MECHANISM-BASED PHARMACOKINETIC-PHARMACODYNAMIC MODELLING OF OPIOIDS: ROLE OF BIOPHASE DISTRIBUTION AND TARGET INTERACTION KINETICS

MECHANISM-BASED PHARMACOKINETIC-PHARMACODYNAMIC MODELLING OF OPIOIDS: ROLE OF BIOPHASE DISTRIBUTION AND TARGET INTERACTION KINETICS

Proefschrift

ter verkrijging van
de graad van Doctor aan de Universiteit Leiden,
op gezag van Rector Magnificus prof.mr. P.F. van der Heijden,
volgens besluit van het College voor Promoties
te verdedigen op dinsdag 18 september 2007
klokke 15.00 uur

door

Dorien Groenendaal
geboren te Velsen
in 1978

Promotiecommissie

Promotor	: Prof. Dr. M. Danhof
Co-promotor	: Dr. E.C.M. de Lange
Referent	: Prof. Dr. W. Couet (Université de Poitiers, Poitiers, France)
Overige leden	: Prof. Dr. A.P. IJzerman Prof. Dr. E.R. de Kloet Prof. Dr. J. van der Greef Prof. Dr. J. Bouwstra

ὥρη μὲν πολέων μύθων, ὥρη δὲ καὶ ὕπνου
There is a time for many words, and there is also a time for sleep
The Odyssey, **book XI**, l. 379

Aan allen die mij dierbaar zijn

The research described in this thesis was conducted at the Division of Pharmacology and the Division of Medicinal Chemistry of the Leiden/Amsterdam Center for Drug Research, Leiden University and the department of Drug Metabolism and Pharmacokinetics of GlaxoSmithKline in Ware, United Kingdom.

The printing of this thesis was financially supported by:
Astellas Pharma Europe B.V.
Leiden/Amsterdam Center for Drug Research
Pharmachemie B.V.

Cover design and lay-out: Roel van de Meent
The picture on the cover represents a photograph of morphine, taken through a microscope with polarized light, by Lars Bech. Copyright Teva Pharmachemie Haarlem, The Netherlands

Printed by Ponsen & Looijen, Wageningen, The Netherlands

ISBN: 987–90–6464–165–7

Section 1
GENERAL INTRODUCTION

Sec1

Chapter 1

PHARMACOKINETIC-PHARMACODYNAMIC MODELLING OF OPIOIDS:
ROLE OF BIOPHASE DISTRIBUTION AND TARGET INTERACTION KINETICS

ABSTRACT

Mechanism-based pharmacokinetic-pharmacodynamic (PK-PD) models contain specific expressions for processes on the causal path between drug administration and response. These models include expressions to describe a) blood pharmacokinetics in blood or plasma, b) biophase distribution, c) kinetics or target binding, d) transduction and e) homeostatic feedback mechanisms.

Previously, the PK-PD correlations of the high efficacy μ-opioid receptor agonists alfentanil, fentanyl and sufentanil have been investigated using quantitative EEG parameters as pharmacodynamic endpoint. In these investigations, the hysteresis observed for fentanyl and sufentanil was described with an effect-compartment model. Furthermore, by simulation it was shown that, in mechanistic terms, the *in vivo* concentration-effect relationships could be explained on the basis of the operational model of agonism, under the assumption of considerable receptor reserve. A limitation of this analysis was however, that all investigated opioids behaved as full agonists. Moreover, complexities at the level of blood-brain barrier (BBB) distribution had not been taken into account.

The main focus of the research in this thesis is on mechanism-based PK-PD modelling of the EEG effects of opioids with special emphasis on 1) the biophase distribution kinetics, which is mainly determined by BBB transport, and 2) interaction with the μ-opioid receptor in the brain as determinants of the time course of the pharmacological effect. To this end, a wide range of opioids with different binding characteristics and intrinsic activities should be investigated. The impact of biophase distribution should be investigated *in vivo* in great detail using intracerebral microdialysis.

CONTENTS

1. PHARMACOKINETIC-PHARMACODYNAMIC MODELLING

The objective of pharmacokinetic-pharmacodynamic (PK-PD) modelling is the characterisation and prediction of the time course of drug effects *in vivo* under physiological and pathological conditions (Breimer & Danhof 1997).

1.1 Classical/empirical approach

Classical PK-PD models consist of three components: (1) a pharmacokinetic model describing the time-course of drug concentration in blood or plasma, (2) a pharmacodynamic model describing the relation between the observed effect and the (predicted) drug concentration and (3) a link model to account for the often observed delay between blood/plasma concentration and effect.

1.1.1 Pharmacokinetic models

In PK-PD modelling, compartmental models are most commonly used to describe the time course of the drug concentration in blood/plasma. In these models drug disposition is characterised as the transfer of drug between interconnected hypothetical compartments, which serves to mimic the drug absorption, distribution and elimination processes. A limitation of this approach is that, although useful for descriptive purposes, it is not truly mechanistic. As a result, it is of limited value for extrapolation and prediction (i.e. interspecies scaling).

1.1.2 Pharmacodynamic models

Pharmacodynamic models describe the relationship between blood or plasma concentration and effect. The most general pharmacodynamic model is the sigmoid E_{max} model. This model is mathematically expressed by the Hill equation (Hill 1910) according to:

$$E = E_0 + \frac{\alpha \cdot C^{n_H}}{EC_{50} + C^{n_H}} \qquad (1)$$

in which E_0 is the no-drug response (baseline), α is the maximum response (intrinsic activity), EC_{50} is the concentration at which 50% of the maximum effect is reached (potency) and n_H is a factor expressing the slope of the sigmoid relationship. A limitation of the Hill equation is that it is not a mechanistic model. Specifically, the model does not provide insight in the factors which determine the shape and the location of the drug concentration-effect relationship. In this respect, it is important that drug concentration-effect relationships are determined by a combination of drug-specific properties (affinity and intrinsic efficacy) and biological system-specific characteristics such as receptor density and the efficiency of receptor-effector coupling (van der Graaf & Danhof 1997), as is illustrated in figure 1. An important factor is that the system-specific properties may differ between biological systems. Moreover, they can be influenced by several

processes like disease, age, chronic treatment and by other drugs. This may explain differences in drug-concentration-effect relationships between biological systems (i.e. species) and individuals (inter-individual variability). Moreover, the parameters of the sigmoid E_{max} model are "mixed" parameters; potency of a drug is determined by both affinity and efficacy and the intrinsic activity is a function of both compound (intrinsic efficacy) and system (receptor density and signal transduction) characteristics. This complicates the prediction of *in vivo* drug concentration-effect relationships on the basis of information from *in vitro* bio-assays.

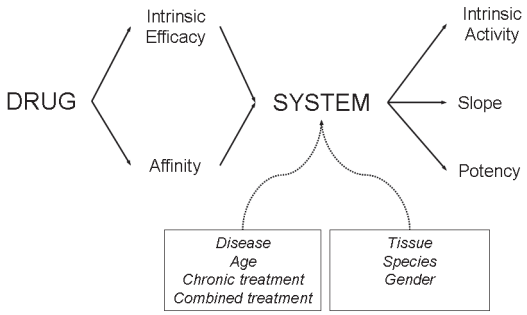

Figure 1: The pharmacodynamics of a drug (potency, intrinsic activity and Hill factor) are dependent on both drug (affinity and intrinsic efficacy) and system-related properties. These system related properties can be influenced by several processes like disease, age, chronic treatment and other drugs. Adapted from Van der Graaf and Danhof (1997).

1.1.3 Link models

For many drugs the relationship between blood/plasma concentration and pharmacological effect is not direct. Often a delay in pharmacological effect (hysteresis) is observed, which can be caused by time dependencies at the level of a) pharmacokinetics and b) pharmacodynamics. To account for delays between drug concentration and response, Segre introduced the concept of a "hypothetical effect compartment" (Segre 1968). Sheiner and co-workers were the first to formalize this concept into a model to describe hysteresis caused by distribution to the biophase (Holford & Sheiner 1982; Sheiner *et al*. 1979). With the effect compartment model the assumption is made that the rate of onset and offset of the drug effect is governed by the rate of drug distribution to the hypothetical "effect-site" (Sheiner *et al*. 1979). This effect-compartment is then linked to the blood concentrations with the rate constant k_{1e} for transport to the effect-site and the rate constant for drug loss k_{eo}. The effect-site distribution is considered to be symmetrical under the assumption that in equilibrium the effect-site concentration equals the blood concentration, where k_{1e} is equal to k_{eo}.

1.2 New approach – distinction between determinants of *in vivo* effects

At present there is a clear trend towards the development and application of mechanism-

based PK-PD models. Mechanism-based PK-PD models differ from the classical empirical descriptive models in that they contain specific expressions to characterise the processes on the causal path between drug administration and effect. These models should contain expressions for a) blood/plasma pharmacokinetics, b) biophase distribution c) kinetics of target binding, d) transduction and e) homeostatic feedback mechanisms (Danhof *et al.* 2005). A schematic diagram of drug action *in vivo* with the major determinants is shown in figure 2.

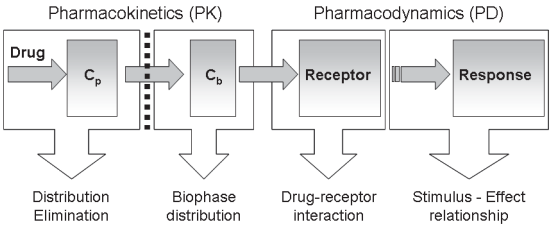

Figure 2: Schematic diagram of drug action in

1.2.1 Blood/plasma pharmacokinetics

To improve the prediction of pharmacokinetics, especially with regard to the extrapolation between species and the understanding of inter-individual variability, the concept of physiologically-based pharmacokinetic (PBPK) modelling has been proposed (Rowland *et al.* 2004). PBPK models are based on physiological principles and typically contain specific expressions for physiological variables such as blood flow to specific organs, binding to plasma proteins and/or tissue components and liver enzyme activity.

1.2.2 Biophase distribution

The concentration at the site of action (the biophase) is an important determinant of the drug effect *in vivo*. For drugs acting at extracellular targets, physicochemical properties (e.g. molecular size) and binding to plasma proteins and other blood constituents can restrict distribution to the biophase. Moreover, for drugs acting at intracellular targets and at targets in tissues that are protected by specific barriers (e.g. the brain), the distribution into the biophase can be influenced by the functionality of transporters. At present, these mechanisms are usually not taken into consideration when modelling biophase distribution kinetics. Yet, this is important since complexities at the level of biophase distribution may affect the derived shape of the concentration-effect relationship (Mandema *et al.* 1991; Visser *et al.* 2002b). Moreover, it may complicate the *in vitro* to *in vivo* extrapolation of parameters characterising the binding affinity of a drug to a specific target (Zuideveld *et al.* 2004). Another important consideration in relation to biophase distribution is whether it is indeed the free drug concentration

that drives the intensity of the pharmacological response. For a number of drugs (i.e. benzodiazepines, synthetic opioids) this seems to be the case (Cox *et al*. 1998; Mandema *et al*. 1991). However, there is still limited experimental evidence that the "free drug hypothesis" is valid under all circumstances. Particularly for drugs with a high affinity to their biological target and for drugs, which are transported by active transport mechanisms to the site of action, the biophase distribution may be non-restrictive.

In general, biophase distribution is dependent on both perfusion and distribution processes. Distribution processes include 1) passive diffusion and 2) transporter-mediated transport. Passive membrane diffusion is dependent on filtration (paracellular transport) and diffusion (transcellular transport), which can both be influenced by binding of the compound to proteins or other blood constituents. The main focus of this thesis is on the mechanisms of biophase distribution and this will be discussed in a separate section.

1.2.3 Kinetics of target binding

At the effect-site in the brain, the relationship between the concentration and the pharmacological effect is dependent on target interaction kinetics and signal transduction. Typically, when analysing concentration-effect relationships of a range of compounds in a given biological system, a single unique transducer function determines the effect and observed differences in concentration-effect relations are related to differences in receptor interaction kinetics in terms of target affinity and intrinsic efficacy.

In recent years, there has been considerable interest in the incorporation of receptor theory in PK-PD modelling for the prediction of *in vivo* concentration-effect relationships (van der Graaf & Danhof 1997). This is important since this enables a separation between drug-specific and biological-specific properties as determinants of the concentration-effect relationships. Modern receptor theory is based on the concept of the occupancy theory as first proposed by Clark (1937). This theory was further refined to describe the effects of partial agonists (Ariens 1954; Stephenson 1956) and receptor reserve (Furchgott 1966). Black and Leff have proposed the operational model of agonism to describe the relationship between drug concentration, receptor interaction and response (Black & Leff 1983). This model consists of two hyperbolic functions to describe the concentration-receptor occupancy and the receptor occupancy-response relationship, respectively, according to:

$$E = E_0 + \frac{E_m \cdot \tau^n \cdot C^n}{(K_A + C)^n + \tau^n \cdot C^n} \qquad (2)$$

where E_m is the maximum effect achievable in the system, K_A is the agonist dissociation equilibrium constant, n is the slope index for the occupancy-effect relationship and τ is the efficacy parameter. This efficacy parameter expressed according to equation:

$$\tau = \frac{R_0}{K_E} \tag{3}$$

where R_0 is the total number of available receptors and K_E is the concentration of the drug-receptor complex required to produce half-maximal effect. The drug-specific properties, the intrinsic activity (α) and the potency (EC_{50}) can than be derived with the following equations:

$$\alpha = \frac{E_{\max} \cdot \tau^n}{\tau^n + 1} \tag{4}$$

$$EC_{50} = \frac{K_A}{\left(2 + \tau^n\right)^{1/n} - 1} \tag{5}$$

Recently, the principles of receptor theory have been successfully applied in the PK-PD analysis of neuroactive steroids (Visser *et al.* 2002a), benzodiazepines (Tuk *et al.* 1999; 2003; Visser *et al.* 2001), adenosine A_1 receptor agonists (van der Graaf *et al.* 1997) and 5-HT_{1A} receptor agonists (Zuideveld *et al.* 2004). PK-PD analysis on the basis of the operational model of agonism of the concentration-effect relationships of adenosine A_1 receptor agonists (van der Graaf *et al.* 1997) and 5-HT_{1A} receptor agonists (Zuideveld *et al.* 2004) have shown that a distinction can be made between drug-related and system-related parameters. For the adenosine A_1 receptor agonists a good correlation was found between the *in vivo* pK_A and the in *vitro* pK_i and between the *in vivo* efficacy parameter τ and the *in vitro* GTP shift. In contrast, for the 5-HT_{1A} receptor agonists a poor correlation was found between the *in vivo* pK_A and the *in vitro* pK_i, whereas a good correlation was found between *in vivo* efficacy parameter τ and the *in vitro* GTP shift. This poor correlation between *in vivo* pK_A and *in vitro* pK_i could in part be explained by differences in blood-brain distribution of the 5-HT_{1A} receptor agonists.

1.2.4 Signal transduction

Within the context of PK-PD modelling, transduction is defined as the cascade of processes that govern the time course of the pharmacological response *in vivo* following drug-induced target activation.

In addition to biophase distribution, time-dependent processes like the synthesis or degradation rate of an endogenous compound can explain hysteresis. To link this time delay between blood/plasma concentration and effect, a family of four physiological indirect response models have been proposed (Dayneka *et al.* 1993), which are based on the following differential equation:

$$\frac{dR}{dt} = k_{in} - k_{out} \cdot R \tag{6}$$

Where *R* is a physiological entity, which is constantly being produced and eliminated

in time, k_{in} is the zero-order rate constant for production of the physiological entity and k_{out} is the first-order rate constant for its loss. These models have been applied to describe the time-courses of a wide array of different drugs (Jusko & Ko 1994), although these models are often not properly validated.
A recent development has been the incorporation of dynamic system analysis to describe complex *in vivo* transduction processes (Zuideveld *et al*. 2001; 2004).

1.2.5 Homeostatic feedback mechanisms

The time course of the pharmacological response is often influenced by *in vivo* homeostatic feedback mechanisms, which may be operative. Such mechanisms may explain observations such as complex pharmacological effect *vs* time profiles. Recently, a model has been developed to describe the complex effect vs time profiles of the hypothermic response following the administration of 5-HT_{1A} receptor agonists to rats (Zuideveld *et al*. 2001; 2004). This model describes the hypothermic effect based on the concept of a set-point and general physiological response model.

2. BIOPHASE DISTRIBUTION OF CNS DRUGS

CNS active drugs have to pass the blood-brain barrier (BBB) to reach their target in the brain to be able to exert their pharmacological effect. This often results in biophase kinetics which are substantially different from plasma pharmacokinetics since BBB transport and brain distribution is often neither instantaneous nor complete (Welty *et al*. 1993).

2.1 Blood-brain barrier

2.1.1 Blood-brain barrier morphology

The BBB is situated at the interface between blood and brain and its main functions are (1) to maintain homeostasis in the brain (Abbott & Romero 1996), (2) selective transport of essential compounds like amino acids and glucose and (3) metabolism and modification of substances before entering the brain, for example proteins and peptides (de Boer & Breimer 1992). The BBB is primarily formed by brain capillary endothelial cells (BCEC) (de Boer & Breimer 1992; Rubin & Staddon 1999), although cells like astrocytes, pericytes and neuronal cells also play an important role in the function of the BBB (Pardridge 1991). The BCECs are distinctly different from peripheral endothelial cells in functional and morphological aspects (Bradbury 1993; de Boer *et al*. 2003). The most specific feature is the presence of tight junctions which prevents paracellular transport of hydrophilic compounds (Brightman & Reese 1969). Moreover, the BCECs express numerous influx and efflux transporters (de Boer *et al*. 2003; Golden & Pollack 1998; Lee *et al*. 2001).

2.1.2 Transport characteristics

Transport across the BBB can be divided into passive and active transport processes (de Lange & Danhof 2002). Passive transport of compounds across the BBB is dependent on physicochemical properties, such as lipophilicity, degree of ionisation and number of hydrogen bonds (van Bree *et al.* 1988). Passive transport (diffusion) across the BBB can either be permeability-limited or cerebral blood flow limited. Permeability-limited BBB transport is applicable for the more hydrophilic drugs that depend on the paracellular route for exchange between blood and brain. This route is restricted by the above-mentioned presence of tight junctions. Lipophilic, small and non-charged drugs more easily diffuse via the transcellular route and in such case blood-flow will mainly determine the transport rate. Active transport can be divided into carrier mediated transport, receptor mediated transport and endocytosis (de Boer *et al.* 2003). A schematic diagram of the transport processes across the BBB is shown in figure 3.

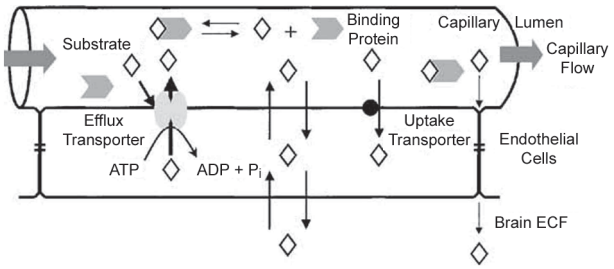

Figure 3: Schematic diagram of substrate flux through the BBB, indicating factors and processes that determine net brain uptake. Uptake and efflux transporters are illustrated on the luminal membrane of the endothelial cells for illustrative purposes only (Golden and Pollack, 2003)

2.1.3 P-Glycoprotein

An important efflux transporter expressed at the luminal face of the BBB is P-glycoprotein (Pgp) (Cordon-Cardo *et al.* 1989). Pgp is a member of the adenosine triphosphate-binding cassette (ABC) super family and is encoded by the multidrug resistance gene (MDR1) (Thiebaut *et al.* 1987). Pgp is a 170 kDa glycosylated membrane protein that consists of an integral membrane protein with twelve putative transmembrane α-helical domains and an energy-coupling domain localized at the cytoplasmatic side of the membrane (Fath & Kolter 1993; Pigeon & Silver 1994). The proposed function of Pgp is mainly to protect the brain from exogenous toxins, to excrete metabolites and furthermore to transport hormones from the brain to the periphery (Borst & Schinkel 1996; Karssen *et al.* 2001). The use of *in vitro* cell systems comprising of MDCK or LLC-PK1 cells transfected with the human MDR1 gene and MDR1a(-/-) (Pgp knock-out) mice (Schinkel *et al.* 1994) has clarified the impact of this efflux transporter on brain concentrations of many drugs including dexamethasone, domperidone, indinavir, digoxin, vinblastine, sparfloxacin, amitryptyline and cyclosporin (de Lange *et al.* 2000; de Lange & Danhof

2002; Kim *et al.* 1998; Meijer *et al.* 1998; Schinkel *et al.* 1995; Schinkel *et al.* 1996; Uhr *et al.* 2000; van der Sandt *et al.* 2001b). Alternatively, co-administration of Pgp inhibitors such as GF120918 (Hyafil *et al.* 1993) and SDZ-PSC 833 (Desrayaud *et al.* 1998; Mayer *et al.* 1997) can change drug distribution into the brain. For example, for the 5-HT_{1A} receptor agonist flesinoxan it was shown that a 5 to 6 fold increase in C_{max} and AUC was observed in brain pharmacokinetics when co-infused with the Pgp inhibitor SDZ-PSC 833 (van der Sandt *et al.* 2001a).

2.2 Distribution processes within the brain

The brain cannot be considered a homogeneous tissue, because it is composed of many anatomical structures with different characteristics (Collins & Dedrick 1983; Gross *et al.* 1986). In general, the main compartments are the brain extracellular fluid (ECF), the intracellular space (ICS) and the brain cerebrospinal fluid (CSF). After passage of the BBB, a drug enters the brain ECF and may thereafter distribute into brain ICS and the CSF (de Lange & Danhof 2002; Walker *et al.* 2000; Wong *et al.* 1993). Brain intracellular distribution is, in general, quantitatively more profound for the more lipophilic drugs and as a consequence the brain ECF concentrations will be relatively lower.

The interplay between the kinetics of BBB transport and intracellular distribution determines the time to equilibrium between plasma and biophase kinetics (Liu *et al.* 2005). With regard to the brain ECF concentrations, active transport out of the brain decreases whereas brain tissue binding increases the time to equilibrium. It should be noted that other than BBB transport, active transporters may also play a role in the intracellular distribution in the brain as indicated by localisation and functional expression of Pgp and MRP in the brain parenchyma (Lee *et al.* 2001).

2.3 Intracerebral microdialysis

Intracerebral microdialysis is very valuable technique for characeterisation of brain distribution kinetics, since it allows the determination of the free drug in the ECF as a function of time. It involves the implantation of a microdialysis probe into tissue, for example a specific region of the brain. The probe, consisting of a hollow tube and a semi-permeable membrane, is constantly perfused with a physiological solution. During perfusion, compounds that are small enough to traverse the membrane will diffuse from higher to lower concentration into the dialysate (Benveniste & Huttemeier 1990; de Lange *et al.* 1999a).

An important aspect of microdialysis is the recovery of the microdialysis probe. The dialysate concentrations do not equal the real ECF concentrations, because of the existence of a constant flow of the perfusion fluid. At early stages of microdialysis research, the *in vitro* recovery was used to calculate the ECF concentrations. However, *in vivo*, several tissue processes influence the recovery (Bungay *et al.* 1990) and therefore *in vivo* recovery methods have been developed including retrodialysis, no-net-flux and the dynamic-no-net-flux (Bouw & Hammarlund-Udenaes 1998; de Lange *et al.* 1997; 1999a; 1999b; 2000; Olson & Justice, Jr. 1993). Many CNS active drugs have their target

at extracellular recognition sites and therefore the ECF concentrations are most closely related to the biophase concentrations.

3. BRAIN AND BIOPHASE DISTRIBUTION MODELS

For PK-PD modelling, often only blood/plasma and effect data are available. In this case, a hypothetical effect-compartment is commonly applied to describe the biophase distribution kinetics. Recently, important progress has been made with the development of the technique of intracerebral microdialysis. It has been demonstrated that the mechanisms of brain distribution kinetics can be investigated in detail *in vivo* using this technique. It is proposed that this may provide novel insights in the mechanisms of the biophase distribution kinetics of CNS active drugs.

3.1. Brain distribution models

Recently, pharmacokinetic models have been developed that allow integrated analysis of microdialysis data which means that recovery calculations are included into the models (Schaddelee *et al*. 2004; Tunblad *et al*. 2004). In addition, population pharmacokinetic modelling of the microdialysis data has provided insight into the BBB transport characteristics of several drugs. These drugs include adenosine A_1 receptor agonists (Schaddelee *et al*. 2004), gabapentin (Wang & Welty 1996), norfloxacin (Chenel *et al*. 2004), fluvoxamine (Geldof *et al*. 2007) and opioids, which will be discussed in a separate section.

3.1.1 Application to adenosine A_1 receptor agonists

Schaddelee and co-workers have proposed a population pharmacokinetic model for estimation of the brain distribution clearance of the synthetic adenosine A_1 receptor agonists, 2'dCPA and MCPA. The model consisted of three compartments for description of the time course of the concentration in blood in combination with three compartments for the brain ECF concentrations (figure 4).

The mass balance in the brain compartments is described with the following differential equations:

$$\frac{dA_4}{dt} = K_{14} \cdot A_1 - K_{41} \cdot A_4 - K_{45} \cdot A_4 + K_{54} \cdot A_5 - K_{46} \cdot A_4 + K_{64} \cdot A_6 \quad (7)$$

$$\frac{dA_5}{dt} = K_{45} \cdot A_4 - K_{54} \cdot A_5 \quad (8)$$

$$\frac{dA_6}{dt} = K_{46} \cdot A_4 - K_{64} \cdot A_6 \quad (9)$$

Where A_1 represents the amount in the central blood compartment, A_4 – A_6 represent the amounts in the respective brain compartment and K_{mn} represents the first-order

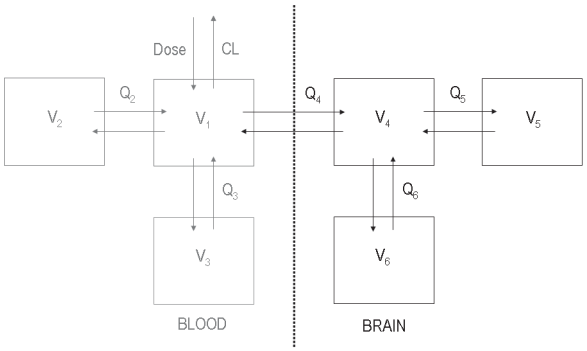

Figure 4: The population pharmacokinetic model for synthetic adenosine A_1 receptor agonists as proposed by Schaddelee and co-workers (2003). The model consists of three compartments to describe the blood pharmacokinetics (grey) and three compartments to describe the brain pharmacokinetics (black). Abbreviations: V= volume of distribution, Q = intercompartmental clearance and CL = body clearance.

transport rate constants from compartment *m* to compartment *n*. The rate constants were related to the inter-compartmental clearances (Q) and compartment volume (V) according to the following equations:

$$K_{mm} = \frac{Q_{m+1}}{V_m} \tag{10}$$

$$K_{mn} = \frac{Q_{m+1}}{V_n} \tag{11}$$

Low distribution clearances into the brain (Q_4) were found, 1.6 ± 0.3 µl/min and 1.9 ± 0.4 µl/min for 2'dCPA and MCPA, respectively, which were consistent with the results from *in vitro* tests. Furthermore, a slow elimination from the brain compartment was observed, indicating that the duration of the CNS effect might be much longer than expected on the basis of the terminal half-life in blood.

3.1.2 Application to the 5-HT$_{1A}$ receptor agonist fluvoxamine

The pharmacokinetics of the 5-HT_{1A} receptor agonist fluvoxamine, were described by simultaneous analysis of plasma, brain ECF and total brain concentrations on the basis of a more physiologically-based pharmacokinetic model. A three compartment model was used to describe the pharmacokinetics in plasma. The brain model to describe both brain ECF and total brain concentrations considers the brain to be composed of two areas (figure 5) and was based on the models proposed by Upton and co-workers (2000). The first area is the perfusion compartment, considered to be in direct contact with the blood flow and in which mass exchange is perfusion limited (shallow perfusion-limited compartment). The second area is the diffusion limited brain ECF compartment (deep brain compartment) in which the concentration is equal to the measured fluvoxamine ECF concentration. This compartment is poorly perfused and distribution is diffusion

limited. Fluvoxamine is not able to enter this compartment directly by perfusion, but only indirectly from the shallow perfusion-limited compartment by diffusion or active transport processes.

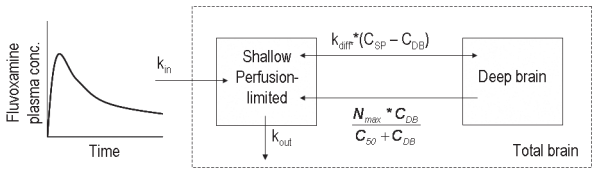

Figure 5: The physiologically-based pharmacokinetic model for fluvoxamine as proposed by Geldof and co-workers (2007). Plasma fluvoxamine concentrations were predicted with a three-compartment model and used as input function for fluvoxamine in the brain. The brain model consists of a shallow perfusion-limited and a deep brain compartment and mass exchange between the shallow perfusion-limited and the deep brain compartment is described by a passive diffusion term and an active saturable efflux process. Abbreviations: k_{in} is the rate constant into the shallow perfusion compartment, k_{out} is the rate constant out of shallow perfusion compartment; k_{diff} is the diffusion rate constant between the shallow perfusion-limited and the deep brain compartment; N_{max} is the maximal active efflux; C_{50} is the fluvoxamine concentration in the perfusion compartment at which 50% of the maximal active efflux is reached and k_{eff} is the active efflux rate constant which is influenced by GF120918.

In this model, the BBB is located between the perfusion and ECF compartment. The mass balance in the brain is determined by both the perfusion and the ECF compartment according to the following equations:

$$\frac{dA_{SP}}{dt} = Q_B \cdot C_{in} - Q_B \cdot C_{out} + N_{SP-DB} \tag{12}$$

$$\frac{dA_{DB}}{dt} = -N_{SP-DB} \tag{13}$$

where A_{SP} is the amount of morphine in the shallow perfusion-limited compartment, Q_B is the effective blood perfusion rate, C_{in} is the concentration entering the perfusion compartment en C_{out} is the concentration leaving the perfusion compartment. $N_{SP\text{-}DB}$ is the net mass exchange between the shallow perfusion-limited and the deep brain compartment and A_{DB} is the amount of fluvoxamine in the deep brain compartment and can include both passive and active transport processes. In case of fluvoxamine, mass exchange between the perfusion and ECF compartment consisted of passive diffusion and an active saturable efflux process, resulting in the following relation:

$$N_{SP-DB} = -k_{diff} \cdot \left(C_{SP} - C_{DB}\right) + \frac{N_{\max} \cdot C_{DB}}{C_{50} + C_{DB}} \tag{14}$$

in which k_{diff} is the diffusion rate constant between the shallow perfusion-limited and deep brain compartment, C_{SP} is the concentration in the deep brain compartment, N_{max}

is the maximal active removal flux and C_{50} is the fluvoxamine concentration in the deep brain compartment at which 50% of saturation of the active removal flux is reached. Under the assumption that rapid equilibrium between fluvoxamine concentrations in the shallow perfusion-limited and the deep brain compartment is reached, the relationship between both compartments can be described as follows:

$$C_{SP} = C_{DB} + \frac{N_{\max}}{k_{dif} f} \cdot \frac{C_{DB}}{C_{50} + C_{DB}} \quad (15)$$

The total amount of fluvoxamine in the brain can be described by:

$$\frac{dA_T}{dt} = \frac{dA_{SP}}{dt} + \frac{dA_{DB}}{dt} = Q_B \cdot C_{in} - Q_B \cdot C_{out} \quad (16)$$

in which A_T represents the total amount of fluvoxamine in the brain. The concentration entering the perfusion compartment (C_{in}) is assumed to be equal to the plasma concentration (C_{plasma}), whereas the concentration leaving the perfusion compartment is determined by the partition coefficient (P) between fluvoxamine in blood and the concentration in the shallow perfusion-limited compartment (C_{SP}).
When aggregating the perfusion rates, partition coefficient and brain distribution volume to the rate constants k_{in} and k_{out}, the differential equation for the total fluvoxamine in the brain can be described by:

$$\frac{dC_T}{dt} = k_{in} \cdot C_{plasma} - k_{out} \cdot C_{SP} \quad (17)$$

in which C_T is the total fluvoxamine concentration in the brain. The relationships between the total brain concentrations and both compartments could be derived on the basis of the partition coefficients for the shallow perfusion-limited and the deep brain compartment.
It was shown that the proposed model could accurately describe the plasma and brain pharmacokinetics of fluvoxamine. Active saturable efflux could be identified, although it remains unclear what transporter at the BBB is involved in the active efflux of fluvoxamine.

3.2 Biophase distribution models

In PK-PD investigations, the biophase distribution kinetics is often described by a 1-compartment biophase distribution model, also known as the effect-compartment model. With the effect compartment model, the assumption is made that the rate of onset and offset of the drug effect is governed by the rate of drug distribution to the hypothetical "effect-site" (Sheiner *et al*. 1979). This effect-compartment is then linked to the blood/plasma concentrations with the rate constant for transport to the biophase k_{1e} and the rate constant for drug loss k_{eo}. The rate of change of the drug concentration in the effect compartment can then be expressed by equation:

$$\frac{dC_e}{dt} = k_{1e} \cdot C_b - k_{eo} \cdot C_e \quad (18)$$

Where C_b represents the blood/plasma concentration and C_e represents the effect-site concentration. Under the assumption that in equilibrium the effect-site concentration equals the blood/plasma concentration, this equation can be simplified to:

$$\frac{dC_e}{dt} = k_{eo} \cdot (C_b - C_e) \quad (19)$$

However, more complex biophase distribution models have also been proposed. For example, for the neuroactive steroid alphaxolone the value of k_{eo} was concentration dependent (Visser *et al.* 2002b). In addition, Mandema and co-workers have reported two equilibration rate constants for the EEG effects of heptabarbital and have shown that the equilibration kinetics of amobarbital were best described with a bi-exponential equilibration function instead of a simple first-order mono-exponential equilibration model (Mandema & Danhof 1990; Mandema *et al.* 1991).

Recently, Chenel and co-workers have simultaneously investigated central nervous system distribution and the PK-PD relationship of the EEG effects of norfloxacin (2004). For this purpose, the combined EEG/microdialysis technique has been used. It was shown that the extensive time delay between EEG effect and plasma concentration of norfloxacin could be best described with an effect compartment model. However, this delay could not be accounted for by restricted BBB transport. Presumably, the drug concentration in brain ECF is not representative for the effect-site concentration of norfloxacin. In contrast, for morphine 80% and for morphine-6-glucuronide 50% of the delay in anti-nociceptive effect could be explained by restricted transport across the BBB (Bouw *et al.* 2000; 2001).

4. PHARMACOKINETIC-PHARMACODYNAMIC MODELLING OF OPIOIDS

4.1 Biophase distribution kinetics of opioids

For the analysis of the PK-PD correlations of opioids, modelling of complex biophase distribution kinetics is important, given the (potential) interaction with active transporters and the wide range in lipophilicity. In previous investigations, morphine and loperamide have been identified as Pgp substrates in two *in vitro* models, comprising of either BCECs or LLC-PK1:MDR1 cells, and in *in vivo* models, in rats and mice (Henthorn *et al.* 1999; Letrent *et al.* 1998; 1999a; 1999b; Mahar Doan *et al.* 2002; Schinkel *et al.* 1995; 1996). Alfentanil and sufentanil were not identified as Pgp substrates within the abovementioned investigations in *in vitro* models, whereas inconsistencies have been reported for fentanyl (Henthorn *et al.* 1999; Wandel *et al.* 2002). For fentanyl, *in situ*

brain perfusion studies have indicated a minimal contribution of Pgp mediated efflux as it was found that the brain uptake of fentanyl was only marginally increased (1.2 fold) in MDR1a (-/-) mice when compared to MDR1a (+/+) mice (Dagenais *et al.* 2004). Nalbuphine, a semi-synthetic opioid analgesic, was also found to be a Pgp substrate in an MDCKII-MDR1 cell-system (Mahar Doan *et al.* 2002).

The BBB transport characteristics of morphine and its metabolites have been studied in great detail using intracerebral microdialysis (Bouw *et al.* 2000; 2001; Xie *et al.* 2000). The brain pharmacokinetics of morphine, morphine-3-glucuronide (M3G) and morphine-6-glucuronide (M6G) were best described with a two compartment brain distribution model. The half-life of morphine in the brain was 44 ± 11 minutes for a dose of 10 mg/kg and was dependent on dose. For M3G and M6G the half-life in the brain was around 70 and 60 minutes, respectively. The brain-to-plasma concentration ratios were 0.28, 0.11 and 0.27 for morphine, M3G and M6G, respectively. All ratios are below 1 indicating that these compounds are actively removed at the BBB. Furthermore, PK-PD studies in rats have revealed that after oral pre-treatment with the specific Pgp inhibitor GF120918, the anti-nociceptive effect of morphine was prolonged due to its prolonged half-life in the brain (Letrent *et al.* 1998; 1999a). Tunblad and co-workers investigated the influence of probenecid on the BBB transport of morphine and found that in the presence of probenecid the steady state brain-to-plasma ratio was increased from 0.29 to 0.39 and that the morphine half-life in the brain increased from 58 to 115 min (2004). In addition, probenecid also decreased the systemic clearance of morphine and decreased the formation of M3G. M3G is also identified as a substrate for the probenecid-sensitive transporters (Xie *et al.* 2000).
In contrast, intracerebral microdialysis studies with the highly lipophilic opioid codeine have shown that a distributional equilibrium is reached rapidly with equal unbound concentrations in blood and brain and without dose dependency (Xie & Hammarlund-Udenaes 1998).

4.2 EEG as a biomarker for opioid receptor activation

Detailed characterisation of the role of biophase distribution kinetics in PK-PD investigations requires the availability of high density pharmacodynamic data. In this respect, quantitative analysis of drug effects on the electroencephalogram (EEG) yields attractive biomarkers, which are continuous, sensitive and reproducible (Dingemanse *et al.* 1988). Another advantage is that EEG effect measurements can be obtained in both laboratory animals and humans which enables interspecies extrapolation of the pharmacodynamics. On the basis of spectral analysis, the EEG can be subdivided into five distinct frequency bands: delta (0.5-4.5 Hz), theta (3.5-8 Hz), alpha (8-12 Hz), beta (12-30 Hz) and gamma (30->70 Hz) (Faulkner *et al.* 1999). Frequencies ranging from below 1 Hz up to around 12 Hz (delta – alpha bands) are readily observable in recordings from subjects during sleep, sedation or relaxed wakefulness. Higher frequencies from 12 Hz

to >70 Hz (beta – gamma bands) can also be seen, but at much lower amplitudes during intense mental activity and following sensory stimulation (Visser 2003).

Quantitative EEG parameters have been widely used as a pharmacodynamic endpoint in pre-clinical and clinical investigations on the PK-PD correlations of a variety of CNS active drugs. This includes barbiturates (Ebling *et al.* 1991), benzodiazepines (Mandema, *et al.* 1991a; 1991b; 1992b), neurosteroids (Visser *et al.* 2002a) and baclofen (Mandema *et al.* 1992a). It has also been shown that the synthetic opioid alfentanil, which is frequently used in anesthesia, produces a progressive slowing of the EEG with a pre-dominant increase in the delta frequency band (0.5-4.5 Hz) of the EEG power spectrum in both animals (Cox *et al.* 1997; Mandema & Wada 1995; Wauquier *et al.* 1988; Young & Khazan 1984) and humans (Scott *et al.* 1985; Wauquier *et al.* 1984; Young & Khazan 1984). After administration of alfentanil the EEG profile changes from high-frequency and low-amplitude to low-frequency and high-amplitude as is illustrated in figure 6.

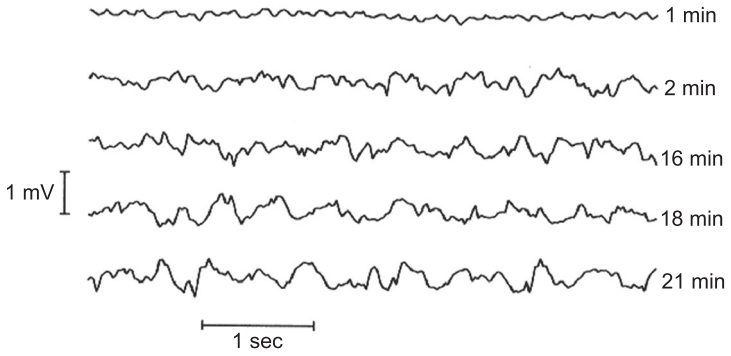

Figure 6: Typical EEG changes in rats upon alfentanil administrations. After administration of alfentanil, a progressive slowing of the EEG is observed with pre-dominant high-amplitude, low-frequency activity (0.5-4.5 Hz) (Cox *et al.* 1997).

4.3 Pharmacokinetic-pharmacodynamic modelling of the EEG effects of opioids

Previously, Cox and co-workers investigated the PK-PD correlations of the EEG effects of synthetic opioids alfentanil, fentanyl and sufentanil after intravenous administration in rats (1998). In these investigations, hysteresis was observed between the pharmacokinetics in blood and the pharmacodynamics for fentanyl and sufentanil whereas a direct correlation was observed for alfentanil. The hysteresis was described with the effect compartment model (equation 9), resulting in k_{eo} values of 0.32 min^{-1} ($t_{1/2,keo}$ = 2.2 min) and 0.17 min^{-1} ($t_{1/2,keo}$ = 4.2 min) for fentanyl and sufentanil, respectively. The pharmacodynamics was described using the sigmoid E_{max} model (equation 1). The interaction at the opioid μ receptor was determined *in vitro* on the basis of displacement of [^{3}H]-naloxone binding in washed rat brain membranes. The value of the 'sodium shift', being the ratio between affinities in the presence and the absence of sodium

chloride, was used as a measure of *in vitro* efficacy. Combination with the *in vitro* receptor binding characteristics showed that the *in vivo* concentration-effect relationships could be explained by the operational model of agonism according to Black and Leff (equation 2) under the assumption of a considerable receptor reserve (Cox *et al.* 1998).

The operational model of agonism has subsequently been used to explain the functional adaptation observed upon repeated administration of the selective μ-opioid receptor agonist, alfentanil. It was proposed that the ~2-fold decrease in potency observed following repeated administration of alfentanil can be explained by a ~40% decrease in the efficacy parameter of the operational model of agonism, τ, which includes both receptor density and coupling efficiency (Cox *et al.* 1998).

Garrido and co-workers further investigated the concept of receptor reserve for the full μ-opioid agonist, alfentanil, *in vivo* by pre-treatment with the irreversible μ antagonist, β-funaltrexamine (β-FNA) (2000). After pre-treatment with β-FNA the *in vivo* concentration-effect relationship of alfentanil was steeper and shifted to higher concentrations. Analysis with the operational model of agonism revealed that the observed changes could be explained by a 70-80% reduction in the alfentanil efficacy. This was consistent with the 40-60% reduction in the number of μ-opioid binding sites in the brain, as determined in an *in vitro* binding assay.

However, so far only simulations have been performed to investigate the role of μ-opioid receptor interaction kinetics. A complication in this analysis was however, that all investigated opioids behaved as full agonists.

5. CONCLUSIONS

In conclusion, to be able to develop a mechanism-based PK-PD model for opioids, a wide range of opioids should be investigated with different binding affinities and intrinsic activities. Moreover, potential complexities caused by interactions with specific transporters at the level of the brain distribution need to be taken into consideration.

6. REFERENCES

Abbott NJ, Romero IA (1996) Transporting therapeutics across the blood-brain barrier. *Mol.Med.Today* **2**: 106-113

Ariens EJ (1954) Affinity and intrinsic activity in the theory of competitive inhibition. I. Problems and theory. *Arch. Int.Pharmacodyn.Ther* **99**: 32-49

Benveniste H, Huttemeier PC (1990) Microdialysis--theory and application. *Prog.Neurobiol.* **35**: 195-215

Black JW, Leff P (1983) Operational models of pharmacological agonism. *Proc.R.Soc.Lond B Biol.Sci.* **220**: 141-162

Borst P, Schinkel AH (1996) What have we learnt thus far from mice with disrupted P-glycoprotein genes? *Eur. J.Cancer* **32A**: 985-990

Bouw MR, Gardmark M, Hammarlund-Udenaes M (2000) Pharmacokinetic-pharmacodynamic modelling of morphine transport across the blood-brain barrier as a cause of the antinociceptive effect delay in rats - a microdialysis study. *Pharm.Res.* **17**: 1220-1227

Bouw MR, Hammarlund-Udenaes M (1998) Methodological aspects of the use of a calibrator in in vivo microdialysis-further development of the retrodialysis method. *Pharm.Res.* **15**: 1673-1679

Bouw MR, Xie R, Tunblad K, Hammarlund-Udenaes M (2001) Blood-brain barrier transport and brain distribution of morphine-6-glucuronide in relation to the antinociceptive effect in rats--pharmacokinetic/pharmacodynamic modelling. *Br.J.Pharmacol,* **134**: 1796-1804

Bradbury MW (1993) The blood-brain barrier. *Exp.Physiol,* **78**: 453-472

Breimer DD, Danhof M (1997) Relevance of the application of pharmacokinetic-pharmacodynamic modelling concepts in drug development. The “wooden shoe’ paradigm. *Clin.Pharmacokinet.* **32**: 259-267

Brightman MW, Reese TS (1969) Junctions between intimately apposed cell membranes in the vertebrate brain. *J.Cell Biol.* **40**: 648-677

Bungay PM, Morrison PF, Dedrick RL (1990) Steady-state theory for quantitative microdialysis of solutes and water in vivo and in vitro. *Life Sci.* **46**: 105-119

Chenel M, Marchand S, Dupuis A, Lamarche I, Paquereau J, Pariat C, Couet W (2004) Simultaneous central nervous system distribution and pharmacokinetic-pharmacodynamic modelling of the electroencephalogram effect of norfloxacin administered at a convulsant dose in rats. *Br.J.Pharmacol* **142**: 323-330

Clark AJ (1937) General Pharmacology. in Heffner’s Handbuch der experimentellen *Pharmacologie Erganzungsband,* Springer, 38-51.

Collins JM, Dedrick RL (1983) Distributed model for drug delivery to CSF and brain tissue. *Am.J.Physiol,* **245**: R303-R310

Cordon-Cardo C, O'Brien JP, Casals D, Rittman-Grauer L, Biedler JL, Melamed MR, Bertino JR (1989) Multidrug-resistance gene (P-glycoprotein) is expressed by endothelial cells at blood-brain barrier sites. *Proc.Natl.Acad.Sci. U.S.A.* **86**: 695-698

Cox EH, Kerbusch T, van der Graaf PH, Danhof M (1998) Pharmacokinetic-pharmacodynamic modeling of the electroencephalogram effect of synthetic opioids in the rat: correlation with the interaction at the mu-opioid receptor. *J Pharmacol.Exp.Ther.* **284**: 1095-1103

Cox EH, Kuipers JA, Danhof M (1998) Pharmacokinetic-pharmacodynamic modelling of the EEG effect of alfentanil in rats: assessment of rapid functional adaptation. *Br.J.Pharmacol* **124**: 1534-1540

Cox EH, Van Hemert JG, Tukker EJ, Danhof M (1997) Pharmacokinetic-pharmacodynamic modelling of the EEG effect of alfentanil in rats. *J Pharmacol.Toxicol.Methods* **38**: 99-108

Dagenais C, Graff CL, Pollack GM (2004) Variable modulation of opioid brain uptake by P-glycoprotein in mice. *Biochem Pharmacol* **67**: 269-276

Danhof M, Alvan G, Dahl SG, Kuhlmann J, Paintaud G (2005) Mechanism-based pharmacokinetic-pharmacodynamic modeling-a new classification of biomarkers. *Pharm.Res.* **22**: 1432-1437

Dayneka NL, Garg V, Jusko WJ (1993) Comparison of four basic models of indirect pharmacodynamic responses. *J.Pharmacokinet.Biopharm.* **21**: 457-478

de Boer AG, Breimer DD (1992) De bloed-hersen barriere en het transport van farmaca. *Janssen medisch wetenschappelijk nieuws:* 149-155

de Boer AG, van der Sandt I, Gaillard PJ (2003) The role of drug transporters at the blood-brain barrier. *Annu.Rev. Pharmacol Toxicol.* **43**: 629-656

de Lange EC, Danhof M (2002) Considerations in the use of cerebrospinal fluid pharmacokinetics to predict brain target concentrations in the clinical setting: implications of the barriers between blood and brain. *Clin. Pharmacokinet.* **41**: 691-703

de Lange EC, Danhof M, de Boer AG, Breimer DD (1997) Methodological considerations of intracerebral microdialysis in pharmacokinetic studies on drug transport across the blood-brain barrier. *Brain Res.Brain Res. Rev.* **25**: 27-49

de Lange EC, de Boer AG, Breimer DD (2000) Methodological issues in microdialysis sampling for pharmacokinetic studies. *Adv.Drug Deliv.Rev.* **45**: 125-148

de Lange EC, de Boer AG, Breimer DD (1999a) Microdialysis for pharmacokinetic analysis of drug transport to the brain. *Adv.Drug Deliv.Rev.* **36**: 211-227

de Lange EC, Marchand S, van den Berg D, van der Sandt I, de Boer AG, Delon A, Bouquet S, Couet W (2000) In vitro and in vivo investigations on fluoroquinolones; effects of the P-glycoprotein efflux transporter on brain distribution of sparfloxacin. *Eur.J.Pharm.Sci.* **12**: 85-93

de Lange EC, de Boer AG, Breimer DD (1999b) Microdialysis for pharmacokinetic analysis of drug transport to the brain. *Advanced Drug Delivery Reviews* **36**: 211-227

Desrayaud S, de Lange EC, Lemaire M, Bruelisauer A, de Boer AG, Breimer DD (1998) Effect of the Mdr1a P-glycoprotein gene disruption on the tissue distribution of SDZ PSC 833, a multidrug resistance-reversing agent, in mice. *J.Pharmacol Exp.Ther* **285**: 438-443

Dingemanse J, Sollie FA, Breimer DD, Danhof M (1988) Pharmacokinetic modeling of the anticonvulsant response of oxazepam in rats using the pentylenetetrazol threshold concentration as pharmacodynamic measure. *J.Pharmacokinet.Biopharm.* **16**: 203-228

Ebling WF, Danhof M, Stanski DR (1991) Pharmacodynamic characterization of the electroencephalographic effects of thiopental in rats. *J.Pharmacokinet.Biopharm.* **19**: 123-143

Fath MJ, Kolter R (1993) ABC transporters: bacterial exporters. *Microbiol.Rev.* **57**: 995-1017

Faulkner HJ, Traub RD, Whittington MA (1999) Anaesthetic/amnesic agents disrupt beta frequency oscillations associated with potentiation of excitatory synaptic potentials in the rat hippocampal slice. *Br.J.Pharmacol* **128**: 1813-1825

Furchgott RF (1966) The use of beta-haloalkylamines in the differentiation of receptors and in the determination of dissociation constants of receptor agonist complexes. in *Advances in Drug Research* NJ Harper & AB Simmonds, eds., Academic Press, New York, 21-55

Garrido M, Gubbens-Stibbe J, Tukker E, Cox E, von Frijtag Drabbe Kunzel J, IJzerman A, Danhof M, van der Graaf PH (2000) Pharmacokinetic-pharmacodynamic analysis of the EEG effect of alfentanil in rats following beta-funaltrexamine-induced mu-opioid receptor “knockdown” in vivo. *Pharm.Res.* **17**: 653-659

Geldof M, Freijer J, van Beijsterveldt L, Danhof M (2007) Physiological pharmacokinetic modeling of non-linear brain distribution of fluvoxamine in the rat. *in press*

Golden PL, Pollack GM (1998) Rationale for influx enhancement versus efflux blockade to increase drug exposure to the brain. *Biopharm.Drug Dispos.* **19**: 263-272

Golden PL, Pollack GM (2003) Blood-brain barrier efflux transport. *J.Pharm.Sci.* **92**: 1739-1753

Gross PM, Sposito NM, Pettersen SE, Fenstermacher JD (1986) Differences in function and structure of the capillary endothelium in gray matter, white matter and a circumventricular organ of rat brain. *Blood Vessels* **23**: 261-270

Henthorn TK, Liu Y, Mahapatro M, Ng KY (1999) Active transport of fentanyl by the blood-brain barrier. *J.Pharmacol. Exp.Ther.* **289**: 1084-1089

Hill AV (1910) The possible effects of the aggregation of the molecules of haemoglobin on its dissociation curve. *J.Physiol.Lond.* **40**.

Holford NH, Sheiner LB (1982) Kinetics of pharmacologic response. *Pharmacol Ther* **16**: 143-166

Hyafil F, Vergely C, Du VP, Grand-Perret T (1993) In vitro and in vivo reversal of multidrug resistance by GF120918, an acridonecarboxamide derivative. *Cancer Res.* **53**: 4595-4602

Jusko WJ, Ko HC (1994) Physiologic indirect response models characterize diverse types of pharmacodynamic effects. *Clin Pharmacol Ther* **56**: 406-419

Karssen AM, Meijer OC, van der Sandt I, Lucassen PJ, de Lange EC, de Boer AG, de Kloet ER (2001) Multidrug resistance P-glycoprotein hampers the access of cortisol but not of corticosterone to mouse and human brain. *Endocrinology* **142**: 2686-2694

Kim RB, Fromm MF, Wandel C, Leake B, Wood AJ, Roden DM, Wilkinson GR (1998) The drug transporter P-glycoprotein limits oral absorption and brain entry of HIV-1 protease inhibitors. *J.Clin Invest* **101**: 289-294

Lee G, Dallas S, Hong M, Bendayan R (2001) Drug transporters in the central nervous system: brain barriers and brain parenchyma considerations. *Pharmacol.Rev.* **53**: 569-596

Letrent SP, Pollack GM, Brouwer KR, Brouwer KL (1998) Effect of GF120918, a potent P-glycoprotein inhibitor, on morphine pharmacokinetics and pharmacodynamics in the rat. *Pharm.Res.* **15**: 599-605

Letrent SP, Pollack GM, Brouwer KR, Brouwer KL (1999a) Effects of a potent and specific P-glycoprotein inhibitor on the blood- brain barrier distribution and antinociceptive effect of morphine in the rat. *Drug Metab Dispos.* **27**: 827-834

Letrent SP, Polli JW, Humphreys JE, Pollack GM, Brouwer KR, Brouwer KL (1999b) P-glycoprotein-mediated transport of morphine in brain capillary endothelial cells. *Biochem.Pharmacol.* **58**: 951-957

Liu X, Smith BJ, Chen C, Callegari E, Becker SL, Chen X, Cianfrogna J, Doran AC, Doran SD, Gibbs JP, Hosea N, Liu J, Nelson FR, Szewc MA, Van Deusen J (2005) Use of a physiologically based pharmacokinetic model to study the time to reach brain equilibrium: an experimental analysis of the role of blood-brain barrier permeability, plasma protein binding, and brain tissue binding. *J.Pharmacol.Exp.Ther.* **313**: 1254-1262

Mahar Doan KM, Humphreys JE, Webster LO, Wring SA, Shampine LJ, Serabjit-Singh CJ, Adkison KK, Polli JW (2002) Passive permeability and P-glycoprotein-mediated efflux differentiate central nervous system (CNS) and non-CNS marketed drugs. *J.Pharmacol.Exp.Ther.* **303**: 1029-1037

Mandema JW, Danhof M (1990) Pharmacokinetic-pharmacodynamic modeling of the central nervous system effects of heptabarbital using aperiodic EEG analysis. *J.Pharmacokinet.Biopharm.* **18**: 459-481

Mandema JW, Heijligers-Feijen CD, Tukker E, de Boer AG, Danhof M (1992a) Modeling of the effect site equilibration kinetics and pharmacodynamics of racemic baclofen and its enantiomers using quantitative EEG effect measures. *J.Pharmacol Exp.Ther* **261**: 88-95

Mandema JW, Sansom LN, Dios-Vieitez MC, Hollander-Jansen M, Danhof M (1991a) Pharmacokinetic-pharmacodynamic modeling of the electroencephalographic effects of benzodiazepines. Correlation with receptor binding and anticonvulsant activity. *J.Pharmacol Exp.Ther* **257**: 472-478

Mandema JW, Tuk B, van Steveninck AL, Breimer DD, Cohen AF, Danhof M (1992b) Pharmacokinetic-pharmacodynamic modeling of the central nervous system effects of midazolam and its main metabolite alpha-hydroxymidazolam in healthy volunteers. *Clin Pharmacol Ther* **51**: 715-728

Mandema JW, Tukker E, Danhof M (1991b) Pharmacokinetic-pharmacodynamic modelling of the EEG effects of midazolam in individual rats: influence of rate and route of administration. *Br.J.Pharmacol* **102**: 663-668

Mandema JW, Veng-Pedersen P, Danhof M (1991c) Estimation of amobarbital plasma-effect site equilibration kinetics. Relevance of polyexponential conductance functions. *J.Pharmacokinet.Biopharm.* **19**: 617-634

Mandema JW, Wada DR (1995) Pharmacodynamic model for acute tolerance development to the electroencephalographic effects of alfentanil in the rat. *J.Pharmacol.Exp.Ther.* **275**: 1185-1194

Mayer U, Wagenaar E, Dorobek B, Beijnen JH, Borst P, Schinkel AH (1997) Full blockade of intestinal P-glycoprotein and extensive inhibition of blood-brain barrier P-glycoprotein by oral treatment of mice with PSC833. *J.Clin.Invest* **100**: 2430-2436

Meijer OC, de Lange EC, Breimer DD, de Boer AG, Workel JO, de Kloet ER (1998) Penetration of dexamethasone into brain glucocorticoid targets is enhanced in mdr1A P-glycoprotein knockout mice. *Endocrinology* **139**: 1789-1793

Olson RJ, Justice JB, Jr. (1993) Quantitative microdialysis under transient conditions. *Anal.Chem.* **65**: 1017-1022

Pardridge WM (1991) *Peptide drug delivery to the brain* Raven Press, New York.

Pigeon RP, Silver RP (1994) Topological and mutational analysis of KpsM, the hydrophobic component of the ABC-transporter involved in the export of polysialic acid in Escherichia coli K1. *Mol.Microbiol.* **14:** 871-881

Rowland M, Balant L, Peck C (2004) Physiologically based pharmacokinetics in drug development and regulatory science: a workshop report (Georgetown University, Washington, DC, May 29-30, 2002). *AAPS.PharmSci.* **6**: E6

Rubin LL, Staddon JM (1999) The cell biology of the blood-brain barrier. *Annu.Rev.Neurosci.* **22**: 11-28

Schaddelee MP, Groenendaal D, DeJongh J, Cleypool CG, IJzerman AP, de Boer AG, Danhof M (2004) Population pharmacokinetic modeling of blood-brain barrier transport of synthetic adenosine A1 receptor agonists. *J Pharmacol Exp.Ther.* **311**: 1138-1146

Schinkel AH, Smit JJ, van Tellingen O, Beijnen JH, Wagenaar E, van Deemter L, Mol CA, van der Valk MA, Robanus-Maandag EC, te Riele HP, Berns AJM, Borst, P (1994) Disruption of the mouse mdr1a P-glycoprotein gene leads to a deficiency in the blood-brain barrier and to increased sensitivity to drugs. *Cell* **77**: 491-502

Schinkel AH, Wagenaar E, Mol CA, van Deemter L (1996) P-glycoprotein in the blood-brain barrier of mice influences the brain penetration and pharmacological activity of many drugs. *J.Clin.Invest* **97**: 2517-2524

Schinkel AH, Wagenaar E, van Deemter L, Mol CA, Borst P (1995) Absence of the mdr1a P-Glycoprotein in mice affects tissue distribution and pharmacokinetics of dexamethasone, digoxin, and cyclosporin A. *J.Clin.Invest* **96**: 1698-1705

Scott JC, Ponganis KV, Stanski DR (1985) EEG quantitation of narcotic effect: the comparative pharmacodynamics of fentanyl and alfentanil. *Anesthesiology* **62**: 234-241

Segre G (1968) Kinetics of interaction between drugs and biological systems. *Farmaco [Sci.]* **23**: 907-918

Sheiner LB, Stanski DR, Vozeh S, Miller RD, Ham J (1979) Simultaneous modeling of pharmacokinetics and pharmacodynamics: application to d-tubocurarine. *Clin Pharmacol Ther* **25**: 358-371

Stephenson RP (1956) A modification of receptor theory. *Br.J.Pharmacol Chemother.* **11**: 379-393

Thiebaut F, Tsuruo T, Hamada H, Gottesman MM, Pastan I, Willingham MC (1987) Cellular localization of the multidrug-resistance gene product P-glycoprotein in normal human tissues. *Proc.Natl.Acad.Sci U.S.A.* **84**: 7735-7738

Tuk B, van Gool T, Danhof M (2003) Mechanism-based pharmacodynamic modeling of the interaction of midazolam, bretazenil, and zolpidem with ethanol. *J Pharmacokinet Pharmacodyn* **29**: 235-250

Tuk B, van Oostenbruggen MF, Herben VM, Mandema JW, Danhof M (1999) Characterization of the pharmacodynamic interaction between parent drug and active metabolite in vivo: midazolam and alpha-OH-midazolam. *J.Pharmacol Exp.Ther* **289**: 1067-1074

Tunblad K, Jonsson EN, Hammarlund-Udenaes M (2004) Morphine blood-brain barrier transport is influenced by probenecid co-administration. *Pharm Res* **20**: 618-623

Uhr M, Steckler T, Yassouridis A, Holsboer F (2000) Penetration of amitriptyline, but not of fluoxetine, into brain is enhanced in mice with blood-brain barrier deficiency due to mdr1a P-glycoprotein gene disruption. *Neuropsychopharmacology* **22**: 380-387

Upton RN, Ludbrook GL, Grant C, Doolette DJ (2000) The effect of altered cerebral blood flow on the cerebral kinetics of thiopental and propofol in sheep. *Anesthesiology* **93**: 1085-1094

van Bree JB, de Boer AG, Danhof M, Ginsel LA, Breimer DD (1988) Characterization of an “in vitro” blood-brain barrier: effects of molecular size and lipophilicity on cerebrovascular endothelial transport rates of drugs. J *Pharmacol Exp.Ther.* **247**: 1233-1239

van der Graaf PH, Danhof M (1997) Analysis of drug-receptor interactions in vivo: a new approach in pharmacokinetic-pharmacodynamic modelling. *Int.J Clin.Pharmacol.Ther.* **35**: 442-446

van der Graaf PH, Van Schaick EA, Mathot RA, IJzerman AP, Danhof M (1997) Mechanism-based pharmacokinetic-pharmacodynamic modeling of the effects of N6-cyclopentyladenosine analogs on heart rate in rat: estimation of in vivo operational affinity and efficacy at adenosine A1 receptors *J.Pharmacol.Exp.Ther.* **283**: 809-816

van der Sandt I, Smolders R, Nabulsi L, Zuideveld KP, de Boer AG, Breimer DD (2001a) Active efflux of the 5-HT(1A) receptor agonist flesinoxan via P-glycoprotein at the blood-brain barrier. *Eur.J.Pharm.Sci.* **14**: 81-86

van der Sandt I, Vos CM, Nabulsi L, Blom-Roosemalen MC, Voorwinden HH, de Boer AG, Breimer DD (2001b) Assessment of active transport of HIV protease inhibitors in various cell lines and the in vitro blood--brain barrier. *AIDS* **15**: 483-491

Visser SA (2003) *Mechanism-based pharmacokinetic-pharmacodynamic modeling of the GABA-A receptor response in vivo*, Leiden Amsterdam Center for Drug Research.

Visser SA, Gladdines WW, van der Graaf PH, Peletier LA, Danhof M (2002a) Neuroactive steroids differ in potency but not in intrinsic efficacy at the GABA(A) receptor in vivo. *J.Pharmacol Exp.Ther* **303**: 616-626

Visser SA, Smulders CJ, Reijers BP, van der Graaf PH, Peletier LA, Danhof M (2002b) Mechanism-based pharmacokinetic-pharmacodynamic modeling of concentration-dependent hysteresis and biphasic electroencephalogram effects of alphaxalone in rats. *J.Pharmacol Exp.Ther* **302**: 1158-1167

Visser SA, Wolters FL, Gubbens-Stibbe JM, Tukker E, van der Graaf PH, Peletier LA, Danhof M (2001) Mechanism-based pharmacokinetic/pharmacodynamic modeling of the electroencephalogram effects of GABAA receptor modulators: in vitro-in vivo correlations. *J Pharmacol Exp Ther* **304**: 88-101

Walker MC, Tong X, Perry H, Alavijeh MS, Patsalos PN (2000) Comparison of serum, cerebrospinal fluid and brain extracellular fluid pharmacokinetics of lamotrigine. *Br.J.Pharmacol* **130**: 242-248

Wandel C, Kim R, Wood M, Wood A (2002) Interaction of morphine, fentanyl, sufentanil, alfentanil, and loperamide with the efflux drug transporter P-glycoprotein. *Anesthesiology* **96**: 913-920

Wang Y, Welty DF (1996) The simultaneous estimation of the influx and efflux blood-brain barrier permeabilities of gabapentin using a microdialysis-pharmacokinetic approach. *Pharm.Res.* **13**: 398-403

Wauquier A, Bovill JG, Sebel PS (1984) Electroencephalographic effects of fentanyl-, sufentanil- and alfentanil anaesthesia in man. *Neuropsychobiology* **11**: 203-206

Wauquier A, De Ryck M, Van den Broeck W, Van Loon J, Melis W, Janssen P (1988) Relationships between quantitative EEG measures and pharmacodynamics of alfentanil in dogs. *Electroencephalogr.Clin Neurophysiol.* **69**: 550-560

Welty DF, Schielke GP, Vartanian MG, Taylor CP (1993) Gabapentin anticonvulsant action in rats: disequilibrium with peak drug concentrations in plasma and brain microdialysate. *Epilepsy Res.* **16**: 175-181

Wong SL, Van Belle K, Sawchuk RJ (1993) Distributional transport kinetics of zidovudine between plasma and brain extracellular fluid/cerebrospinal fluid in the rabbit: investigation of the inhibitory effect of probenecid utilizing microdialysis. *J.Pharmacol Exp.Ther* **264**: 899-909

Xie R, Bouw MR, Hammarlund-Udenaes M (2000) Modelling of the blood-brain barrier transport of morphine-3-glucuronide studied using microdialysis in the rat: involvement of probenecid-sensitive transport. *Br.J.Pharmacol* **131**: 1784-1792

Xie R, Hammarlund-Udenaes M (1998) Blood-brain barrier equilibration of codeine in rats studied with microdialysis. *Pharm.Res.* **15**: 570-575

Young GA, Khazan N (1984) Differential neuropharmacological effects of mu, kappa and sigma opioid agonists on cortical EEG power spectra in the rat. Stereospecificity and naloxone antagonism. *Neuropharmacology* **23**: 1161-1165

Zuideveld KP, Maas HJ, Treijtel N, Hulshof J, van der Graaf PH, Peletier LA, Danhof M (2001) A set-point model with oscillatory behavior predicts the time course of 8-OH-DPAT-induced hypothermia. *Am.J.Physiol Regul.Integr. Comp Physiol* **281**: R2059-R2071

Zuideveld KP, van der Graaf PH, Newgreen D, Thurlow R, Petty N, Jordan P, Peletier LA, Danhof M (2004) Mechanism-based pharmacokinetic-pharmacodynamic modeling of 5-HT1A receptor agonists: estimation of in vivo affinity and intrinsic efficacy on body temperature in rats *J.Pharmacol Exp.Ther* **308**: 1012-1020

Chapter 2

SCOPE AND OUTLINE OF INVESTIGATIONS

1. GENERAL OBJECTIVES AND BACKGROUND

The objective of the research described in this thesis was the development of a mechanism-based pharmacokinetic-pharmacodynamic (PK-PD) model for the electro-encephalogram (EEG) effects of opioids. The central effects of opioids are determined by four main processes: (1) blood/plasma pharmacokinetics, (2) biophase distribution, which is mainly determined by blood-brain barrier (BBB) transport, (3) receptor interaction kinetics and (4) signal transduction. Under the assumption that within a single species the signal transduction mechanisms are equal for all opioids, the focus of this thesis was to characterise the role of biophase distribution and receptor interaction kinetics on the pharmacokinetic-pharmacodynamic (PK-PD) relationships of opioids.

In the investigations described in this thesis, a panel of opioids with a wide range of pharmacological and physicochemical properties was used. These drugs were specifically selected because of their (partial) agonistic properties at the μ-opioid receptor. The change in the delta frequency band (0.5-4.5 Hz) of the EEG was used as a pharmacodynamic endpoint because it is a sensitive and continuous measure of the central effects of opioids (Dingemanse *et al.* 1988). Previously, the EEG effects of the opioids alfentanil, fentanyl and sufentanil have been investigated. In these investigations, PK-PD analysis was performed with the effect compartment model, to account for hysteresis between the blood concentration and effect. This analysis showed that these opioids all behaved as high efficacy agonists albeit that differences in potency and hysteresis were observed (Cox *et al.* 1998).
To identify a mechanism-based PK-PD model, morphine, nalbuphine and butorphanol were included as model drugs. Morphine is the classical agonist of the μ-opioid receptor (Dhawan *et al.* 1996) and its biophase distribution is known to be complex, because of the interaction with the efflux transporters at the BBB, such as P-glycoprotein (Pgp) at the BBB (Henthorn *et al.* 1999; Letrent *et al.* 1998; 1999a;. 1999b; Mahar Doan *et al.* 2002; Schinkel *et al.* 1995; 1996). Nalbuphine and butorphanol are structurally related to morphine and have previously been identified as partial agonists *in vivo* (Emmerson *et al.* 1996). Nalbuphine was identified as a Pgp substrate *in vitro* (Mahar Doan *et al.*, 2002). So far little is known about the biophase distribution kinetics of nalbuphine and butorphanol.

2. CHARACTERISATION OF THE ROLE OF BIOPHASE DISTRIBUTION

The main objective of the research described in *section 2* was the characterisation of the role of biophase distribution in the PK-PD relationships of the selected opioids. Restricted transport across the BBB can be a critical factor in the PK-PD relationships of opioids. Apart from restricted paracellular diffusion by the presence of tight junctions between the endothelial cells of the BBB, active transport mechanisms may play an

important role, especially for Pgp-mediated efflux.

For the investigation of the PK-PD relationships of morphine, butorphanol and nalbuphine and the characterisation of BBB transport of morphine, first a sensitive HPLC method was developed to analyse blood and brain microdialysate concentrations. The method consisted of a liquid-liquid extraction with ethyl acetate of the blood samples followed by injection on an HPLC system coupled to electrochemical detection. The development and validation of this method is discussed in **chapter 3**. The microdialysate samples were injected without sample pre-treatment. The sample pre-treatment of blood samples was dependent on the compound. For morphine, an alkaline extraction was sufficient whereas for nalbuphine and butorphanol both and acidic and alkaline extraction were required. The mobile phase was a mixture of 0.1 M sodium phosphate buffer, methanol and octane-sulfonic acid with ratio and pH depending on compound and matrix. The limits of quantification in blood samples were 25, 50 and 25 ng/mL for nalbuphine, butorphanol and morphine, respectively and 0.5 ng/mL for morphine in microdialysate samples. Based on sample volume, sensitivity and reproducibility, these assays proved to be suitable for PK-PD studies.

Next, the membrane transport characteristics of opioids were investigated *in vitro*. The focus was on the relative contribution of passive permeability and Pgp-mediated efflux. The studies were conducted in an *in vitro* cell system using monolayers of either the MDCK:MDR1 cells, which were transfected with the MDR1 gene encoding for human P-glycoprotein (Pgp), or LLC-PK1:MDR1a cells, which were transfected with the MDR1a gene encoding for rodent Pgp (**chapter 4**). The interaction of the opioids with Pgp was determined a) indirectly by investigating the inhibition of Pgp-mediated efflux of ^{3}H-digoxin and b) directly by a substrate assessment study. In the latter study, the transport of opioids in the presence and absence of the potent and specific Pgp inhibitor GF120918 (Hyafil *et al*. 1993) was determined. The passive permeability, as reflected by the Papp, of the different opioids was determined in the presence of GF120918. In addition, regression analysis was performed to investigate the relationships between the physico-chemical properties and the P_{app} values. These studies have shown that the influence of Pgp on membrane transport is highly dependent on the passive permeability. Alfentanil, fentanyl and sufentanil have affinity for Pgp but the contribution of Pgp mediated transport to the overall transport rate is minimal because of the high passive permeability rates (>500 nm/sec). In contrast, Pgp has a significant influence on the transport of morphine, presumably because the passive permeability is very low (16 nm/sec).

For morphine, the role of biophase distribution kinetics in the PK-PD correlation was investigated using a novel combined EEG/microdialysis technique that allows simultaneous characterisation of both the brain extracellular fluid (ECF) concentration

and the EEG effect. In these investigations a wide dose range was investigated (4 to 40 mg/kg). The influence of Pgp was investigated by co-infusion of GF120918.

In **chapter 5**, the relative contributions of passive and active transport mechanisms of morphine across the BBB *in vivo* were determined in a quantitative manner upon intravenous administration of two distinct doses of morphine, 4 and 40 mg/kg. Complex brain distribution kinetics was observed in these investigations. Specifically, analysis of the brain microdialysate concentrations showed non-linear distribution kinetics in brain ECF with increasing dose and a distinct effect of Pgp inhibition by GF120918. To describe the complex brain distribution kinetics, a one compartment brain distribution model was developed, with separate expressions for passive diffusion, active saturable influx and active efflux. This active efflux component could be partly reduced by co-infusion with GF120918.

The focus of **chapter 6** was on the influence of biophase distribution and Pgp interaction on the EEG effects of morphine and to compare the biophase distribution kinetics for the EEG with the kinetics of morphine distribution to the brain ECF. Profound hysteresis was observed between blood concentrations and EEG effect. To describe the biophase distribution kinetics of morphine, an extended-catenary biophase distribution model was proposed. This model consists of two sequential compartments (a transfer and an effect compartment) and two rate constants; the k_{1e} which describes the transport through the transfer compartment and the keo, which describes the loss from the effect compartment. Co-infusion of GF120918 only influenced the k_{eo} and different values were found for k_{1e} and k_{eo}. The observation that GF120918 affects the efflux of morphine is consistent with the observations on the distribution in brain ECF. The predicted morphine biophase concentration-time profiles, however were distinctly different from the brain ECF concentration-time profiles as estimated by intracerebral microdialysis.

3. PHARMACOKINETIC-PHARMACODYNAMIC MODELLING OF THE EEG EFFECTS OF OPIOIDS

In *section 3* the PK-PD relationships of the whole set of opioids were evaluated on the basis of model discrimination. For the biophase distribution kinetics, two different models were investigated for each opioid (**chapter 7**): (1) the one-compartment biophase distribution model and (2) the extended-catenary biophase distribution model as proposed for morphine in chapter 6. Both symmetrical and a-symmetrical transport to the biophase was investigated. It was shown that only morphine displays complex biophase distribution kinetics, since the biophase distribution of the other opioids were best described with the one-compartment distribution model. Interestingly, a statistically significant correlation was observed between the values of k_{1e} and the *in vitro* passive permeability. It could be concluded that the relative contribution of passive

permeability and the interaction with transporters determines the complex biophase distribution of opioids.

In addition, the link between the *in vivo* concentration effect-relationships and the interaction at the μ-opioid receptor was investigated (**chapter 8**). The predicted biophase concentrations were used to analyse the concentration-effect relationships simultaneously with the empirical E_{max} model. Further analysis of the pharmacodynamic data was performed on the basis of the operational model of agonism as proposed by Black and Leff (1983) with the values of the system maximum E_m (123 μV) and n (1.44) constrained to the values of alfentanil which displayed the highest intrinsic activity. Between the opioids, wide differences in both *in vivo* affinity and intrinsic efficacy were observed. When the estimated *in vivo* pK_A values were correlated with the *in vitro* pK_i values, indications for two distinct subpopulations were obtained. In addition, a poor correlation was observed between the *in vitro* Na/GTP-shift and the *in vivo* log τ. These observations might be explained by 1) the involvement of active transport processes in distribution from blood to brain, 2) the existence of μ-opioid receptor subtypes and 3) the interaction with other types of opioid receptors.

4. SUMMARY, CONCLUSIONS AND PERSPECTIVES

To conclude this thesis, in *section 4* (**chapter 9**) the results of the separate studies are reviewed and discussed and perspectives for future research are presented.

5. REFERENCES

Black JW, Leff P (1983) Operational models of pharmacological agonism. *Proc.R.Soc.Lond B Biol.Sci.* **220**: 141-162

Cox EH, Kerbusch T, van der Graaf PH, Danhof M (1998) Pharmacokinetic-pharmacodynamic modeling of the electroencephalogram effect of synthetic opioids in the rat: correlation with the interaction at the mu-opioid receptor. *J Pharmacol.Exp.Ther.* **284**: 1095-1103

Dhawan BN, Cesselin F, Raghubir R, Reisine T, Bradley PB, Portoghese PS, Hamon M (1996) International Union of Pharmacology. XII. Classification of opioid receptors. *Pharmacol.Rev.* **48**: 567-592

Dingemanse J, Sollie FA, Breimer DD, Danhof M (1988) Pharmacokinetic modeling of the anticonvulsant response of oxazepam in rats using the pentylenetetrazol threshold concentration as pharmacodynamic measure. *J.Pharmacokinet.Biopharm.* **16**: 203-228

Emmerson PJ, Clark MJ, Mansour A, Akil H, Woods JH, Medzihradsky F (1996) Characterization of opioid agonist efficacy in a C6 glioma cell line expressing the mu opioid receptor. *J.Pharmacol.Exp.Ther.* **278**: 1121-1127

Henthorn TK, Liu Y, Mahapatro M, Ng KY (1999) Active transport of fentanyl by the blood-brain barrier. *J.Pharmacol. Exp.Ther.* **289**: 1084-1089

Hyafil F, Vergely C, Du VP, Grand-Perret T (1993) In vitro and in vivo reversal of multidrug resistance by GF120918, an acridonecarboxamide derivative. *Cancer Res.* **53**: 4595-4602

Letrent SP, Pollack GM, Brouwer KR, Brouwer KL (1998) Effect of GF120918, a potent P-glycoprotein inhibitor, on morphine pharmacokinetics and pharmacodynamics in the rat. *Pharm.Res.* **15**: 599-605

Letrent SP, Pollack GM, Brouwer KR, Brouwer KL (1999a) Effects of a potent and specific P-glycoprotein inhibitor on the blood- brain barrier distribution and antinociceptive effect of morphine in the rat. *Drug Metab Dispos.* **27**: 827-834

Letrent SP, Polli JW, Humphreys JE, Pollack GM, Brouwer KR, Brouwer KL (1999b) P-glycoprotein-mediated transport of morphine in brain capillary endothelial cells. *Biochem.Pharmacol.* **58**: 951-957

Mahar Doan KM, Humphreys JE, Webster LO, Wring SA, Shampine LJ, Serabjit-Singh CJ, Adkison KK, Polli JW (2002) Passive permeability and P-glycoprotein-mediated efflux differentiate central nervous system (CNS) and non-CNS marketed drugs. *J.Pharmacol.Exp.Ther.* **303**: 1029-1037

Schinkel AH, Wagenaar E, Mol CA, van Deemter L (1996) P-glycoprotein in the blood-brain barrier of mice influences the brain penetration and pharmacological activity of many drugs. *J.Clin.Invest* **97**: 2517-2524

Schinkel AH, Wagenaar E, van Deemter L, Mol CA, Borst P (1995) Absence of the mdr1a P-Glycoprotein in mice affects tissue distribution and pharmacokinetics of dexamethasone, digoxin, and cyclosporin *A. J.Clin.Invest* **96**: 1698-1705

Section 2

CHARACTERISATION OF THE ROLE OF BIOPHASE DISTRIBUTION

Chapter 3

HIGH-PERFORMANCE LIQUID CHROMATOGRAPHY OF NALBUPHINE, BUTORPHANOL AND MORPHINE IN BLOOD AND BRAIN MICRODIALYSATE SAMPLES: APPLICATION TO PHARMACOKINETIC-PHARMACODYNAMIC STUDIES IN RATS

Dorien Groenendaal, Margret C.M. Blom-Roosemalen, Meindert Danhof and Elizabeth C.M. de Lange

Division of Pharmacology, Leiden/Amsterdam Center for Drug Research, Leiden University, Leiden, the Netherlands

Published in the Journal of Chromatography B (2005) **822**, 230-237

ABSTRACT

A rapid and sensitive assay for quantification of nalbuphine, butorphanol and morphine in blood (50µl) and brain microdialysate (~40µl) samples was developed. Blood samples were extracted with ethyl acetate. Analysis was performed with high performance liquid chromatography coupled to an electrochemical detector. The mobile phase was a mixture of 0.1M sodium phosphate buffer, methanol and octane-sulfonic acid with ratio and pH depending on compound and matrix. The limits of quantification in blood samples were 25, 50 and 25 ng/ml for nalbuphine, butorphanol and morphine, respectively and 0.5 ng/ml for morphine in microdialysate samples. Based on sample volume, sensitivity and reproducibility, these assays are particularly suitable for pharmacokinetic-pharmacodynamic studies in rodents.

INTRODUCTION

Opioids are widely used in clinical anaesthesia, analgesia and treatment of drug abuse. For example, the natural opioid morphine, the semi-synthetic nalbuphine and the synthetic butorphanol are used in analgesia, whereas the synthetic opioids alfentanil, fentanyl, sufentanil and remifentanil have been developed for use in anaesthesia. However, optimal dosing for these drugs is difficult, due to the development of tolerance, risk of addiction and side effects like respiratory depression.

At present there is a considerable interest in the development of μ-opioid receptor partial agonists, since these compounds in theory have a much-improved selectivity of action. A mechanism-based pharmacokinetic-pharmacodynamic (PK-PD) approach can provide insight into factors that determine pharmacodynamic behaviour of μ-opioid receptor agonists *in vivo* by distinction between drug and biological system characteristics (van der Graaf & Danhof 1997). Recently, the effects of the opioids alfentanil, fentanyl and sufentanil have been studied *in vivo* in a chronically instrumented rat model, using the amplitude in the 0.5-4.5 Hz frequency band of the electroencephalogram (EEG) as a pharmacodynamic endpoint (Cox *et al.* 1998). On the basis of mechanism-based PK-PD analysis, it was shown that these opioids all behave as full agonists *in vivo*. Subsequently, the model has been successfully applied to characterise the *in vivo* pharmacodynamic properties of the novel synthetic opioid remifentanil and its active metabolite GR90291 (Cox *et al.* 1999), showing that they also behave as full agonists at the μ-opioid receptor. Current research on the PK-PD correlations of opioids focuses on nalbuphine, butorphanol and morphine (figure 1).

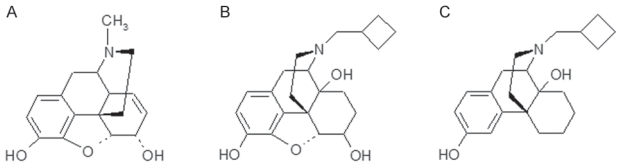

Figure 1: Chemical structures of the opioids morphine (A), nalbuphine (B) and butorphanol (C)

Nalbuphine and butorphanol were selected because they behave as partial agonists at the μ-opioid receptor (Cherny 1996; Emmerson *et al.* 1996; Garner *et al.* 1997; Pallasch & Gill 1985). An important feature of morphine is that blood-brain barrier (BBB) transport is a major determinant of its *in vivo* effect (Bouw *et al.* 2000).

To be able to study the PK-PD correlations of nalbuphine, butorphanol and morphine in the rat EEG model a convenient, rapid and sensitive analytical assay should be developed for the analysis of concentrations in small blood samples. In addition, for morphine the free concentrations in brain microdialysate should be obtained to get insight into the BBB transport, but because of the small sample volume and the low concentrations a highly sensitive HPLC method is required (Benveniste & Huttemeier 1990; Bouw *et al.* 2000; de Lange *et al.* 1999).

Several methods of analysis have been reported for nalbuphine, butorphanol and morphine. These methods include radio-immunoassay and HPLC combined with electrochemical, ultraviolet or fluorescence detection (Pittman *et al.* 1980; Willey *et al.* 1994). More recently, analysis methods with gas chromatography and liquid chromatography coupled to mass-spectrometric detection have been developed (Grinstead 1991; Kanazawa *et al.* 1998; Volk *et al.* 1996). These methods are exceptionally robust and sensitive, but the access to the instrumentation is often limited.
For the analysis of nalbuphine, the published reports focus on HPLC with electrochemical detection (Aitkenhead *et al.* 1988; Nicolle *et al.* 1995; 1997), but these methods require relatively large sample volumes (500 µl). In addition, for analysis of morphine and its metabolites often HPLC analysis with electrochemical and fluorescence detection is described for detection of morphine, the metabolite morphine-6-glucoride (M6G) and morphine-3-glucoronide (M3G), respectively (Drost *et al.* 1984; Joel *et al.* 2002; Liaw *et al.* 1998; Svensson 1986). However, for most assays relatively large plasma volumes are required (1 ml) which precludes application in pre-clinical animal investigations. Therefore, a rapid and highly sensitive HPLC assay was developed which requires only small blood samples (50 – 200 µl) to quantify nalbuphine, butorphanol, morphine. This assay was also able to quantify morphine concentrations in microdialysate samples (20 – 60 µl).

EXPERIMENTAL

Materials

Morphine hydrochloride was purchased from Pharmachemie (Haarlem, The Netherlands), nalbuphine hydrochloride and nalorphine hydrochloride were purchased from Sigma Aldrich (Zwijndrecht, The Netherlands) and butorphanol tartrate was purchased from Sigma Aldrich (St. Louis, MI, USA). Millipore water (resistivity 18.2 MΩ.cm) was obtained from a Milli-Q® PF Plus system (Millipore B.V., Amsterdam, The Netherlands). Methanol (HPLC grade) was obtained from Biosolve BV (Valkenswaard, The Netherlands). Ethyl acetate was purchased from Fischer Scientific ('s Hertogenbosch, The Netherlands) and distilled prior to use. All other chemicals were of analytical grade (Baker, Deventer, The Netherlands).

General instrumentation

The HPLC system consisted of an LC-10AD HPLC pump (Shimadzu, 's Hertogenbosch, The Netherlands), a Waters 717 plus autosampler (Waters, Etten-Leur, The Netherlands), a pulse damper (Antec Leyden, Zoeterwoude, The Netherlands) and a digital electrochemical amperometric detector (DECADE, software version 3.02, Antec Leyden, The Netherlands). The electrochemical detector consisted of a VT-03 electrochemical flow cell combined with a 25 µm spacer and an *in situ* Ag/AgCl (ISAAC) reference

electrode operating in the DC mode. For morphine analysis, a standard Ag/AgCl reference electrode, filled with a saturated KCl solution was used. Data acquisition and processing was performed using the Empower® data-acquisition software (Waters, Etten-Leur, The Netherlands).

Extraction procedure for blood samples

For determination of nalbuphine and butorphanol blood concentrations, 50 µl of internal standard solution (butorphanol for nalbuphine analysis and vice versa) was added to hemolysed blood samples (50 – 200 µl blood + 400 µl Millipore water) in glass centrifuge tubes. Next, 500 µl of 1.7 mM phosphoric acid (pH 2.3) and 3 ml of ethyl acetate were added and the mixture was vortexed for 5 min. After centrifugation for 10 min at 4000 rpm, the organic layer was discarded and 500 µl of a 0.15 M carbonate buffer (pH 11) supplemented with EDTA (2.7 mM) was added. Next, 5 ml of ethyl acetate was added and the mixture was vortexed for 5 min. After centrifugation (10 min at 4000 rpm), the organic layer was transferred into a clean glass tube and evaporated to dryness under reduced pressure on a vacuum vortex evaporator (Buchler Instruments, Fort Lee, NJ, USA) at 37°C. The residue was dissolved in 100 µl mobile phase of which 10 – 75 µl was injected into the HPLC system.

For determination of morphine blood concentrations, 50 µl of internal standard solution (nalorphine) was added to hemolysed blood samples (50 – 200 µl blood + 400 µl Millipore water) in glass centrifuge tubes. Next 500 µl 0.15 M carbonate buffer (pH 11) supplemented with EDTA (2.7 mM) and 5 ml of ethyl acetate was added and the mixture was vortexed for 5 min. After centrifugation (10 min at 4000 rpm), the organic layer was transferred into a clean tube and evaporated to dryness under reduced pressure on a vacuum vortex evaporator at 37°C. The residue was dissolved in 100 µl mobile phase of which 10 – 75 µl was injected into the HPLC system.

Analysis of nalbuphine, butorphanol and morphine concentrations in blood samples

Chromatography of blood samples was performed on an Ultrasphere® C18 5 µm column (4.6 mm I.D. x 150 mm) (Alltech, Breda, The Netherlands) equipped with a refill guard column (2 mm I.D. x 20 mm) (Upchurch Scientific, Oak Harbor, WA, USA), packed with C18 (particle size 20-40 µm) (Alltech, Breda, The Netherlands), at a constant temperature of 30 °C.

The mobile phase was a mixture of 0.1 M sodium phosphate buffer (pH 5.5) and methanol (65:35, v/v) for nalbuphine and butorphanol, whereas for morphine a mixture of 0.1 M sodium phosphate buffer (pH 4) and methanol (75:25, v/v). All mobile phases were supplemented with a total concentration 20 mg/l EDTA (sodium salt). The mobile phase for nalbuphine and butorphanol also contained 5 mM KCl whereas for morphine analysis 2 mM octane-sulfonic acid was added. Mobile phase solvents were filtered through a 0.2 µm nylon filter (Alltech, Breda, The Netherlands), mixed and degassed

continuously with helium. The flow rate was set at 1 ml/min. The optimal working potential for nalbuphine, butorphanol and morphine were +0.85 V, +0.85 V and +0.75 V, respectively, as determined by a voltammogram and sensitivity plot.

Analysis of morphine concentrations in brain microdialysate samples

For analysis of morphine brain microdialysate concentrations, 2 µl of internal standard (nalorphine) solution was added per 5 µl of sample. The samples were injected into the HPLC system without further sample pre-treatment. Chromatography of brain microdialysate samples was performed on a Ultrasphere® C18 column (2 mm I.D. x 150 mm) (Alltech, Breda, The Netherlands) at a constant temperature of 35 °C. The mobile phase was a mixture of 0.1 M sodium phosphate buffer (pH 2.5) and methanol (75:25, v/v), supplemented with 20 mg/L EDTA (sodium salt) and 10 mM octane-sulfonicacid. Mobile phase solvents were filtered through a 0.2 µm nylon filter, mixed and degassed continuously with helium. The flow rate was set at 0.2 ml/min. The optimal working potential for morphine was +0.80 V, as determined by a voltammogram and sensitivity plot.

Reagents and standard solutions

For analysis of blood samples, the stock solutions of nalbuphine, butorphanol, morphine and nalorphine were prepared at a concentration of 1 mg/ml (free base) in Millipore water. The stock solutions were diluted with Millipore water to obtain calibration solutions (range 25 – 10000 ng/ml). Internal standard solutions were prepared by dilution of the stock solutions to a concentration of 250, 2500 and 500 ng/ml for nalbuphine, butorphanol and nalorphine, respectively.

For analysis of brain microdialysate samples, a stock solution of morphine was prepared at a concentration of 1 mg/ml (free base) in microdialysis perfusion fluid. Internal standard solution was prepared by dilution of the stock solution to 500 ng/ml nalorphine in perfusion fluid. Microdialysis perfusion fluid comprised of phosphate buffer (2 mM, pH 7.4) containing 145 mM sodium, 2.7 mM potassium, 1.2 mM calcium, 1.0 mM magnesium, 150 mM chloride and 0.2 mM ascorbate (Moghaddam & Bunney 1989). The stock solutions were stored at –20 °C up to three months. The assay solutions were stored at 4 °C up to four weeks.

Calibration and validation

On each day of blood sample analysis, a 10-point calibration curve was prepared by spiking 50 µl of blood hemolysed in 400 µl water with 50 µl of calibration solution and 50 µl of the internal standard solution. For analysis of brain microdialysates, a 10-point calibration curve was prepared with 40 µl of calibration solutions in perfusion fluid and 16 µl of internal standard solution in Millipore water.

Samples were processed as described above and peak ratios of nalbuphine-butorphanol, butorphanol-nalbuphine or morphine-nalorphine were calculated. Calibration curves

were constructed by weighted linear regression [weight factor = 1/ (peak height ratio)^2] according to the method implemented in the data-acquisition program Empower®.
Quality control samples of fixed concentrations were prepared to determine intra- and inter-assay variability. Extraction yields were determined by comparing the peak ratios after extraction from blood with the peak ratios of not-extracted standards.

Pharmacokinetic-pharmacodynamic study in rats

Chronically instrumented male Wistar rats, weighing 250 – 300 g were used in the experiments. Nine days before the experiment, seven cortical EEG electrodes were implanted into the skull. A number of rats used for the morphine studies were implanted with four cortical EEG electrodes and a CMA/12 microdialysis guide (Aurora Borealis Control, Schoonebeek, The Netherlands) which was replaced by the microdialysis probe (CMA/12, 4 mm) 24 hours before the experiment. Two days before the experiments three cannulas were implanted for drug administration and serial blood sampling. Two cannulas were implanted in the right jugular vein for opioid and midazolam infusion and one cannula was implanted in the left femoral artery to collect blood samples. The surgical procedures were performed under anaesthesia of 0.1 mg/kg Domitor® (intramuscular injection, 1 mg/ml medetomidine hydrochloride, Pfizer, Capelle aan de IJssel, The Netherlands) and 1 mg/kg Ketanest® (subcutaneous injection, 50 mg/ml ketamine base, Parke Davis, Hoofddorp, The Netherlands). After surgery, rats received a single dose of ampicilline trihydrate (0.6 ml/kg of a 200 mg/ml solution, A.U.V., Cuijk, The Netherlands).
At the day of the experiment, the rats received an intravenous infusion of midazolam (5.5 mg/kg/h) and either nalbuphine (10 mg/kg in 10 min), butorphanol (10 mg/kg in 10 min) or morphine (4 mg/kg in 10 min). Midazolam was administered continuously to prevent opioid induced seizures (Cox *et al.* 1997). To reach steady state rapidly, midazolam was administered with a Wagner infusion (Wagner 1974). The midazolam infusion was started 30 min before opioid infusion. A total number between 15 and 20 arterial blood samples were collected over a period of 4 hours at fixed time intervals and immediately hemolysed in Millipore water. The samples were stored at – 20°C until analysis.
During the experiment, the EEG was recorded continuously. After off-line fast Fourier transformation using the data analysis software Spike2 version 4.60, (Cambridge Electronic Design limited, Cambridge, UK), the absolute amplitude in the delta-frequency range in 5 s epochs were averaged over 1 min intervals.
The pharmacokinetics of nalbuphine, butorphanol and morphine were quantified for each individual rat using the least squares minimisation algorithm (weight = 1/(y predicted)^2) of the WinNonlin Pro package V.1.5 (Pharsight Corporation, Mountain View, CA, USA). For nalbuphine, butorphanol and morphine a standard two-compartment model (Gibaldi & Perrier 1982) best described the concentration-time profile by the Akaike Information Criteria (Akaike 1974).

RESULTS AND DISCUSSION

Chromatography

The sample pre-treatment by liquid-liquid extraction provided a good sample clean up as shown in figure 2. For nalbuphine and butorphanol a two-step extraction procedure was required because of interfering peaks, whereas for morphine a one-step extraction was sufficient (figure 3).

Retention times for nalbuphine and butorphanol were 6 and 11 min, respectively with a mobile phase containing 35 % methanol and 65 % 0.1 M phosphate buffer pH 5.5. Retention times for morphine and internal standard nalorphine were 5 and 11 min,

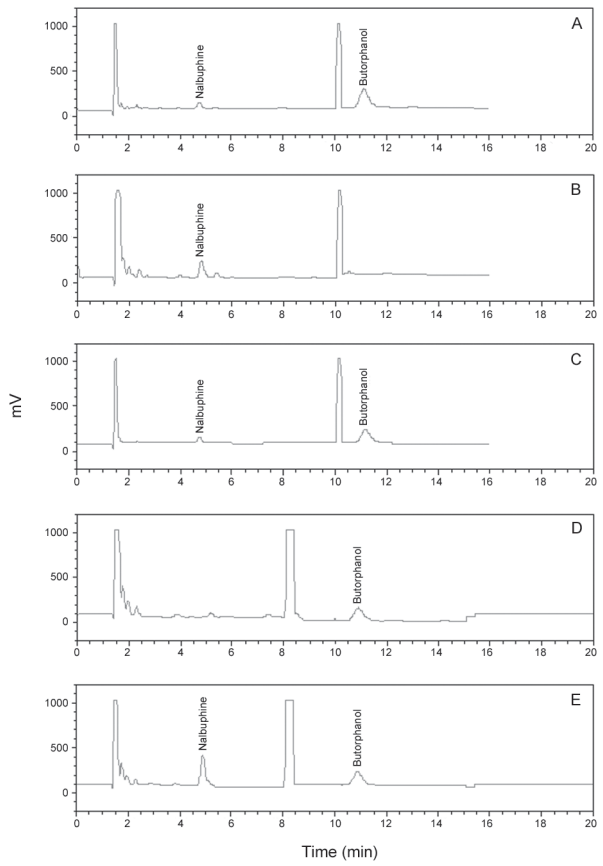

Figure 2: Chromatograms of an extract of blank blood spiked with nalbuphine (250 ng/ml) and butorphanol (2500 ng/ml)(A), blank blood spiked with either internal standard nalbuphine (250 ng/ml) or internal standard butorphanol (2500 ng/ml) (B and D) and blood obtained from a rat at 12 min after start of an infusion of 10 mg/kg butorphanol in 10 min (concentration 1931 ng/ml)(C) or after having received and infusion of 10 mg/kg nalbuphine in 10 min (concentration 1955 ng/ml)(E).

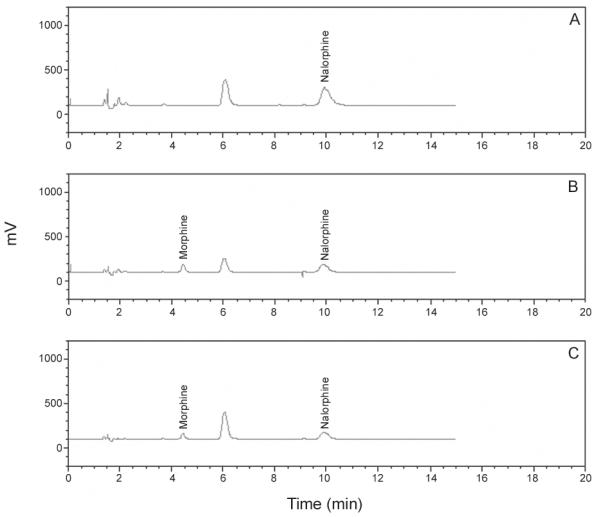

Figure 3: Chromatograms of an extract of blank blood spiked with internal standard nalorphine (500 ng/ml) (A), blank blood spiked with morphine (1000 ng/ml) and internal standard nalorphine (500 ng/ml) (B) and blood obtained from a rat at 12 min after the start of an infusion of 4 mg/kg morphine in 10 min (morphine concentration 767 ng/ml) (C).

respectively with a mobile phase containing 25% methanol, 75 % 0.1 M phosphate buffer pH 4 and 2 mM octane-sulfonicacid. For the analysis of morphine, the mobile phase was adjusted because morphine did not have enough retention on the column with the conditions used for nalbuphine and butorphanol. To improve retention, 2 mM octane-sulfonic acid was added as an ion-pair. The pH was adjusted to improve the peak shape.

Table 1 summarises the recovery after extraction, the accuracy and reproducibility of the analysis. For nalbuphine, butorphanol and morphine intra- and inter-assay were less than 20 % in the concentration range of 25–10000 ng/ml. The weighted linear regression equations (mean ± SEM) for nalbuphine (N=9), butorphanol (N=5) and morphine (N=15) were y = (1.212 ± 0.055)x + (-7.195 ± 2.394), y = (0.0020 ± 0.0003)x + (-0.0629 ± 0.0127) and y = (0.0011 ± 0.0001)x + (-0.0045 ± 0.0015), respectively. Corresponding coefficients of correlation were (0.978 ± 0.003), (0.993 ± 0.001) and (0.996 ± 0.001), indicating the linearity of the methods. Using 50 µl blood, the limit of detection for nalbuphine, butorphanol and morphine was 25, 50 and 25 ng/ml (signal to noise ratio = 3), respectively. The main difference of the methods described here and the methods described in the literature is the sample size. All methods are described for studies in humans or relatively large laboratory animals (dogs, pigs, rabbits), whereas the method described here was especially for application to studies in small laboratory animals (rats). For example, for the analysis of nalbuphine Nicolle and co-workers (1995; 1997) used plasma samples

Table 1: Validation of the determination of nalbuphine (N), butorphanol (B) and morphine (M): recovery, intra-assay and inter-assay variability, coefficients of variation and accuracy. Results are expressed as mean ± SEM.

	Added (ng/ml)	Recovery (N=3)	Intra-assay (N=3)			Inter-assay (N=5)		
			Found (ng/ml)	CV (%)	Accuracy (%)	Found (ng/ml)	CV (%)	Accuracy (%)
N	100	67±2	-	-	-	-	-	-
	250	-	265±17	11	106	263±12	13	105
	1000	71±5	-	-	-	-	-	-
	2500	-	2553±28	1.9	102	2936±80	7	117
	10000	78±4	-	-	-	-	-	-
B	100	64±14	-	-	-	-	-	-
	250	-	248±6	4.7	99	213±10	10	86
	1000	85±8	-	-	-	-	-	-
	2500	-	2530±51	3.5	101	2550±62	5	102
	10000	80±8	-	-	-	-	-	-
M	250	62±4	239±5	4.4	96	257±5	6	103
	3000	58±4	2630±97	8.2	88	3268±82	9	109

of 500 µl whereas in our studies blood samples of 50-200 µl were used. When whole blood samples are used for drug analysis, more samples can be collected from a subject and therefore more information about the individual pharmacokinetic profiles can be obtained. Another advantage of our method is that one general method is applicable for three opioids. Nalbuphine and butorphanol samples can be analysed with the same HPLC-conditions and sample pre-treatment, whereas for morphine only slight modifications are required.

For morphine administration, drug concentrations were also determination in brain microdialysate. No sample pre-treatment was required to clean up the samples as is shown in figure 4. The weighted linear regression equation (mean ± SEM) for morphine (N=9) was $y = (16.644 \pm 0.269)x + (-6.484 \pm 0.565)$ and corresponding coefficient of correlation was (0.994 ± 0.001), indicating the linearity of the method. Using 40 µl microdialysate, the limit of detection for morphine was 0.5 ng/ml (signal to noise ratio = 3).

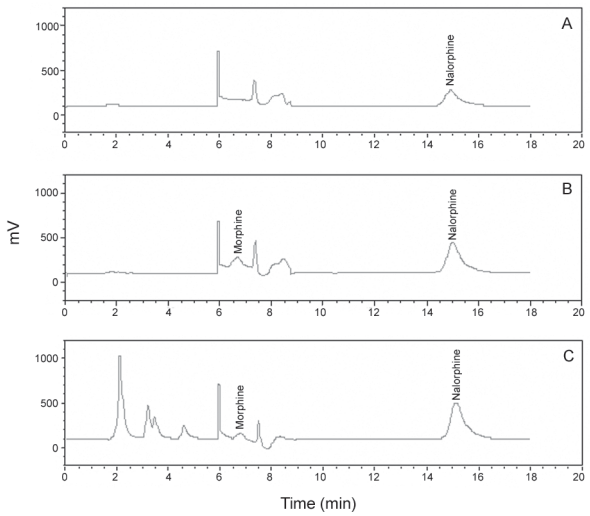

Figure 4: Chromatograms of blank microdialysate spiked with internal standard nalorphine (500 ng/ml) (A), microdialysate spiked with morphine (10 ng/ml) and internal standard nalorphine (500 ng/ml) (B) and a microdialysate fraction obtained from a rat 40-60 min after the start of an infusion of 4 mg/kg morphine in 10 min (morphine concentration 6.1 ng/ml) (C).

Study in rats

Figure 5a and 5b show representative blood concentration-time profiles for an intravenous administration of 10 mg/kg nalbuphine in 10 min and 10 mg/kg butorphanol in 10 min. The values for clearance, volume of distribution at steady state and terminal half-life were estimated for each individual rat (table 2).

Table 2: Average pharmacokinetic parameter estimates (Mean ± SEM) obtained with a two-compartment pharmacokinetic model for nalbuphine, butorphanol and morphine after a 10-min intravenous infusion.

Compound	Dose (mg/kg)	N	Cl (ml/min)	Vd_{ss} (ml)	Elimination half life (min)
Nalbuphine	10	8	38.7 ± 3.3	1917 ± 385	56.0 ± 7.0
Butorphanol	10	6	22.8 ± 3.3	1242 ± 193	62.4 ± 14.0
Morphine	4	14	24.1 ± 2.1	881 ± 117	44.1 ± 4.7

Figure 5c shows a representative blood and brain microdialysate concentration-time profile for an intravenous infusion of 4 mg/kg morphine in 10 min. To emphasise the application to PK-PD studies, figure 5 also shows the time-course of the change in amplitude of the delta-frequency band (0.5 - 4.5 Hz) of the EEG during and after administration of nalbuphine, butorphanol or morphine. Combination of both the detailed concentration-time and effect-time relationship revealed a complex concentration-effect relationship, which is currently being investigated by PK-PD modelling.

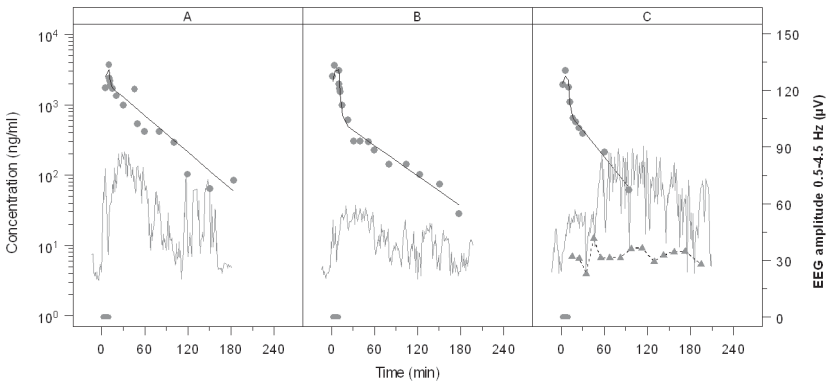

Figure 5: Typical blood concentration-time profiles (filled circles, left ordinate) and EEG amplitudes in delta-frequency range versus time (grey solid line, right ordinate) in rats following intravenous infusion of 10 mg/kg nalbuphine (A), 10 mg/kg butorphanol (B) or 4 mg/kg morphine (C) in 10 min. Panel C also shows the brain microdialysate concentration-time profile of morphine (dotted line). The solid line represents the best description of the plasma concentrations according to a two-compartment pharmacokinetic model.

CONCLUSIONS

A simple and sensitive HPLC method has been developed for the analysis of nalbuphine, butorphanol and morphine in biological samples. The short duration of the analysis, the sample size, the sensitivity, the reproducibility and the simplicity of the methods used make these assays particularly useful for PK-PD studies in small laboratory animals in which large numbers of samples have to be analysed.
In combination with the EEG measurements, concentration-effect profiles can be obtained in individual rats, which can then be used for quantitative analysis of μ-opioid receptor mediated responses *in vivo*. The analysis of the brain microdialysate concentrations of morphine allows the characterisation of the BBB transport of morphine and its influence on the concentration-effect relationships.

ACKNOWLEDGEMENTS

The authors wish to acknowledge the technical assistance of Andrea Rosier, Dennis de Mik and Susanne Bos-van Maastricht. The described work was financially supported by GlaxoSmithKline, United Kingdom.

REFERENCES

Aitkenhead AR, Lin ES, Achola KJ (1988) The pharmacokinetics of oral and intravenous nalbuphine in healthy volunteers. *Br.J.Clin.Pharmacol.* **25:** 264-268

Akaike H (1974) A new look at the statistical model identification. *IEEE Trans.Automat.Control* **19:** 716-723

Benveniste H, Huttemeier PC (1990) Microdialysis--theory and application. *Prog.Neurobiol.* **35:** 195-215

Bouw MR, Gardmark M, Hammarlund-Udenaes M (2000) Pharmacokinetic-pharmacodynamic modelling of morphine transport across the blood-brain barrier as a cause of the antinociceptive effect delay in rats--a microdialysis study. *Pharm.Res.* **17:** 1220-1227

Cherny NI (1996) Opioid analgesics: comparative features and prescribing guidelines. *Drugs* **51:** 713-737

Cox EH, Kerbusch T, van der Graaf PH, Danhof M (1998) Pharmacokinetic-pharmacodynamic modeling of the electroencephalogram effect of synthetic opioids in the rat: correlation with the interaction at the mu-opioid receptor. *J Pharmacol.Exp.Ther.* **284:** 1095-1103

Cox EH, Langemeijer MW, Gubbens-Stibbe JM, Muir KT, Danhof M (1999) The comparative pharmacodynamics of remifentanil and its metabolite, GR90291, in a rat electroencephalographic model. *Anesthesiology* **90:** 535-544

Cox EH, van Hemert JG, Tukker EJ, Danhof M (1997) Pharmacokinetic-pharmacodynamic modelling of the EEG effect of alfentanil in rats. *J Pharmacol.Toxicol.Methods* **38:** 99-108

de Lange EC, de Boer BA, Breimer DD (1999) Microdialysis for pharmacokinetic analysis of drug transport to the brain. *Adv.Drug Deliv.Rev.* **36:** 211-227

Drost RH, van Ooijen RD, Ionescu T, Maes RA (1984) Determination of morphine in serum and cerebrospinal fluid by gas chromatography and selected ion monitoring after reversed-phase column extraction. *J Chromatogr* **310:** 193-198

Emmerson PJ, Clark MJ, Mansour A, Akil H, Woods JH, Medzihradsky F (1996) Characterization of opioid agonist efficacy in a C6 glioma cell line expressing the mu opioid receptor. *J.Pharmacol.Exp.Ther.* **278:** 1121-1127

Garner HR, Burke TF, Lawhorn CD, Stoner JM, Wessinger WD (1997) Butorphanol-mediated antinociception in mice: partial agonist effects and mu receptor involvement. *J.Pharmacol.Exp.Ther.* **282:** 1253-1261

Gibaldi M, Perrier D (1982) Noncompartmental analysis based on statistical moment theory. in *Pharmacokinetics, 2 edn*, Marcel Dekker, New York, 409-424

Grinstead GF (1991) A closer look at acetyl and pentafluoropropionyl derivatives for quantitative analysis of morphine and codeine by gas chromatography/mass spectrometry. *J.Anal.Toxicol.* **15:** 293-298

Joel SP, Osborne RJ, Slevin ML (2002) An improved method for the simultaneous determination of morphine and its principal glucuronide metabolites. *J Chromatogr* **430:** 394-399

Kanazawa H, Konishi Y, Matsushima Y, Takahashi T (1998) Determination of sedatives and anesthetics in plasma by liquid chromatography-mass spectrometry with a desalting system. *J.Chromatogr.A* **797:** 227-236

Liaw WJ, Ho ST, Wang JJ, Hu OY, Li JH (1998) Determination of morphine by high-performance liquid chromatography with electrochemical detection: application to human and rabbit pharmacokinetic studies. *J Chromatogr B Biomed.Sci.Appl.* **714:** 237-245

Moghaddam B, Bunney BS (1989) Ionic composition of microdialysis perfusing solution alters the pharmacological responsiveness and basal outflow of striatal dopamine. *J.Neurochem.* **53:** 652-654

Nicolle E, Michaut S, Serre-Debeauvais F, Bessard G (1995) Rapid and sensitive high-performance liquid chromatographic assay for nalbuphine in plasma. *J.Chromatogr.B Biomed.Appl.* **663:** 111-117

Nicolle E, Veitl S, Guimier C, Bessard G (1997) Modified method of nalbuphine determination in plasma: validation and application to pharmacokinetics of the rectal route. *J.Chromatogr.B Biomed.Sci.Appl.* **690:** 89-97

Pallasch TJ, Gill CJ (1985) Butorphanol and nalbuphine: a pharmacologic comparison. *Oral Surg.Oral Med.Oral Pathol.* **59:** 15-20

Pittman KA, Smyth RD, Mayol RF (1980) Serum levels of butorphanol by radioimmunoassay. *J.Pharm.Sci.* **69:** 160-163

Svensson JO (1986) Determination of morphine, morphine-6-glucoronide and normorphine in plasma and urine with high-performance liquid chromatography and electrochemical detection. *J.Chromatogr* **375:** 174-178

van der Graaf PH Danhof M (1997) Analysis of drug-receptor interactions in vivo: a new approach in pharmacokinetic-pharmacodynamic modelling. *Int.J Clin.Pharmacol.Ther.* **35:** 442-446

Volk KJ, Klohr SE, Rourick RA, Kerns EH, Lee MS (1996) Profiling impurities and degradants of butorphanol tartrate using liquid chromatography/mass spectrometry and liquid chromatography/tandem mass spectrometry substructural techniques. *J.Pharm.Biomed.Anal.* **14:** 1663-1674

Wagner JG (1974) A safe method for rapidly achieving plasma concentration plateaus. *Clin.Pharmacol.Ther.* **16:** 691-700

Willey TA, Duncan GF, Tay LK, Pittman KA, Farmen RH (1994) High-performance liquid chromatographic method for the quantitative determination of butorphanol, hydroxybutorphanol, and norbutorphanol in human urine using fluorescence detection. *J.Chromatogr.* **652:** 171-178

Chapter 4

MEMBRANE TRANSPORT OF OPIOIDS: RELATIVE CONTRIBUTION OF P-GLYCOPROTEIN MEDIATED TRANSPORT AND PASSIVE PERMEABILITY *IN VITRO*

Dorien Groenendaal[1], Dennis de Mik[1], Glynis Nicholls[2], Andrew D. Ayrton[2], Anne Hersey[3], Meindert Danhof[1] and Elizabeth C.M. de Lange[1]

[1]Leiden Amsterdam Center for Drug Research, Leiden University, Division of Pharmacology, Leiden, The Netherlands, [2]GlaxoSmithKline, Drug Metabolism and Pharmacokinetics, Ware and Welwyn, Hertfordshire, United Kingdom, [3]GlaxoSmithKline, Computational and Structural Sciences, Stevenage, Hertfordshire, United Kingdom

ABSTRACT

Restricted transport across the blood-brain barrier (BBB) can be a critical factor in the development of mechanism-based pharmacokinetic/pharmacodynamic (PK-PD) models for the central effects of opioids. In this study, the P-glycoprotein (Pgp) interaction and the apparent transmembrane passive permeability rates (P_{app}) of a wide range of opioids were investigated, This was performed *in vitro*, using monolayers of MDCK:MDR1 and LLC-PK1:MDR1a cells. The opioids alfentanil, fentanyl, sufentanil, loperamide and morphine were able to inhibit Pgp mediated efflux of ^{3}H-digoxin in MDCK:MDR1 and LLC-PK1:MDR1a cells, whereas no inhibition was observed for butorphanol, nalbuphine, and the morphine metabolites M3G and M6G. Moreover, active transport by Pgp was found for loperamide and morphine. The P_{app} values were determined in the presence of the Pgp inhibitor GF120918. High transmembrane passive permeability rates (>500 nm/sec) were found for alfentanil, fentanyl, sufentanil and butorphanol, whereas the permeability rates of loperamide (206 nm/sec), nalbuphine (156 nm/sec) and morphine (16 nm/sec) were relatively low. It is concluded that the contributions of both Pgp mediated transport and transmembrane passive permeability rates are of importance for the influence of BBB transport on the PK-PD relationships of opioids. Alfentanil, fentanyl, sufentanil and butorphanol have high passive permeability rates and the relative contribution of Pgp mediated transport, if any, is therefore considered as not significant. In contrast, nalbuphine, morphine and loperamide have low passive permeabilities and therefore the net transmembrane transport is significantly influenced by Pgp mediated transport.

INTRODUCTION

The objective of pharmacokinetic-pharmacodynamic (PK-PD) modelling is the prediction of the time course of drug effects under physiological and pathological conditions (Breimer & Danhof 1997). At present there is a clear trend towards the development and application of mechanism-based PK-PD models. Mechanism-based PK-PD models differ from empirical descriptive models in that they contain specific expressions to characterise the processes on the causal path between drug administration and effect. These processes include 1) biophase distribution, 2) target site activation, 3) transduction and 4) the influence of *in vivo* homeostatic feedback mechanisms (Danhof *et al*. 2005). An important feature of PK-PD models is further the strict distinction between drug and system specific characteristics (van der Graaf & Danhof 1997). Our interest is to develop a mechanism-based PK-PD model for the central effects of opioids. In these investigations alfentanil, fentanyl, sufentanil, nalbuphine, butorphanol, morphine and loperamide (figure 1) are used as model drugs, because they differ widely in affinity and intrinsic efficacy at the μ-opioid receptor.

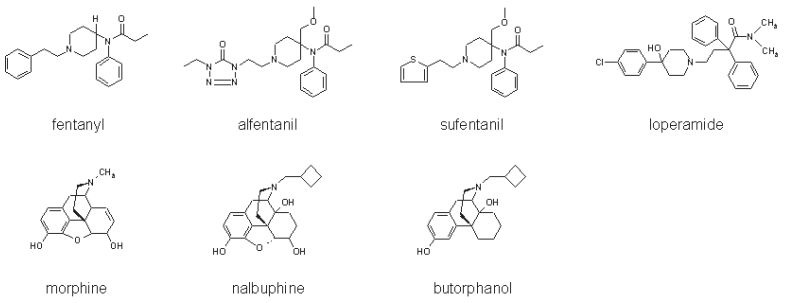

Figure 1: The chemical structures of the opioids investigated in these studies. Two categories of opioids can be identified; the ones derived from fentanyl and the ones derived from morphine.

To determine the complex *in vivo* concentration-effect relationships of these opioids, the transport across the blood-brain barrier (BBB) needs to be taken into consideration.
Recently, the effects of the opioids alfentanil, fentanyl and sufentanil have been studied *in vivo* in a chronically instrumented rat model, using the amplitude in the 0.5-4.5 Hz frequency band of the electroencephalogram (EEG) as a pharmacodynamic endpoint (Cox *et al*. 1998). However, the role of BBB transport as a mechanism for the observed hysteresis of these opioids has so far not been explored in detail. This is important since active transporters at the BBB may influence both the rate and extent of transport into the brain, and thereby the estimation of the parameters in the complex PK-PD relationships of centrally acting drugs (de Lange *et al*. 2005).

Transport across the BBB can be divided into passive and active transport processes (de Lange & Danhof 2002). Passive transport of compounds across the BBB is dependent on physicochemical properties, such as lipophilicity, degree of ionisation and number of hydrogen bonds (van Bree *et al.* 1988). Active transport can be divided into carrier mediated transport, receptor mediated transport and endocytosis (de Boer *et al.* 2003). Several transporters are present at the BBB to transport endogenous compounds such as amino acids, glucose etc. An important efflux transporter expressed at the luminal face of the BBB is P-glycoprotein (Pgp). Pgp is a member of the adenosine triphosphate-binding cassette super family and is encoded by the multidrug resistance gene (MDR1) (Thiebaut *et al.* 1987). This transporter has been shown to have an important influence on the BBB transport of a wide range of drugs (de Lange & Danhof 2002; Schinkel *et al.* 1995; Schinkel *et al.* 1996).

In previous investigations, morphine and loperamide have been identified as Pgp substrates in both *in vitro* models, comprising of either brain capillary endothelial cells or LLC-PK1:MDR1 cells, and *in vivo* models, in rats and mice (Wandel *et al.* 2002, Letrent *et al.* 1999b; Mahar Doan *et al.* 2002; Schinkel *et al.* 1995, 1996). Furthermore, PK-PD studies in rats have revealed that after oral pre-treatment with the specific Pgp inhibitor GF120918, the anti-nociceptive effect of morphine was prolonged due to its prolonged half-life in the brain (Letrent *et al.* 1998, 1999a). Alfentanil and sufentanil were not identified as Pgp substrates within the abovementioned investigations in *in vitro* models, whereas inconsistencies have been reported for fentanyl (Henthorn *et al.* 1999; Wandel *et al.* 2002). In addition, for fentanyl, *in situ* brain perfusion studies indicated Pgp mediated efflux as it was found that the brain uptake of fentanyl is slightly increased (1.2 fold) in MDR1a (-/-) mice when compared to MDR1a (+/+) mice (Dagenais *et al.* 2004; Mahar Doan *et al.* 2002; Schinkel *et al.* 1995, 1996). Nalbuphine, a semi-synthetic opioid analgesic, was also found to be a Pgp substrate in a MDCKII-MDR1 cell-system (Mahar Doan *et al.* 2002), whereas to our knowledge so far no studies have performed on butorphanol.

The aim of the present study was to identify the membrane transport characteristics with respect to the relative contribution of Pgp mediated (efflux) transport and passive transmembrane permeability rate (P_{app}), for a series of opioids including alfentanil, fentanyl, sufentanil, nalbuphine, butorphanol, morphine and loperamide. The chemical structures of these opioids are shown in figure 1. The opioids were tested in an *in vitro* cell system, comprising of monolayers of MDCKII:MDR1 or LLC-PK1:MDR1a cells. Regression analysis was used to investigate the relationships between P_{app} and physicochemical properties of the opioids. These properties included polar surface area, lipophilicity (cLogP) and the predicted BBB permeability based on the number of hydrogen donors and acceptors, according to the Abraham equation (Abraham *et al.* 1994).

MATERIALS AND METHODS

Materials

Fentanyl citrate, morphine sulphate, nalbuphine hydrochloride, butorphanol tartrate, loperamide hydrochloride, morphine-3-glucuronide, morphine-6-glucuronide and lucifer yellow were obtained from Sigma Aldrich (United Kingdom). Alfentanil hydrochloride and sufentanil citrate were kindly provided by Janssen Pharmaceutica (Beerse, Belgium). GF120918 and SB-243213 were supplied by GlaxoSmithKline. ^{3}H-amprenavir (specific activity 0.13 Ci/mmol), ^{3}H-digoxin (specific activity 37 Ci/mmol) and ^{3}H-loperamide (specific activity 10 Ci/mmol) were obtained from Amersham.
The stock solutions of the opioids and GF120918 were prepared in DMSO (Sigma Aldrich, United Kingdom). The GSK internal standard solution was prepared in ammonium acetate/methanol (50/50 v/v). The lucifer yellow solution was prepared in Millipore water (18.2MΩ.cm). All other chemicals were of analytical grade.
All cell-culture reagents were obtained from Invitrogen (United Kingdom). BD Falcon™ HTS 24-Multiwell Inserts (24-well, 0.31 cm^2, 0.1 µm pore size) were obtained from Becton-Dickinson (United Kingdom).

Cell lines

MDCKII:MDR1; Madine Darby Canine Kidney type II cells transfected with the human MDR1 gene (MDCKII:MDR1) were cultured in DMEM – glutamax media, formulated with D-glucose (4.5 g/l), L-alanyl-glutamine and phenol red and supplemented with penicillin (10000 U/ml)-streptomycin (10000 µg/ml) and 10% (v/v) fetal calf serum at 37 °C and 5% CO_2. Cells were trypsinised every 4 days. For the studies, the cells were seeded onto BD Falcon™ HTS 24-Multiwell Inserts at a seeding density of 50000 cells/well and grown for 3 days in DMEM full media.
LLC-PK1:MDR1a; Porcine kidney epithelial cells transfected with the mouse MDR1a gene (LLC-PK1:MDR1a) were cultured in M199 media, formulated with Earle's salts, L-glutamine, phenol red and sodium bicarbonate (2.2 g/L) and supplemented with penicillin (10000 U/ml)-streptomycin (10000 µg/ml) and 10% (v/v) fetal calf serum at 37 °C and 5% CO_2. The cells were trypsinised every 4 days and sub-cultured in M199 media containing 2 mM vincristine as a selection agent. For the studies, the cells were seeded onto BD Falcon™ HTS 24-Multiwell Inserts at a seeding density of 75000 cells/well and grown for 3 days in M199 media without the selection agent vincristine.

General experimental procedures on transmembrane transport studies

Transport experiments were performed using monolayers of both the MDCKII:MDR1 and the LLC-PK1:MDR1a cells. As an integrity check, prior to the experiment, the trans-epithelial electrical resistance (TEER) of each monolayer was measured with an EVOM™ voltohmmeter (World Precision Instruments, Stevenage, United Kingdom). The experiments were performed in transport buffer consisting of DMEM containing

25 mM HEPES without phenol red and sodium pyruvate. The experiments were started with pre-incubation of the monolayers for 15 min at 37°C with transport buffer to which either the Pgp inhibitor GF120818 or the vehicle (0.5% DMSO) was added. After the pre-incubation period, the transport buffer was removed and the test solutions were added. All test solutions were prepared from stock solutions, that were prepared in 100% DMSO (opioids at 100 mM; GF120918 at 2 mM). To prepare the test solutions, the stock solutions were diluted further with transportbuffer. The test solutions ultimately contained 0.5% DMSO. The monolayers were incubated with the test solutions for a test period of 90 min at 37°C under continuous shaking. All experiments were performed automatically using the robotic TECAN™ genesis workstation (TECAN, Reading, United Kingdom).
The reference drugs for membrane integrity towards paracellular transport (lucifer yellow, 10 µM) and for Pgp-efflux functionality (amprenavir, 3 µM) were included in each experiment to test the integrity and quality of the monolayer. Lucifer yellow was added to each well, whereas amprenavir was only added to two wells as a positive control. After the test period of 90 min, 100 µl samples were collected to be analysed on the concentrations of the references lucifer yellow and amprenavir, as well as the test compound.

Inhibition of Pgp mediated efflux of ^{3}H-digoxin, the "^{3}H-digoxin transport inhibition factor"

The experiments on inhibition of Pgp mediated transport by either the Pgp inhibitor GF120918 or by the seven selected opioids were performed in duplicate using monolayers of both the MDCKII:MDR1 and the LLC-PK1:MDR1a cells. Transport measurements were performed in basolateral-to-apical direction (b→a). This would correspond to BBB transport in the direction from brain into blood (efflux).
In addition to alfentanil, fentanyl, sufentanil, nalbuphine, butorphanol, morphine and loperamide, the morphine metabolites, morphine-3-glucoronide (M3G) and morphine-6-glucoronide (M6G) were also included in these studies. Stock solutions of opioids (100 mM) and GF120918 (2 mM) were prepared. The monolayers were pre-incubated with transport buffer containing either GF120918 (2 µM) or opioid (100 µM) at both the basolateral and apical side. At time = 0, the experiment was started by addition of ^{3}H-digoxin (3 µM) for testing the inhibitory action of the opioids and the morphine metabolites. As a positive control ^{3}H-amprenavir was added to two of the wells and lucifer yellow was added to all the wells to check for monolayer integrity. The ^{3}H-digoxin transport inhibition factor was calculated (see data analysis).

Pgp substrate assessment studies; the "Pgp substrate efflux ratio"

Pgp substrate assessment studies were performed in duplicate using monolayers of the MDCKII:MDR1 cells. Transport experiments were performed both into the apical-to-basolateral (a→b) as the basolateral-to-apical (b→a) direction. The stock solutions of the opioids contained final concentrations of 3 mM in DMSO. The pre-incubation solutions

contained vehicle (0.5% DMSO) or GF120918 (2 µM in 0.5% DMSO) in transport buffer. The test solutions contained vehicle (0.5% DMSO) or GF120918 (2 µM), lucifer yellow and one of the opioids (3 µM) or amprenavir (3 µM). The "Pgp substrate efflux ratio" was calculated (see data analysis).

Sample analysis

^{3}H-amprenavir, ^{3}H-loperamide and ^{3}H-digoxin samples were dried down at 37°C and analysed with a Topcount NXT™ microplate scintillation counter (Perkin Elmer, Beaconsfield, United Kingdom), 2 min per sample.

Alfentanil, fentanyl, sufentanil and butorphanol were analysed by dual high-performance liquid chromatography with tandem mass spectrometry (HPLC-LC/MS/MS). The system consisted of an API-365 (Applied Biosystems, Warrington, United Kingdom) LC/MS/MS employing positive ion turbospray ionisation with a CTC HTS PAL autosampler (CTC Analytics, Hitchin, United Kingdom). HPLC was conducted on a 50 mm x 2.1 mm HyPURITY column (ThermoHypersil, Runcorn, United Kingdom) at a flow rate of 0.8 ml/min and a split ratio of 1:2. The mobile phase consisted of two solvents: (A) 10 mM ammonium acetate pH 4 and (B) 100% acetonitrile. The gradient profile was set at 0 min on 80% A and 20% B, at 1 min on 0% A and 100% B and at 1.1 min on 80% A and 20% B. The total run time was 1.5 min. Data acquisition was performed with PE Sciex version 1.1 (Applied Biosystems, Warrington, United Kingdom) and data were reported as the ratio of test compound peak area over internal standard peak area.

Nalbuphine and morphine samples were analysed by high performance liquid chromatography with electrochemical detection (HPLC-ECD) as described previously (Groenendaal *et al.* 2005 – chapter 3). Briefly, the nalbuphine samples were transferred into glass tubes and the internal standard butorphanol (50 µl, 2500 ng/ml) was added. The samples were acidified with phosphoric acid (0.15 mM, pH 2.3, 500 µl) and extracted with 3 ml of ethyl acetate. After extraction, the organic layer was discarded. Subsequently, the samples were alkalinised with carbonate buffer (0.15 mM, pH 11, 500 µl) and extracted with 5 ml of ethyl acetate. The organic layer was transferred into clean glass tubes and evaporated to dryness under reduced pressure at 37 °C. For morphine samples, only the alkaline extraction with carbonate buffer and ethyl acetate was performed. The HPLC system consisted of an LC-10AD HPLC pump (Shimadzu, Kyoto, Japan), a Waters 717 plus autosampler (Waters, Milford, MA, USA), a pulse damper (Antec Leyden, Rijnsburg, The Netherlands) and a digital electrochemical amperometric detector (DECADE, software version 3.02) from Antec Leyden. The electrochemical detector consisted of a VT-03 electrochemical flow cell combined with a 25 µm spacer and an Ag/AgCl reference electrode operating in the DC mode at a temperature of 30 °C, set at a voltage of 0.85V and 0.75V for nalbuphine and morphine, respectively.

Chromatography was performed on C18 ODS Ultrasphere 5 µm column (4.6 mm I.D. x 150 mm) (Alltech, Breda, The Netherlands) equipped with a refill guard column. The mobile phase was a mixture of 0.1 M phosphate buffer (pH 5.5) and methanol (65:35, v/v) for nalbuphine and butorphanol and a mixture of 0.1 M phosphate buffer (pH 4) and methanol (75:25, v/v) for morphine and contained a total concentration of 5 mM KCl and 20 mg/l EDTA. The mobile phase for morphine also contained 2.0 mM octanesulfonic acid. The flow rate was set at 1 ml/min. Data acquisition and processing was performed using the Empower integration software (Waters, Milford, MA, USA).

The lucifer yellow samples were analysed by a Polarstar® fluorescence microplate reader with λ_{ex}=430 nm and λ_{em}=538 nm (BMG-Labtech, Aylesbury, United Kingdom).

Data analysis

For the Pgp inhibition studies, the amount of ^{3}H-digoxin transported from the basolateral to apical (b→a, "brain to blood") side of both monolayers of the MDCKII:MDR1 and the LLC-PK1:MDR1a was calculated in the presence and absence of either the vehicle, the Pgp inhibitor GF120918 or the opioid. The ^{3}H-digoxin transport inhibition factor was calculated as the amount of ^{3}H-digoxin transported from b→a in the presence of the opioid or GF120918, respectively, divided by the amount of ^{3}H-digoxin transported from b→a in the presence of the vehicle (control).

For the Pgp substrate assessment studies, the Pgp substrate efflux ratio was calculated by the amount of opioid or the Pgp substrate ^{3}H-amprenavir as the positive control being transported from basolateral to apical (b→a) side, divided by the amount of opioid or ^{3}H-amprenavir transported from apical to basolateral (a→b) side of the MDCKII:MDR1 monolayer. Involvement of Pgp mediated efflux was considered significant for values of the Pgp substrate efflux ratio >1.5 (Mahar Doan *et al.* 2002).
To exclude potential contributions of other transporters to this Pgp substrate efflux ratio, experiments were also performed in the presence of the Pgp inhibitor GF120918, for which this substrate efflux ratio should decease to 1, if the asymmetrical membrane transport of the opioid was indeed only caused by Pgp.

The transmembrane passive permeability rate; the "P_{app}" values

The apparent transmembrane passive permeability rate P_{app} (nm/sec) of the compounds was calculated using the equation:

$$P_{app} = -\left(\frac{V_R \cdot V_D}{(V_R + V_D)\cdot A \cdot t}\right)\cdot \ln\left\{1 - \frac{CR(t)}{\langle C(t)\rangle}\right\} \qquad (1)$$

where V_D and V_R are the donor (basolateral) and receiver (apical) chamber volumes (cm^3) respectively, A is the area of the monolayer (cm^2), t is the time after the start of the experiments (s), $C_R(t)$ is the drug concentration in the receiver (apical) chamber and

$\langle C(t) \rangle$ is described by equation 2:

$$\langle C(t) \rangle = \frac{V_D \cdot C_D(t) + V_R \cdot C_R(t)}{V_D + V_R} \quad (2)$$

where $\langle C(t) \rangle$ describes the average concentration of the compound on both sides of the monolayer, V_D and V_R are the donor (basolateral) and receiver (apical) chamber volumes (cm^3) and $C_D(t)$ and $C_R(t)$ are the donor (basolateral) and receiver (apical) concentrations at time *t* (Tran *et al.* 2004; 2005). This calculation of P_{app} takes into account the loss of drug from the donor compartment, which results in a better estimation of the P_{app}.

In all studies, the ^{3}H-amprenavir substrate efflux ratios, the apparent transmembrane passive permeability rate of lucifer yellow and the mass balance values were used as controls for the quality (integrity and Pgp functionality) of each monolayer.

The mass balance was calculated with the following equation:

$$\langle C(t) \rangle = \frac{V_D \cdot C_D(t) + V_R \cdot C_R(t)}{V_D + V_R} \quad (3)$$

where $\%MB$ is the mass balance, A_{rt} is the drug amount in receiver chamber at time (t), A_{dt} is the drug amount in donor chamber at time (t) and A_{d0} is the drug amount in the donor chamber at t=0.
The data from experiments were only included when the value for the Pgp substrate efflux ratio of ^{3}H-amprenavir was > 16, the value of the transmembrane passive apparent permeability rate of lucifer yellow < 50 nm/sec and the value for the mass balance > 70 %.

It should be noted that for nalbuphine literature values were used (Mahar Doan *et al.* 2002). The nalbuphine efflux ratio was determined at a donor concentration of 10 µM. The Pgp substrate efflux ratio for morphine was calculated at a donor concentration of 100 µM only, as at other concentrations no receiver concentrations were detectable. The apparent permeability rate for morphine was calculated at a donor concentration 100 µM, but without GF120918 and a→b.

Quantitative structure activity relationships – physico-chemical relationships

The Log octanol/water partition coefficients (cLogP) and molar refractivity values (CMR) were calculated using Daylight Software v4.71/82 (Daylight Chemical Information Systems Inc., Irvine, CA). Polar surface areas (PSA) were calculated according to Ertl and co-workers (Ertl *et al.* 2000). An *in silico* predictor of passive BBB transport was also determined based on the Abraham equation (Abraham *et al.* 1994):

$$LogBB = -0.038 + 0198 \cdot R_2 - 0.687 \cdot \pi_2^H - 0.715 \cdot \alpha_2^H - 0.698 \cdot \beta_2^H + 0.995 \cdot V_x \quad (4)$$

where *LogBB* is the logarithm of the blood-brain concentration ratio and R_2, π^H_2, α^H_2, β^H_2 and V_x are defined as the excess molar refractivity, dipolarity/polarisability, hydrogen bond acidity, hydrogen bond basicity and the solute McGowan volume, respectively, as described by Platts (Platts *et al*. 1999).

Statistical analysis

The data obtained from the studies on the inhibition of Pgp mediated efflux of ^{3}H-digoxin (the ^{3}H-digoxin transport inhibition factor) and on the Pgp substrate efflux ratio were analysed using an unpaired Student's t-test (two-tailed) or one-way analysis of variance (ANOVA) (Graphpad Instat®, version 3.00). A value of $p<0.05$ was considered a significant difference. Linear regression analysis of the P_{app}, cLogP, PSA and LogBB values was performed using S-plus (version 6.0 professional, release 1, Insightful corporation, USA) without a weight factor at a confidence level of 0.95. All data are expressed as mean ± SEM, unless indicated otherwise. Each experiment was performed in duplicate in at least three separate experiments.

RESULTS

Opioid inhibition of Pgp mediated efflux of ^{3}H-digoxin –"the ^{3}H-digoxin transport inhibition factor"

The inhibitory properties of the seven selected opioids and the morphine metabolites M3G and M6G were studied in MDCKII:MDR1 and LLC-PK1:MDR1a cells. Transport of ^{3}H-digoxin from the basolateral to the apical side of the monolayers was measured in the presence of vehicle, 2 mM GF120918 or 100 mM of the opioids. The results are shown in figure 2.

Alfentanil, fentanyl, sufentanil, morphine and loperamide were able to inhibit the Pgp mediated ^{3}H-digoxin transport in both cell-lines. In contrast, nalbuphine and butorphanol, M3G and M6G could not. According to the ^{3}H-digoxin transport inhibition factor, a ranking can be made. For the opioids the ranking (strong to weak) is as follows: fentanyl, sufentanil, loperamide, alfentanil, morphine and nalbuphine / butorphanol. This ranking was similar for both cell-lines. Furthermore, the inhibition of Pgp mediated efflux of ^{3}H-digoxin by the opioids was significantly weaker than by the Pgp inhibitor GF120918.

Pgp substrate assessment – "the Pgp substrate efflux ratio"

The next step was to determine the Pgp substrate efflux ratio of the opioids in the monolayers of the MDCKII:MDR1 cells. The results are shown in figure 3. No statistically significant differences were found in the Pgp substrate efflux ratios for alfentanil, fentanyl, sufentanil and butorphanol in the presence or absence of GF120918. For loperamide, a Pgp substrate efflux ratio of 4 was found. This efflux ratio decreased to 1.0 in the presence of GF120918, indicating that the asymmetrical transport was

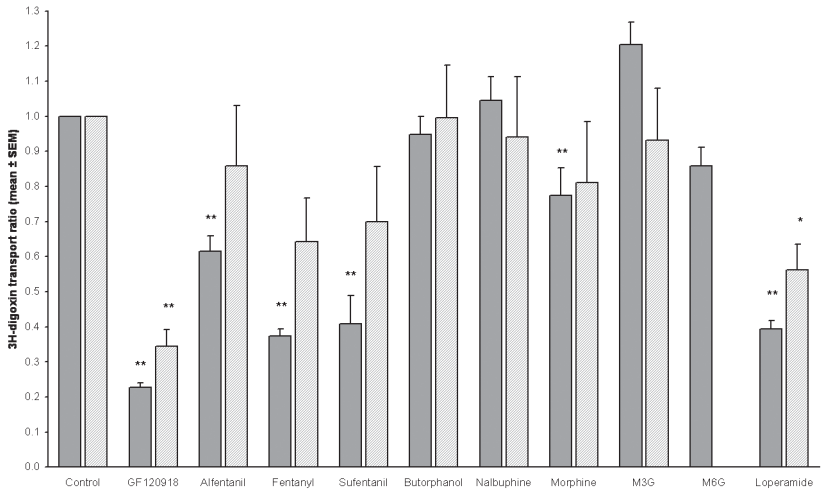

Figure 2: ^{3}H-digoxin transport inhibition factors in the presence of vehicle (control), 2 μM GF120918 or 100 μM opioid in MDCK:MDR1 (solid bars) and LLC-PK1:MDR1a cells (striped bars). The ^{3}H-digoxin transport inhibition factors are represented as a fraction of the control. Statistically significant differences were denoted as ** for P<0.01, * for P<0.05: for control versus opioid/GF120918.

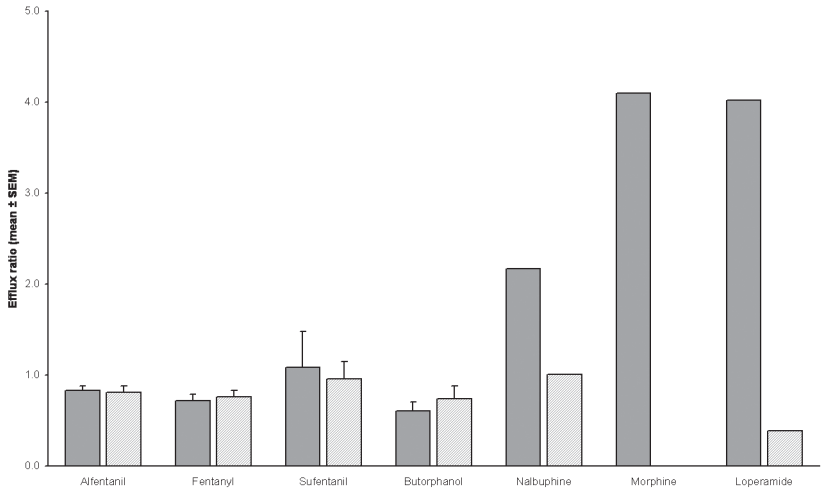

Figure 3: Assessment of opioid transport by Pgp. The Pgp substrate efflux ratios for the tested opioids, using the monolayers of MDCK:MDR1 cells. The efflux ratios were determined in the presence of vehicle (dark bars) as well as in the presence of 2 μM GF120918 (light bars). An efflux ratio larger than 1.5 was considered to reflect a significant involvement of Pgp in membrane transport. For nalbuphine literature values were used (Mahar Doan *et al.* 2002).

caused by Pgp solely. For morphine and nalbuphine the concentrations in the receiving compartment were below the limit of quantification of the assay when using the donor concentration of 3 µM. Therefore, the values obtained at a donor concentration of 10 or 100 µM for nalbuphine and morphine were used, respectively.

Apparent transmembrane passive permeability rates; the P_{app} values

The P_{app} values of the opioids were calculated on the basis of the amount transported across the monolayer over time (nm/s), in both directions, in the presence of GF120918. The results are shown in figure 4.

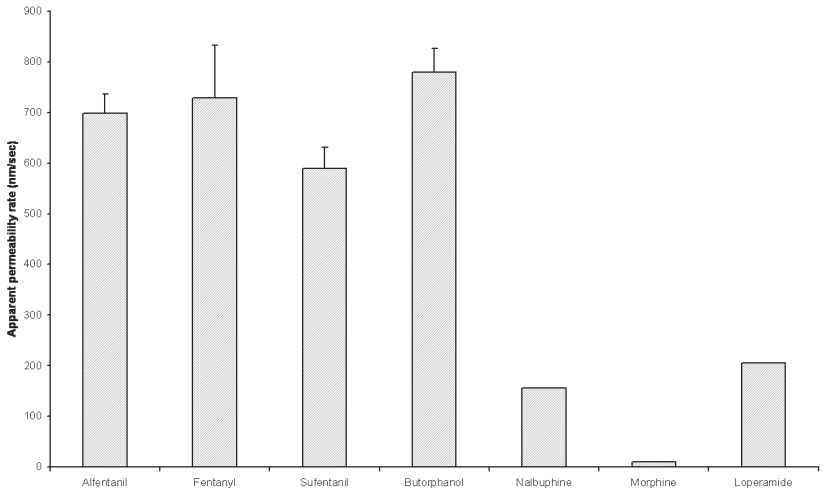

Figure 4: Calculated apparent transmembrane passive permeability rate values of the opioids across the MDCK: MDR1 monolayer, as determined at a donor concentration of 3µM of the opioid in the presence of the Pgp inhibitor GF120918. For nalbuphine literature values were used (Mahar Doan et al. 2002).

P_{app} values > 500 nm/s were found for alfentanil, fentanyl, sufentanil and butorphanol, whereas the P_{app} values of nalbuphine and loperamide were 156 and 206 nm/s, respectively. For morphine, the P_{app} value was 11 nm/s, indicating that almost no morphine is transported across the monolayer within the experimental period of 90 min.

Quantitative structure activity relationships: physico-chemical relationships

The values of P_{app}, cLogP, LogBB, PSA and CMR are listed in table 1. Regression analysis was performed to investigate the possible correlations between the apparent permeability and the physico-chemical properties of the selected opioids. Linear regression was performed with the P_{app} and $LogP_{app}$ values, but no significant correlations were found. However, the $LogP_{app}$ values gave slightly better correlations (figure 5).

Table 1: Physicochemical properties of opioids

			Abraham equation							
Name	**Mw**	**cLogP**	R_2	π^H_2	α^H_2	β^H_2	V_x	**LogBB**	**PSA**	**CMR**
Alfentanil	416.6	2.1	2.58	3.02	0	2.04	3.26	0.277	85.5	11.5
Fentanyl	336.5	3.6	2.08	2.21	0	1.23	2.84	0.886	23.6	10.4
Sufentanil	386.6	3.6	2.07	2.26	0	1.49	3.11	0.932	32.8	11.3
Nalbuphine	357.5	1.4	2.34	1.91	0.81	2.08	2.62	-0.247	73.2	9.6
Butorphanol	327.5	3.7	2.02	1.7	0.8	1.48	2.61	0.253	43.7	9.5
Morphine	285.4	0.6	2.1	1.68	0.55	1.76	2.06	-0.28	52.9	7.7
Loperamide	477.1	4.7	2.85	2.98	0.35	2.11	3.77	0.566	43.8	14.1

Abbreviations: Mw – molecular weight, cLogP – calculated LogP value, which is indicative for lipophilicity, R_2, π^H_2, α^H_2, β^H_2 and V_x – descriptors for Abraham equation, LogBB = BBB transport on basis of Abraham equation PSA = polar surface area (Å), and CMR = calculated molecular refractivity, which is indicative for size of molecule.

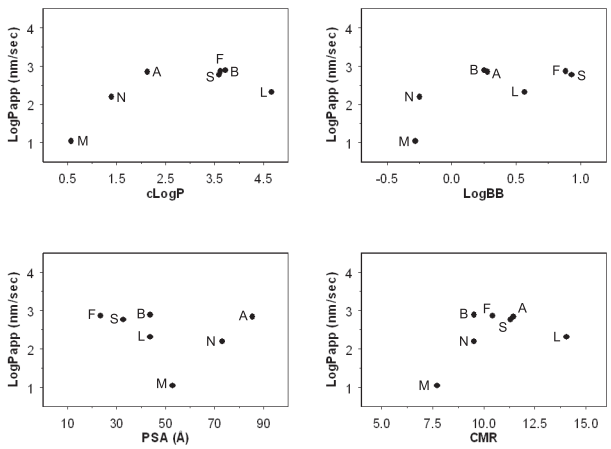

Figure 5: Correlation between the $LogP_{app}$ and the physicochemical properties of the opioids. The compounds are depicted with the first letter of the opioid name.

DISCUSSION

The main objective of these studies was to characterise the membrane transport characteristics of the opioids alfentanil, fentanyl, sufentanil, nalbuphine, butorphanol, morphine and loperamide. The focus was on the relative contributions of the passive membrane permeability rates and Pgp mediated active transport as mechanisms that determine the overall membrane passage. This is important for the development of a mechanism-based PK-PD model for the central effects of opioids, since opioids have to pass the membrane of the the BBB in order to reach their target and to exert their central effect.

Large differences were found between the opioids in the values for passive transmembrane permeability rates (P_{app}) and for the interaction with Pgp. The results show that the contribution of Pgp mediated transport should be taken into account for opioids with a low passive transmembrane permeability rate, whereas for opioids with a high passive permeability rate no significant contribution of Pgp mediated transport on membrane passage is to be expected.
The biophase kinetics of a CNS drug is an important determinant in the time course and intensity of its CNS effects. Apart from plasma pharmacokinetics, the mechanisms that determine CNS biophase kinetics include the rate and extent of BBB transport, and the kinetics of distribution and elimination within the brain. Transport across the BBB can be divided into passive and active transport processes (de Lange & Danhof 2002). Active transport processes are mediated by transporters, such as the Pgp, which has been shown to be an important efflux transporter at the BBB for many drugs. Therefore, the relative contribution of Pgp on overall BBB membrane transport is of interest. Our approach was to characterise the contribution of Pgp mediated transport, relative to passive membrane diffusion, on the overall membrane transport. Investigations were performed for the whole set of opioids, using a robust *in vitro* system composed of monolayers of Pgp-expressing cells. Monolayers of both MDCKII-MDR1 (transfected with the human MDR1 gene that encodes for Pgp) and of LLC-PK1:MDR1a cells (transfected with the mouse MDR1a gene) were used in these studies. These cell systems were chosen because of their very tight junction, which is similar to brain endothelia cells. If significant differences in Pgp mediated transport by the human and rodent gene products would be identified, these findings could be used to improve interspecies extrapolation of PK-PD relationships.

A number of *in vitro* studies has been performed with monolayers of LLC-PK1:MDR1 cells. However, these studies mainly focussed on morphine, loperamide and fentanyl (Schinkel *et al.* 1995, 1996; Wandel *et al.* 2002). Nalbuphine was only investigated once (Mahar Doan *et al.* 2002), whereas butorphanol has never been tested for Pgp interaction. For our ultimate goal, which is the development of a mechanistic PK-PD model for opioids, it was necessary to test all the selected opioids for Pgp interaction in the same experimental design. Moreover, unlike in previous studies, here the relative contribution of Pgp mediated efflux relative to the passive membrane transport component was explicitely addressed.

The inhibition of Pgp mediated efflux of ^{3}H-digoxin by the opioid (the ^{3}H-digoxin inhibition factor) was determined at a concentration of 100 µM of the opioid or 3 µM GF120918. The transport of ^{3}H-digoxin was measured from basolateral to apical direction (what would correspond with brain efflux). Efflux ratios were not calculated because the transport from apical to basolateral was very low and therefore the variability was between the wells was very high when efflux ratios were used. Inhibition of

Pgp mediated transport of ^{3}H-digoxin was found for alfentanil, fentanyl, sufentanil and loperamide, in accordance with the results found by Wandel and co-workers (Wandel *et al*. 2002). Interestingly, in our experiments morphine was identified as a Pgp inhibitor. In contrast, Wandel and co-workers (2002) did not show an inhibition of Pgp mediated efflux of ^{3}H-digoxin when using a 5-fold lower morphine concentration. This indicates that the interaction of morphine and Pgp is relatively weak. No inhibition of Pgp mediated efflux of ^{3}H-digoxin was found for nalbuphine, butorphanol and the morphine metabolites M3G and M6G. GF120918 inhibited the ^{3}H-digoxin efflux to 20%. Interestingly, the ^{3}H-digoxin transport ratio could not be completely inhibited by GF120918 although GF120918 is a very potent Pgp inhibitor. This indicates that other transporters might be involved in the efflux of ^{3}H-digoxin. In general, identical results were obtained using either the MDCKII:MDR1 or the LLC-PK1:MDR1a monolayers, though the variability in the LLC-PK1:MDR1a cells was a little higer. Taken together, these inhibition studies show that Pgp could influence the membrane transport characteristics of alfentanil, fentanyl, sufentanil, morphine and loperamide.

The Pgp substrate efflux ratio was determined for all opioids. For alfentanil, fentanyl and sufentanil no Pgp mediated transport could be found, in accordance with literature (Wandel *et al.* 2002). For loperamide a Pgp efflux ratio value of 4 was found, confirming that loperamide is a strong Pgp substrate (Schinkel *et al*. 1995, 1996; Wandel *et al.* 2002). For morphine and nalbuphine, the Pgp substrate efflux ratio was initially determined at a donor concentration of 3 µM. Under these conditions the concentrations in the acceptor phase were below the limit of quantification of the assay. Therefore, morphine has been investigated at a donor concentration of 100 µM and was clearly detected as Pgp substrate (with an efflux ratio of 4). For nalbuphine, literature values were included (Mahar Doan *et al*. 2002) to calculate a Pgp substrate efflux ratio value of 2. This would indicate that nalbuphine is a substrate for Pgp, while an absence of inhibition of Pgp mediated transport of ^{3}H-digoxin by nalbuphine was found. This apparent contradiction might be explained by the existence of several Pgp binding sites (Martin *et al*. 2000).

The P_{app} values of <50, 50-250, >250 nm/sec were considered as low, moderate and high, respectively. Thus, for morphine a low permeability was found; for loperamide and nalbuphine a moderate permeability, and for alfentanil, fentanyl, sufentanil and butorphanol a high permeability. For alfentanil, fentanyl and sufentanil the high P_{app} values explain why these opioids could not be identified as Pgp substrates. The potential contribution of Pgp mediated transport to the overall membrane transport is too low to be detected, and therefore not of any significance. In contrast, for loperamide and morphine, the P_{app} values were very low, which means that their Pgp mediated transport is of more much relevance in the overall membrane passage. To summarise, these results emphasise that the passive transmembrane permeability rates should be considered when investigating the impact of Pgp interaction on membrane transport.

Our interest was to predict the impact of BBB transport on the *in vivo* PK-PD relationships of opioids. In the current experiment *in vitro* cell systems have been used, made up from kidney epithelium cells, for its robustness. For an extrapolation of the results found in this study to the *in vivo* BBB transport characteristics it should be realised that the BBB is comprised of brain capillary endothelial cells, which may differ from the kidney epithelial cells used in this study in terms of membrane characteristics and paracellular spaces, while also the functionality of Pgp may differ. Such differences may explain why fentanyl, in a study using an *in vitro* cell-system comprising of brain capillary endothelial cells, could be identified as a borderline Pgp substrate (Henthorn *et al.* 1999). However, though small quantitative differences may exist between epithelial and endothelial membranes, the investigation of a whole set of opioids in a similar set-up will provide useful information on transport characteristics, which can be related to the differences observed in the *in vivo* PK-PD relationships. Therefore, based on the P_{app} values, it is to be expected that for morphine, loperamide and nalbuphine, passive transport across the BBB membrane plays a role in the PK-PD relation of centrally mediated effects. For alfentanil, fentanyl, sufentanil and butorphanol, a significant influence of BBB transport can be excluded. However, biophase pharmacokinetic processes like distribution within the brain should still be considered (Liu *et al*. 2005).

Based on the results presented here, a role of Pgp and BBB transport is expected *in vivo* for loperamide, morphine and potentially nalbuphine. Previously, the distribution of ^{3}H-loperamide has been investigated in MDR1a wild-type and knock-out mice. A 13.5 times higher concentration of ^{3}H-loperamide was found in the brain of knock-out mice compared with the wild-type (Schinkel *et al*. 1996). For morphine, Letrent and co-workers showed that the anti-nociceptive effect in rats was prolonged after oral administration of GF120918, due to its prolonged half-life of in the brain (Letrent *et al.* 1998, 1999a). For fentanyl, in MDR1a wild-type and knock-out mice it was shown that Pgp has a very small effect on the distribution and the anti-nociceptive effect (Dagenais *et al*. 2004;Thompson *et al*. 2000). However, it should be noted that variability in the anti-nociceptive data is relatively high and that the influence of Pgp on pharmacokinetics in blood and plasma was not considered in this study. For alfentanil, fentanyl, sufentanil and butorphanol no significant influence of Pgp and BBB transport on their central effects is expected.

In the last years, several *in silico* methods have been developed to predict passive BBB transport on the basis of physico-chemical properties, as reviewed by Clark and Norinder (Clark 2003; Norinder & Haeberlein 2002). These methods include the relationship between polar surface area and BBB penetration (Clark 1999; Kelder *et al*. 1999; Norinder & Haeberlein 2002; van de Waterbeemd *et al.* 1998). Abraham and co-workers have developed an *in silico* method that predicts passive BBB transport on the basis of several descriptors, including excess molar refraction, dipolarity/polarisability,

hydrogen bonding and size of the molecule (Abraham *et al.* 1994). Recently, it has been found that the dynamic polar surface area (non-linear) and logBB as calculated by the Abraham equation (linear) were significantly related to the *in vitro* BBB clearance values of a set of 11 structurally highly related adenosine A_1 receptor agonists (Schaddelee *et al.* 2003). It was therefore of interest to investigate the potential of *in silico* prediction of the *in vitro* values for passive membrane transport for the whole set of opioids in this study. Thus, the relationships between P_{app} values and physicochemical properties were investigated by regression analysis. No significant correlations could be identified. This may be explained by the limited number of opioids included in the present analysis. Moreover, these opioids can be divided in two structurally different groups (figure 1). Taken together, in this stage, no conclusions can be drawn about the predictability of BBB transport of opioids on the basis of physicochemical properties.

It is concluded that the relative contribution of both Pgp mediated transport and passive permeability across the BBB should be considered in the PK-PD relationships of opioids. For alfentanil, fentanyl, sufentanil and butorphanol, all having a high passive permeability value, membrane transport will be insensitive to Pgp. For nalbuphine, morphine and loperamide membrane transport is influenced by active Pgp transport, because of their low passive permeability membrane transport rates.

ACKNOWLEDGEMENTS

The authors wish to acknowledge the technical assistance of Nipa Shah and Caroline Brough (Drug Metabolism and Pharmacokinetics, GlaxoSmithKline, United Kingdom), Rebecca Scott and Phil Dennif (World Wide Bio-analysis, GlaxoSmithKline, United Kingdom) and Margret Blom (Department of Pharmacology, LACDR, The Netherlands). The described work was financially supported by GlaxoSmithKline, United Kingdom.

REFERENCES

Abraham MH, Chadha HS, Mitchell RC (1994) Hydrogen bonding. 33. Factors that influence the distribution of solutes between blood and brain. *J.Pharm.Sci.* **83:** 1257-1268

Breimer DD, Danhof M (1997) Relevance of the application of pharmacokinetic-pharmacodynamic modelling concepts in drug development. The “wooden shoe” paradigm. *Clin.Pharmacokinet.* **32:** 259-267

Clark DE (1999) Rapid calculation of polar molecular surface area and its application to the prediction of transport phenomena. 2. Prediction of blood-brain barrier penetration. *J.Pharm.Sci.* **88:** 815-821

Clark DE (2003) In silico prediction of blood-brain barrier permeation. *Drug Discov.Today* **8:** 927-933

Cox EH, Kerbusch T, van der Graaf PH, Danhof M (1998) Pharmacokinetic-pharmacodynamic modeling of the electroencephalogram effect of synthetic opioids in the rat: correlation with the interaction at the mu-opioid receptor. *J Pharmacol.Exp.Ther.* **284:** 1095-1103

Dagenais C, Graff CL, Pollack GM (2004) Variable modulation of opioid brain uptake by P-glycoprotein in mice. *Biochem Pharmacol* **67:** 269-276

Danhof M, Alvan G, Dahl SG, Kuhlmann J, Paintaud G (2005) Mechanism-based pharmacokinetic-pharmacodynamic modeling-a new classification of biomarkers. *Pharm.Res.* **22:** 1432-1437

De Boer AG, Van der Sandt I, Gaillard PJ (2003) The role of drug transporters at the blood-brain barrier. *Annu. Rev.Pharmacol Toxicol.* **43:** 629-656

De Lange EC, Danhof M (2002) Considerations in the use of cerebrospinal fluid pharmacokinetics to predict brain target concentrations in the clinical setting: implications of the barriers between blood and brain. *Clin. Pharmacokinet.* **41:** 691-703

Ertl P, Rohde B, Selzer P (2000) Fast calculation of molecular polar surface area as a sum of fragment-based contributions and its application to the prediction of drug transport properties. *Journal of Medicinal Chemistry* **43:** 3714-3717

Groenendaal D, Blom-Roosemalen MC, Danhof M, de Lange EC (2005) High-performance liquid chromatography of nalbuphine, butorphanol and morphine in blood and brain microdialysate samples: application to pharmacokinetic/ pharmacodynamic studies in rats. *J.Chromatogr.B Analyt.Technol.Biomed.Life Sci.* **822:** 230-237

Henthorn TK, Liu Y, Mahapatro M, Ng KY (1999) Active transport of fentanyl by the blood-brain barrier. *J.Pharmacol. Exp.Ther.* **289:** 1084-1089

Kelder J, Grootenhuis PD, Bayada DM, Delbressine LP, Ploemen JP (1999) Polar molecular surface as a dominating determinant for oral absorption and brain penetration of drugs. *Pharm.Res.* **16:** 1514-1519

Letrent SP, Pollack GM, Brouwer KR, Brouwer KL (1998) Effect of GF120918, a potent P-glycoprotein inhibitor, on morphine pharmacokinetics and pharmacodynamics in the rat. *Pharm.Res.* **15:** 599-605

Letrent SP, Pollack GM, Brouwer KR, Brouwer KL (1999a) Effects of a potent and specific P-glycoprotein inhibitor on the blood- brain barrier distribution and antinociceptive effect of morphine in the rat. *Drug Metab Dispos.* **27:** 827-834

Letrent SP, Polli JW, Humphreys JE, Pollack GM, Brouwer KR, Brouwer KL (1999b) P-glycoprotein-mediated transport of morphine in brain capillary endothelial cells. *Biochem.Pharmacol.* **58:** 951-957

Liu X, Smith BJ, Chen C, Callegari E, Becker SL, Chen X, Cianfrogna J, Doran AC, Doran SD, Gibbs JP, Hosea N, Liu J, Nelson FR, Szewc MA, Van Deusen J (2005) Use of a physiologically based pharmacokinetic model to study the time to reach brain equilibrium: an experimental analysis of the role of blood-brain barrier permeability, plasma protein binding, and brain tissue binding. *J.Pharmacol.Exp.Ther.* **313:** 1254-1262

Mahar Doan KM, Humphreys JE, Webster LO, Wring SA, Shampine LJ, Serabjit-Singh CJ, Adkison KK, Polli JW (2002) Passive permeability and P-glycoprotein-mediated efflux differentiate central nervous system (CNS) and non-CNS marketed drugs. *J.Pharmacol.Exp.Ther.* **303:** 1029-1037

Martin C, Berridge G, Higgins CF, Mistry P, Charlton P, Callaghan R (2000) Communication between multiple drug binding sites on P-glycoprotein. *Mol.Pharmacol.* **58:** 624-632

Norinder U, Haeberlein M (2002) Computational approaches to the prediction of the blood-brain distribution. *Adv. Drug Deliv.Rev.* **54:** 291-313

Platts JA, Butina D, Abraham MH, Hersey A (1999) Estimation of molecular linear free energy relation descriptors using a group contribution approach. *J.Chem.Inform.Comp.Sci.* **39:** 835-845

Schaddelee MP, Voorwinden HL, Groenendaal D, Hersey A, IJzerman AP, Danhof M, de Boer AG (2003) Blood-brain barrier transport of synthetic adenosine A1 receptor agonists in vitro: structure transport relationships. *Eur. J Pharm.Sci* **20:** 347-356

Schinkel AH, Wagenaar E, Mol CA, van Deemter L (1996) P-glycoprotein in the blood-brain barrier of mice influences the brain penetration and pharmacological activity of many drugs. *J.Clin.Invest* **97:** 2517-2524

Schinkel AH, Wagenaar E, van Deemter L, Mol CA, Borst P (1995) Absence of the mdr1a P-Glycoprotein in mice affects tissue distribution and pharmacokinetics of dexamethasone, digoxin, and cyclosporin A. *J.Clin.Invest* **96:** 1698-1705

Thiebaut F, Tsuruo T, Hamada H, Gottesman MM, Pastan I, Willingham MC (1987) Cellular localization of the multidrug-resistance gene product P-glycoprotein in normal human tissues. *Proc.Natl.Acad.Sci U.S.A.* **84:** 7735-7738

Thompson SJ, Koszdin K, Bernards CM (2000) Opiate-induced analgesia is increased and prolonged in mice lacking P- glycoprotein. *Anesthesiology* **92:** 1392-1399

Tran TT, Mittal A, Aldinger T, Polli JW, Ayrton A, Ellens H, Bentz J (2005) The elementary mass action rate constants of P-gp transport for a confluent monolayer of MDCKII-hMDR1 cells. *Biophysical Journal* **88:** 715-738

Tran TT, Mittal A, Gales T, Maleeff B, Aldinger T, Polli JW, Ayrton A, Ellens H, Bentz J (2004) Exact kinetic analysis of passive transport across a polarized confluent MDCK cell monolayer modeled as a single barrier. *J.Pharm.Sci.* **93:** 2108-2123

Van Bree JB, de Boer AG, Danhof M, Ginsel LA, Breimer DD (1988) Characterization of an “in vitro” blood-brain barrier: effects of molecular size and lipophilicity on cerebrovascular endothelial transport rates of drugs. *J.Pharmacol Exp.Ther*. **247:** 1233-1239

Van de Waterbeemd H, Camenisch G, Folkers G, Chretien JR, Raevsky OA (1998) Estimation of blood-brain barrier crossing of drugs using molecular size and shape, and H-bonding descriptors. *J Drug Target* **6:** 151-165

van der Graaf PH, Danhof M (1997) Analysis of drug-receptor interactions in vivo: a new approach in pharmacokinetic-pharmacodynamic modelling *Int.J Clin.Pharmacol.Ther.* **35:** 442-446

Wandel C, Kim R, Wood M, Wood A (2002) Interaction of morphine, fentanyl, sufentanil, alfentanil, and loperamide with the efflux drug transporter P-glycoprotein. *Anesthesiology* **96:** 913-920

Chapter 5

POPULATION PHARMACOKINETIC MODELLING OF NON-LINEAR BRAIN DISTRIBUTION OF MORPHINE: INFLUENCE OF ACTIVE SATURABLE INFLUX AND P-GLYCOPROTEIN MEDIATED EFFLUX

Dorien Groenendaal[1], Jan Freijer[2], Dennis de Mik[1], M. René Bouw[3], Meindert Danhof[1,2] and Elizabeth C.M. de Lange[1]

[1]Leiden Amsterdam Center for Drug Research, Leiden University, Division of Pharmacology, Leiden, The Netherlands, [2]LAP&P Consultants BV, Leiden, The Netherlands, [3]GlaxoSmithKline, Clinical Pharmacokinetics Neurology, Harlow, United Kingdom

British Journal of Pharmacology (2007) **151**, 701-712

SUMMARY

Background and purpose

Biophase equilibration must be considered to get more insight into the mechanisms underlying the pharmacokinetic-pharmacodynamic (PK-PD) correlations of opioids. The objective was to characterise in a quantitative manner the non-linear brain distribution kinetics of morphine.

Experimental approach

Male rats received a 10-min infusion of 4 mg/kg of morphine, combined with a continuous infusion of the Pgp inhibitor GF120918 or vehicle, or 40 mg/kg. Unbound extracellular fluid (ECF) concentrations obtained by intracerebral microdialysis and total blood concentrations were analysed using a population modelling approach.

Key results

Blood pharmacokinetics of morphine was best described with a three-compartment model and was not influenced by GF120918. Non-linear distribution kinetics in brain ECF was observed with increasing dose. A one compartment distribution model was developed, with separate expressions for passive diffusion, active saturable influx and active efflux by Pgp. The passive diffusion rate constant was 0.0014 min^{-1}. The active efflux rate constant decreased from 0.0195 min^{-1} to 0.0113 min^{-1} in the presence of GF120918. The active influx was insensitive to GF120918 and had a maximum transport (N_{max}/V_{ecf}) of 0.66 ng/min·ml and is already saturated at low concentrations of morphine (C_{50} = 9.9 ng/ml).

Conclusions and implications

Brain distribution of morphine is determined by 1) limited passive diffusion, 2) active efflux, reduced by 42% by Pgp inhibition and 3) low capacity active uptake. This implies blood concentration-dependency and sensitivity to drug-interactions. These factors should be taken into account in further investigations on PK-PD correlations of morphine.

INTRODUCTION

The influence of biophase equilibration must be considered to get more insight into the mechanisms underlying the pharmacokinetic-pharmacodynamic (PK-PD) correlation of opioids. Biophase equilibration is mainly determined by blood brain-barrier (BBB) transport. The influence of BBB transport is dependent on (1) the morphology and functionality of the brain capillary endothelial cells representing the BBB, (2) the physiochemical properties of the drug and (3) the affinity of the drug for specific transporters present at the BBB. Transport across the BBB can be divided in passive and active transport processes. An important efflux transporter at the BBB is P-glycoprotein (Pgp), which is a member of the adenosine triphosphate-binding cassette super family and is encoded by the multidrug resistance gene (MDR1) (Thiebaut *et al.* 1987). This transporter has been shown to have an important influence on the brain distribution of a wide range of drugs (de Lange & Danhof 2002; Schinkel *et al.* 1995; 1996).

It is known from literature that opioids are substrate for Pgp (Henthorn *et al.* 1999; Letrent *et al.* 1998; 1999a; 1999b; Mahar Doan *et al.* 2002; Schinkel *et al.* 1995; 1996) (Henthorn *et al.* 1999; Wandel *et al.* 2002). Recently, the relative contribution of Pgp mediated transport and passive permeability on the membrane transport of a wide range of opioids have been studied in an *in vitro* cell system comprising of MDCKII cells transfected with the human Pgp (chapter 4). It was shown that the influence of Pgp on membrane transport is highly dependent on the passive permeability of the opioids. Passive permeability is dependent on physicochemical properties like lipophilicity (van Bree *et al.* 1988); hydrophilic drugs are expected to have a low passive permeability whereas lipophilic drugs often have a high passive permeability. Alfentanil, fentanyl and sufentanil all have affinity for Pgp but the influence of Pgp mediated transport is minimal because of the high passive permeability rates of these opioids. In contrast, Pgp has as significant influence on the transport of morphine, loperamide and nalbuphine, because their passive permeability is relatively low. For morphine, transcortical microdialysis studies in Pgp-deficient mice (mdr1a -/- mice) and wild-type (mdr1a +/+) mice have shown that active transport mechanisms influence the brain distribution *in vivo* (Xie *et al.* 1999). In addition, brain perfusion studies have shown that the brain uptake is 1.24 times higher in mdr1a -/- mice compared to mdr1a +/+ mice (Dagenais *et al.* 2004).
Furthermore, PK-PD studies in rats have revealed that after oral pre-treatment with the specific Pgp inhibitor GF120918, the anti-nociceptive effect of morphine was prolonged due to its prolonged half-life in the brain (Letrent *et al.* 1998; 1999a). Bouw and co-workers have proposed a compartmental model to account for the delay of the anti-nociceptive effect of morphine relative to corresponding plasma concentrations (Bouw *et al.* 2000; 2001). It was found that BBB transport accounts for 84% of the observed hysteresis of morphine.

The present investigations focus on the BBB transport of morphine in relation to the effect on the electroencephalogram (EEG) (Groenendaal *et al*., 2007 – chapter 6). For this purpose, the combined-EEG/microdialysis technique has been developed, which allows simultaneous investigation of both BBB transport and quantitative EEG monitoring in the same rat. The objective of this study was to characterise in a quantitative manner the relative contributions of passive and active transport mechanisms of morphine across the BBB upon intravenous administration of two distinct doses of morphine.

METHODS

Study design

In order to investigate the influence of BBB transport on the PK-PD correlation of the EEG effect of morphine, the study was divided in three separate experiments, (1) EEG experiments, (2) combined EEG/MD experiments and (3) MD experiments. An overview of the experimental groups is shown in table 1. This paper focuses on the investigation of the transport mechanisms of morphine across the BBB (experiment 2 and 3) on the basis of population PK analysis of blood and extracellular fluid concentrations. The PK-PD analysis of the EEG effect of morphine (experiment 1 and 2) will be discussed in a separate paper (Groenendaal *et al*., 2007 – chapter 6).

Table 1: Experimental design of the studies investigating the PK-PD relationships of the EEG effects of morphine in rats

Dose	Treatment	Method	N	Bodyweight (kg)	Perfusate conc (ng/kg)		
					0	50	500
4 mg/kg	Vehicle	EEG	7	0.294 ± 0.023	n/a	n/a	n/a
		EEG/MD	14	0.297 ± 0.014	N =10	N = 3	N = 3
		MD	3	0.304 ± 0.023	N = 3		
	GF120918	EEG/MD	20	0.300 ± 0.030	N = 10	N = 5	N = 5
10 mg/kg	Vehicle	EEG	7	0.260 ± 0.015	n/a	n/a	n/a
40 mg/kg	Vehicle	EEG	5	0.273 ± 0.026	n/a	n/a	n/a
		EEG/MD	15	0.306 ± 0.019	N = 9	N = 3	N = 3

Chemicals

Morphine hydrochloride was purchased from Pharmachemie (Haarlem, The Netherlands) and GF120918 was kindly provided by GlaxoSmithKline (United Kingdom). Midazolam was obtained from BUFA (Uitgeest, The Netherlands). Vecuronium bromide (Norcuron®), heparin (20 U/ml) and physiological saline (0.9%) were both obtained from the hospital pharmacy of the Leiden University Medical

Center (Leiden, The Netherlands). All chemicals were of analytical grade and solvents were of HPLC grade.

Microdialysis materials

Microdialysis probes, CMA/12 (4 mm, 400 µm inner diameter, 500 µm outer diameter) were supplied by Aurora Borealis Control BV (Schoonebeek, The Netherlands). The probe consisted of a polycarbonate-polyether co-polymeric membrane with a molecular cut-off of 20 kDa. The perfusion solution for microdialysis contained (in mM): NaCl 145, KCl 0.6, $MgCl_2$ 1.0, $CaCl_2$ 1.2 and ascorbic acid 0.2 in phosphate buffer, pH 7.4 (Moghaddam & Bunney 1989). The probes were connected to a BAS Beehive infusion pump (Bioanalytical systems Inc., Indiana, USA) with polyethylene tubing (O.D. 0.61 mm, I.D. 0.28 mm) supplied by Aurora Borealis Control BV (Schoonebeek, The Netherlands). Before use, the probes were activated according to the manufacturer's protocol (CMA, Sweden).

Animals

The protocol of these studies was approved by the Committee of Animal Experimentation of the Leiden University. Male Wistar rats weighing between 250-350 grams (Charles River, Maastricht, The Netherlands) were housed in groups for at least 7 days under standard environmental conditions (temperature 21 °C, humidity 60% and 12/12 hour dark/light cycle, with lights on at 7 AM). The animals had access to standard laboratory chow (RMH-TM, Hope Farms, Woerden, The Netherlands) and acidified water *ad libitum*. During the experiments, the animals were deprived of food and water.

Surgical procedures

The rats were divided into two different groups, the EEG/MD group (N=52) and the MD group (N=3). All rats were anesthetized with an intramuscular injection of 0.1 mg/kg Domitor® (1 mg ml-1 medetomidine hydrochloride, Pfizer, Capelle a/d IJssel, The Netherlands) and a subcutaneous injection of 1 mg/kg Ketalar® (50 mg/ml Ketaminebase, Parke-Davis, Hoofddorp, The Netherlands). Ten days before the start of the experiments, four cortical electrodes were stereotactically implanted into the skull of the EEG rats as described before (Cox *et al.* 1997). Briefly, the electrodes were placed at the locations 11 mm anterior and 2,5 mm lateral (F_l), 3 mm anterior and 3,5 mm lateral (C_l) and 3 mm posterior and 2,5 mm lateral (O_l) to lambda. A reference electrode was placed on lambda. In addition, a CMA/12 guide cannula with a dummy probe was placed in the striatum of the right brain hemisphere (anterior-posterior: +0.5 mm, lateral: +2.7 mm with bregma as reference and ventral: -3.5 mm ventral to the skull). The MD rats were only instrumented with a CMA/12 guide cannula with a dummy probe. The miniature connector and guide cannula were insulated and fixed to the skull with dental acrylic cement. For drug administration and the collection of blood samples, four indwelling cannulas were implanted to all groups of rats, one in

the right femoral artery for collection of serial blood samples and two in the left jugular vein (interna and externa) for morphine and midazolam administration. The fourth cannula was implanted into the right femoral vein to administer GF120918 or vehicle and vecuronium bromide. All cannulas were made from pyrogen free polyethylene tubing (Portex Limited, Hythe, Kent, United Kingdom). The arterial cannula consisted of 4 cm (I.D.=0.28, O.D.=0.61 mm) polyethylene tubing heat-sealed to 18 cm polyethylene tubing (I.D.=0.58, O.D.=0.96 mm). The venous cannula consisted of 3 cm (I.D.=0.28, O.D.=0.61 mm) polyethylene tubing heat-sealed to 10 cm polyethylene tubing (I.D.=0.58, O.D.=0.96 mm). The cannulas were subcutaneously tunnelled to the back of the neck of the rats. In order to prevent clotting the cannulas were filled with a 25% (w/v) polyvinylpyrrolidone (PVP, Brocacef, Maarssen, The Netherlands) solution in saline containing 50 IU/ml heparin (Pharmacy, Leiden University Medical Centre, Leiden, The Netherlands). During the surgical procedures, the body temperature of the rats was maintained constant at 38 °C using a CMA/140 temperature controller (Aurora Borealis, Schoonebeek, The Netherlands). After surgery, 4 mg ampicilline (A.U.V., Cuijk, The Netherlands) was administered to aid recovery. At 16 to 24 hours before the experiments, the dummy microdialysis probe was removed from the microdialysis guide and replaced by the brain probe (CMA/12, 4 mm membrane).

Microdialysis probe recovery

The microdialysis probe recovery was investigated both *in vitro* and *in vivo*. To check the flow rate through the microdialysis probes, the samples were collected in pre-weighed collection vials. At the end of the experiment, the vials were weighed to determine the volume collected within the sampling interval and thereby the flow rate.When the flow rate was too low (lower than 95% of 2µl/min) or too variable, the results were omitted from data analysis. The *in vitro* recovery was investigated to check the probe response time to changes in the bulk or perfusate in terms of rate and extent, as well as symmetry (gain=loss). Therefore, the probes were placed in blank perfusion fluid and perfused with blank perfusion fluid for 90 min to stabilize the system. Next, the probes were placed in perfusion fluid containing either 50 ng/ml or 500 ng/ml morphine and perfused with blank perfusion fluid for 90 min to determine the gain (equation 1).

$$\text{Recovery} = \frac{C_{out}}{C_b} \qquad (1)$$

Where C_{out} represents the morphine concentration in the dialysate outflow, and C_b represents the bath concentration in which the probes are placed. After a washout period (blank perfusion fluid in both bath and probe) of 90 min, the probes were placed in blank perfusion fluid and flushed with either 50 ng/ml or 500 ng/ml to determine the recovery using the retrodialysis method (Bouw & Hammarlund-Udenaes 1998). During the experiments, 15 minute fractions were collected at a flow rate of 2 µl/min. The *in vitro* recovery of morphine was calculated by measuring the loss of morphine

from the probe into the bath according to equation:

$$\text{Recovery}_{invivo} = \frac{C_{in} - C_{out}}{C_{in}} \quad (2)$$

Where C_{in} is the morphine concentration flushed through the microdialysis probe and C_{out} is the morphine concentration in the dialysate outflow. The recovery was also determined *in vivo* to take into account the influence of periprobe processes (Bungay *et al.* 1990) and was used to calculate ECF concentrations from microdialysate concentrations. The experiment was performed according to a combined retro-DNNF method to determine *in vivo* recovery in order to obtain concentration- as well as time-dependent recovery values of morphine. The probes were perfused for 60 min with a blank perfusion solution to stabilise the microdialysis and to obtain blank samples. Subsequently, according to a retrodialysis approach (Bouw & Hammarlund-Udenaes, 1998) the microdialysis probes were perfused with morphine concentrations of 0, 50 or 500 ng/ml (see table 1) for a period of 60 minutes before the intravenous administration of morphine, to determine whether the loss of morphine from the probe was concentration dependent or influenced by GF120918. The perfusion concentrations were maintained during the full experiment, according to the DNNF principle (Olson & Justice, Jr., 1993), in order to determine time-dependent values for *in vivo* recovery after iv administration of morphine. However, in contradiction to previous results for morphine in mice (Xie *et al.* 1999), in this case no conclusions could be drawn from the microdialysis data obtained for the DNNF rats after iv administration of morphine. Therefore these data were omitted from further analysis. The *in vivo* recovery was calculated from the retrodialysis period on the basis of the retrodialysis data of the 50 and 500 ng/ml perfusion concentrations (equation 2) and used to correct the microdialysis values obtained from the group of rats with the blank perfusion.

Experimental procedures

The EEG/MD rats were randomly divided in three groups and received a 10-min intravenous infusion of 4 or 40 mg/kg morphine combined with a continuous infusion of the Pgp inhibitor GF120918 or vehicle (figure 2). The MD rats all received a 10-min infusion of 4 mg/kg morphine and a continuous infusion of GF120918. Morphine hydrochloride was dissolved in saline. GF120918 infusion consisted of a 1-min bolus infusion of 6 mg/kg dissolved in DMSO followed by a continuous infusion of 25 ng/min dissolved in DMSO/glucose/cyclodextrine 5/5/10% in saline. All rats also received a continuous infusion of midazolam to prevent opioid induced seizure activity at a rate of 5.5 mg/kg·h (Cox *et al.* 1997). Midazolam solutions were prepared in physiological saline containing an equimolar concentration of hydrochloric acid, based on the body weight of the rat. To reach steady state rapidly, midazolam was administered according to a Wagner infusion scheme, with an initial infusion rate of 3 times the steady state infusion rate for 16 min (Wagner 1974).

All experiments started between 8.30 and 9.30 AM to minimise the influences of circadian rhythms. At the start of the experiment (t=-120 min), EEG recording was started (when applicable), the microdialysis probes were equilibrated for 60 min and the GF120918 or vehicle infusion was started. After 30 min (t=-90 min), midazolam infusion was started followed by the retrodialysis phase of the experiment (t=-60 min). Thereafter, at t=0 morphine was administered in a zero-order infusion for 10 minutes using a BAS Beehive infusion pump (Bioanalytical systems Inc., Indiana, USA). During the experiment, a total number of between 25 and 30 dialysate fractions (10 to 60 µl each) at a flow rate of 2 µl/min and 15 arterial blood samples (50 to 200 µl) were collected at pre-defined time intervals for determination of morphine concentrations. Additionally, 6 blood samples (50 µl) were collected for determination of GF120918 and midazolam concentrations. The total volume of blood collected did not exceed 2 ml (including blood gas samples, see below). During the experiments, body temperature was stabilised between 37.5 and 38.5 °C using a CMA/140 temperature controller (Aurora Borealis, Schoonebeek, The Netherlands). Bipolar EEG leads on the left hemisphere (C_l-O_l) were continuously monitored and analysed off-line with fast-Fourier transformation. Changes in the amplitudes in the δ-frequency band of the EEG (0.5-4.5 Hz) were used as a pharmacodynamic endpoint. Details of the EEG effect measurements will be presented in a separate paper.

Monitoring of blood gas status and artificial ventilation

During and after the infusion of morphine, arterial blood samples were collected to monitor arterial pH, pO_2 and pCO_2 levels using a Corning 248 Blood Gas Analyzer (Bayer, Meidrecht, The Netherlands) and to identify respiratory depression. During and after administration of 40 mg/kg morphine, severe respiratory depression and muscle rigidity occurred. These rats were artificially ventilated with preheated air (32 °C) using an Amsterdam Infant Ventilator, model MK3 (Hoekloos, Amsterdam, The Netherlands) through a custom made ventilation mask as described by Cox and co-workers (Cox *et al*. 1997). The ventilation settings were: ventilation frequency 62 beats/min, I-E ratio 1:2 and air supply flow rate 0.7-1.0 l/min. 5 minutes after start of the morphine infusion, the rats received an intravenous bolus dose of 0.15 mg vecuronium bromide dissolved in saline and artificial ventilation was started. Vecuronium bromide was used to counteract muscle rigidity to enable artificial ventilation. Vecuronium doses of 0.10 mg were administered repeatedly when muscle rigidity re-appeared until respiratory activity re-occurred. Blood gas status was carefully monitored during and after artificial ventilation.

Drug analysis

Morphine blood samples – Samples were analysed by high performance liquid chromatography with electrochemical detection (HPLC-ECD) as described previously (Groenendaal *et al.* 2005 – chapter 3). Briefly, after addition of internal standard

(nalorphine 500 ng/ml, 50 µl) the blood samples were alkalinised with carbonate buffer (0.15 mM, pH 11, 500 µl) and extracted with 5 ml ethyl acetate. The organic layer was transferred into clean glass tubes and evaporated to dryness under reduced pressure at 37 °C. The HPLC system consisted of a LC-10AD HPLC pump (Shimadzu, Kyoto, Japan), a Waters 717 plus autosampler (Waters, Milford, MA, USA), a pulse damper (Antec Leyden, Zoeterwoude, The Netherlands) and a digital electrochemical amperometric detector (DECADE, software version 3.02) from Antec Leyden. The electrochemical detector consisted of a VT-03 electrochemical flow cell combined with a 25 µm spacer and an Ag/AgCl reference electrode operating in the DC mode at a temperature of 30 °C, set at a voltage of +0.75V. Chromatography was performed on C18 Ultrasphere® 5 µm column (4.6 mm I.D. x 150 mm) (Alltech, Breda, The Netherlands) equipped with a refill guard column. The mobile phase was a mixture of 0.1 M phosphate buffer (pH 4) and methanol (75:25, v/v) and contained a total concentration of 20 mg/l EDTA and 2.0 mM octane-sulfonic acid. The flow rate was set at 1 ml/min. Data acquisition and processing was performed using the Empower integration software (Waters, Milford, MA, USA). The intra- and inter-assay variation was less than 10% and the lower limit of quantification was 25 ng/ml for a 50 µl blood sample.

Morphine dialysate samples – Samples were analysed by high performance liquid chromatography with electrochemical detection (HPLC-ECD) as described previously (Groenendaal *et al*., 2005 – chapter 3). The samples were analysed without sample pre-treatment. Internal standard nalorphine (500 ng/ml) was added to the samples in a 2:5 ratio, which means 2 µl of internal standard solution for every 5 µl of sample. Since the volume of the microdialysate samples varied throughout the experiment, this method was required to keep the concentration of internal standard constant in all samples. The HPLC system was the same as described for the blood samples. The electrochemical detector consisted of a VT-03 electrochemical flow cell combined with a 25 µm spacer and an Ag/AgCl reference electrode operating in the DC mode at a temperature of 30 °C, set at a voltage of +0.85V. Chromatography was performed on C18 Ultrasphere® 5 µm column (2.0 mm I.D. x 150 mm) (Alltech, Breda, The Netherlands) equipped with a refill guard column. The mobile phase was a mixture of 0.1 M phosphate buffer (pH 2.5) and methanol (75:25, v/v) and contained a total concentration of 20 mg/l EDTA and 10 mM octane-sulfonic acid. The flow rate was set at 0.15 ml/min. Data acquisition and processing was performed using the Empower integration software (Waters, Milford, MA, USA). The lower limit of quantification was 0.5 ng/ml for a 40 µl dialysate sample. The intra-assay variation was less than 0.1% and inter-assay variation was less than 10%.

GF120918 blood samples – Samples were analysed by high performance liquid chromatography with fluorescence detection. After addition of internal standard (chloropromazine, 500 ng/ml, 50 µl) the samples were alkalinised with sodium

hydroxide (0.1 M, 500 µl) and extracted with ethyl acetate. After centrifugation (10 min, 4000 rpm), the organic layer was transferred into clean glass tubes and evaporated to dryness under reduced pressure at 37 °C. The HPLC system consisted of a LC-10AD HPLC pump (Shimadzu, Kyoto, Japan), a Waters 717 plus auto sampler (Waters, Milford, MA, USA), and a fluorescence detector (Perkin Elmer) set at λ_{ex} = 260 nm and λ_{em} = 460 nm. Chromatography was performed on a stainless-steel Microsphere® C18 3 µm cartridge column (10 mm x 4.6 mm I.D.) (Chrompack Nederland BV, Bergen op Zoom, The Netherlands). The mobile phase was a mixture of 0.4 M acetate buffer (pH 4.6) and acetonitrile (50:50, v/v). The flow rate was set at 1 ml/min. Data acquisition and processing was performed using the Empower integration software (Waters, Milford, MA, USA). The intra- and inter-assay variation was less than 20% and the lower limit of quantification was 100 ng/ml for a 50 µl blood sample.

Midazolam blood samples – Samples were analysed as described previously by Mandema and co-workers (Mandema *et al.* 1991). The method consisted of a liquid-liquid extraction with NaOH and dichloromethane/petroleumether (45/55, v/v). After extraction, samples were injected onto an HPLC coupled to an ultraviolet detector. The intra- and inter-assay variation was less than 6% and the lower limit of quantification was 50 ng/ml for a 50 µl blood sample.

Pharmacokinetic data analysis

The pharmacokinetic data of both blood and brain ECF were analysed using non-linear mixed effect modelling as implemented in the NONMEM software version V, level 1.1 (Beal & Sheiner 1999). Parameter estimation was undertaken using the first-order conditional estimation method (FOCE interaction). All fitting procedures were performed on an IBM-compatible computer (Pentium IV, 1500 MHz) running under Windows XP with the Fortran Compiler Compaq Visual Fortran version 6.1. Structural model selection for both the blood and the ECF PK model was based on the likelihood ratio test, diagnostic plots (observed concentrations vs. individual and population predicted concentrations, weighted residuals vs. predicted time and concentrations), parameter correlations and precision in parameter estimates. The likelihood ratio test is based on a comparison of the minimum value of the objective function (MVOF) of two models. The significance level was set at 0.01, which corresponds to a decrease of MVOF of 6.6 points when an extra parameter is included in the structural model under the assumption that the difference in MVOF between two nested models is χ^2 distributed. The inter-animal variability in the pharmacokinetic parameters was assumed to be log normally distributed:

$$P_i = P_{typ} \cdot \exp(\eta_i) \quad (3)$$

with

$$\eta_i \sim N(0, \omega^2) \quad (4)$$

where P_i is the individual value of the model parameter P, P_{typ} is the typical value (population value) of parameter P in the population, and η_i is realisation from a normally distributed inter-animal random variable with mean zero and variance ω^2. Inter-individual variability was investigated for each parameter and was fixed to zero when no significant decrease in the MVOF was obtained. Correlations between the inter-individual variability of the various parameters were graphically explored.
The residual error, which accounts for unexplained errors (e.g. measurement and experimental errors) in the blood drug concentrations, was best described with a proportional error model according to equation:

$$C_{obs,ij} = C_{pred,ij} \cdot (1 + \varepsilon_{ij}) \quad (5)$$

with

$$\varepsilon_i \sim N(0, \sigma^2) \quad (6)$$

where $C_{obs,ij}$ is the j-th observation of the i-th individual, $C_{pred,ij}$ is the predicted concentration and ε_{ij} is from a normally distributed residual random variable with mean zero and variance σ^2.
The accuracy of the pharmacokinetic models was investigated by an internal validation method, the visual predictive check (Cox *et al.* 1999; Duffull & Aarons 2000; Yano *et al.* 2001). With this method, 1000 curves were simulated from the final PK parameter estimates. The median, lower (2.5%) and upper (97.5%) limit of the interquantile range of the simulated concentrations were calculated and compared with the position of the observations.

Pharmacokinetic analysis of blood profiles

For the development of the pharmacokinetic structural models for blood, both two- and three-compartment models were tested. On the basis of model selection criteria a three-compartment model was chosen. Pharmacokinetic analysis was performed with the PREDPP subroutines ADVAN 11 TRANS 4 implemented in NONMEM with estimation of the pharmacokinetic parameters clearance (Cl), inter-compartmental clearances (Q2 and Q3) and the volumes of distribution (V1, V2 and V3).
To refine the pharmacokinetic model, the relationship between bodyweight and the different parameters was explored graphically. The following equation was used to model the parameter as a function of bodyweight *(BW)*:

$$P_i = \theta_1 \cdot (1 + \theta_2 \cdot (BW_i - medianBW)) \quad (7)$$

where P_i is the individual value of a model parameter and θ_1 and θ_2 are the intercept and slope factor of the relationship between the individual parameter and bodyweight.
In addition the influence of co-infusion of GF120918 was also tested with the following the following equation:

$$P_i = \theta_3 \cdot (1 - GF120918_i) + \theta_4 \cdot (GF120918_i) \quad (8)$$

In which GF120918 is a factor, set to 1 if GF120918 is co-infused and set to 0 if vehicle is co-infused.

Pharmacokinetic analysis of morphine brain distribution

Simulations were performed to evaluate the influence of different transport mechanisms on the transport of morphine across the BBB. The simulations were performed using Berkeley Madonna (version 8.0.1, Macey & Oyster) and were based on the approach by Hammarlund and co-workers (1997). The population parameter values of the blood PK model were used in the simulations. The non-linear transport model contains specific expressions for 1) passive diffusion, 2) an active saturable uptake mechanism and 3) an active efflux by Pgp (figure 1).

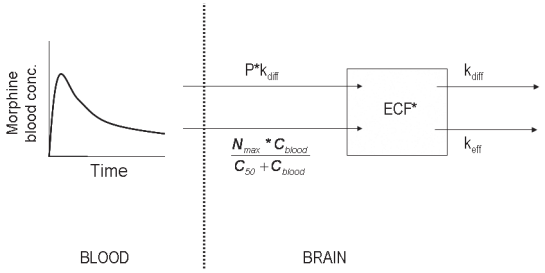

Figure 1: A schematic overview of the non-linear transport model to describe the brain ECF data. The morphine blood pharmacokinetics are described with a three-compartment model and used as input function for morphine in the brain. The brain model consists of one brain compartment and mass exchange between blood and brain is described with separate expressions for passive diffusion, active saturable influx and active efflux by Pgp, which could be influenced by GF120918. Abbreviations: k_{diff} is the diffusion rate constant between blood and brain compartment; N_{max} is the maximum active influx; C_{50} is the morphine blood concentration at which 50% of the maximum active influx is reached and k_{eff} is the active efflux rate constant, which is influenced by GF120918.

The transport model is based on indications from literature on the active uptake of morphine (Xie *et al*., 1999), simulations of different transport processes (Hammarlund-Udenaes *et al*. 1997) and the models proposed by Upton and co-workers (Upton *et al*. 2000; Xie *et al*. 1999). The model consists of one brain ECF compartment which is poorly perfused and diffusion limited. The BBB is located between the blood and ECF compartment.

The mass exchange between the blood and ECF compartment consists of three terms, a passive diffusion flux $Q_{diff}\cdot(C_{blood}-C_{ecf})$, an active saturable influx and an active Pgp mediated efflux which can be described following equation:

$$\frac{dA_{ecf}}{dt} = Q_{diff}\cdot\left(C_{blood}-C_{ecf}\right)+\frac{N_{\max}\cdot C_{blood}}{C_{50}+C_{blood}}-Q_{eff}\cdot C_{ecf} \qquad (9)$$

in which the right side of the equation represents the net mass exchange between the blood and ECF compartment. A_{ecf} is the amount of morphine in the ECF compartment,

Q_{diff} is the diffusion clearance, C_{blood} is the concentration in the central blood compartment, C_{ecf} is the concentration in the ECF compartment, Nmax is the maximal active influx, C_{50} is the morphine concentration in the blood compartment at which 50% of the maximal active influx is reached and (Q_{eff}.C_{ecf}) is the active efflux by Pgp which is influenced by GF120918.

Accordingly, the concentration in the ECF compartment can be described as:

$$\frac{dC_{ecf}}{dt} = \frac{Q_{diff}}{V_{ecf}} \cdot \left(C_{blood} - C_{ecf}\right) + \frac{N_{\max}}{V_{ecf}} \cdot \frac{C_{blood}}{C_{50} + C_{blood}} - \frac{Q_{eff}}{V_{ecf}} \cdot C_{ecf} \qquad (10)$$

Parameter aggregation yields:

$$k_{diff} = \frac{Q_{diff}}{V_{ecf}} \qquad N_{max}* = \frac{N_{max}}{V_{ecf}} \qquad k_{eff} = \frac{Q_{eff}}{V_{ecf}} \qquad (11)$$

Where k_{diff} is the diffusion rate constant and k_{eff} is the active efflux rate constant.

Pharmacokinetic analysis of brain ECF profiles

For the development of the pharmacokinetic structural models for brain ECF, the PREDPP subroutine ADVAN6 was used, which is a general nonlinear model that uses the numerical solution of the differential equations. The influence of co-infusion of GF120918 on the PK parameter was investigated following equation 8.

RESULTS

Pharmacokinetics in blood

Figure 2 shows the observed, population predicted and 2.5% and 97.5% quantiles for morphine concentrations in blood, after administration of a 10-min infusion of 4, 10 and 40 mg/kg in the presence of vehicle or GF120918. Based on the MVOF and diagnostics, the pharmacokinetics of morphine in blood was best described with a three-compartment model and was not influenced by co-infusion of GF120918. A tendency towards dose-dependent elimination was observed (figure 2). The parameters were estimated accurately with acceptable coefficient of variance (table 2). Covariate analysis showed linear relationships between bodyweight and Cl and between bodyweight and V2. The accuracy of the models was investigated using the predictive check. The selected PK models could well predict the time course of morphine after intravenous infusion as is shown by the population prediction and the quantiles (figure 2).

Table 2: Population pharmacokinetic parameter estimates of morphine in blood obtained with a three compartment model.

Parameter		Estimate	CV%	LLCI – ULCI
Structural model				
Cl (ml/min)				
	Intercept	20	5.6	18.5 – 23.1
	Slopefactor	5.35	25.2	5.66 – 11.3
V1 (ml)		68.1	16.7	45.8 – 90.4
Q2 (ml/min)		15.5	11.3	12.1 – 18.9
V2 (ml)				
	Intercept	739	7.6	629 – 849
	Slopefactor	8.5	17.1	2.70 – 7.99
Q3 (ml/min)		17.8	18.4	11.4 – 24.2
V3 (ml)		133	15.9	91.6 – 174
Interanimal variability				
ω^2 Cl		0.129	17.2	0.085 – 0.173
ω^2 V2		0.099	24.7	0.051 – 0.147
Residual variability				
Proportional error		0.074	10.2	0.059 – 0.089

Abbreviations: Cl = clearance; Q2/Q3 = inter-compartmental clearances; V1 = volume of distribution in central compartment, V2/V3 = volumes of distribution in peripheral compartment; slopefactor = linear relationship between bodyweight and Cl or V2; CV% = coefficient of variation; LLCI = lower limit of confidence interval; ULCI = upper limit of confidence interval.

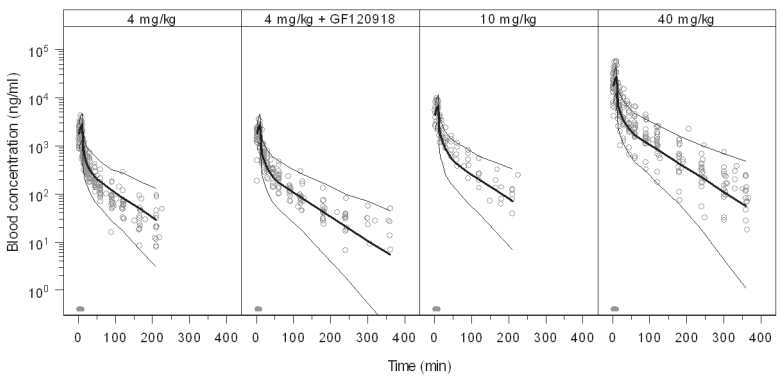

Figure 2: Pharmacokinetics of morphine in blood. Observed (grey dots), population predicted (solid line) and 2.5% and 97.5% quantiles (dotted lines) are depicted for each dose group. The grey bar indicates the infusion time.

GF120918 blood concentrations

Three blood samples were collected for determination of the GF120918 concentrations in blood. The first sample was collected at the end of the bolus infusion and the mean (± SEM) concentration in blood was 11650 ± 2560 ng/ml. The second and third blood samples were collected randomly from start of the morphine infusion until the end of the experiment. The mean (± SEM) GF120918 concentration in blood was 214 ± 16 ng/ml, which was sufficient to block Pgp (GSK, personal communication).

Midazolam blood concentrations

Three blood samples were collected for determination of the midazolam concentrations in blood. The first sample was collected prior to morphine administration and the mean (± SEM) concentration in blood was 879 ± 75 ng/ml. The second and third blood samples were collected randomly from the start of the morphine infusion until the end of the experiment. The mean (± SEM) midazolam concentration in blood was 937 ± 56 ng/ml, which was sufficient to suppress potential opioid-induced seizure activity (Cox *et al*. 1997).

Recovery of the microdialysis probes

The *in vitro* recovery experiments showed that gain is equal to loss, indicating that no adhesion to probe materials occurs with an instantaneous reflection of bulk morphine concentrations. The individual recovery values were calculated on the basis of six microdialysis fractions. The average recovery values *in vitro* were 25 ± 5.0 and 24 ± 5.6 % for retrodialysis solutions of 50 and 500 ng/ml, respectively.

The average recovery values *in vivo*, as determined with prior to systemic administration of morphine, were 16 ± 9.9 and 20 ± 3.5 % for retrodialysis solutions of 65 and 622 ng/ml. No difference was found between the vehicle and GF120918 pre-treated group, indicating that co-infusion of GF120918 does not influence the *in vivo* recovery. Since the experimental design does not allow estimation of individual recovery values, for the 4 mg/kg and the 4 mg/kg + GF120918 group the average recovery value of 16.1% is used and for the 40 mg/kg group a value of 20.3 % was used.

Pharmacokinetics in brain ECF

Morphine brain distribution kinetics was investigated using two distinctly different doses for an extensive period of 4-6 hours. With this approach data were collected over a broad concentration range, which allowed detailed pharmacokinetic analysis. The individual observed morphine concentrations in brain ECF are shown in figure 3.

The brain ECF concentrations increased rapidly after start of the morphine infusion, the maximum concentration of morphine was observed within 40 minutes after start of the infusion for the 4 mg/kg groups and within 20 min for the 40 mg/kg group. For the 4 mg/kg groups, after 20 min a relatively stable plateau in morphine brain ECF concentrations was reached. However, for the 40 mg/kg a clear decline in brain ECF

concentration was observed. When morphine concentrations were normalised to a dose of 4 mg/kg, the non-linearity in distribution kinetics in brain ECF was evident (figure 4). Moreover, at higher doses a reduction of the dose-normalized AUC is observed. The dose-normalised AUC was calculated over the largest common interval (0 – 165 min) using the log-linear trapezoidal rule and had mean values of 6810 ± 1890, 8460 ± 2790 and 3990 ± 2180 ng·h/ml for the 4 mg/kg, mg/kg + GF120918 and the 40 mg/kg group, respectively.

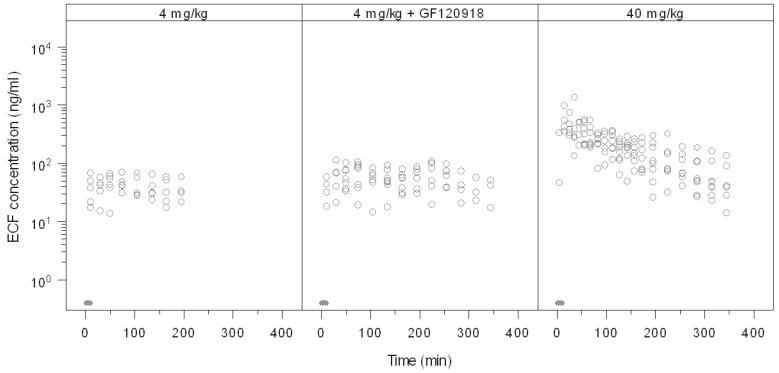

Figure 3: Observed morphine brain ECF concentrations for each dose group. The grey bar indicates the infusion time.

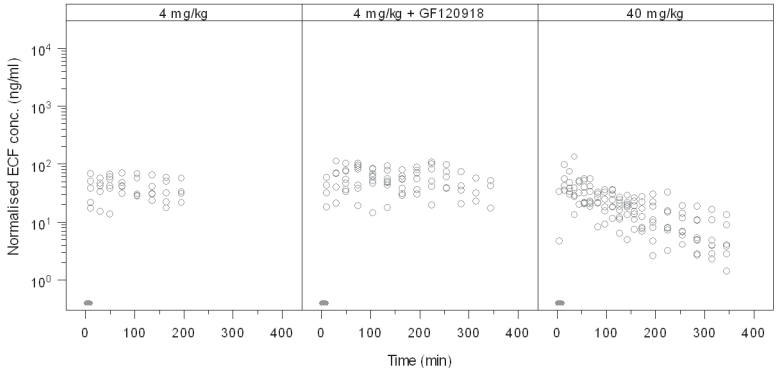

Figure 4: Observed morphine brain ECF concentrations after normalisation for dose (normalisation dose 4 mg/kg). The grey bar indicates the infusion time. The dose is depicted at the top of each panel.

For the 4 mg/kg dose group, the net elimination from the brain was much slower compared to the 40 mg/kg dose group. This process could not be described with a linear brain model, and the profiles suggested that transport of morphine is influenced both by an active influx transport process and the active efflux transport, mediated by Pgp. The active influx was supposed to be saturated already at low concentrations of morphine (4 mg/kg).

This behaviour of the proposed brain distribution model was evaluated using simulations in Berkeley Madonna. Figure 5 shows the simulated time courses of the brain ECF concentrations upon administration of morphine with doses ranging from 4 to 40 mg/kg in the absence and presence of GF120918. Results show that, consistent with the observations in the experiments, relatively stable 'plateau' brain ECF concentrations or morphine are observed at low doses, while with increasing doses a clear decline is observed.

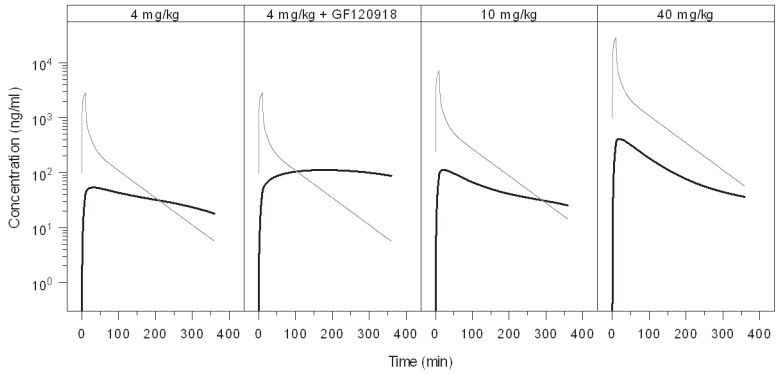

Figure 5: Simulations of the proposed non-linear transport model, consisting of separate expressions for passive diffusion, active saturable influx and active efflux by Pgp, which could be influenced by GF120918. The grey line represents the pharmacokinetics in plasma and the black lines the pharmacokinetics in brain ECF.

Next, the non-linear transport model was fitted to the data and resulted in a good description of the brain ECF profiles. Morphine concentrations could be adequately described with this model as shown in figure 6 and table 3. Specifically, when the active efflux of morphine in the presence of GF120918 was set to zero, this resulted in a significant worsening of the fit. The best fit was obtained when different values of the efflux rate constant keff were estimated for the presence or absence of GF120918. In the presence of GF120918, the value of the efflux rate constant keff decreased from 0.0195 to 0.0113 min^{-1}. This suggests that around 50% of the active efflux process is mediated by transporters other than Pgp.

In the population analysis, precise estimates could be obtained for all parameters. The coefficients of variation were all below 50% except for the C_{50} which was estimated at 71.5%. Inter-animal variability (ω^2) was estimated for k_{diff} and k_{eff} and was 0.238 and 0.080, respectively. In addition, a correlation was found between the post-hoc individual estimates of k_{diff} and k_{eff} and therefore a covariance block was included in the final model. Inter-animal variability could not be estimated accurately for the other parameters and was therefore fixed to zero. The individually observed morphine brain ECF concentrations do not deviate substantially from individual predicted concentrations as is shown by the goodness-of-fit plots (figure 7). The weighted residuals, which is the difference between observed and predicted morphine ECF concentrations, were

randomly distributed around zero in time, indicating that the structural model is plausible. In general the model can predict the brain ECF concentration adequately as is shown in figures 6 and 7. The model development was mainly driven by knowledge of different transport processes, such as efflux by Pgp (Xie *et al*., 1999, Letrent *et al*., 1999).

Table 3: Population pharmacokinetic parameter estimates of the non-linear transport model of morphine in brain ECF

Parameter		Estimate	CV%	LLCI – ULCI
Structural model				
k_{diff} (min^{-1})		0.001	12.6	0.0010 – 0.0017
k_{eff} (min^{-1})				
	-GF120918	0.0195	12.2	0.0149 – 0.0241
	+GF120918	0.0113	25.4	0.0057 – 0.0169
N_{max}* (ng/min)		0.658	26.1	0.321 – 0.995
C_{50} (ng/min)		9.92	71.5	-3.97 – 23.8
Interanimal variability				
$\omega^2 k_{diff}$		0.238	56.3	-0.025 – 0.501
$\omega^2 k_{eff}$		0.08	36.8	0.022 – 0.137
$\omega^2 k_{eff} \sim \omega^2 k_{eff}$		0.059	85	-0.039 – 0.158
Residual variability				
Proportional error		0.094	21.4	0.055 – 0.134

Abbreviations: k_{diff} = diffusion rate constant; k_{eff} = active efflux rate constant; N_{max} = maximum active influx; C_{50} = morphine blood concentration at which 50% of the maximal active influx is reached; CV% = coefficient of variation; LLCI = lower limit of confidence interval; ULCI = upper limit of confidence interval.*

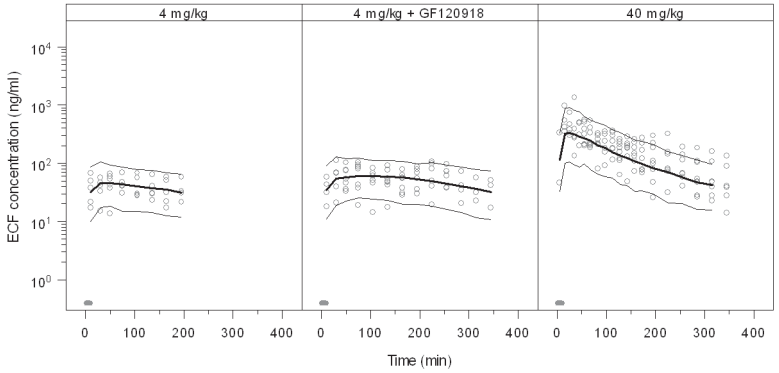

Figure 6: Pharmacokinetics of morphine in brain ECF. Observed (grey dots), population predicted (solid line) and 2.5% and 97.5% quantiles (dotted lines) are depicted for each dose group. The grey bar indicates the infusion time.

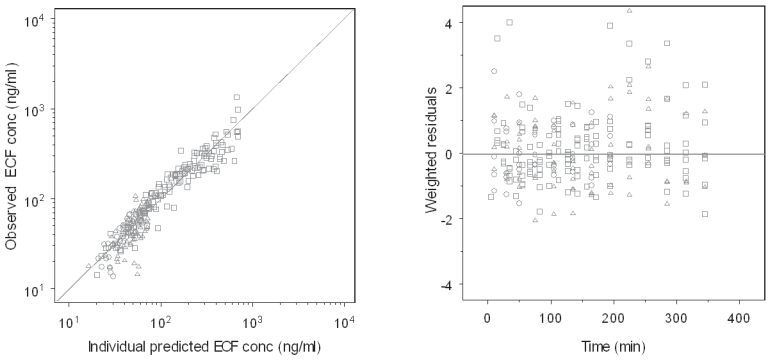

Figure 7: Goodness-of-fit plots of morphine concentrations in brain ECF for the non-linear transport model. In the left panel a scatterplot is depicted of the observed morphine concentrations versus the individual model predictions. The line represents the line of unity. In the right panel a scatterplot is depicted of weighted residuals versus time (right panel). The circles represent the data of the 4 mg/kg group, the triangles represent the 4 mg/kg + GF120918 group and the squares represent the 40 mg/kg group.

DISCUSSION

The influence of biophase equilibration must be considered to get more insight into the mechanisms underlying the pharmacokinetic-pharmacodynamic (PK-PD) correlation of opioids. Biophase equilibration is mainly determined by blood brain-barrier (BBB) transport. For morphine clear indications exist that BBB transport influences the biophase equilibration (Bouw *et al.* 2000). As part of the present investigations that focus on the BBB transport of morphine in relation to the PK-PD correlation for the effect on the electroencephalogram (EEG) (Groenendaal *et al.*, 2007 – chapter 6), the objective of the present study was to characterise, in a quantitative manner, the influence of passive and active transport mechanisms of morphine across the BBB. To this end, a large concentration-range of morphine in blood and brain ECF following intravenous administration 4 mg/kg, in the presence and absence of GF120918, and 40 mg/kg have been analysed on the basis of a three compartment pharmacokinetic model and a one compartment brain distribution model, respectively. It was deduced that BBB transport of morphine consists of passive diffusion, in parallel with active saturable influx and active efflux mechanisms.

Pharmacokinetics in blood

The pharmacokinetics of morphine in blood was best described by a three-compartment model, based on blood concentration data up to 360 min after the start of the morphine infusion. In previous studies plasma pharmacokinetics were described with a two-compartment model, for data up to 180 min (Bouw *et al.* 2000; Tunblad *et al.* 2004). This longer sampling period allows a more detailed analysis of the terminal phase of the

morphine pharmacokinetics, especially following the administration of a higher dose (40 mg/kg). A tendency towards dose-dependent elimination was observed (figure 2). However, there are no indications from literature for a dose-dependent elimination of morphine, nor could it be identified on the basis of the current data.
It is known that morphine is metabolised into glucuronides. The main metabolite in rats is morphine-3-glucuronide (M3G). In humans, morphine is also metabolised into M6G. However, upon intravenous administration of morphine in rats, M6G has not been detected in plasma (Coughtrie *et al*., 1989, van Grugten *et al*., 1997, Salem and Hope, 1997). Research has shown that M3G only has minor antinociceptive effects (Ekblom *et al*. 1993; Gardmark *et al*. 1993), it has not been analysed in this study. Also, because M3G is not a Pgp substrate (Letrent *et al*. 1999a; Xie *et al*. 1999), the potential influence of M3G on P-glycoprotein interaction could be excluded. On that basis it seems highly unlikely that the glucuronide metabolites are of significant influence on the BBB transport in our experiments.

Distribution into brain ECF

The proposed novel brain distribution model is rather complex; in contrast to previously proposed models it contains a passive diffusion component and two active transport mechanisms, contributing to the influx and the efflux, respectively. The transport model is based on indications from literature on the active uptake of morphine (Xie *et al*., 1999), simulations of different transport processes across the BBB (Hammarlund-Udenaes *et al*. 1997) and the models proposed by Upton and co-workers (2000).

To describe transport from blood to brain over a large concentration-range, a model was developed by a stepwise approach. Linear brain distribution models with and without active efflux could not describe the data. Next, a model was developed that consisted of a perfusion (cerebral blood flow-limited) compartment and a deeper membrane-limited compartment (the brain ECF). However, this perfusion component could not be identified nor did inclusion of this term yield a significant improvement in the goodness-of-fit. For this reason, the perfusion term was removed from the model. This indicated that cerebral blood flow is not a rate-limiting step in the transport of morphine across the BBB. This was expected on the basis of its physico-chemical properties (logP of ~0.7, and pKa of 7.9) and literature data on *in vivo* uptake clearance. A clearance value of 0.010 ml/min·g brain was found in mice (Dagenais et al 2001), and values ranging from 0.011 to 0.014 ml/min·g brain in rat (Bouw *et al*., 2000 ; Tunblad *et al*., 2004). and an *in situ* PS value of 0.008 ml/min·g brain in rat (Wu *et al*., 1997). These values are much lower than cerebral blood flow values of around 1-2 ml/min·g brain in mice and rats.

The non-linearity in the brain ECF concentration data indicated the presence of active efflux that was sensitive to inhibition by GF120918 as well as the presence of active saturable influx. Since, the uptake into the brain is composed of passive diffusion and

active influx, the uptake clearance (Cl_{in}) is not a single value and can therefore not be directly compared with literature data. However, based on the literature values of Clin ranging between 0.011-0.014 ml/min·g brain obtained with a rather similar experimental setting (Bouw *et al.* 2000; Tunblad *et al.* 2004), it can be concluded that this value is much smaller than rat CBF. At high doses, like many other opioids, morphine induces respiratory depression as a side-effect, which results in a decrease in pO_2, an increase in pCO_2 and a decrease in pH. To keep these changes to a minimum, in our experiments artificial ventilation was applied at the 40 mg/kg dose of morphine. Passive diffusion of morphine (with pKa of 7.9) into the brain pH dependent; at higher pH values, because of relatively more neutral morphine molecules available. This has been demonstrated experimentally by Bouw and co-workers (2000). The artificial ventilation in our experiments prevented a decrease in pH and therefore probably has resulted in a higher value for the passive diffusion uptake clearance in our study.

The influence of an active saturable influx transporter has never been proposed in population pharmacokinetic analyses. In an earlier study using microdialysis in mice, the presence of an active influx process was already indicated by brain/blood ratios that were much higher at low blood concentrations, both in MDR1a (+/+) and (-/-) mice (Xie *et al.* 1999). These observations also indicated that the active influx is not sensitive to changes in Pgp efflux. Our study is the first to characterize such an active influx in quantitative terms. Other studies only had access to concentrations after a single morphine dose of 1 mg/kg with low resolution PK microdialysis data of 30 min intervals (Letrent *et al.* 1998; 1999a) or concentrations that resulted from a dose range of 10 and 40 mg kg-1 that probably already had saturated the active influx component (Bouw *et al.* 2000). However, Letrent and co-workers (1999) found morphine brain ECF/blood ratios of ~0.5 which were about 2-fold higher compared to the brain ECF/plasma ratio of ~0.25 found by Bouw and co-workers (2000). This also supports the existence of active influx at lower blood concentrations. It remains to be elucidated, however, if such active influx is also present in and relevant for the human situation.

Several *in vitro* and *in vivo* studies have shown that morphine is a substrate for Pgp (Dagenais *et al.* 2004; Letrent *et al.* 1998; 1999a; 1999b; Schinkel *et al.* 1995; Wandel *et al.* 2002; Xie *et al.* 1999). In this study, a clear influence of active brain efflux could also be identified, as a two-fold difference in keff existed in the presence and absence of GF120918. Interestingly, the active efflux component could not be blocked completely with GF120918. The mean GF120918 blood concentration was 214 ng/ml, which was sufficient to completely block Pgp *in vivo* (personal communication with GSK) and therefore it appears that morphine efflux from the brain is also mediated by transporters other than Pgp. Tunblad and co-workers showed that morphine is also substrate for the probenecid-sensitive transporters at the BBB. Co-administration of probenecid resulted in a decrease in efflux clearance of morphine from the brain (Tunblad *et al.*, 2004).

Apart from the Pgp inhibitor GF120918, two other drugs were co-administered to morphine in this study. First, midazolam was continuously administered to prevent opioid-induced seizure activity and second, vecuronium bromide was used for muscle relaxation to enable artificial ventilation. An important question is whether these drugs could influence Pgp functionality. For midazolam, an inhibitory effect on Pgp functionality *in vitro*, has been shown, only at high concentrations (100 µM) (Mahar Doan *et al*. 2002; Tolle-Sander *et al*. 2003). The steady-state concentrations in our experiments were around 3 µM and present in all conditions tested and therefore the influence of midazolam on Pgp could be neglected. For vecuronium bromide we could not find any indications on a drug interaction with morphine.

In conclusion, the BBB transport of morphine could be accurately described with a model based on (slow) passive diffusion, combined with both active efflux and active saturable influx. This active efflux is partly explained by the interaction of morphine with Pgp. These observations indicate a blood concentration-dependency and sensitivity to drug-interactions. The complex brain distribution kinetics of morphine has an important impact for investigations on the PK-PD correlation of morphine.

ACKNOWLEDGEMENTS

The authors gratefully acknowledge the technical assistance of M.C.M. Blom-Roosemalen, S.M. Bos-van Maastricht and P. Looijmans. The supply of GF120918 by GlaxoSmithKline in the United Kingdom is highly appreciated. These investigations were financially supported by GlaxoSmithKline in the United Kingdom.

REFERENCES

Beal SL, Sheiner LB (1999) *NONMEM users guide* San Francisco, CA

Bouw MR, Gardmark M, Hammarlund-Udenaes M (2000) Pharmacokinetic-pharmaco-dynamic modelling of morphine transport across the blood-brain barrier as a cause of the antinociceptive effect delay in rats--a microdialysis study. *Pharm.Res.* **17:** 1220-1227

Bouw MR, Hammarlund-Udenaes M (1998) Methodological aspects of the use of a calibrator in in vivo microdialysis-further development of the retrodialysis method. *Pharm.Res.* **15:** 1673-1679

Bouw MR, Xie R, Tunblad K, Hammarlund-Udenaes M (2001) Blood-brain barrier transport and brain distribution of morphine-6-glucuronide in relation to the antinociceptive effect in rats--pharmacokinetic/pharmacodynamic modelling. *Br.J.Pharmacol* **134:** 1796-1804

Bungay PM, Morrison PF, Dedrick RL (1990) Steady-state theory for quantitative microdialysis of solutes and water in vivo and in vitro. *Life Sci.* **46:** 105-119

Coughtrie MW, Ask B, Rane A, Burchell B, Hume R (1989) The enantioselective glucuronidation of morphine in rats and humans. Evidence for the involvement of more than one UDP-glucuronosyltransferase isoenzyme. *Biochem Pharmacol* **38:** 3273-3280

Cox EH, Van Hemert JG, Tukker EJ, Danhof M (1997) Pharmacokinetic-pharmacodynamic modelling of the EEG effect of alfentanil in rats. *J Pharmacol.Toxicol.Methods* **38:** 99-108

Cox EH, Veyrat-Follet C, Beal SL, Fuseau E, Kenkare S, Sheiner LB (1999) A population pharmacokinetic-pharmacodynamic analysis of repeated measures time-to-event pharmaco-dynamic responses: the antiemetic effect of ondansetron. *J.Pharmacokinet.Biopharm.* **27:** 625-644

Dagenais C, Graff CL, Pollack GM (2004) Variable modulation of opioid brain uptake by P-glycoprotein in mice. *Biochem Pharmacol* **67:** 269-276

de Lange EC, Danhof M (2002) Considerations in the use of cerebrospinal fluid pharmacokinetics to predict brain target concentrations in the clinical setting: implications of the barriers between blood and brain. *Clin. Pharmacokinet.* **41:** 691-703

Duffull SB, Aarons L (2000) Development of a sequential linked pharmacokinetic and pharmacodynamic simulation model for ivabradine in healthy volunteers. *Eur.J.Pharm.Sci.* **10:** 275-284

Ekblom M, Gardmark M, Hammarlund-Udenaes M (1993) Pharmacokinetics and pharmacodynamics of morphine-3-glucuronide in rats and its influence on the antinociceptive effect of morphine. *Biopharm.Drug Dispos.* **14:** 1-11

Gardmark M, Ekblom M, Bouw R, Hammarlund-Udenaes M (1993) Quantification of effect delay and acute tolerance development to morphine in the rat. *J.Pharmacol.Exp.Ther.* **267:** 1061-1067

Groenendaal D, Blom-Roosemalen MC, Danhof M, de Lange EC (2005) High-performance liquid chromatography of nalbuphine, butorphanol and morphine in blood and brain microdialysate samples: application to pharmacokinetic/pharmacodynamic studies in rats. *J.Chromatogr.B Analyt.Technol.Biomed.Life Sci.* **822:** 230-237

Groenendaal D, Freijer J, de Mik D, Bouw MR, Danhof M, de Lange EC (2007) Influence of biophase distribution and P-glycoprotein interaction on pharmacokinetic-pharmacodynamic modelling of the effects of morphine on the EEG. *Br.J.Pharmacol.* **515:** 713-720

Hammarlund-Udenaes M, Paalzow LK, de Lange EC (1997) Drug equilibration across the blood-brain barrier--pharmacokinetic considerations based on the microdialysis method. *Pharm.Res.* **14:** 128-134

Henthorn TK, Liu Y, Mahapatro M, Ng KY (1999) Active transport of fentanyl by the blood-brain barrier. *J.Pharmacol. Exp.Ther.* **289:** 1084-1089

Letrent SP, Pollack GM, Brouwer KR, Brouwer KL (1998) Effect of GF120918, a potent P-glycoprotein inhibitor, on morphine pharmacokinetics and pharmacodynamics in the rat. *Pharm.Res.* **15:** 599-605

Letrent SP, Pollack GM, Brouwer KR, Brouwer KL (1999a) Effects of a potent and specific P-glycoprotein inhibitor on the blood- brain barrier distribution and antinociceptive effect of morphine in the rat. *Drug Metab Dispos.* **27:** 827-834

Letrent SP, Polli JW, Humphreys JE, Pollack GM, Brouwer KR, Brouwer KL (1999b) P-glycoprotein-mediated transport of morphine in brain capillary endothelial cells. *Biochem.Pharmacol.* **58:** 951-957

Mahar Doan KM, Humphreys JE, Webster LO, Wring SA, Shampine LJ, Serabjit-Singh CJ, Adkison KK, Polli JW (2002) Passive permeability and P-glycoprotein-mediated efflux differentiate central nervous system (CNS) and non-CNS marketed drugs. *J.Pharmacol.Exp.Ther.* **303:** 1029-1037

Mandema JW, Tukker E, Danhof M (1991) Pharmacokinetic-pharmacodynamic modelling of the EEG effects of midazolam in individual rats: influence of rate and route of administration. *Br.J.Pharmacol* **102:** 663-668

Moghaddam B, Bunney BS (1989) Ionic composition of microdialysis perfusing solution alters the pharmacological responsiveness and basal outflow of striatal dopamine. *J.Neurochem.* **53:** 652-654

Olson RJ, Justice JB, Jr. (1993) Quantitative microdialysis under transient conditions. *Anal. Chem.* **65:** 1017-1022

Salem A, Hope W (1997) Role of morphine glucuronide metabolites in morphine dependence in the rat. *Pharmacol Biochem.Behav.* **57:** 801-807

Schinkel AH, Wagenaar E, Mol CA, van Deemter L (1996) P-glycoprotein in the blood-brain barrier of mice influences the brain penetration and pharmacological activity of many drugs. *J.Clin.Invest* **97:** 2517-2524

Schinkel AH, Wagenaar E, van Deemter L, Mol CA, Borst P (1995) Absence of the mdr1a P-Glycoprotein in mice affects tissue distribution and pharmacokinetics of dexamethasone, digoxin, and cyclosporin A. *J.Clin.Invest* **96:** 1698-1705

Thiebaut F, Tsuruo T, Hamada H, Gottesman MM, Pastan I, Willingham MC (1987) Cellular localization of the multidrug-resistance gene product P-glycoprotein in normal human tissues. *Proc.Natl.Acad.Sci U.S.A.* **84:** 7735-7738

Tolle-Sander S, Rautio J, Wring S, Polli JW, Polli JE (2003) Midazolam exhibits characteristics of a highly permeable P-glycoprotein substrate. *Pharm.Res.* **20:** 757-764

Tunblad K, Jonsson EN, Hammarlund-Udenaes M (2004) Morphine blood-brain barrier transport is influenced by probenecid co-administration. *Pharm Res* **20:** 618-623

Upton RN, Ludbrook GL, Grant C, Doolette DJ (2000) The effect of altered cerebral blood flow on the cerebral kinetics of thiopental and propofol in sheep. *Anesthesiology* **93:** 1085-1094

van Bree JB, de Boer AG, Danhof M, Ginsel LA, Breimer DD (1988) Characterization of an “in vitro” blood-brain barrier: effects of molecular size and lipophilicity on cerebrovascular endothelial transport rates of drugs. *J Pharmacol Exp.Ther.* **247:** 1233-1239

van Crugten JT, Somogyi AA, Nation RL, Reynolds G (1997) Concentration-effect relationships of morphine and morphine-6 beta-glucuronide in the rat. *Clin Exp.Pharmacol Physiol* **24:** 359-364

Wagner JG (1974) A safe method for rapidly achieving plasma concentration plateaus. *Clin.Pharmacol.Ther.* **16:** 691-700

Wandel C, Kim R, Wood M, Wood A (2002) Interaction of morphine, fentanyl, sufentanil, alfentanil, and loperamide with the efflux drug transporter P-glycoprotein. *Anesthesiology* **96:** 913-920

Xie R, Hammarlund-Udenaes M, de Boer AG, de Lange EC (1999) The role of P-glycoprotein in blood-brain barrier transport of morphine: transcortical microdialysis studies in mdr1a (-/-) and mdr1a (+/+) mice. *Br.J.Pharmacol.* **128:** 563-568

Yano Y, Beal SL, Sheiner LB (2001) Evaluating pharmacokinetic/pharmacodynamic models using the posterior predictive check. *J.Pharmacokinet.Pharmacodyn.* **28:** 171-192

Chapter 6

PHARMACOKINETIC-PHARMACODYNAMIC MODELLING OF THE ELECTROENCEPHALOGRAM EFFECTS OF MORPHINE:

INFLUENCE OF BIOPHASE DISTRIBUTION AND P-GLYCOPROTEIN INTERACTION

Dorien Groenendaal[1], Jan Freijer[2], Dennis de Mik[1], M. René Bouw[3], Meindert Danhof[1,2] and Elizabeth C.M. de Lange[1]

[1]Leiden Amsterdam Center for Drug Research, Leiden University, Division of Pharmacology, Leiden, The Netherlands, [2]LAP&P Consultants BV, Leiden, The Netherlands, [3]GlaxoSmithKline, Clinical Pharmacokinetics Neurology, Harlow, United Kingdom

British Journal of Pharmacology (2007) **151**, 713-720

SUMMARY

Background and purpose

The aim was to investigate the influence of biophase distribution including P-glycoprotein (Pgp) functionality on the pharmacokinetic-pharmacodynamic correlation of morphine.

Experimental approach

Male rats received a 10-min infusion of morphine as 4 mg/kg, combined with a continuous infusion of the Pgp inhibitor GF120918 or vehicle, 10 or 40 mg/kg. EEG signals were recorded continuously and blood samples were collected.

Key results

Profound hysteresis was observed between morphine blood concentrations and EEG effect. Only the offset of the EEG effect was influenced by GF120918. Biophase distribution was best described with an extended-catenary biophase distribution model, with a sequential transfer and effect compartment. The rate constant for transport through the transfer compartment (k_{1e}) was 0.038 min^{-1}, being unaffected by GF120918. In contrast, the rate constant for the loss from the effect compartment (k_{eo}) decreased 60% by GF120918, from 0.043 to 0.015 min^{-1}. The EEG effect was directly related to the concentrations in the effect compartment using the sigmoidal E_{max} model. The values of the pharmacodynamic parameters E_0, E_{max}, EC_{50} and Hill factor were 45.0 μV, 44.5 μV, 451 ng/ml and 2.3, respectively.

Conclusions and implications

The effects of GF120918 on the distribution kinetics of morphine in the effect compartment were consistent with recent observations on the distribution in brain extracellular fluid (ECF) as estimated by intracerebral microdialysis. However, the time-course of morphine concentrations at the site of action in the brain, as deduced from the biophase model, is distinctly different from the brain ECF concentrations.

INTRODUCTION

Mechanism-based pharmacokinetic-pharmacodynamic (PK-PD) models for the central action of opioids contain expressions for a) blood pharmacokinetics, b) biophase distribution, which is mainly determined by blood-brain barrier (BBB) transport, c) receptor interaction kinetics and d) signal transduction (Danhof *et al.* 2005). Especially for morphine, biophase distribution is an important determinant of the onset and duration of the effect because of its hydrophilic nature and the interaction with the efflux transporter P-glycoprotein (Pgp). Research on the influence of biophase distribution on morphine PK-PD relationships has so far primarily focussed on rather empirical biophase distribution model. Bouw and co-workers have proposed a single biophase compartment model to account for the delay of the anti-nociceptive effect of morphine relative to corresponding plasma concentrations (Bouw *et al.* 2000). It was found that BBB transport accounts for 84% of the observed hysteresis. For morphine, a limited number of studies have focused on the role of active transport mechanisms at the BBB. Specifically, it has been shown that after oral pre-treatment with the specific Pgp inhibitor GF120918, the anti-nociceptive effect of morphine was prolonged due to its prolonged half-life in the brain, presumably resulting from inhibition of Pgp as an active efflux mechanism (Letrent *et al.* 1998; 1999). Moreover, the role of transporters other than Pgp efflux at the BBB on brain distribution of morphine has been indicated by interaction studies with probenecid (Tunblad *et al.*, 2004).
In recent investigations, the brain distribution of morphine has been characterised in greater detail with intracerebral microdialysis (Groenendaal *et al.*, 2007 - chapter 5). Brain distribution was non-linear and was successfully described by a complex brain distribution model with specific expression for 1) passive diffusion, 2) active saturable influx and 3) active efflux which could in part be inhibited by GF120918. Against this background, it is of considerable interest to characterise in a mechanistic manner the biophase distribution kinetics of morphine in a PK-PD investigation.

Detailed characterisation of the biophase distribution kinetics requires the availability of high density pharmacodynamic data. In this respect, quantitative analysis of drug effects on the electroencephalogram (EEG) yields attractive biomarkers, which are continuous, sensitive and reproducible (Dingemanse *et al.* 1988). Meanwhile, quantitative EEG parameters have been widely used as a pharmacodynamic endpoint in pre-clinical and clinical investigations on the PK-PD correlations of a variety of CNS active drugs. It has also been shown that the synthetic opioid alfentanil, which is frequently used in anesthesia produces a progressive slowing of the EEG with a pre-dominant increase in the delta frequency band (0.5-4.5 Hz) of the EEG power spectrum in both animals (Cox *et al.* 1997; Mandema & Wada 1995; Wauquier *et al.* 1988; Young & Khazan 1984) and humans (Scott *et al.* 1985; Wauquier *et al.* 1984; Young & Khazan 1984). Meanwhile the increase in the delta frequency band of the EEG has been widely used as a biomarker in

numerous studies on the PK-PD correlations of synthetic opioids. In preclinical studies it has been demonstrated that the increase in the delta frequency band of the EEG reflect μ-opioid receptor activation (Cox *et al.* 1997; 1998; 1999). Moreover, in clinical studies, this biomarker has been validated as a surrogate marker for depth of anaesthesia (Egan *et al.* 1996; Lemmens *et al.* 1995; Scott *et al.* 1991; Scott *et al.* 1985).
The aim of the present study was to investigate the influence of biophase distribution and Pgp interaction at the BBB on the PK-PD relationships of morphine and to compare the time course of the predicted effect-site concentrations with the time course of the brain extracellular fluid (ECF) concentrations as determined by intracerebral microdialysis.

METHODS

The pharmacokinetics in blood and pharmacodynamics were investigated in two sets of experiments, the classic EEG experiments and the EEG/MD experiments. The details of the EEG/MD experiments have been described previously (Groenendaal *et al.* 2007 - chapter 5).

Surgical procedures

Details on the anaesthesia and surgical procedures have been described previously (Groenendaal *et al.* 2007 - chapter 5). For the EEG experiments, seven cortical electrodes were stereotaxically implanted into the skull of rats ten days before the start of the experiments as described before (Cox *et al.* 1996). Briefly, the electrodes were placed at the locations 11 mm anterior and 2,5 mm lateral (F_l and F_r), 3 mm anterior and 3,5 mm lateral (C_l and C_r) and 3 mm posterior and 2,5 mm lateral (O_l and O_r) to lambda. A reference electrode was placed on lambda. Stainless-steel crews were used as electrodes and connected to a miniature connector. For the EEG/MD experiments, the rats were chronically instrumented with four EEG electrodes at the F_l, C_l, O_l and reference position and with a CMA/12 guide cannula with a dummy probe placed in the striatum of the right brain hemisphere (anterior-posterior: +0.5 mm, lateral: +2.7 mm with bregma as reference and ventral: -3.5 mm ventral to the skull).

Experimental procedures

All experimental procedures were identical for both the EEG groups and the EEG/MD groups, as described previously (Groenendaal *et al.* 2007 - chapter 5). The EEG signal was continuously monitored via bipolar EEG leads on the left hemisphere (Cl-Ol) using a Nihon-Kohden AB-621G Bioelectric Amplifier (Hoekloos BV, Amsterdam, The Netherlands) and concurrently digitized at a rate of 256 Hz using a CED 1401plus interface (CED, Cambridge, United Kingdom). The digitized signal was transferred into a Pentium III computer and stored on hard disk for off-line analysis. For each 5-sec epoch, quantitative EEG parameters were obtained off-line by Fast Fourier Transformation

with a user-defined script within the software package Spike2 for Windows, version 3.18 (CED, Cambridge, United Kingdom). Changes in the amplitudes in the δ-frequency band of the EEG (0.5-4.5 Hz) averaged over 1-minute time intervals were used as a pharmacodynamic endpoint. Further reduction of the EEG data was performed by averaging the signals over predetermined time intervals using a user-defined script within the software package Matlab®, version 6.1 (The Mathworks Inc., Gouda, The Netherlands). The size of the intervals was dependent on the different periods of the experiment. The intervals were 3 min for baseline, 3 min between start of infusion (time = 0) and 75 min, 5 min between 75 and 200 min after start of infusion and 10 min between 200 and 360 min after start of the infusion. These intervals were chosen on the basis on visual inspection of the 1-min datafile.
Blood samples were analysed for morphine, GF120918 and midazolam as described previously (Groenendaal *et al.* 2005 - chapter 3).

Data analysis

The details on the general modelling procedures have been described previously (Groenendaal *et al.* 2007 - chapter 5). The EEG effects of morphine were analysed using non-linear mixed effect modelling as implemented in the NONMEM software version V, level 1.1 (Beal & Sheiner 1999). Population analysis was undertaken using the first-order conditional estimation method (FOCE interaction). Individual pharmacokinetic parameter estimates were used as input for the pharmacodynamic models. Individual blood concentrations were calculated at the times of the EEG measurements.

The selection of the biophase distribution model

A profound delay in the EEG effect (hysteresis) of morphine was observed. The hysteresis was characterized on the basis of two biophase distribution models: A) the one-compartment biophase distribution model, also known as the effect-compartment model and B) the extended-catenary biophase distribution model (figure 1).

A) One-compartment biophase distribution model

Hysteresis is often characterised on the basis of the one-compartment biophase distribution model. With this model the assumption is made that the rate of onset and offset of the drug effect is governed by the rate of drug distribution to the hypothetical "effect-site" (Sheiner *et al.* 1979). This effect-compartment is then linked to the blood concentrations with the rate constant k_{1e} and the rate constant for drug loss k_{eo}. The rate of change of the drug concentration in the effect compartment can then be expressed by equation:

$$\frac{dC_e}{dt} = k_{1e} \cdot C_b - k_{eo} \cdot C_e \qquad (1)$$

Where C_b represents the blood concentration and C_e represents the effect-site

concentration. Under the assumption that in equilibrium the effect-site concentration equals the blood concentration, this equation can be simplified to:

$$\frac{dC_e}{dt} = k_{eo} \cdot (C_b - C_e) \quad (2)$$

This model describes a symmetrical biophase. In contrast, when k_{1e} is not equal to k_{eo}, the biophase is considered to be a-symmetrical. Both models were investigated.

B) Extended-catenary biophase distribution model

The extended-catenary biophase distribution model consists of two sequential compartments, a transfer (e_t) and an effect (e) compartment which was based on the "tank-in-series" models described by Upton and co-workers and provides a simple method for accounting for dispersion of drug in transit through the brain (Upton *et al.* 2000). The rate of change of the concentrations in the effect compartments can then be described as follows:

$$\frac{dC_{e_t}}{dt} = k_{1e} \cdot C_b - k_{1e} \cdot C_{e_t} \quad (3)$$

$$\frac{dC_e}{dt} = k_{1e} \cdot C_{e_t} - k_{eo} \cdot C_e \quad (4)$$

where C_{et} and C_e describe the concentrations in the transfer and effect-compartment, respectively. The concentrations in the effect-compartment were then linked to the pharmacological effect. Both the symmetrical ($k_{1e}=k_{eo}$) and the asymmetrical ($k_{1e}\neq k_{eo}$) biophase models were investigated.

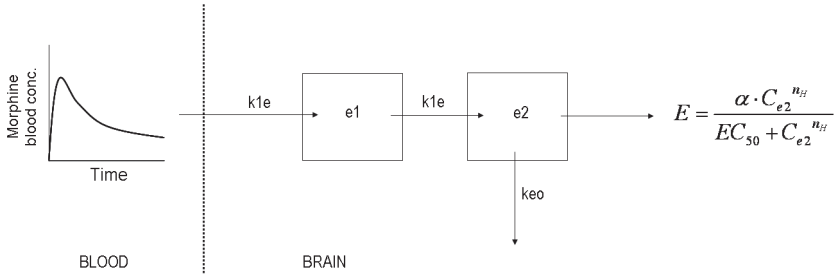

Figure 1: A schematic overview of the one-compartment distribution model (panel A) and the extended-catenary biophase distribution model (panel B) to describe the biophase kinetics of morphine. The blood pharmacokinetics were described with a three-compartment model and used as input function for morphine in the brain. The one-compartment distribution model consists of one effect compartment (e), whereas the biophase distribution model consists of two sequential compartments, the transfer (et) and the effect (e) compartment. The concentrations in the effect compartment were related to the EEG effect on the basis of the sigmoidal Emax model. Abbreviations: k_{1e} represents the rate constant for transport through the transfer compartment; k_{eo} represents the rate constant for loss from the effect compartment and is influenced by GF120918; Emax represent the intrinsic activity and EC_{50} represents the potency.

PK-PD analysis of the EEG effect

For the development of the structural PK-PD model for the EEG effect of morphine, the PREDPP subroutine ADVAN6 was used, which is a general nonlinear model that uses a numerical solution of the differential equations.

After hysteresis minimization, the individual concentration-effect relationships were fitted to the sigmoidal E_{max} model:

$$E = E_0 + \frac{E_{\max} \cdot C_e^{\,n_H}}{EC_{50}^{\,n_H} + C_e^{\,n_H}} \tag{5}$$

Where E_0 is the no-drug response, E_{max} is the intrinsic activity, EC_{50} is the potency and n_H is the slope factor.

In the experiments described here, two experimental approaches were used, the EEG method and the EEG/MD method. Since the removal of three EEG electrodes and the subsequent implantation of a microdialysis probe could possibly result in a change in baseline EEG, a covariate was included in the analysis to validate the EEG/MD method. The following equation was used:

$$P_i = \theta_1 \cdot (1 - METHOD_i) + \theta_2 \cdot (METHOD_i) \tag{6}$$

where P_i is the individual value of model parameter and θ_1 and θ_2 are the parameter values obtained with METHOD=1 for EEG/MD and METHOD=0 for EEG.

The influence of co-infusion of GF120918 on the biophase distribution rate constants was tested with the following equation:

$$P_i = \theta_3 \cdot (1 + \theta_4 \cdot GF\ 120918_i) \tag{7}$$

Where P_i is the individual value of model parameter and θ_3 and θ_4 are the parameter estimate and Pgp inhibition value and GF120918 is a factor, set to 1 if GF120918 is co-infused and set to 0 is vehicle is co-infused.

Inter-animal variability on E_0 and E_{max} was described with a proportional variability model according to equation:

$$P_i = P_{typ} \cdot (1 + \eta_i) \tag{8}$$

with

$$\eta_i \sim N(0, \omega^2) \tag{9}$$

where P_i is the individual value of the model parameter P, P_{typ} is the typical value (population value) of parameter P in the population, and η_i is inter-animal random variable. The assumption was made that all other parameters were log normal distributed with mean zero and variance ω^2.

The inter-animal variability on all other parameters was described with an exponential error model according to equation:

$$P_i = P_{typ} \cdot \exp(\eta_i) \quad (10)$$

with

$$\eta_i \sim N(0, \omega^2) \quad (11)$$

Inter-animal variability was investigated for each parameter and was fixed to zero when the MVOF did not improve. Correlations between the inter-animal variability of the various parameters were graphically explored. In addition, correlations between the PD parameters and dose and between the PD parameters and the co-infusion of GF120918 were also investigated graphically.

The residual error, which accounts for unexplained errors (such as measurement and experimental errors) in the EEG measurements, was best described with a proportional error model according to equation:

$$C_{obs,ij} = C_{pred,ij} \cdot (1 + \varepsilon_{ij}) \quad (12)$$

where $C_{obs,ij}$ is the *j*-th observation of the *i*-th individual, $C_{pred,ij}$ is the predicted concentration and ε_{ij} is a realisation from the normally distributed residual random variable with mean zero and variance σ^2:

$$\varepsilon_i \sim N(0, \sigma^2) \quad (13)$$

RESULTS

Pharmacodynamics and hysteresis

After the start of the morphine infusion, a gradual increase in the EEG effect, expressed as the absolute amplitude in the 0.5-4.5 Hz frequency range, was observed. The maximal effect was 60 µV and was observed around 20 minutes after the end of the morphine infusion. The duration of the effect (from the start of the infusion until the return to baseline values) was around 180 minutes following the infusion of 4 and 10 mg/kg morphine whereas after a dose of 4 mg/kg combined with GF120918 or 40 mg/kg morphine the duration of the effect was around 360 minutes. In figure 2, the pharmacokinetics and the pharmacodynamics of a typical rat of each experimental group are shown. It was found that the derived blood concentration-EEG effect relationships showed profound hysteresis for all experimental groups (figure 3), which was counter clockwise.

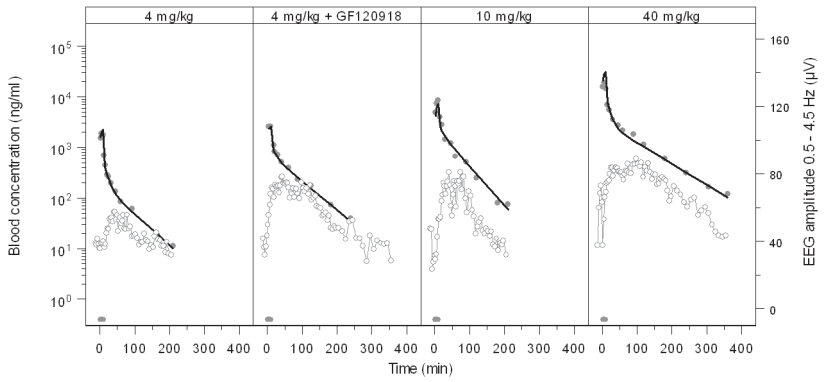

Figure 2: Pharmacokinetics and pharmacodynamics of a typical rat after administration of the opioids. Observed blood concentrations (grey dots), individual predicted blood concentrations (black line) and observed EEG effect (grey open dots) are depicted for each dose group. The grey bar indicates the infusion time.

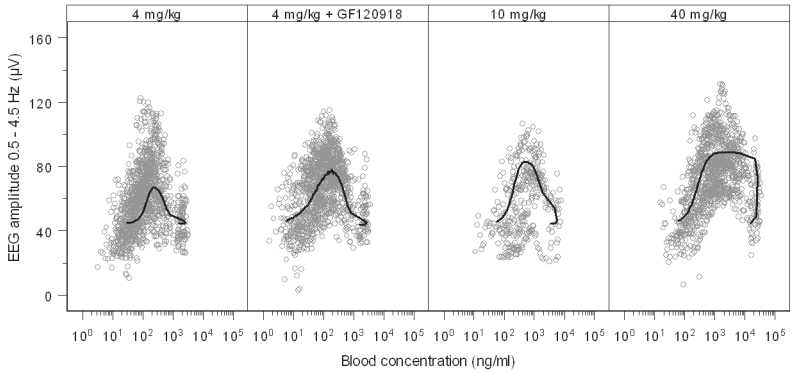

Figure 3: PK-PD relationship after administration of morphine. Observed (grey dots) and population predictions (black line) are depicted for each dose group. A clear counter clockwise hysteresis loop was observed for all morphine doses.

The selection of the biophase distribution model

In order to describe the observed hysteresis, two biophase distribution models were proposed: 1) the one compartment distribution model and 2) the extended-catenary biophase distribution model. First, the biophase distribution kinetics was fitted according to the one-compartment biophase distribution model. Both the symmetrical and a-symmetrical effect compartment model was tested. With the symmetrical ($k_{1e}=k_{eo}$) biophase distribution no results were obtained (minimisation terminated) whereas with the asymmetrical ($k_{1e}\neq k_{eo}$) effect compartment model no precise estimates could be obtained and bias was observed between the observed and predicted values Therefore, the extended-catenary biophase distribution model was proposed, consisting of two sequential compartments; a transfer and an effect compartment. Both

the symmetrical and asymmetrical model was used. The asymmetrical model resulted in the lowest objective function, 24671 ($k_{1e} \neq k_{eo}$) versus 24936 ($k_{1e} = k_{eo}$) and precise estimates of the parameters of the biophase distribution kinetics were obtained (table 1).

Table 1: Population pharmacokinetic parameter estimates of the biophase distribution of morphine obtained with the extended-catenary biophase distribution model

Parameter		Estimate	CV%	LLCI – ULCI
Structural model				
k_{1e} (min^{-1})		0.038	8.4	0.0315 – 0.0441
k_{eo} (min^{-1})				
	-GF120918	0.0426	10	0.0342 – 0.0510
	+GF120918#	0.0152		
Pgp inhibition factor		-0.644	-7.3	-0.736 – -0.552
Interindividual variability				
ω^2 k_{eo}		0.237	20.2	0.143 – 0.331

 # k_{eo}(+GF120918) = k_{eo}(-GF120918)(1+Pgp inhibition factor)*

Abbreviations: k_{1e} = rate constant for transport to the effect-site; k_{eo} = rate constant for the loss from the effect-site; CV% = coefficient of variation; LLCI = lower limit of confidence interval; ULCI = upper limit of confidence interval

The value of the rate constant for transport through the transfer compartment (k_{1e}) was 0.038 min^{-1} and was unaffected by the co-administration of GF120918. The values for transport rate constants for the loss from the effect compartment (k_{eo}) in the presence and absence of GF120918 were 0.0015 min^{-1} and 0.043 min^{-1}, respectively. The population predictions of blood and biophase concentration-time profiles are shown in figure 4.

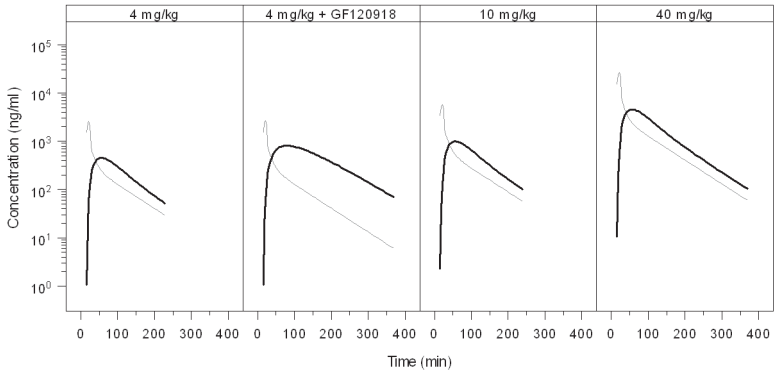

Figure 4: Population predicted blood and biophase concentration-time profiles of morphine obtained with the extended-catenary biophase distribution model. The grey lines represent the blood concentration-time profiles and the black lines represent the biophase concentration-time profiles.

The best fit was obtained when the influence of GF120918 was described with a Pgp inhibition factor that influences the keo. This Pgp inhibition factor was estimated at a value of –0.64 indicating that in the presence of GF120918, the k_{eo} is decreased with 64% from 0.043 to 0.015 min^{-1}. The inter-animal variability (ω^2) on k_{eo} was estimated with an exponential error model and was equal to 0.237. The inter-animal variability could not be estimated for the other parameters and were therefore fixed to zero.

Pharmacokinetic-pharmacodynamic analysis of the EEG effect

The individual predicted biophase concentrations were related to the EEG effect on the basis of the sigmoidal Emax pharmacodynamic model. Since the EEG and EEG/MD experiments were performed in parallel, covariate analysis was included to investigate the influence of the microdialysis probe on the pharmacodynamic parameters. Since no differences were observed in E_0 and E_{max} values between the EEG and the EEG/MD group, a single parameter value was estimated. Morphine PK-PD relationships were accurately described as shown in figure 5 and table 2.

Table 2: Population pharmacodynamic parameter estimates of morphine EEG effect obtained with the sigmoidal Emax model after hysteresis minimisation with the extended-catenary biophase distribution model.

Parameter	Estimate	CV%	LLCI – ULCI
Structural model			
E_0 (μV)	44.6	2.3	42.6 – 46.6
E_{max} (μV)	44.5	8	37.5 – 51.5
EC_{50} (ng ml^{-1})	451	17.3	298 - 604
N	2.32	10.4	1.85 – 2.79
Interindividual variability			
ω^2 k_{E0}	0.034	17.8	0.022 – 0.045
ω^2 k_{Emax}	0.121	24.1	0.064 – 0.178
Residual variability			
Proportional error	0.027	7.6	0.023 – 0.031

Abbreviations: E_0 is the no-drug response; E_{max} is the intrinsic activity; EC_{50} is the potency; n_H is the slope factor; CV% = coefficient of variation; LLCI = lower limit of confidence interval; ULCI = upper limit of confidence interval

Co-infusion of GF120918 did not influence the pharmacodynamic parameters. The values of the pharmacodynamic parameters E_0, E_{max}, EC_{50} and nH were 45.0 μV, 44.5 μV, 451 ng/ml and 2.3, respectively. Inter-animal variability (ω^2) was estimated with a proportional error model for E_0 and Emax and was equal to 0.034 and 0.121, respectively. Inter-animal variability could not be estimated for the other parameters and were therefore fixed to zero. Graphical analysis showed that no significant correlations

were observed between the estimates of the PD parameters and dose and between PD parameter estimates and co-infusion of GF120918.

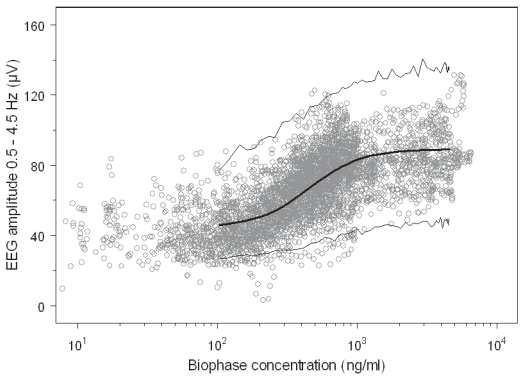

Figure 5: PK-PD relationships of the opioids after hysteresis minimisation with the extended-catenary biophase distribution model. Observed (grey dots), population predicted (solid line) and 2.5% and 97.5% quantiles (dotted lines) are depicted versus the predicted biophase concentration as shown in figure 4. The PK-PD relationship was obtained using the extended-catenary biophase distribution model to describe the distribution to the effect-site and the sigmoidal Emax model to relate the biophase concentrations to the EEG effect.

DISCUSSION

Biophase distribution can be defined as the distribution processes between the blood and the effect-site. The aim of the present study was to investigate the influence of biophase distribution and Pgp interaction at the BBB on the PK-PD relationships of morphine and to compare the time course of the predicted effect-site concentrations with the time course of the brain ECF concentrations as determined by intracerebral microdialysis.

So far the PK-PD investigations of morphine have focussed on the anti-nociceptive effects (Bouw *et al*. 2000; Letrent *et al*.1998). In these studies, the hysteresis has been described with the standard symmetrical effect compartment model consisting of a single effect compartment, where k_{1e} is equal to k_{eo}. In these models, a wide difference in k_{eo} values (hysteresis) was observed; the k_{eo} values were 0.228 min^{-1} and 0.022 min^{-1}, for the doses of 1 mg/kg and 10/40 mg/kg, respectively. This difference may be explained by the different dose used (1 mg/kg versus 10/40 mg/kg), the difference in infusion speed (bolus versus 10 min infusion) and the differences in experimental set-up to measure the anti-nociceptive effect (hot-lamp tail-flick latency assay versus electrical stimulation vocalisation method). With anti-nociceptive effect measurements only a limited number of data points can be obtained, which may limit a detailed PK-PD analysis.

Morphine induces both analgesia and sedation. Changes in EEG are often used as a measure to reflect the depth of sedation or anaesthesia (Stanski 1992). As EEG effect

measurements have the advantage of being continuous, sensitive, objective and reproducible, EEG has been used in this study to investigate the influence of biophase distribution on the PK-PD relationship of morphine. Between rats, only very small differences were observed in baseline (E_0) values, indicating the robustness of the EEG model. The method, either EEG or EEG/MD, had no influence on the E_0 and E_{max}.
A profound counter clockwise hysteresis was observed for the concentration-effect relationships of each group, which may result from the formation of metabolites that influence the effect of morphine. In rats, only the metabolite M3G is formed in significant amounts. Since the affinity of M3G for the μ-opioid receptor is much lower compared to morphine (Bartlett & Smith 1995; de Jong *et al.* 2005; Loser *et al.* 1996), it was concluded that the influence of M3G on the observed hysteresis could be neglected. Therefore, M3G was not quantitated in the present study. The hysteresis of the EEG effects of morphine was characterized on the basis of two biophase distribution models: A) the one-compartment biophase distribution model, also known as the effect-compartment model and B) the extended-catenary biophase distribution model. The biophase distribution kinetics could neither be described with the symmetrical nor the asymmetrical one-compartment biophase distribution model, indicating that the biophase distribution process of the EEG effect included multiple distribution processes. Therefore the extended-catenary biophase distribution model was developed. This model consists of two sequential biophase-compartments; the transfer and the effect compartment. The extended-catenary biophase distribution model is based on a "tank-in-series" model as proposed by Upton and co-workers (Upton *et al.* 2000). This model provides a simple method for accounting for dispersion of drug in the transit through the brain (Upton *et al.* 1999). The concentrations in the effect compartment were related to the EEG effects, defined by the rate constant for transport through the transfer compartment (k_{1e}) and for loss from the effect compartment (k_{eo}). These rate constants are distinctly different since only the k_{eo} could be influenced by co-infusion of the specific and potent Pgp inhibitor GF120918.
The biophase distribution observed for morphine is more complex compared to other opioids. For alfentanil, the biophase distribution was too fast to be identified, while for fentanyl and sufentanil, the hysteresis could be described with simple k_{eo} values of 0.32 min^{-1} and 0.17 min^{-1}, for fentanyl and sufentanil, respectively (Cox *et al.*, 1998). These observations confirm that application of morphine as an anaesthetic is more difficult compared to fentanyl-like opioids.

The pharmacodynamic parameters of the EEG effects of morphine could be accurately described with the sigmoidal E_{max} model. All EEG experiments were performed in the presence of a steady state infusion of midazolam to prevent opioid induced seizure activity. Since a constant midazolam concentration was present in all treatment groups, the comparison of the biophase distribution and EEG effect is still valid. In addition, midazolam is a weak Pgp inhibitor, but is not transported by Pgp (Mahar Doan *et al.*

2002) and therefore the influence of midazolam could be neglected.

The next step was to correlate the biophase distribution kinetics with the previously investigated brain ECF distribution pharmacokinetics (Groenendaal *et al*., 2007 – chapter 5). To describe the brain ECF distribution kinetics a non-linear transport model was proposed consisting of one brain compartment with distinction between passive diffusion, active linear efflux which is partly mediated by Pgp and active saturable influx by a yet unknown transport mechanism. In contrast, the extended-catenary biophase distribution model consists of two sequential compartments. There were no indications for non-linearity in the biophase distribution kinetics of morphine. The difference between the models indicates that transport into the brain ECF is distinctly different from transport to the effect-site. Transport into the brain ECF is dependent on both passive diffusion and active saturable influx, whereas for biophase distribution the transport to the effect-site is a linear process. The effects of GF120918 on the distribution kinetics of morphine in the effect compartments were consistent with recent observations on the distribution in brain ECF (Groenendaal *et al*., 2007 – chapter 5). When comparing the concentration-time profiles in brain ECF and biophase, it could be noted that they were distinctly different (figure 6). The concentration in brain

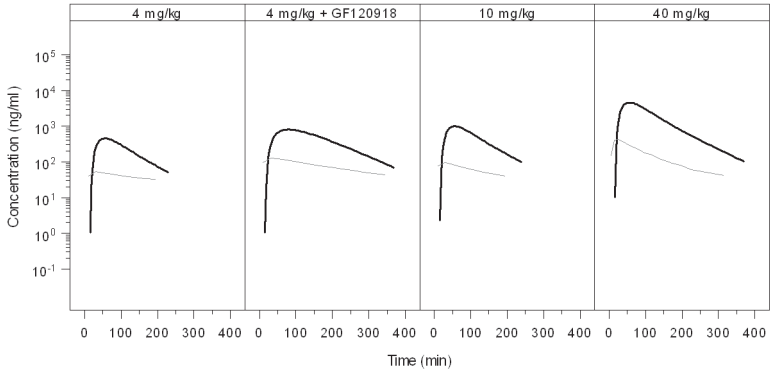

Figure 6: Comparison of the population predicted biophase concentration-time profiles (black lines) and the population predicted brain ECF fluid concentration-time profiles (grey lines) as obtained previously (see companion paper). It is shown that the time-course of the biophase concentrations differs substantially from the time-course of the brain ECF concentrations indicating that biophase equilibration is slower than transport into the brain ECF.

ECF peaked early, whereas the maximum biophase concentration showed a profound delay. In addition, at the low dose of morphine a "plateau" was observed in brain ECF whereas in the biophase concentrations a clear decline over time was observed. These observations indicate that the brain ECF cannot be used to explain the hysteresis. This is in contrast with the observation by Bouw and co-workers where 85% of the observed hysteresis for the anti-nociceptive effect could be explained by distribution into the brain ECF (2000). In addition, Bouw and co-workers did not identify the active uptake of

morphine in the brain ECF. This indicates that the site of action for the anti-nociceptive effects is distinctly different from that for the EEG effect.
A discrepancy between the predicted effect-site concentration and the measured CNS time course has also been observed for the EEG effects of amobarbital, where the amobarbital effect-site concentrations did not reflect the measured cerebrospinal fluid concentrations (Mandema *et al*. 1991). In addition, Chenel and co-workers showed that the extensive time delay between EEG effect and plasma concentrations of norfloxacin, best described with an effect-compartment model, could not be explained by slow distribution to the biophase (Chenel *et al*. 2004). For norfloxacin the brain ECF concentrations peaked very early, whereas the EEG effect was delayed, which was also seen for morphine. For norfloxacin the brain ECF profiles were parallel to the plasma profiles whereas for morphine a non-linearity was observed at the low dose (4 mg/kg). Chenel and co-workers showed that the k_{eo} did not decrease when the ECF data were included in the PK-PD analysis, whereas for morphine the brain ECF and EEG effects could not be analysed simultaneously.

In conclusion, the biophase distribution kinetics of morphine was adequately described with the extended-catenary biophase distribution model. Comparison with the previously developed non-linear distribution model for morphine distribution into the brain showed that the time-course of morphine at the site of action in the brain is distinctly different from the brain ECF concentrations as estimated by intracerebral microdialysis.

ACKNOWLEDGEMENTS

The authors gratefully acknowledge the technical assistance of M.C.M. Blom-Roosemalen, S.M. Bos-van Maastricht and P. Looijmans. The supply of GF120918 by GlaxoSmithKline in the United Kingdom is highly appreciated. These investigations were financially supported by GlaxoSmithKline in the United Kingdom.

REFERENCES

Bartlett SE, Smith MT (1995) The apparent affinity of morphine-3-glucuronide at mu1-opioid receptors results from morphine contamination: demonstration using HPLC and radioligand binding *Life Sci.* **57:** 609-615

Beal SL, Sheiner LB (1999) *NONMEM users guide* San Francisco, CA

Bouw MR, Gardmark M, Hammarlund-Udenaes M (2000) Pharmacokinetic-pharmacodynamic modelling of morphine transport across the blood-brain barrier as a cause of the antinociceptive effect delay in rats--a microdialysis study *Pharm.Res.* **17:** 1220-1227

Chenel M, Marchand S, Dupuis A, Lamarche I, Paquereau J, Pariat C, Couet W (2004) Simultaneous central nervous system distribution and pharmacokinetic-pharmacodynamic modelling of the electroencephalogram effect of norfloxacin administered at a convulsant dose in rats *Br.J.Pharmacol* **142:** 323-330

Cox EH, Kerbusch T, van der Graaf PH, Danhof M (1998) Pharmacokinetic-pharmacodynamic modeling of the electroencephalogram effect of synthetic opioids in the rat: correlation with the interaction at the mu-opioid receptor *J Pharmacol. Exp. Ther.* **284:** 1095-1103

Cox EH, Langemeijer MW, Gubbens-Stibbe JM, Muir KT, Danhof M (1999) The comparative pharmacodynamics of remifentanil and its metabolite, GR90291, in a rat electroencephalographic model *Anesthesiology* **90:** 535-544

Cox EH, Van Hemert JG, Tukker EJ, Danhof M (1997) Pharmacokinetic-pharmacodynamic modelling of the EEG effect of alfentanil in rats. *J Pharmacol. Toxicol. Methods* **38:** 99-108

Danhof M, Alvan G, Dahl SG, Kuhlmann J, Paintaud G (2005) Mechanism-based pharmacokinetic-pharmacodynamic modeling-a new classification of biomarkers. *Pharm.Res.* **22:** 1432-1437

de Jong LA, Kramer K, Kroeze MP, Bischoff R, Uges DR, Franke JP (2005) Development and validation of a radioreceptor assay for the determination of morphine and its active metabolites in serum. *J. Pharm. Biomed. Anal.* **39:** 964-971

Dingemanse J, Sollie FA, Breimer DD, Danhof M (1988) Pharmacokinetic modeling of the anticonvulsant response of oxazepam in rats using the pentylenetetrazol threshold concentration as pharmacodynamic measure. *J. Pharmacokinet. Biopharm.* **16:** 203-228

Egan TD, Minto CF, Hermann DJ, Barr J, Muir KT, Shafer SL (1996) Remifentanil versus alfentanil: comparative pharmacokinetics and pharmacodynamics in healthy adult male volunteers. *Anesthesiology* **84:** 821-833

Groenendaal D, Blom-Roosemalen MC, Danhof M, de Lange EC (2005) High-performance liquid chromatography of nalbuphine, butorphanol and morphine in blood and brain microdialysate samples: application to pharmacokinetic/pharmacodynamic studies in rats. *J. Chromatogr. B Analyt. Technol. Biomed. Life Sci.* **822:** 230-237

Groenendaal D, Freijer J, de Mik D, Bouw MR, Danhof M, de Lange EC (2007) Population pharmacokinetic modelling of non-linear brain distribution of morphine: influence of active saturable influx and P-glycoprotein mediated efflux. *Br. J.Pharmacol.* **515:** 701-712

Lemmens HJ, Egan TD, Fiset P, Stanski DR (1995) Pharmacokinetic/dynamic assessment in drug development: application to the investigational opioid mirfentanil. *Anesth. Analg.* **80:** 1206-1211

Letrent SP, Pollack GM, Brouwer KR, Brouwer KL (1998) Effect of GF120918, a potent P-glycoprotein inhibitor, on morphine pharmacokinetics and pharmacodynamics in the rat. *Pharm. Res.* **15:** 599-605

Letrent SP, Pollack GM, Brouwer KR, Brouwer KL (1999) Effects of a potent and specific P-glycoprotein inhibitor on the blood- brain barrier distribution and antinociceptive effect of morphine in the rat. *Drug Metab Dispos.* **27:** 827-834

Loser SV, Meyer J, Freudenthaler S, Sattler M, Desel C, Meineke I, Gundert-Remy U (1996) Morphine-6-O-beta-D-glucuronide but not morphine-3-O-beta-D-glucuronide binds to mu-, delta- and kappa- specific opioid binding sites in cerebral membranes. *Naunyn Schmiedebergs Arch. Pharmacol* **354:** 192-197

Mahar Doan KM, Humphreys JE, Webster LO, Wring SA, Shampine LJ, Serabjit-Singh CJ, Adkison KK, Polli JW (2002) Passive permeability and P-glycoprotein-mediated efflux differentiate central nervous system (CNS) and non-CNS marketed drugs. *J. Pharmacol. Exp. Ther.* **303:** 1029-1037

Mandema JW, Veng-Pedersen P, Danhof M (1991) Estimation of amobarbital plasma-effect site equilibration kinetics. Relevance of polyexponential conductance functions. *J. Pharmacokinet. Biopharm.* **19:** 617-634

Mandema JW, Wada DR (1995) Pharmacodynamic model for acute tolerance development to the electroencephalographic effects of alfentanil in the rat. *J.Pharmacol.Exp.Ther.* **275:** 1185-1194

Scott JC, Cooke JE, Stanski DR (1991) Electroencephalographic quantitation of opioid effect: comparative pharmacodynamics of fentanyl and sufentanil. *Anesthesiology* **74:** 34-42

Scott JC, Ponganis KV, Stanski DR (1985) EEG quantitation of narcotic effect: the comparative pharmacodynamics of fentanyl and alfentanil. *Anesthesiology* **62:** 234-241

Sheiner LB, Stanski DR, Vozeh S, Miller RD, Ham J (1979) Simultaneous modeling of pharmacokinetics and pharmacodynamics: application to d-tubocurarine. *Clin Pharmacol Ther* **25:** 358-371

Stanski DR (1992) Pharmacodynamic modeling of anesthetic EEG drug effects. *Annu. Rev. Pharmacol Toxicol.* **32:** 423-447

Tunblad K, Jonsson EN, Hammarlund-Udenaes M (2004) Morphine blood-brain barrier transport is influenced by probenecid co-administration. *Pharm Res* **20:** 618-623

Upton RN, Huang YF, Mather LE, Doolette DJ (1999) The relationship between the myocardial kinetics of meperidine and its effect on myocardial contractility: model-independent analysis and optimal regional model. *J. Pharmacol Exp. Ther* **290:** 694-701

Upton RN, Ludbrook GL, Grant C, Doolette DJ (2000) The effect of altered cerebral blood flow on the cerebral kinetics of thiopental and propofol in sheep. *Anesthesiology* **93:** 1085-1094

Wauquier A, Bovill JG, Sebel PS (1984) Electroencephalographic effects of fentanyl-, sufentanil- and alfentanil anaesthesia in man. *Neuropsychobiology* **11:** 203-206

Wauquier A, De Ryck M, Van den Broeck W, Van Loon J, Melis W, Janssen P (1988) Relationships between quantitative EEG measures and pharmacodynamics of alfentanil in dogs. Electroencephalogr. *Clin Neurophysiol.* **69:** 550-560

Young GA, Khazan N (1984) Differential neuropharmacological effects of mu, kappa and sigma opioid agonists on cortical EEG power spectra in the rat. Stereospecificity and naloxone antagonism. *Neuropharmacology* **23:** 1161-1165

Section 3

PHARMACOKINETIC-PHARMACODYNAMIC MODELLING OF THE EEG EFFECTS OF OPIOIDS

Chapter 7

PHARMACOKINETIC-PHARMACODYNAMIC MODELLING OF THE EEG EFFECTS OF OPIOIDS: THE ROLE OF COMPLEX BIOPHASE DISTRIBUTION KINETICS

Dorien Groenendaal[1], Jan Freijer[2], Andrea Rosier[1], Dennis de Mik[1], Glynis Nicholls[3], Anne Hersey[4], Andrew D Ayrton[3], Meindert Danhof[1,2] and Elizabeth C.M. de Lange[1]

[1]Leiden/Amsterdam Center for Drug Research, Leiden University, Division of Pharmacology, Leiden, The Netherlands, [2]LAP&P Consultants BV, Leiden, The Netherlands, [3]GlaxoSmithKline, Drug Metabolism and Pharmacokinetics, Ware, United Kingdom, [4]GlaxoSmithKline, Computational and Structural Sciences, Stevenage, United Kingdom

Submitted for publication

ABSTRACT

The objective of this investigation was to characterize the role of complex biophase distribution kinetics in the pharmacokinetic-pharmacodynamic correlation of a wide range of opioids. Following intravenous infusion of morphine, alfentanil, fentanyl, sufentanil, butorphanol and nalbuphine the time course of the EEG effect was determined in conjunction with blood concentrations. Different biophase distribution models were tested for their ability to describe hysteresis between blood concentration and effect. For morphine, hysteresis was best described by an extended catenary biophase distribution model with different values for k_{1e} and k_{eo} of 0.038 ± 0.003 and 0.043 ± 0.003 min^{-1}, respectively. For the other opioids hysteresis was best described by a one-compartment biophase distribution model with identical values for k_{1e} and k_{eo}. Between the different opioids, the values of k1e ranged from 0.04 and 0.47 min^{-1}. The correlation between concentration and EEG effect was successfully described by the sigmoidal Emax pharmacodynamic model. Between opioids significant differences in potency (EC50 range: 1.2 - 451 ng/ml) and intrinsic activity (α range: 18 –109 μV) were observed.

In addition, membrane transport characteristics of the opioids were investigated *in vitro*, using MDCK:MDR1 cells and *in silico* with QSAR analysis. A statistically significant correlation was observed between the values of the *in vivo* k1e and the apparent passive permeability as determined *in vitro* in MDCK:MDR1 monolayers.

It is concluded that unlike other opioids, only morphine displays complex biophase distribution kinetics, which can be explained by its relatively low passive permeability and the interaction with active transporters at the blood-brain barrier.

INTRODUCTION

Biophase distribution kinetics can be an important determinant of the pharmacokinetic-pharmacodynamic (PK-PD) correlations of CNS active drugs, and is often described by a one-compartment biophase distribution model, also known as the effect-compartment model. With the effect compartment model the assumption is made that the rate of onset and offset of the drug effect is governed by the rate of drug distribution to the hypothetical "effect-site" (Sheiner *et al.* 1979). This effect-compartment is then linked to the blood concentrations with the rate constant k1e and the rate constant for drug loss k_{eo}. Typically, the biophase distribution is considered to be symmetrical under the assumption that in equilibrium the effect-site concentration equals the blood concentration, in other words, where k_{1e} is equal to k_{eo}. However, also more complex biophase distribution models have been proposed. For example, for the neuroactive steroid alphaxolone a concentration dependent k_{eo} was observed (Visser *et al.* 2002). It was shown that the k_{eo} was correlated to the C_{max} in plasma. In addition, Mandema and co-workers have reported two equilibration rate constants for the dual effects of heptabarbital and have shown that the equilibration kinetics of amobarbital were best described with a bi-exponential transducer function instead of a simple first-order mono-exponential equilibration model (Mandema & Danhof 1990; Mandema *et al.* 1991b).

For opioids, modelling of complex biophase distribution kinetics is of interest, given the interaction with active transporters and the wide range in lipophilicity. In previous investigations, morphine and loperamide have been identified as substrates for P-glycoprotein (Pgp) in both *in vitro* and *in vivo* models (Letrent *et al.* 1999b; Mahar Doan *et al.* 2002; Schinkel *et al.* 1995; 1996;Wandel *et al.* 2002). Furthermore, PK-PD studies in rats have revealed that after oral pre-treatment with the specific Pgp inhibitor GF120918, the anti-nociceptive effect of morphine was prolonged due to its prolonged half-life in the brain (Letrent *et al.* 1998; 1999a). Alfentanil and sufentanil were not identified as Pgp substrates within the abovementioned *in vitro* studies, whereas inconsistencies have been reported for fentanyl (Henthorn *et al.* 1999; Wandel *et al.* 2002). In addition, for fentanyl, *in situ* brain perfusion studies indicated Pgp mediated efflux (Dagenais, Graff, & Pollack 2004). Nalbuphine, a semi-synthetic opioid analgesic, was also found to be a Pgp substrate in a MDCKII-MDR1 cell-system (Mahar Doan *et al.* 2002), whereas to our knowledge so far no studies have been performed on butorphanol.

In order to study the differences in biophase distribution kinetics between opioids, an *in vivo* model is required that is able to study changes in pharmacological effects in great detail. Previous investigations have shown that quantitative analysis of the increase in the delta frequency band of the electroencephalogram (EEG) is a suitable biomarker for the PK-PD correlation of opioids (Cox *et al.* 1998; Groenendaal *et al.* 2007 – chapter 6).

PK-PD analysis with the one-compartment biophase distribution model showed that only small differences were observed between alfentanil, fentanyl and sufentanil, no hysteresis (k_{eo}) was observed for alfentanil, whereas for fentanyl and sufentanil the k_{eo} values were 0.32 min^{-1} and 0.17 min^{-1}, respectively. In this analysis, all opioids behaved as full agonists with an intrinsic activity of around 100 µV, but differed in potency (EC_{50} values of 1.43 – 289 ng/ml). For morphine profound hysteresis was observed between the blood pharmacokinetics and EEG effects. Co-infusion of the Pgp inhibitor GF120918 prolonged the offset of the EEG effect but had no influence on the onset of the hysteresis. The biophase distribution kinetics were best described with the extended-catenary biophase distribution model, consisting of two sequential effect compartments (i.e. a transfer and an effect compartment) and two rate constants for transport through the transfer compartment (k_{1e}) and for loss from the effect compartment (k_{eo}) (Groenendaal *et al*. 2007 – chapter 6). In this study, morphine behaved as a low efficacy agonist with an intrinsic activity of 44.5 µV.

The objective of the study presented here was to study the biophase distribution kinetics in the PK-PD correlation of a wide range of opioids. The opioids selected were alfentanil, fentanyl, sufentanil, morphine, butorphanol and nalbuphine (figure 1).

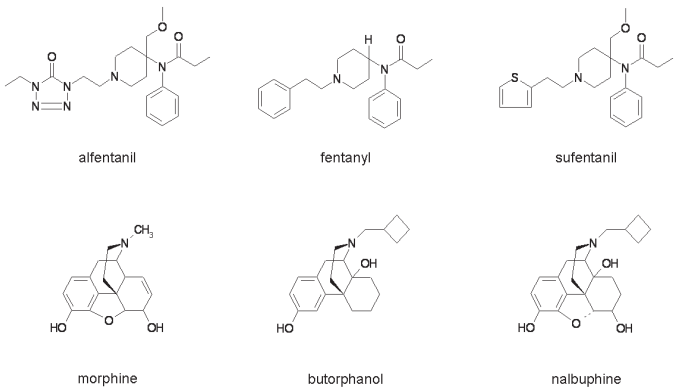

Figure 1: Chemical structures of the opioids. The individual names of the compounds are depicted below the chemical structures.

Nalbuphine and butorphanol were added because they behave as partial agonists *in vivo* (Emmerson *et al.* 1996). The biophase distribution kinetics was investigated with both the one-compartment biophase distribution model, and the extended-catenary biophase distribution model as previously proposed for morphine (Groenendaal *et al*., 2007 – chapter 6). *In vitro* and *in silico* studies were also included to investigate the membrane transport characteristics of all the opioids with respect to P-glycoprotein interaction, apparent membrane permeability and physico-chemical properties. The predicted effect-site concentrations were related to the EEG effect on basis of the sigmoidal E_{max} pharmacodynamic model.

MATERIALS AND METHODS

Animals and surgical procedures

The protocol of these studies was approved by the Committee of Animal Experimentation of the Leiden University. Male Wistar rats weighing between 250-350 grams were housed in groups for at least 7 days under standard environmental conditions (temperature 21 °C, humidity 60% and 12/12 hour dark/light cycle, with lights on at 7 a.m.). The animals had access to standard laboratory chow (RMH-TM, Hope Farms, Woerden, The Netherlands) and acidified water *ad libitum*.

Nine days before the start of the experiments, seven cortical electrodes were implanted into the skull as described before (Cox *et al*. 1997). Briefly, the electrodes were placed at the locations 11 mm anterior and 2,5 mm lateral (F_l and F_r), 3 mm anterior and 3,5 mm lateral (C_l and C_r) and 3 mm posterior and 2,5 mm lateral (O_l and O_r) to lambda. A reference electrode was placed on lambda. Stainless-steel screws were used as electrodes and connected to a miniature connector, which was insulated and fixed to the skull with dental acrylic cement.

Two days before the start of the experiments, three/four indwelling cannulas were implanted, one in the right femoral artery for collection of serial blood samples and two in the left jugular vein (interna and externa) for opioid and midazolam administration. The fourth cannula was implanted into the right femoral vein to administer vecuronium bromide which was only required for the experiments with alfentanil, fentanyl, sufentanil and morphine. All cannulas were made from pyrogen free polyethylene tubing (Portex Limited, Hythe, Kent, United Kingdom). The arterial cannula consisted of 4 cm (I.D.=0.28, O.D.=0.61 mm) polyethylene tubing heat-sealed to 18 cm polyethylene tubing (I.D.=0.58, O.D.=0.96 mm). The venous cannula consisted of 3 cm (I.D.=0.28, O.D.=0.61 mm) polyethylene tubing heat-sealed to 10 cm polyethylene tubing (I.D.=0.58, O.D.=0.96 mm). The cannulas were subcutaneously tunnelled to the back of the neck of the rats. In order to prevent clotting the cannulas were filled with a 25% (w/v) polyvinylpyrrolidone (PVP, Brocacef, Maarssen, The Netherlands) solution in saline containing 50 IU/ml heparin (Pharmacy, Leiden University Medical Centre, Leiden, The Netherlands).

All rats were anesthetized with an intramuscular injection of 0.1 mg/kg Domitor® (1 mg/ml medetomidine hydrochloride, Pfizer, Capelle a/d IJssel, The Netherlands) and subcutaneous injection of 1 mg/kg Ketalar® (50 mg/ml Ketaminebase, Parke-Davis, Hoofddorp, The Netherlands). After the first surgery, 4 mg ampicilline (A.U.V., Cuijk, The Netherlands) was administered to aid recovery.

Drugs and dosages

Alfentanil hydrochloride, fentanyl citrate and sufentanil citrate were kindly donated by Johnson& Johnson Pharmaceutical Research and Development, a Division of Janssen

Pharmaceutica N.V (Beerse, Belgium). Morphine hydrochloride was purchased from Pharmachemie (Haarlem, The Netherlands), nalbuphine hydrochloride and nalorphine hydrochloride were purchased from Sigma Aldrich (Zwijndrecht, The Netherlands) and butorphanol tartrate was purchased from Sigma Aldrich (St. Louis, MI, USA). Midazolam was obtained from BUFA (Uitgeest, The Netherlands). Vecuronium bromide (Norcuron®) was obtained from the hospital pharmacy of the Leiden University Medical Center (Leiden, The Netherlands).

Solutions of the opioids were prepared in physiological saline (0.9%) on the day of the experiment. 500-1500 µl of the infusion solution was administered to each rat. The doses and concentrations are expressed as free base and the concentrations of the infusion solutions were based on the body weight of each rat. Midazolam was administered to prevent opioid induced seizures at a rate of 5.5 mg/kg/h (Cox *et al.* 1997). To reach steady state rapidly, midazolam was administered according to a Wagner infusion scheme, with an initial infusion rate of 3 times the steady state infusion rate for 16 min (Wagner 1974). Vecuronium bromide solutions were prepared at a concentration of 2 mg/ml in physiological saline, independent of body weight.

Pharmacokinetic/pharmacodynamic experiments

The original data and details of the experiments with alfentanil, fentanyl, sufentanil and morphine have been published previously (Cox *et al.*1998; Groenendaal *et al.* 2007 – chapter 6). The experimental protocols for nalbuphine and butorphanol were similar as described for alfentanil, fentanyl and sufentanil. Animals were randomly assigned to the treatment groups. Detailed information regarding the complete experimental design are shown in table 1.

All experiments were started between 8.30 and 9.30 a.m. to minimize influences of circadian rhythms. During the experiments, the animals were deprived of food and water. Bipolar EEG leads on the left hemisphere (C_l-O_l) were continuously monitored using a Nihon-Kohden AB-621G Bioelectric Amplifier (Hoekloos BV, Amsterdam, The Netherlands) and concurrently digitized at a rate of 256 Hz using a CED 1401plus interface (CED, Cambridge, United Kingdom). The digitized signal was transferred into a Pentium III computer and stored on hard disk for off-line analysis. For each 5-sec epoch, quantitative EEG parameters were obtained off-line by Fast Fourier Transformation with a user-defined script within the software package Spike2 for Windows, version 3.18 (CED, Cambridge, United Kingdom). Changes in the amplitudes in the δ-frequency band of the EEG (0.5-4.5 Hz) averaged over 1-minute time intervals were used as a pharmacodynamic endpoint. Further reduction of the EEG data was performed by averaging the signals over predetermined time intervals using a user-defined script within the software package Matlab®, version 6.1 (The Mathworks Inc., Gouda, The Netherlands).

Table 1: Experimental design of the studies investigating the PK-PD relationships of the EEG effects of opioids.

Compound	N	Dose (mg/kg)	Infusion time (min)	Body weight (kg)
Morphine[b]	24	4	10	0.297 ± 0.003
	7	10	10	0.260 ± 0.006
	18	40	10	0.298 ± 0.006
Alfentanil[a]	7	3.14	40	0.278 ± 0.005
Fentanyl[a]	8	0.15	20	0.290 ± 0.012
Sufentanil[a]	7	0.03	40	0.297 ± 0.006
Butorphanol	7	2.5	10	0.284 ± 0.006
	6	5	10	0.260 ± 0.002
	6	10	10	0.254 ± 0.004
Nalbuphine	6	5	10	0.275 ± 0.009
	9	10	10	0.273 ± 0.006
	5	15	10	0.283 ± 0.006[c]
Saline	6	n/a	10	0.290 ± 0.007

[a]*Experiments described previously by Cox et al. 1997*

[b]*Experiments described previously by Groenendaal et al. 2006*

[c]*Not included in the analysis because of severe systemic side effects during and after the opioid infusion*

The EEG baseline was recorded for 15 min. Thereafter, midazolam infusion was started. 30 minutes after the start of the midazolam infusion, the opioids were administered in a zero-order infusion using a BAS Beehive infusion pump (Bioanalytical systems Inc., Indiana, USA). The EEG signals were recorded up to a maximum of 360 minutes after start of the opioid infusions. For determination of opioid and midazolam concentrations, serial arterial blood samples were collected at predetermined time intervals and immediately hemolysed with 0.5 ml of millipore water and stored at –20 °C.

During and after the infusion of the opioids, respiratory depression occurred. Arterial blood samples were collected to monitor arterial pH, pO_2 and pCO_2 levels using a Corning 248 Blood Gas Analyzer (Bayer, Mijdrecht, The Netherlands). During and after administration of 40 mg/kg morphine, alfentanil, fentanyl and sufentanil, severe respiratory depression and muscle rigidity occurred. These rats were artificially ventilated with preheated air (32 °C) using an Amsterdam Infant Ventilator, model MK3 (Hoekloos, Amsterdam, The Netherlands) through a custom made ventilation mask as described by Cox and co-workers (1997). The ventilation settings were: ventilation frequency 62 beats/min, I-E ratio 1:2 and air supply flow rate 0.7-1.0 l/min. 5 minutes after start of the infusion, the rats received an intravenous bolus dose of 0.15 mg vecuronium bromide and artificial ventilation was started. Vecuronium doses of 0.10 mg were administered repeatedly when muscle rigidity re-appeared until respiratory activity resumed. Blood gas status was carefully monitored during the whole experiment.

During the experiments, body temperature was stabilized between 37.5 and 38.5 °C using a CMA/140 temperature controller (Aurora Borealis, Schoonebeek, The Netherlands).

Drug analysis

The analysis methods for the opioids in blood samples have been described previously (Cox *et al*. 1997; 1998; Groenendaal *et al*. 2005 – chapter 3). The blood concentrations of alfentanil were determined by gas chromatography with nitrogen-phosphorus detection, after a liquid-liquid extraction of the hemolyzed blood samples with sodium triphosphate and pentane. The intra- and interassay variability was generally less than 5% and the lower limit of quantification was 1 ng/ml for a 0.1 ml sample. The blood concentrations of fentanyl and sufentanil were determined by radio-immunoassay, after liquid-liquid extraction of the samples with sodium hydroxide and n-heptane/ isoamylalcohol (98.5/1.5, v/v). The intra- and inter-assay variability were less than 40% and the lower limits of quantification were 0.040 ng/ml for a 1 ml sample obtained at the end of the experiment for both fentanyl and sufentanil.

Morphine, nalbuphine and butorphanol blood samples were analyzed by an HPLC method coupled to an electrochemical detector, after a liquid-liquid extraction of the hemolyzed blood samples with phosphoric acid and/or sodium carbonate and ethyl acetate. The intra- and inter-assay variation was less than 15% for morphine, nalbuphine and butorphanol. The lower limits of quantification for a 50 µl blood sample were 25, 25 and 50 ng/ml for morphine, nalbuphine and butorphanol, respectively (Groenendaal *et al*. 2005 – chapter 3).

The blood concentrations of midazolam were determined as described previously by Mandema and co-workers (Mandema *et al*. 1991a). The method consisted of a liquid-liquid extraction with NaOH and dichloromethane/petroleumether (45/55, v/v). After extraction, samples were injected onto an HPLC coupled to an ultraviolet detector. The intra- and inter-assay variation was less than 6% and the lower limit of quantification was 50 ng/ml for a 50 µl blood sample.

Pharmacokinetic-pharmacodynamic data analysis

The pharmacokinetic and pharmacodynamic data of the opioids were analysed using non-linear mixed effect modelling as implemented in the NONMEM software version V, level 1.1 (Beal & Sheiner 1999). Population analysis was undertaken using the first-order conditional estimation method (FOCE interaction) for pharmacokinetic analysis. All fitting procedures were performed on an IBM-compatible computer (Pentium IV, 1500 MHz) running under Windows XP with the Fortran Compiler Compaq Visual Fortran version 6.1.

Pharmacokinetic analysis

For the development of the pharmacokinetic structural models for the opioids, both two- and three-compartment models were tested. Model selection was based on the likelihood ratio test, diagnostic plots (observed concentrations vs. individual and population predicted concentrations, weighted residuals vs. predicted time and concentrations), parameter correlations and precision in parameter estimates. The likelihood criteria

test is based on a comparison of the minimum value of the objective function (MVOF) of two models. The significance level was set at 0.01 which corresponds to a decrease of MVOF of 6.6 points when an extra parameter is included in the structural model under the assumption that the difference in MVOF between the two nested models is χ^2 distributed. On the basis of model selection criteria a three-compartment model was chosen for alfentanil, morphine and nalbuphine, whereas a two-compartment model was the best choice for fentanyl, sufentanil and butorphanol. Pharmacokinetic analysis was performed with the PREDPP subroutines ADVAN 11 TRANS 4 (three-compartment model) and ADVAN 3 TRANS 4 (two-compartment model) implemented in NONMEM. For a three compartment model the pharmacokinetic parameters clearance (Cl), inter-compartemental clearances (Q2 and Q3) and the volumes of distribution (V1, V2 and V3) are estimated whereas Q3 and V3 are excluded when using a two-compartment model.

The interanimal variability in the pharmacokinetic parameters was assumed to be log normally distributed:

$$P_i = P_{typ} \cdot \exp(\eta_i) \tag{1}$$

with

$$\eta_i \sim N(0, \omega^2) \tag{2}$$

where P_i is the individual value of the model parameter P, P_{typ} is the typical value (population value) of parameter P in the population, and η^i is the realization from a normally distributed inter-animal random variable with mean zero and variance ω^2. Inter-animal variability was investigated for each parameter and was fixed to zero when the MVOF did not improve. Correlations between the inter-animal variability of the various parameters were graphically explored.

The residual error, which accounts for unexplained errors (e.g. measurement and experimental errors), in the blood drug concentrations was best described with a proportional error model according to equation:

$$C_{obs,ij} = C_{pred,ij} \cdot (1 + \varepsilon_{ij}) \tag{3}$$

with

$$\varepsilon_i \sim N(0, \sigma^2) \tag{4}$$

Where $C_{obs,ij}$ is the *j*-th observation of the *i*-th individual, $C_{pred,ij}$ is the predicted concentration and ε_{ij} is the normally distributed residual random variable with mean zero and variance σ^2.

To refine the pharmacokinetic models, the relationship between bodyweight and the different parameters was explored graphically. The following equation was used to model the parameter as a function of bodyweight (*BW*):

$$P_i = \theta_i + \theta_j \cdot (BW - median(BW)) \quad (5)$$

where P_i is the individual value of model parameter P and θ_i and θ_j are the intercept and slope of the relationship between the parameter and bodyweight.
The accuracy of the pharmacokinetic was investigated by an internal validation method, the predictive check (Cox *et al.* 1999; Yano *et al.* 2001). With this method, 1000 curves were simulated from the final PK parameter estimates. The median, lower (2.5%) and upper (97.5%) limit of the interquantile range of the simulated concentrations were calculated and compared with the positions of the observations.
Individual pharmacokinetic parameter estimates were used as input for the pharmacodynamic models. Individual blood concentrations were calculated at the times of the EEG measurements.

Biophase distribution models

In this study, the changes in the delta frequency band of the EEG are used as a measure of drug response. A delay in effect (hysteresis) was observed for all opioids except alfentanil. The hysteresis was characterized on the basis of two biophase distribution models: A) the one-compartment biophase distribution model, also known as the effect-compartment model and B) the extended-catenary biophase distribution model.

A) One-compartment biophase distribution model

With the one-compartment distribution model, the effect-compartment is linked to the blood concentrations with the rate constant k1e and the rate constant for drug loss keo. The rate of change of the drug concentration in the effect compartment can then be expressed by equation:

$$\frac{dC_e}{dt} = k_{1e} \cdot C_b - k_{eo} \cdot C_e \quad (6)$$

where C_b represents the blood concentration and C_e represents the effect-site concentration. Under the assumption that in equilibrium the effect-site concentration equals the blood concentration, this equation can be simplified to:

$$\frac{dC_e}{dt} = k_{eo} \cdot (C_b - C_e) \quad (7)$$

This model describes a symmetrical biophase. In contrast, when k_{1e} is not equal to k_{eo}, the biophase is considered to be asymmetrical. For all opioids both models were investigated.

B) Extended-catenary biophase distribution model

With the extended-catenary biophase distribution model, an extra effect-compartment is added to describe the delay in pharmacological response. The rate of change of the

concentrations in the effect compartments can then be described as follows:

$$\frac{dC_{et}}{dt} = k_{1e} \cdot C_b - k_{1e} \cdot C_{et} \quad (4)$$

$$\frac{dC_e}{dt} = k_{1e} \cdot C_{et} - k_{eo} \cdot C_e \quad (4)$$

where C_{et} and C_{e1} describe the concentrations in the transfer and effect-compartment, respectively. The concentrations in the second effect-compartment will then be linked to the pharmacological effect. Both the symmetrical (k_{1e}=k_{eo}) and the asymmetrical (k_{1e}≠k_{eo}) biophase models were investigated.

A schematic diagram of the PK-PD models used in the analysis is shown in figure 2.

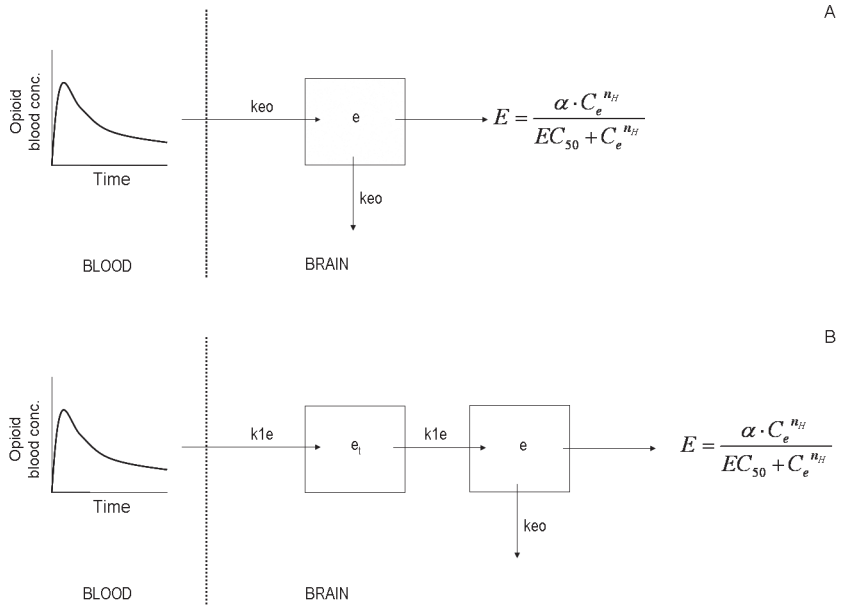

Figure 2: A schematic overview of the PK-PD models used in the analysis. Panel A shows the one-compartment biophase distribution, also known as the effect-compartment model, consisting of one effect (e) compartment. Panel B shows the extended catenary biophase distribution model which consists of two sequential effect compartments, the transfer (et) and the effect (e) compartment. The concentrations in the effect compartment were related to the EEG effect (Groenendaal *et al.* 2007 – chapter 6). The blood pharmacokinetics was used as input function.

PK-PD analysis

After hysteresis minimization, the individual concentration-effect relationships were fitted simultaneously to the Hill equation:

$$E = E_0 + \frac{\alpha \cdot C^{n_H}}{EC_{50}{}^{n_H} + C^{n_H}} \quad (10)$$

where E_0 is the no-drug response, α is the intrinsic activity, EC_{50} is the potency and n_H is the slope factor. The stochastic part of the model, used to describe the inter-animal variability in the pharmacodynamic parameters consisted of a proportional error model for E_0 and α (equation 11) and an exponential error model for EC_{50} (equation 1).

$$P_i = P_{typ} \cdot (1 + \eta_i) \quad (11)$$

with

$$\eta_i \sim N(0, \omega^2) \quad (11)$$

Similar to the pharmacokinetics, the residual error in the pharmacodynamics could be best described with a proportional error model according to equation 6. The accuracy of the pharmacodynamic models was investigated by an internal validation method, the predictive check as explained for the pharmacokinetics.

In vitro transport characteristics

The interaction with Pgp and the apparent membrane permeability (P_{app}) were determined *in vitro* using monolayers of MDCK:MDR1 cells. The cells were cultered in DMEM – glutamax media, formulated with D-glucose (4.5 g/l), L-alanyl-glutamine and phenol red and supplemented with penicillin (10000 U/ml)-streptomycin (10000 µg/ml) and 10% (v/v) fetal calf serum at 37 °C and 5% CO2. Cells were trypsined every 4 days. For the studies, cells were seeded onto BD Falcon™ HTS 24-Multiwell Inserts at a seeding density of 50000 cells/well and grown for 3 days in DMEM full media.

Before each experiment, transepithelial electrical resistance was measured with an EVOMTM voltohmmeter (World Precision Instruments, Stevenage, United Kingdom). The experiments were performed in transport buffer (DMEM containing 25 mM HEPES without phenol red and sodium pyruvate). Cells were pre-incubated with transport buffer containing GF120918 (2 µM) or vehicle (0.5% DMSO) for 15 min at 37°C. After removal of pre-incubation solutions, the test solutions were added and the cells were incubated for 90 min at 37°C under continuous shaking. Donor test solutions contained DMSO or GF120918, lucifer yellow (10 µM) and opioid (3 µM) or amprenavir (3 µM). Receiver test solutions were identical to the pre-incubation solutions. All experiments were performed automatically using the robotic TECANTM genesis workstation (TECAN, Reading, United Kingdom). Reference drugs for paracellular transport (lucifer yellow) and Pgp-efflux (amprenavir) were included in each experiment to test the integrity and quality of the monolayer. After 90 min of incubation, 100 µl samples were

collected to determine lucifer yellow, amprenavir and test compound concentrations. Transport was measured in two directions: apical-to-basolateral (a→b) and basolateral-to-apical (b→a) and in duplicate.

Alfentanil, fentanyl, sufentanil and butorphanol were analysed by dual high-performance liquid chromatography with tandem mass spectrometry (LC/MS/MS). The system consisted of an API-365 (Applied Biosystems, Warrington, United Kingdom) LC/MS/MS employing positive ion turbospray ionisation with a CTC HTS PAL autosampler (CTC Analytics, Hitchin, United Kingdom). Chromatography was conducted on a 50 mm x 2.1 mm HyPURITY column (ThermoHypersil, Runcorn, United Kingdom) at a flow rate of 0.8 ml/min and a split ratio of 1:2. The mobile phase consisted of two solvents: (A) 10 mM ammonium acetate pH 4 and (B) 100% acetonitrile. The gradient profile was at 0 min 80% A and 20% B, at 1 min 0% A and 100% B and at 1.1 min 80% A and 20% B. Total run time was 1.5 min. Data acquisition was performed with PE Sciex version 1.1 (Applied biosystems, Warrington, United Kingdom) and data were reported at the ratio of test compound peak area over internal standard peak area.
Nalbuphine and morphine samples were analysed by high performance liquid chromatography with electrochemical detection (HPLC-ECD) as described above for the samples from the PK-PD studies.
Lucifer yellow samples were analysed by a Polarstar® fluorescence microplate reader with λ_{ex}=430 nm and λ_{em}=538 nm (BMG-Labtech, Aylesbury, United Kingdom).

The efflux ratio was calculated by dividing the amount transported from basolateral to apical (b→a) by the amount transported from apical to basolateral (a→b). Involvement of Pgp mediated efflux was identified if the efflux ratio was >1.5 (Mahar Doan *et al.* 2002). To confirm that efflux was due to Pgp-mediated transport, the efflux ratio was also determined in the presence of the Pgp inhibitor GF120918. In the presence of GF120918, the efflux ratio should decrease to 1. The apparent permeability of the compounds was calculated using the equation:

$$P_{app} = -\left(\frac{V_R \cdot V_D}{(V_R + V_D)\cdot A \cdot t}\right)\cdot \ln\left\{1 - \frac{CR(t)}{\langle C(t)\rangle}\right\} \qquad (13)$$

where P_{app} represents the apparent permeability in nm/sec, V_D and V_R are the donor and receiver chamber volumes (cm^3), A is the area of the permeability barrier (cm^2), t is the time of the measurements (s), $C_R(t)$ is the drug concentration in the receiver chamber and $\langle C(t)\rangle$ is described by equation 11.

$$\langle C(t)\rangle = \frac{V_D \cdot C_D(t) + V_R \cdot C_R(t)}{V_D + V_R} \qquad (14)$$

where $\langle C(t)\rangle$ describes the average system concentration, V_D and V_R are the donor and receiver chamber volumes (cm^3) and $C_D(t)$ and $C_R(t)$ are the donor and receiver

concentrations at time *t* (Tran *et al*. 2004; 2005).
In all studies, amprenavir efflux ratios, apparent permeability of lucifer yellow and mass balance were used as controls. The mass balance was calculated using the equation:

$$\%MB = \frac{A_{rt} + A_{dt}}{A_{d0}} \cdot 100 \quad (15)$$

where $\%MB$ is the mass balance, A_{rt} is the drug amount in receiver chamber at time (t), A_{dt} is the drug amount in donor chamber at time (t) and A_{d0} is the drug amount in the donor chamber at t=0. This calculation of P_{app} takes into account the loss of drug from the donor compartment, which results in a better estimation of the P_{app}.

Experiments were only included when efflux ratio of amprenavir > 16 and when apparent permeability of lucifer yellow < 50 nm/sec and mass balance > 70 %.

Quantitative structure activity relationships – physico-chemical relationships

Log octanol/water partition coefficients (cLogP) was calculated using Daylight Software v4.71/82 (Daylight Chemical Information Systems Inc., Irvine, CA). Polar surface areas (PSA) were calculated according to Ertl and co-workers (2000). A predictor of BBB transport characteristics was also determined based on the Abraham equation (Abraham *et al*. 1994):

$$LogBB = -0.038 + 0198 \cdot R_2 - 0.687 \cdot \pi_2^H - 0.715 \cdot \alpha_2^H - 0.698 \cdot \beta_2^H + 0.995 \cdot V_x \quad (16)$$

where *LogBB* is the logarithm of the blood-brain concentration ratio and R_2, π^H_2, a^H_2, β^H_2 and V_x are defined as the excess molar refractivity, dipolarity/polarisability, hydrogen bond acidity, hydrogen bond basicity and the solute McGowan volume, respectively, as described by Platts and co-workers (Platts *et al*. 1999).

Statistical analysis

The *in vitro* data were analysed using an unpaired Student's t-test (two-tailed) or one-way analysis of variance (ANOVA) (Graphpad Instat®) version 3.00). A value of $p<0.05$ was considered a significant difference. All data are expressed as mean ± SEM, unless indicated otherwise. Each experiment was performed at least three times. Linear regression analysis of *in vivo* k1e with the *in vitro* P_{app} and the physicochemical properties (cLogP, PSA, LogBB) were performed in S-plus 6.0 professional, release 1 (Insightful corporation, USA) using a confidence level of 0.95 and no weight factor.

RESULTS

Pharmacokinetics

Figure 3 shows the observed, population predicted and 2.5% and 97.5% quantiles for 3.14 mg/kg alfentanil in 40 min, 0.15 mg/kg fentanyl in 20 min, 0.030 mg/kg sufentanil in 40 min, 4/10/40 mg/kg morphine in 10 min, butorphanol 2.5/5/10 mg/kg in 10 min and nalbuphine 5/10 mg/kg in 10 min. The pharmacokinetics of fentanyl, sufentanil and butorphanol were best described with a two-compartment model, whereas a three-compartment pharmacokinetic model was used for alfentanil, morphine and nalbuphine. All parameters were estimated accurately as shown in table 2. Covariate analysis showed a linear relationship between bodyweight and CL for fentanyl, a linear relationship between bodyweight and V2 for butorphanol and linear relationships between bodyweight and CL and bodyweight and V2 for morphine. No individual differences in posthoc values were found between the different dosages of morphine, butorphanol and nalbuphine. Between the opioids, differences were observed between the pharmacokinetic parameter values, especially for the volume of the peripheral compartments (V2+V3), ranging from 175 to 1845 ml for alfentanil and nalbuphine, respectively.

Table 2: Population blood pharmacokinetic parameter estimates and standard error of estimate (mean ± SE) for C_l, V_1, Q_2, V_2, Q_3 and V_3. The variances (ω^2) describing the inter-individual variability are shown in parentheses.

Compound	Cl (ml/min)	V1 (ml)	Q2 (ml/min)	V2 (ml)	Q3 (ml/min)	V3 (ml)
Morphine	20.8 ± 1.2	68 ± 11	15.5 ± 1.8	739 ± 56	17.8 ± 3.3	133 ± 21
	-0.13	(--)	(--)	-0.1	(--)	(--)
Alfentanil	10.0 ± 0.8	19 ± 5	22.9 ± 2.6	111 ± 10	1.97 ± 0.3	64 ± 14
	-0.03	(--)	(--)	-0.01	(--)	-0.06
Fentanyl	11.5 ± 1.2	98 ± 9	11.4 ± 2.8	586 ± 94	--	--
	-0.02	(--)	(--)	-0.03	(--)	(--)
Sufentanil	20.6 ± 2.7	113 ± 42	31.2 ± 3.6	1370 ± 204	--	--
	-0.07	(--)	(--)	-0.06	(--)	(--)
Butorphanol	22.9 ± 2.3	81 ± 23	58.8 ± 5.9	1030 ± 89	--	--
	-0.14	(--)	(--)	-0.09	(--)	(--)
Nalbuphine	39.0 ± 3.0	130 ± 29	37.8 ± 4.7	1580 ± 294	44.2 ± 12.4	265 ± 74
	-0.04	(--)	(--)	-0.34	(--)	-0.27

The accuracy of the models was investigated using the predictive check. The selected PK models could well predict the time course of the opioids after intravenous infusion as shown in figure 3.

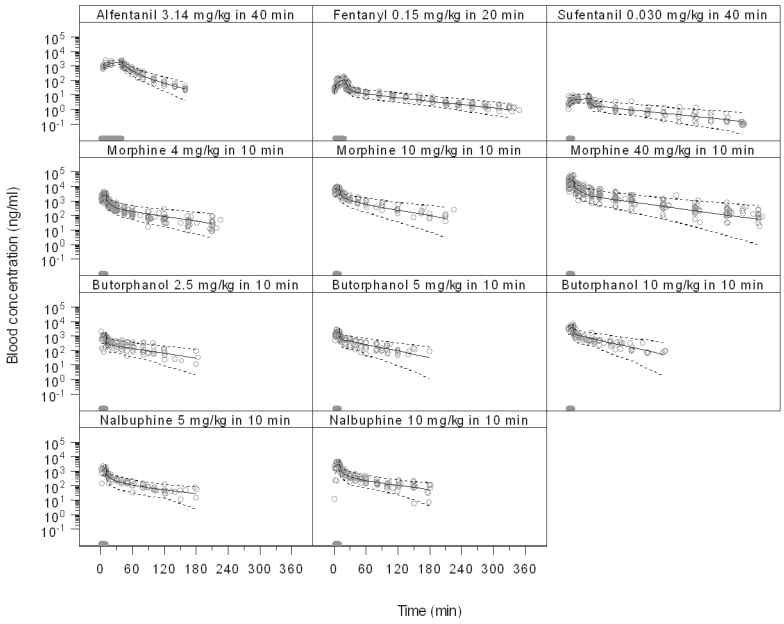

Figure 3: Blood pharmacokinetics of the opioids. Observed (grey dots), population predicted (solid line) and 2.5% and 97.5% quantiles (dotted lines) are depicted for each individual opioid per dose. The name of the compound and the dose are depicted at the top of each panel. Time in minutes is depicted on the x-axis and the blood concentration is depicted on the y-axis on a logarithmic scale. The grey bar indicates the infusion time.

Pharmacodynamics and hysteresis

After start of the opioid infusion, a gradual increase in EEG effect was observed, expressed as absolute amplitude in the 0.5-4.5 Hz frequency range. Large differences in onset of the effect and maximum effect were observed between the opioids (figures 4 and 5). For example, for alfentanil the maximum effect was observed at the end of the infusion, whereas for morphine, the maximal effect was observed around 20 minutes after the end of the infusion. The maximum effect (α) of alfentanil and sufentanil were around 100 μV, whereas for fentanyl, morphine, butorphanol and nalbuphine and butorphanol the maximum effect was 78, 45, 57 and 18 μV, respectively. Duration of the effect (from the start of the infusion until the return to baseline values) was around 180 minutes for alfentanil, 4 and 10 mg/kg morphine, all doses of butorphanol and nalbuphine, whereas for fentanyl, sufentanil and 40 mg/kg morphine, the duration of the effect was around 360 min. The baseline values for alfentanil, fentanyl and

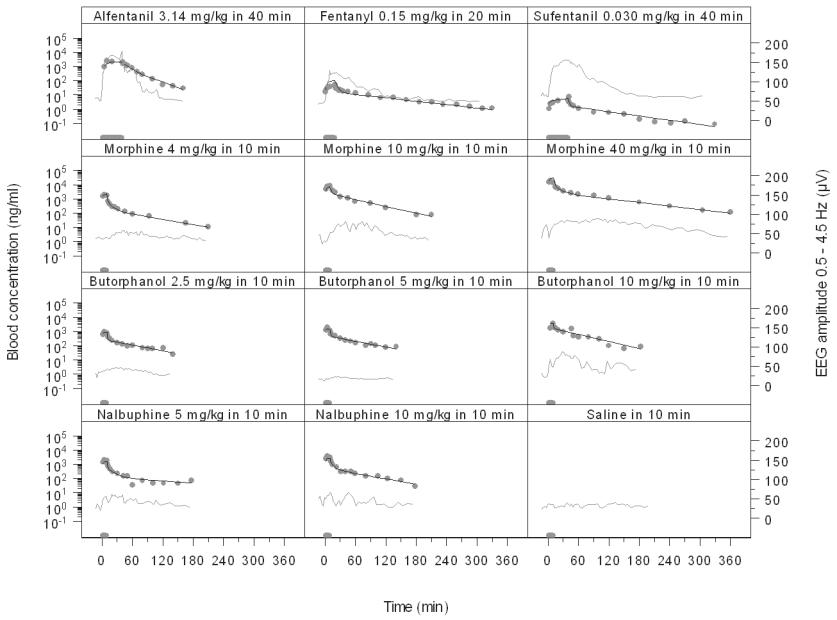

Figure 4: Blood pharmacokinetics and EEG effect (pharmacodynamics) of a typical rat after administration of the opioids. Observed concentrations (grey dots), individual predicted concentrations (black line) and observed effect are depicted for each individual opioid per dose. The grey bar indicates the infusion time. Time in minutes is depicted on the x-axis, the blood concentration is depicted on the left y-axis on a logarithmic scale and the effect as EEG amplitude in the d-frequency range is depicted on the right y-axis on a linear scale. The name of the compound and the dose are depicted at the top of each panel.

sufentanil were significantly higher than the baseline values for morphine, butorphanol and nalbuphine. This is probably caused by differences in surgical and experimental conditions, since the data for alfentanil, fentanyl and sufentanil have been collected and published previously (Cox *et al.* 1998). Validation experiments with fentanyl indicated that a difference in baseline does not affect the actual effect-time profile and maximal effect (data not shown).

The individual pharmacokinetic parameters were used to calculate the blood concentrations at the time points of the individual EEG measurements. The derived concentration-effect relationships showed hysteresis for all opioids, except alfentanil. For each opioid and each dose the concentration-effect relationships are shown in figure 5.

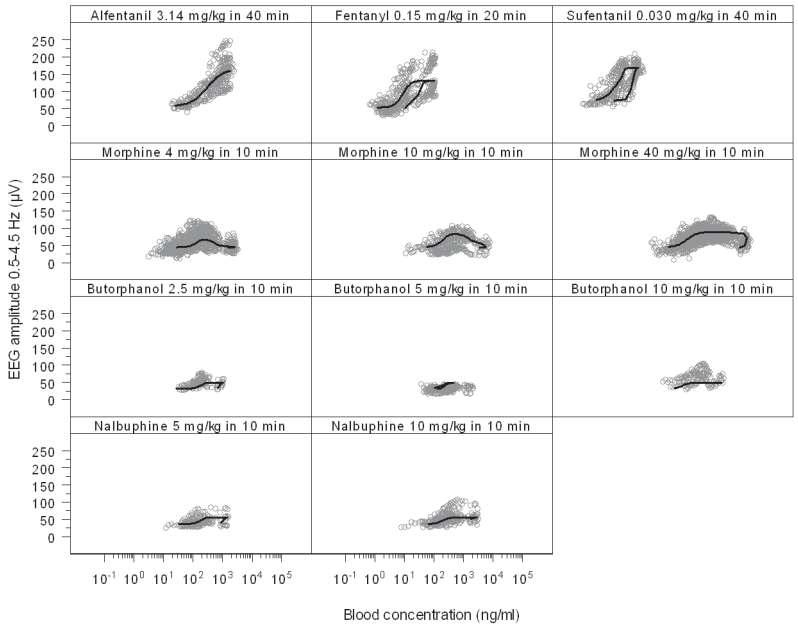

Figure 5: The PK-PD relationship after administration of the opioids. Observed (grey dots) and individual predictions (black line) are depicted for each individual opioid per dose. Blood concentrations are depicted on the x-axis on a logarithmic scale and the EEG amplitude in the d-frequency range is depicted on the y-axis on a linear scale. A hysteresis loop was observed for all opioids, except alfentanil.

Biophase distribution models

Both the one-compartment distribution model and the extended-catenary biophase distribution model were investigated for all opioids except alfentanil, including the symmetrical and a-symmetrical biophase distribution kinetics. A summary of the goodness-of-fit of the four biophase distribution models is shown in table 3. For morphine the extended-catenary biophase distribution model best described the biophase distribution kinetics as has been shown previously (Groenendaal *et al.*, 2007 – chapter 6). In contrast, for fentanyl, sufentanil, nalbuphine and butorphanol, the symmetrical one-compartment biophase distribution model best described the transport to the effect-site. A-symmetrical biophase distribution kinetics could not be identified for the opioids except for morphine. Analysis with the extended-catenary biophase distribution model resulted in an increase in minimum value of objective function or did not result in successful minimization. The k_{1e} values for transport to the effect-site (is equal to k_{eo} except for morphine) ranged from 0.47 min^{-1} ($t_{1/2,k1e}$ = 1.45 min) for fentanyl to 0.04 min^{-1} ($t_{1/2,k1e}$ = 17.3 min) for morphine (table 5). Based on the k1e values the following range in distribution kinetics could be identified: alfentanil (value close to infinity) > fentanyl (0.47 min^{-1}) > butorphanol (0.21 min^{-1}) > nalbuphine (0.20 min^{-1}) > sufentanil (0.17 min^{-1}) > morphine (0.04 min^{-1}).

Table 3: Summary of goodness-of-fit based on the minimum value of objective function, of four biophase distribution models containing expressions for transport to the effect-site and loss from the effect site. This models include the symmetrical ($k_{1e}=k_{eo}$) and a-symmetrical ($k_{1e}\neq k_{eo}$) extended-catenary biophase distribution model and the symmetrical ($k_{1e}=k_{eo}$) and a-symmetrical ($k_{1e}\neq k_{eo}$) one-compartment distribution model.

Compound	One-compartment biophase distribution model		Extended-catenarybiophase distribution model	
	$k_{1e}=k_{eo}$	$k_{1e}\neq k_{eo}$	$k_{1e}=k_{eo}$	$k_{1e}\neq k_{eo}$
Morphine	m.t.	25234	24936	24671
Fentanyl	2497	2497	2504	m.t.
Sufentanil	2297	2298	2324	m.t.
Butorphanol	2542	2542	2620	m.t.
Nalbuphine	2796	2796	2793	2793

Abbreviations: m.t.= minimization terminated

Note: alfentanil is not included in this analysis since no hysteresis was observed.

PK-PD analysis

After hysteresis minimization, the effect site (biophase) concentration-effect relationships were analysed with the Hill equation (equation 3), resulting in estimates for baseline (E_0), intrinsic activity (α), potency (EC_{50}) and slope (n^H). The effect-site concentration-effect relationship of each opioid is shown in figure 6. The highest intrinsic activity was found for alfentanil (109 µV) and the lowest for butorphanol (18 µV). Based on the intrinsic activity, the following range of agonism could be identified: alfentanil (109 µV) > sufentanil (99 µV) > fentanyl (78 µV) > nalbuphine (57 µV) > morphine (45 µV) > butorphanol (18 µV). The estimated pharmacodynamic parameters are shown in table 4.

In vitro transport characteristics and QSAR modeling

The *in vitro* transport characteristics of the opioids were investigated in MDCK: MDR1 cells expressing the human Pgp. Substrate assessment studies were performed to identify Pgp substrates and to calculate the P_{app} value, a measure of the passive membrane transport.

No statistically significant differences were found in the Pgp substrate efflux ratios for alfentanil, fentanyl, sufentanil and butorphanol in the presence or absence of GF120918. For morphine and nalbuphine the concentrations in the receiver compartment were below the limit of quantification of the assay when using the donor concentration of 3 µM. However, at a donor concentration of 100 µM morphine was identified as a Pgp substrate. For nalbuphine literature values were used (Mahar Doan, Humphreys *et al*. 2002). At a donor concentration of 10 µM, nalbuphine was identified as a Pgp substrate. The experimental settings used by Mahar Doan and co-workers were similar to the

Table 4: Population pharmacodynamic estimates and standard error of estimate (mean ± SE) for, intrinsic activity (α), potency (EC_{50}), Hill slope (n_H) and baseline (E_0). The variances (ω^2) describing the inter-individual variability are shown in parentheses.

Compound	k_{1e} (min^{-1})	k_{eo} (min^{-1})	E_0 (μV)	α (μV)	EC_{50} (ng/ml)	n_H
Morphine	0.038 ± 0.003	0.043 ± 0.003	45 ± 1	45 ± 4	451 ± 78	2.3 ± 0.2
		-0.24	-0.03	-0.12	(--)	(--)
Alfentanil	--	--	56 ± 2	109 ± 13	303 ± 56	1.6 ± 0.2
			-0.01	-0.11	-0.16	(--)
Fentanyl	0.47 ± 0.10	0.47 ± 0.10	53 ± 4	78 ± 9	8.9 ± 0.8	3.2 ± 0.3
			-0.06	-0.11	-0.04	(--)
Sufentanil	0.17 ± 0.05	0.17 ± 0.05	72 ± 4	99 ± 8	1.2 ± 0.2	2.1 ± 0.4
			-0.02	-0.02	-0.21	(--)
Butorphanol	0.21 ± 0.03	0.21 ± 0.03	32 ± 2	18 ± 4	195 ± 34	4.1 ± 0.8
			-0.05	-0.73	-0.36	(--)
Nalbuphine	0.20 ± 0.04	0.20 ± 0.04	37 ± 2	57 ± 4	205 ± 24	3.4 ± 0.6
			-0.03	-0.07	-0.15	(--)

Note: For morphine the extended catenary biophase distribution model was used to describe the biophase distribution, for fentanyl, sufentanil, butorphanol and nalbuphine the one-compartment distribution model was used, whereas no hysteresis was observed for alfentanil.

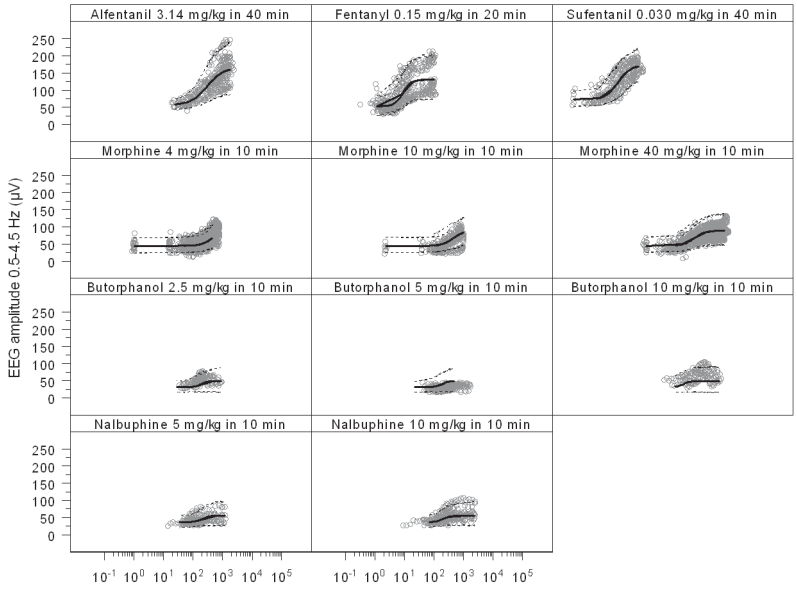

Figure 6: PK-PD relationships of the opioids after hysteresis minimisation. Observed (grey dots), population predicted (solid line) and 2.5% and 97.5% quantiles (dotted lines) are depicted for each individual opioid per dose. The name of the compound is depicted at the top of each panel. The predicted lines were obtained using the effect-compartment model with the Hill equation.

ones used in the present investigation and therefore the use of literature values was justified.

The P_{app} values of the opioids were calculated on the basis of the amount transported across the monolayer over time (nm/s), in both directions, in the presence of GF120918. P_{app} values > 500 nm/s were found for alfentanil, fentanyl, sufentanil and butorphanol, whereas the P_{app} values of nalbuphine and loperamide were 156 and 206 nm/s, respectively. For morphine, the P_{app} value was 16 nm/s, indicating that almost no morphine is transported across the monolayer within the experimental period of 90 min.

The efflux ratios in the absence and presence of GF120918, the P_{app} values and the calculated cLogP, logBB and PSA are listed in table 5.

Table 5: Results of the *in vitro* transport studies in MDCK:MDR1 cells and physico-chemical properties. In vitro studies: averaged (mean ± SEM, n=3) estimate of efflux ratio (transport b →a / transport a → b) and apparent permeability (P_{app}). Each determination was carried out in duplicate. For nalbuphine literature values were used (Mahar Doan et al. 2002). The efflux ratio was determined at a donor concentration of 3 µM, except for nalbuphine

Compound	Efflux ratio		Papp (nm/sec)	cLogP	LogBB	PSA (Á)
	Buffer	GF120918				
Morphine	4.1	n.d.	16	0.6	-0.28	52.9
Alfentanil	0.83 ± 0.05	1.05 ± 0.11	698 ± 39	2.1	0.277	85.5
Fentanyl	0.72 ± 0.07	0.81 ± 0.07	728 ± 105	3.6	0.886	23.6
Sufentanil	1.09 ± 0.39	0.76 ± 0.07	590 ± 42	3.6	0.932	32.8
Butorphanol	0.61 ± 0.10	0.74 ± 0.14	779 ± 48	3.7	0.253	43.7
Nalbuphine	2.17	1.01	156 ± 0.1	1.4	-0.247	73.2

Abbreviations: cLogP – calculated LogP value, which is indicative for lipophilicity, LogBB - BBB transport on basis of Abraham equation, PSA - polar surface area (Á) and n.d. – not determined.

In vitro/in silico/in vivo correlations

Regression analysis was performed to investigate the possible correlations between the *in vivo* k_{1e} and the *in vitro* P_{app} and the *in vivo* k1e with the physico-chemical properties of the selected opioids. The results are shown in figure 7. For all opioids except morphine, the k_{1e} was equal to the keo. For morphine the k1e was estimated separately. A significant correlation was found between the *in vitro* P_{app} and the *in vivo* k_{1e}, which could be described on the basis of: $k_{1e} = 0.13*\log P_{app} - 0.09$. For physicochemical properties, no significant correlations could be identified.

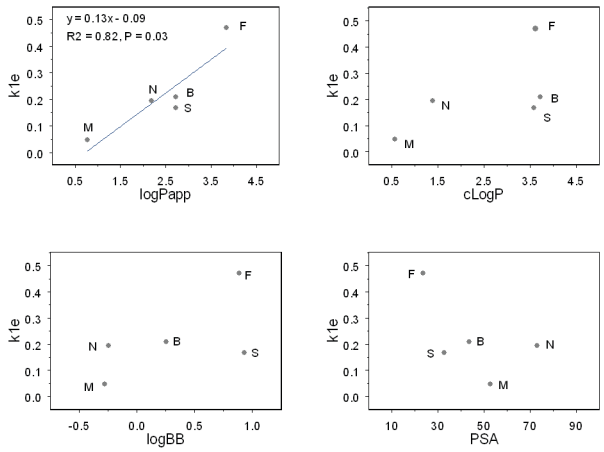

Figure 7: Correlation between the k_{1e} and the P_{app} and the k_{1e} and the physicochemical properties of the opioids. The compounds are depicted with the first letter of the opioid name.

DISCUSSION

The objectives of the study presented here were to study the biophase distribution kinetics in the PK-PD correlation of a wide range of opioids. Previously, the biophase distribution kinetics of morphine have been investigated in the rat EEG model, which were best described with the extended-catenary biophase distribution model. This model consists of two sequential effect compartments (i.e. a shallow and a deep effect compartment) and two rate constants for transport through the transfer compartment (k1e) and for loss from the effect compartment (keo) (Groenendaal *et al*., 2007 – chapter 6). Morphine behaved as a low efficacy agonist with an intrinsic activity of 44.5 µV. It was of interest to extent the investigations on the biophase distribution kinetics for a wide range of opioids. In the current study, two biophase distribution models were investigated, with respect to intrinsic activity and onset of the EEG effect: 1) the one-compartment biophase distribution model (the effect-compartment model) and 2) the extended-catenary biophase distribution model. The predicted biophase concentrations were related to the EEG effect on the basis of the sigmoidal Emax pharmacodynamic model. In addition, *in vitro* and *in silico* studies were also included to investigate the membrane transport characteristics of opioids with respect to P-glycoprotein interaction, apparent membrane permeability and physico-chemical properties.

Pharmacokinetics

The pharmacokinetics of all opioids could be successfully described using population PK analysis. For fentanyl, sufentanil and butorphanol, a two-compartment model

best described the data whereas for alfentanil, morphine and nalbuphine a three-compartment model was most suitable. Previously, Cox and co-workers used a two-compartment model to describe the pharmacokinetics of alfentanil (1997; 1998). However, in the present analysis a population approach was used for the analysis whereas Cox and co-workers analyzed the data per individual. With a population approach both intra- and inter-individual variability are taken into account, thereby increasing the power of the models. All pharmacokinetic parameters could be accurately estimated as shown in table 2. Internal validation with the predictive check confirmed the accuracy of the pharmacokinetic models. Differences were found in the pharmacokinetic characteristics of the opioids, especially in the volume of distribution of the peripheral compartments. For alfentanil a total peripheral volume of 175 ml was found in contrast to nalbuphine where a total peripheral volume of 1845 ml was observed, indicating the butorphanol is widely distributed into tissues compared to alfentanil. The clearance values ranged from 10 ml/min for alfentanil to 39 ml/min for nalbuphine.

Biophase distribution models

Both the one-compartment distribution model and the extended-catenary biophase distribution model were investigated for all opioids, including the symmetrical and a-symmetrical biophase distribution kinetics. The concentration-effect profiles (figure 5) revealed that for all opioids except alfentanil, a delay in effect was observed. Therefore, for alfentanil no distribution models were tested. The biophase distribution kinetics of morphine were best described with the extended-catenary biophase distribution model as shown previously (Groenendaal *et al*., 2007 – chapter 6), with different values for k_{1e} and k_{eo} (asymmetrical biophase). When the data from the rats co-infused with GF120918 were removed from the analysis, the asymmetrical biophase distribution could still be identified. The values for k_{1e} and k_{eo} were 0.038 min^{-1} and 0.043 min^{-1}, respectively. Simplification to the asymmetrical model resulted in a significant increase in objective function and a significant worsening of the fit.

The symmetrical one-compartment biophase distribution model, where $k_{1e}=k_{eo,}$ yielded the most accurate parameter estimates for the biophase distribution kinetics of fentanyl, sufentanil and butorphanol. The use of the a-symmetrical one-compartment biophase model did not result in an improvement of the accuracy of the parameters, while no parameter estimates could be obtained when using the extended-catenary biophase distribution model. These findings were expected since the delay in the EEG effect was relatively short, as is confirmed by the k_{1e} values of 0.47 min^{-1}, 0.17 min^{-1} and 0.21 min^{-1} for fentanyl, sufentanil and butorphanol, respectively. For nalbuphine, a small increase of 2 points in objective function was observed when the biophase distribution was simplified from the extended-biophase distribution model to the one-compartment distribution model. The accuracy of the parameter estimates did not improve and therefore, it was concluded that the simplest model, the one-compartment model was most appropriate to describe the biophase distribution kinetics of nalbuphine. In

addition, asymmetrical distribution could not be identified for nalbuphine and the estimated k_{1e} (and k_{eo}) value was 0.20 min^{-1}.

PK-PD analysis

The differences in intrinsic activity were shown by the PK-PD analysis with the empirical Hill equation. Alfentanil, fentanyl and sufentanil behaved as high efficacy agonists and all displayed the same intrinsic activity of around 100 µV, although the intrinsic activity of fentanyl was slightly lower (78 µV). Morphine, butorphanol and nalbuphine had an intrinsic activity of 45, 18 and 57 µV, respectively, and could therefore be classified as low efficacy agonists. Only small differences were observed in parameter estimates when compared to the paper by Cox and co-workers (1998) indicating that estimation of the inter-animal variability in the population approach and the difference in the pharmacokinetic model for alfentanil does not significantly influence the outcome of the PK-PD modelling. Furthermore, it should be mentioned that the estimation of the pharmacodynamic parameters of butorphanol was difficult, because the changes in EEG amplitude were only marginal compared to the baseline EEG taking into consideration the noise in the EEG signal. This is reflected in the inter-animal variability for the intrinsic activity of butorphanol. For all the opioids this value is around 0.1 whereas for butorphanol this value is 0.73 suggesting that the model has difficulties estimating the intrinsic activity. The EEG effects of butorphanol have the lowest intrinsic activity and the estimate for the Hill factor of 4.1 suggests an on-off response.

In vitro transport characteristics and QSAR modelling

In vitro studies were performed to investigate the contribution of Pgp and P_{app} in transport to the effect site. Morphine and nalbuphine were identified as Pgp substrates whereas for the other opioids, alfentanil, fentanyl, sufentanil and butorphanol, no Pgp-mediated transport was identified. The results were in accordance with literature (Wandel *et al*. 2002). Furthermore, it was shown that the P_{app} in the presence of GF120918 of alfentanil, fentanyl, sufentanil and butorphanol (> 500 nm/sec) was much higher compared to nalbuphine (156 nm/sec) and in particular for morphine with a calculated P_{app} of only 16 nm/sec. The P_{app} values of <50, 50-250, >250 nm/sec were considered as low, moderate and high, respectively. These results indicate that transport to the biophase will not be rate-limiting for alfentanil, fentanyl, sufentanil and butorphanol, due to their very high passive permeabilities, while it should be taken into account for nalbuphine and especially morphine.

For the opioids, to investigate the predictability of the *in vivo* results based on *in vitro* and *in silico* data, a regression analysis was performed to specifically test the correlations between the *in vivo* k1e and the *in vitro* Papp and that between the *in vivo* k_{1e} and the physico-chemical properties as determined *in silico*. The physicochemical properties that were investigated are cLogP, logBB and PSA. cLogP is a measure for lipophilicity

of the compound, logBB is a prediction of the transport characteristics across the BBB, whereas PSA represent the area (size) of the compound. A significant correlation was found between the k_{1e} and the passive permeability which could be described on the basis of: $k_{1e} = 0.13*\log P_{app} - 0.09$ ($R^2 = 0.83$, P=0.03). No significant correlations could be identified between the k1e and the physico-chemical properties, although some trends were observed. Probably, the number of opioids was too limited and moreover these opioids could be divided into two structurally different groups (figure 1). It is therefore expected that the correlations will improve upon inclusion of more opioids. However, based on currently available data, it is concluded that in the *in vitro* P_{app} is a better predictor for the *in vivo* k_{1e} than were the physico-chemical properties. However, it should be taken into consideration that processes other the BBB transport, such as distribution within the brain, can also have an impact on the biophase distribution kinetics (Liu *et al*. 2005).

It is concluded that within the wide range of opioids used in this study, only morphine displays complex biophase distribution kinetics, which can be explained by its relatively low passive permeability and the interaction with active transporters at the blood-brain barrier.

ACKNOWLEDGEMENTS

The authors gratefully acknowledge the technical assistance M.C.M. Blom-Roosemalen, S.M. Bos-van Maastricht and P. Looijmans.

REFERENCES

Abraham MH, Chadha HS, Mitchell RC (1994) Hydrogen bonding. 33. Factors that influence the distribution of solutes between blood and brain. *J.Pharm.Sci.* **83:** 1257-1268

Beal SL, Sheiner LB (1999) *NONMEM users guide* San Francisco, CA

Cox EH, Kerbusch T, van der Graaf PH, Danhof M (1998) Pharmacokinetic-pharmacodynamic modeling of the electroencephalogram effect of synthetic opioids in the rat: correlation with the interaction at the mu-opioid receptor. *J Pharmacol.Exp.Ther.* **284:** 1095-1103

Cox EH, Van Hemert JG, Tukker EJ, Danhof M (1997) Pharmacokinetic-pharmacodynamic modelling of the EEG effect of alfentanil in rats. *J Pharmacol.Toxicol.Methods* **38:** 99-108

Cox EH, Veyrat-Follet C, Beal SL, Fuseau E, Kenkare S, Sheiner LB (1999) A population pharmacokinetic-pharmacodynamic analysis of repeated measures time-to-event pharmacodynamic responses: the antiemetic effect of ondansetron. *J.Pharmacokinet.Biopharm.* **27:** 625-644

Dagenais C, Graff CL, Pollack GM (2004) Variable modulation of opioid brain uptake by P-glycoprotein in mice. *Biochem Pharmacol* **67:** 269-276

Emmerson PJ, Clark MJ, Mansour A, Akil H, Woods JH, Medzihradsky F (1996) Characterization of opioid agonist efficacy in a C6 glioma cell line expressing the mu opioid receptor. *J.Pharmacol.Exp.Ther.* **278:** 1121-1127

Ertl P, Rohde B, Selzer P (2000) Fast calculation of molecular polar surface area as a sum of fragment-based contributions and its application to the prediction of drug transport properties. *Journal of Medicinal Chemistry* **43:** 3714-3717

Groenendaal D, Blom-Roosemalen MC, Danhof M, Lange EC (2005) High-performance liquid chromatography of nalbuphine, butorphanol and morphine in blood and brain microdialysate samples: application to pharmacokinetic/pharmacodynamic studies in rats. *J.Chromatogr.B Analyt.Technol.Biomed.Life Sci.* **822:** 230-237

Groenendaal D, Freijer J, de Mik D, Bouw MR, Danhof M, Lange EC (2007) Influence of biophase distribution and P-glycoprotein interaction on pharmacokinetic-pharmacodynamic modelling of the effects of morphine on the EEG. *Br.J.Pharmacol.* **515:** 713-720

Henthorn TK, Liu Y, Mahapatro M, Ng KY (1999) Active transport of fentanyl by the blood-brain barrier. *J.Pharmacol.Exp.Ther.* **289:** 1084-1089

Letrent SP, Pollack GM, Brouwer KR, Brouwer KL (1998) Effect of GF120918, a potent P-glycoprotein inhibitor, on morphine pharmacokinetics and pharmacodynamics in the rat. *Pharm.Res.* **15:** 599-605

Letrent SP, Pollack GM, Brouwer KR, Brouwer KL (1999a) Effects of a potent and specific P-glycoprotein inhibitor on the blood- brain barrier distribution and antinociceptive effect of morphine in the rat. *Drug Metab Dispos.* **27:** 827-834

Letrent SP, Polli JW, Humphreys JE, Pollack GM, Brouwer KR, Brouwer KL (1999b) P-glycoprotein-mediated transport of morphine in brain capillary endothelial cells. *Biochem.Pharmacol.* **58:** 951-957

Liu X, Smith BJ, Chen C, Callegari E, Becker SL, Chen X, Cianfrogna J, Doran AC, Doran SD, Gibbs JP, Hosea N, Liu J, Nelson FR, Szewc MA, Van Deusen J (2005) Use of a physiologically based pharmacokinetic model to study the time to reach brain equilibrium: an experimental analysis of the role of blood-brain barrier permeability, plasma protein binding, and brain tissue binding. *J.Pharmacol.Exp.Ther.* **313:** 1254-1262

Mahar Doan KM, Humphreys JE, Webster LO, Wring SA, Shampine LJ, Serabjit-Singh CJ, Adkison KK, Polli JW (2002) Passive permeability and P-glycoprotein-mediated efflux differentiate central nervous system (CNS) and non-CNS marketed drugs. *J.Pharmacol.Exp.Ther.* **303:** 1029-1037

Mandema JW, Danhof M (1990) Pharmacokinetic-pharmacodynamic modeling of the central nervous system effects of heptabarbital using aperiodic EEG analysis. *J.Pharmacokinet.Biopharm.* **18:** 459-481

Mandema JW, Tukker E, Danhof M (1991a) Pharmacokinetic-pharmacodynamic modelling of the EEG effects of midazolam in individual rats: influence of rate and route of administration. *Br.J.Pharmacol* **102:** 663-668

Mandema JW, Veng-Pedersen P, Danhof M (1991b) Estimation of amobarbital plasma-effect site equilibration kinetics. Relevance of polyexponential conductance functions. *J.Pharmacokinet.Biopharm.* **19:** 617-634

Platts JA, Butina D, Abraham MH, Hersey A (1999) Estimation of molecular linear free energy relation descriptors using a group contribution approach. *J.Chem.Inform.Comp.Sci.* **39:** 835-845

Schinkel AH, Wagenaar E, Mol CA, van Deemter L (1996) P-glycoprotein in the blood-brain barrier of mice influences the brain penetration and pharmacological activity of many drugs. *J.Clin.Invest* **97:** 2517-2524

Schinkel AH, Wagenaar E, van Deemter L, Mol CA, Borst P (1995) Absence of the mdr1a P-Glycoprotein in mice affects tissue distribution and pharmacokinetics of dexamethasone, digoxin, and cyclosporin A. *J.Clin.Invest* **96:** 1698-1705

Sheiner LB, Stanski DR, Vozeh S, Miller RD, Ham J (1979) Simultaneous modeling of pharmacokinetics and pharmacodynamics: application to d-tubocurarine. *Clin Pharmacol Ther* **25:** 358-371

Tran TT, Mittal A, Aldinger T, Polli JW, Ayrton A, Ellens H, Bentz J (2005) The elementary mass action rate constants of P-gp transport for a confluent monolayer of MDCKII-hMDR1 cells. *Biophysical Journal* **88:** 715-738

Tran TT, Mittal A, Gales T, Maleeff B, Aldinger T, Polli JW, Ayrton A, Ellens H, Bentz J (2004) Exact kinetic analysis of passive transport across a polarized confluent MDCK cell monolayer modeled as a single barrier. *J. Pharm.Sci.* **93:** 2108-2123

Visser SA, Smulders CJ, Reijers BP, van der Graaf PH, Peletier LA, Danhof M (2002) Mechanism-based pharmacokinetic-pharmacodynamic modeling of concentration-dependent hysteresis and biphasic electroencephalogram effects of alphaxalone in rats. *J.Pharmacol Exp.Ther* **302:** 1158-1167

Wagner JG (1974) A safe method for rapidly achieving plasma concentration plateaus. *Clin.Pharmacol.Ther.* **16:** 691-700

Wandel C, Kim R, Wood M, Wood A (2002) Interaction of morphine, fentanyl, sufentanil, alfentanil, and loperamide with the efflux drug transporter P-glycoprotein. *Anesthesiology* **96:** 913-920

Yano Y, Beal SL, Sheiner LB (2001) Evaluating pharmacokinetic/pharmacodynamic models using the posterior predictive check. *J.Pharmacokinet.Pharmacodyn.* **28:** 171-192

Chapter 8

IDENTIFICATION OF THE OPERATIONAL MODEL OF AGONISM FOR THE EEG EFFECTS OF OPIOIDS: ESTIMATION OF THE *IN VIVO* AFFINITY AND INTRINSIC EFFICACY AT THE μ-OPIOID RECEPTOR

Dorien Groenendaal[1], Jan Freijer[2], Jacobien von Frijtag Drabbe Kunzel[3], Adriaan P. IJzerman[3], Piet Hein van der Graaf[4], Meindert Danhof[1,2] and Elizabeth C.M. de Lange[1]

[1]Leiden Amsterdam Center for Drug Research, Leiden University, Division of Pharmacology, Leiden, The Netherlands, [2]LAP&P Consultants BV, Leiden, The Netherlands, [3]Leiden Amsterdam Center for Drug Research, Leiden University, Division of Medicinal Chemistry, Leiden, The Netherlands, [4]Pfizer Ltd, Department of Pharmacokinetics, Dynamics and Metabolism, Sandwich, United Kingdom

In preparation

ABSTRACT

The objective of the current study was to identify the operational model of agonism for the EEG effects of opioids. Unbound biophase concentration-EEG effect relationships of the opioids alfentanil, fentanyl, sufentanil, morphine, butorphanol and nalbuphine were simultaneously analysed with a) the Hill equation and b) the operational model of agonism.

Individual concentration-effect relationships were analysed with the Hill equation and showed that large differences in potency (EC_{50} range 0.22 – 1215 nM) and intrinsic efficacy (α range 0.11 – 1).

Subsequent analysis with the operational model of agonism was performed with the values of the system maximum Em (123 μV) and n (1.44) constrained to the values of alfentanil which displayed the highest intrinsic activity. The values of the *in vivo* affinity parameter pK_A ranged from 5.64 (morphine) to 9.15 (sufentanil) and of the efficacy parameter log τ from 0.421 for alfentanil to -0.342 for nalbuphine. When the estimated *in vivo* pK_A values were correlated with the *in vitro* pK_i values, indications for two distinct subpopulations were obtained. In addition, a poor correlation was observed between the *in vitro* Na/GTP-shift and the *in vivo* log τ indicating that the *in vitro* efficacy measures cannot predict the *in vivo* EEG effect. These observations might be explained by 1) the involvement of active transport processes in distribution from blood to biophase, 2) the existence of μ-opioid receptor subtypes and 3) the interaction with other types of opioid receptors.

INTRODUCTION

Mechanism-based pharmacokinetic-pharmacodynamic (PK-PD) models contain specific expressions for processes on the causal path between drug administration and effect. This includes expressions to describe a) the pharmacokinetics in blood or plasma, b) the biophase distribution kinetics, which for CNS-active drugs includes blood-brain barrier transport (BBB) transport, c) target binding and activation and d) transduction (Danhof *et al.* 2007). Recent investigations on the PK-PD correlations of opioids (alfentanil, fentanyl, sufentanil, morphine, butorphanol and nalbuphine) have focused on the role of biophase distribution kinetics as a determinant of the time course of the EEG effect as a biomarker for μ-opioid receptor activation. A number of structurally different biophase distribution models have been proposed and these models have been successfully applied to derive the biophase concentration-EEG effect relationships of this wide range of opioids (Groenendaal *et al*., 2007 – chapter 6, chapter 7). It has been shown that particularly for morphine the functionality of transporters at the BBB is a major determinant of the time-course of the EEG effect as a biomarker of μ-opioid receptor activation (Groenendaal *et al*., 2007 – chapter 6).

The biophase concentration effect relationships of opioids have so far primarily been described on the basis of the sigmoidal E_{max} pharmacodynamic model (Hill equation). Moreover, an analysis of the relationship between the *in vivo* pharmacodynamic parameters and the *in vitro* receptor binding characteristics has not been accomplished. In this respect it is important that although the Hill equation is useful for descriptive purpose, it provides only limited insight in the factors that determine the shape and the location of the concentration-effect relationships (van der Graaf *et al.* 1997). Specifically, the potency (EC_{50}) and intrinsic activity (E_{max}) are functions of both compound (i.e. target affinity, intrinsic efficacy) and system (i.e. receptor density and signal transduction) characteristics. To fully understand the *in vivo* concentration-effect relationships, more mechanistic modelling approaches are needed to describe target binding and activation processes, including a clear distinction between drug-specific and biological system-specific properties (Danhof *et al.* 2005; 2007).
In the recent years, important progress has been made with the incorporation of receptor theory in PK-PD modelling for the prediction of *in vivo* concentration-effect relationships (van der Graaf & Danhof 1997b). Meanwhile, receptor theory has been successfully applied in the PK-PD analysis of adenosine A1 receptor agonists (van der Graaf *et al.* 1997; 1999) benzodiazepines (Tuk *et al.* 1999; 2003; Visser *et al.* 2001), neuroactive steroids (Visser *et al.* 2002) and 5-HT1A receptor agonists (Zuideveld *et al.* 2004). For the adenosine A_1 receptor agonists a good correlation was observed between the *in vivo* pK_A and the *in vitro* pK_i and also between the *in vivo* efficacy parameter τ and the *in vitro* GTP shift thus enabling the prediction of *in vivo* concentration-effect relationships. In addition, excellent *in vitro-in vivo* correlations have also been observed

for benzodiazepines and neuroactive steroids (Visser *et al.* 2002). In contrast, for the 5-HT_{1A} receptor agonists, despite a good correlation between *in vivo* efficacy parameter τ and the *in vitro* GTP shift, a rather poor correlation was found between the *in vivo* pK_A and the *in vitro* pK_i. This could in part be explained by complexities at the level of blood-brain distribution (Zuideveld *et al.* 2004).

So far, limited progress has been made with the incorporation of receptor theory in mechanism-based PK-PD models of opioids. For the opioids alfentanil, fentanyl and sufentanil, it has been shown by simulation that the concentration-effect relationships could be explained by the operational model of agonism under the assumption of a considerable receptor reserve (Cox *et al.* 1998). Moreover, after pre-treatment with the irreversible μ-opioid receptor antagonist β-funaltrexamine, a shift in the concentration-effect relationship of alfentanil was observed, which is consistent with the 40-60% reduction in the number of specific μ-opioid binding sites as shown in an *in vitro* receptor bioassay (Garrido *et al.* 2000). However, despite these efforts, a formal incorporation of receptor theory in a mechanism-based PK-PD model of opioids has not been accomplished. Complexities at the level of biophase distribution are presumably kinetics were an important factor in this respect.

The objective of the current study was to simultaneously analyse the biophase concentration-effect relationships of six opioids (alfentanil, fentanyl, sufentanil, butorphanol and nalbuphine), as obtained in a previous investigation (chapter 7), with the operational model of agonism. The relationships between the values of the drug-specific parameters receptor affinity (K_A) and intrinsic efficacy (τ), as determined with the operational model of agonism, and the estimates of the receptor affinity and intrinsic efficacy, as determined in an *in vitro* binding assay, are also analysed.

MATERIALS AND METHODS

In vivo PK-PD experiments

The details of the PK-PD experiments have been described previously (chapter 7). Briefly, these studies were conducted in male Wistar rats (Charles River, Maastricht, The Netherlands) weighing between 250 and 300 grams. Nine days prior to the experiments, seven cortical electrodes were implanted for continuous EEG monitoring. In addition, three/four indwelling cannulas were implanted, one in the right femoral artery for collection of serial blood samples and two in the left jugular vein (interna and externa) for opioid and midazolam administration. The fourth cannula was implanted into the right femoral vein to administer vecuronium bromide which was only required for the experiments with alfentanil, fentanyl, sufentanil and morphine. At the day of the experiments, after recording of the EEG baseline, the opioids or saline were administered in a zero-order infusion. The EEG signals were recorded up to a maximum of 360 minutes after start of the opioid infusions. An overview of the experimental groups is shown in table 1. During and after the infusion of the opioids, arterial blood

Table 1: Experimental design of the studies investigating the PK-PD relationships of the EEG effects of opioids in rats.

Compound	N	Dose (mg/kg)	Infusion time (min)	Body weight (kg)
Alfentanil[a]	7	3.14	40	0.278 ± 0.005
Fentanyl[a]	8	0.15	20	0.290 ± 0.012
Sufentanil[a]	7	0.03	40	0.297 ± 0.006
Morphine[b]	24	4	10	0.297 ± 0.003
	7	10	10	0.260 ± 0.006
	18	40	10	0.298 ± 0.006
Butorphanol[b]	7	2.5	10	0.284 ± 0.006
	6	5	10	0.260 ± 0.002
	6	10	10	0.254 ± 0.004
Nalbuphine[b]	6	5	10	0.275 ± 0.009
	9	10	10	0.273 ± 0.006
Saline[b]	6	n/a	10	0.290 ± 0.007

[a]*Experiments described previously by Cox et al. 1997*

[b]*Experiments described previously by Groenendaal et al. 2007c*

samples were collected to monitor arterial pH, pO2 and pCO2 levels. During and after administration of 40 mg/kg morphine, alfentanil, fentanyl and sufentanil, artificial ventilated was required to maintain arterial blood gas values within physiological limits. For determination of drug concentrations, serial arterial blood samples were collected at predetermined time intervals and immediately haemolysed with 0.5 ml of millipore water and stored at –20 °C pending analysis with gas chromatography (Cox *et al*. 1997), radio-immunoassay (Cox *et al*. 1998) or HPLC coupled to electrochemical detection (Groenendaal *et al*. 2005 – chapter 3). Changes in the amplitudes in the δ-frequency band of the EEG (0.5-4.5 Hz) averaged over 1-minute time intervals were used as a pharmacodynamic endpoint. Further reduction of the EEG data was performed by averaging the signals over predetermined time intervals.

Protein binding

Protein binding of morphine, nalbuphine and butorphanol was determined *ex vivo*, whereas for alfentanil, fentanyl and sufentanil literature values were used (Meuldermans *et al*.1982). For determination of the degree of plasma protein binding, blood samples were collected and incubated with morphine, nalbuphine or butorphanol for 1 hour at 37 °C. The concentrations were 100, 1000 and 5000 ng/ml for nalbuphine and butorphanol and 250, 2500 and 25000 ng/ml for morphine. Blood was centrifuged and from the remaining plasma, the free fraction was isolated using ultra filtration (Centrifee, Millipore Corporation, Belford, MA).

In vitro receptor binding assays

Brain homogenates were prepared according to the method of (Lohse *et al.*1984). Briefly, Wistar rat brains (minus cerebellum and corpus striatum) were collected in 0.32 M sucrose solution and homogenized at 25 °C. The suspension was centrifuged for 10 minutes at 1000 rpm and the supernatant was collected. Next, the supernatant was centrifuged for 30 min at 31000 rpm at 4 °C and the remaining pellet was resuspended and centrifuged (15 minutes, 31000 rpm) twice in 50 mM Tris-HCl solution. The remaining pellet was resuspended in 20 ml Tris-HCl and aliquotted. The protein concentration in the stock-homogenate was 15 mg/ml, as determined with the Pierce Micro BCA assay (Pierce, Rockford, IL). Before the experiments, the brain homogenate was diluted to 1.5 mg/ml.

First, the μ-opioid receptor binding characteristics of the radioligand ^{3}H-naloxone (Amersham, specific activity 63 Ci/mmol), K_d and B_{max}, were determined in a saturation experiment. Brain aliquots of 100 μl were incubated with various concentrations (0.5 – 12 nM) of ^{3}H-naloxone at 25 °C. After 30 minutes, the incubation was stopped by adding 1 ml 50 mM Tris-HCl buffer of 4 °C and the samples were filtered through a presoaked glass fiber filter (Whatman GF/B) and eluted six times using 3 ml 50 mM Tris-HCl buffer of 4 °C. The filters were submerged in 3.5 ml Packard Ultima Gold scintillation fluid and radioactivity was measured for 5 minutes by a Hewlett Packard Tri-Carb 1500 liquid scintillation counter. Non-specific binding was determined by calculating the binding of ^{3}H-naloxone in the presence of 10^{-4} M fentanyl. Free radioligand concentrations were calculated by subtracting the non-specific binding from the total concentrations. In the displacement studies, the concentration of ^{3}H-naloxone was equivalent to the K_d value as determined in the saturation experiments in the presence of buffer.

Secondly, the μ-opioid receptor binding was determined by displacement of ^{3}H-naloxone. Brain homogenate aliquots of 100 μl were incubated with 2.5 nM ^{3}H-naloxone at various concentrations of the opioids (10^{-10} – 10^{-5} M). The experimental conditions were similar as described above with the exception of the number of elutions, which was three times in the displacement studies.

To investigate the agonistic character of the opioids, the receptor affinity of the opioids and 3H-naloxone was determined in the presence of buffer, 100 mM NaCl or 1 mM GTP. Previously, it has been shown that the shift in Ki observed after incubation with a high concentration of sodium (100 mM) is a reflection of the agonist efficacy of the ligand (Pert & Snyder 1974). The sodium shift is expressed as the ratio between the Ki in the presence and absence of 100 mM NaCl. Another measure of efficacy is the GTP shift, which is ratio between the Ki in the presence and absence of 1 mM GTP (see (Kenakin 1996)). In each experiment, the binding characteristics were determined in buffer, 100 mM NaCl and 1 mM GTP to minimise inter-assay variability. All experiments were repeated three times and within an experiment duplicates were obtained.

Data analysis

Both the blood pharmacokinetics and the EEG effects of the opioids were analysed using non-linear mixed effect modelling as implemented in the NONMEM software version V, level 1.1 (Beal & Sheiner 1999). Population analysis was undertaken using the first-order conditional estimation method (FOCE interaction). All fitting procedures were performed on an IBM-compatible computer (Pentium IV, 1500 MHz) running under Windows XP with the Fortran Compiler Compaq Visual Fortran version 6.1.

Blood pharmacokinetics and biophase distribution analysis

The population analyses of the blood pharmacokinetics and the biophase distribution kinetics of the various opioids have been described previously (chapter 7). Briefly, the pharmacokinetics of alfentanil, morphine and nalbuphine were best described with a three-compartment model whereas a two-compartment model best described the pharmacokinetics of fentanyl, sufentanil and butorphanol. The biophase distribution kinetics of morphine was best described with the extended-catenary biophase distribution model, while for the other opioids the one-compartment distribution was preferred.

PK-PD analysis

The derived biophase concentrations were converted from ng/ml to nM and corrected for protein binding. The concentration effect relationships were then simultaneously analysed with the sigmoid E_{max} model (Hill equation) using the following equation:

$$E = E_0 + \frac{E_{\max} \cdot \alpha \cdot C_{e,u}{}^{n_H}}{EC_{50,u}{}^{n_H} + C_{e,u}{}^{n_H}} \quad (1)$$

where E_{max} is the maximum effect of the drug with highest intrinsic activity (alfentanil), while α is the fraction of the E_{max} that can be reached by the opioid other the alfentanil; for alfentanil α =1, $EC_{50,u}$ is the potency expressed as the unbound concentration, $C_{e,u}$ is the unbound biophase concentration and n_H is the Hill factor, describing the steepness of the concentration-effect relationships.

Inter-animal variability on E_{max} or n_H (when applicable) was described with a additive error model according to equation:

$$P_i = P_{typ} + \eta_i \quad (2)$$

with

$$\eta_i \sim N(0, \omega^2) \quad (3)$$

where P_i is the individual value of the model parameter *P*, P_{typ} is the typical value (population value) of parameter P in the population, and η_i is inter-animal random variable.

The inter-animal variability on all other parameters was described with a log normal

distribution, using:

$$P_i = P_{typ} \cdot \exp(\eta_i) \quad (4)$$

with

$$\eta_i \sim N(0, \omega^2) \quad (5)$$

Inter-animal variability was investigated for each parameter and was fixed to zero when the MVOF did not improve. Correlations between the inter-animal variability of the various parameters were graphically explored. In addition, correlations between the PD parameters and dose and between the PD parameters and the co-infusion of GF120918 were also investigated graphically.

The residual error, which accounts for unexplained errors (such as measurement and experimental errors) in the EEG measurements, was best described with an additive error model according to equation:

$$C_{obs,ij} = C_{pred,ij} + \varepsilon_{ij} \quad (6)$$

where $C_{obs,ij}$ is the *j*-th observation of the *i*-th individual, $C_{pred,ij}$ is the predicted concentration and ε_{ij} is a realisation from the normally distributed residual random variable with mean zero and variance σ^2:

$$\varepsilon_i \sim N(0, \sigma^2) \quad (7)$$

Next, the *in vivo* concentration-effect relationships were analysed according to the operational model of agonism (Black & Leff 1983):

$$E = E_0 + \frac{E_m \cdot \tau^n \cdot C^n}{(K_A + C)^n + \tau^n \cdot C^n} \quad (8)$$

where E_m is the maximum effect achievable in the system, K_A is the agonist dissociation equilibrium constant, n is the slope index for the occupancy-effect relationship and τ is the efficacy parameter. This efficacy parameter is expressed according to equation:

$$\tau = \frac{R_0}{K_E} \quad (9)$$

where R_0 is the total number of available receptors in the biological system and K_E is the concentration of the drug-receptor complex required to produce the half-maximal effect for that drug.

Inter-animal variability on the parameters was described according to equations 2 and 3. The residual error was best described with a proportional error model according to

equation:

$$C_{obs,ij} = C_{pred,ij} \cdot \left(1 + \varepsilon_{ij}\right) \tag{10}$$

where $C_{obs,ij}$ is the *j*-th observation of the *i*-th individual, $C_{pred,ij}$ is the predicted concentration and ε_{ij} is a realisation from the normally distributed residual random variable with mean zero and variance σ^2:

$$\varepsilon_i \sim N\left(0, \sigma^2\right) \tag{11}$$

In vitro receptor binding

The receptor binding characteristics of the radioligand 3H-naloxone and the opioids were analysed using the non-linear regression curve-fitting program GraphPad Prism, version IV (Graphpad Software Inc, San Diego, CA).The receptor binding characteristics of 3H-naloxone were determined by fitting the data, as obtained from the saturation experiments, to the following equation:

$$B = \frac{B_{\max} \cdot C_f}{K_d + C_f} \tag{12}$$

where B is the number of receptors occupied, B_{max} is the total number of specific binding sites, K_d is the ligand concentration at which 50% of the receptors is occupied and C_f is the free ligand (^{3}H-naloxone) concentration.

The IC_{50} values for the six opioids were determined by fitting the data, as obtained with the displacement experiments, to the following equation:

$$B = \frac{B_0 \cdot IC_{50}}{IC_{50} + C_d} \tag{13}$$

in which B_0 is the specific binding for the radioligand in the absence of the displacer (opioid) and C_d is the concentration of the displacer added and IC_{50} is the opioid concentration that displaces 50% of the radioligand ^{3}H-naloxone. The K_i values were calculated from the IC_{50} values according to the Cheng-Prusoff equation:

$$K_i = \frac{IC_{50}}{1 + \left(L^* / K_d^*\right)} \tag{14}$$

where L^* is the concentration of ^{3}H-naloxone and K_d^* is the equilibration dissociation constant of ^{3}H-naloxone as obtained from the saturation experiment.

RESULTS

In vivo concentration-effect relationships

After administration of the opioids, a gradual increase in the delta frequency (0.5-4.5 Hz) band of the EEG was observed (figure 1).

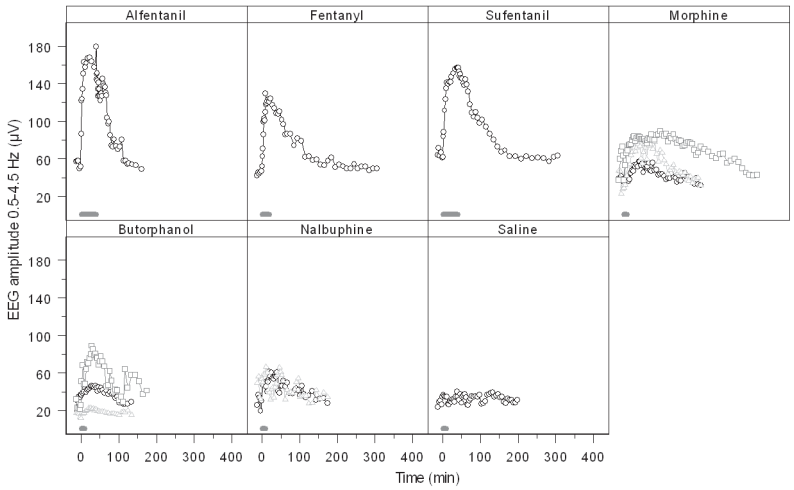

Figure 1: EEG amplitude –time profile of a typical rat after intravenous administration of alfentanil 3.14 mg/kg in 40 min, fentanyl 0.15 mg/kg in 20 min, sufentanil 0.03 mg/kg in 40 min, morphine 4 (black circles), 10 (light gray triangles) and 40 (gray squares) mg/kg in 10 min, butorphanol 2.5 (black circles), 5 (light gray triangles) and 10 (gray squares) mg/kg in 10 min, nalbuphine 5 (black circles) and10 (light gray triangles) mg/kg in 10 min and saline.

Previously, the pharmacokinetics in blood and the biophase distribution kinetics have been investigated (chapter 7). The pharmacokinetics in blood of alfentanil, morphine and nalbuphine were best described with a three compartment model, whereas for fentanyl, sufentanil and butorphanol, a two-compartment model best described the pharmacokinetics in blood. The fraction unbound (mean ± SD) was 0.77 ± 0.01, 0.25 ± 0.06 and 0.097 ± 0.021 for morphine, nalbuphine and butorphanol, respectively. No differences were found between the different concentrations tested (data not shown). For alfentanil, fentanyl and sufentanil literature values of the fraction were used. These values were 0.164, 0.166 and 0.069 for alfentanil, fentanyl and sufentanil, respectively (Meuldermans *et al*. 1982). For all opioids except alfentanil and morphine, biophase distribution was best described with a one-compartment distribution model for all opioids except morphine. For morphine, the extended-catenary biophase distribution model was developed which consists of two sequential distribution compartments.
The results of the simultaneous analysis of the unbound biophase concentration-effect relationships of all six opioids are shown in figure 2. Analysis with the Hill equation was performed on all individual concentration-effect data to provide estimates

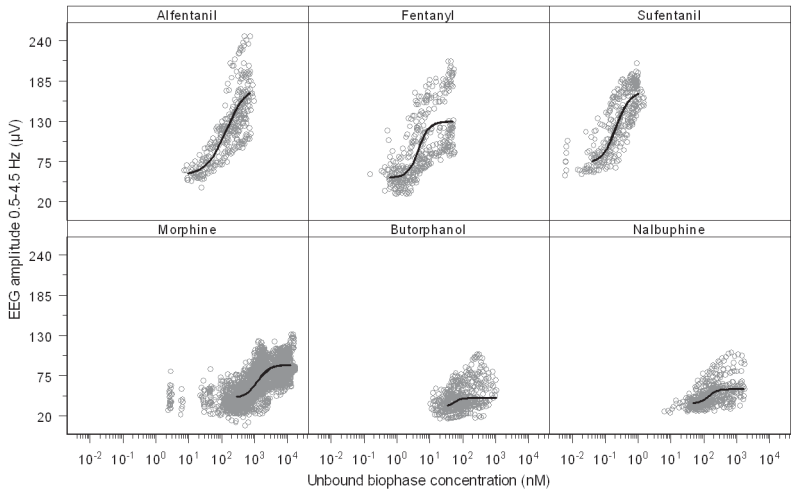

Figure 2: Unbound biophase concentration-effect relationships for the effect on the delta-frequency (0.5-4.5 Hz) band of the EEG after intravenous infusion of the opioids alfentanil, fentanyl, sufentanil, morphine, butorphanol and nalbuphine. The grey dots represent the individual observations and the solid and dashed lines were obtained by simultaneous fitting of the data to the Hill equation.

(mean ± SEM and ω^2 for inter-animal variation) of the PD parameters including maximum achievable effect (E_{max}), the fraction of the E_{max} that can be reached by the opioid (α), the potency expressed as the unbound concentration ($EC_{50,u}$) and the Hill factor (n_H). The derived parameters are shown in table 2.

Table 2: Population pharmacodynamic estimates and standard error of estimate (mean ± SE) for, Emax, fraction of Emax (α), potency (EC50) and Hill slope (nH). The variances (w2) describing the inter-individual variability are shown in parentheses.

Compound	E_{max} (μV)	F	EC_{50u} (nM)	n_H
Alfentanil	123±13	1 FIXED	136±29	1.44±0.16
	-878		-0.2	(--)
Sufentanil		0.81±0.10	0.21±0.03	2.06±0.26
		(--)	-0.21	(--)
Fentanyl		0.62±0.11	4.48±0.40	2.74±0.22
		-0.06	-0.06	(--)
Morphine		0.36±0.05	1223±42	2.51±0.14
		-0.09	(--)	(--)
Nalbuphine		0.16±0.03	141±4	3.34±0.43
		-0.13	-0.13	(--)
Butorphanol		0.10±0.03	54±10	3.97±0.59
		-0.74	-0.33	(--)

Between the opioids, large differences in intrinsic activity and potency were observed with values of α ranging from 1 (alfentanil) to 0.10 (butorphanol) and of $EC_{50,u}$, ranging from 0.21 nM (sufentanil) to 1223 nM (morphine).

Mechanism-based analysis: estimation of in vivo affinity and intrinsic efficacy at the μ-opioid receptor

Individual unbound biophase concentration-effect relationships for all agonists, as obtained by the analysis with the Hill equation, were simultaneously analysed on the basis of the operational model of agonism according to the comparative method with n = 1.44 and E_{max} = 123 ± 13 μV. The *in vivo* pK_A of sufentanil was fixed to the *in vitro* pK_i value in the presence of 100 mM NaCl or in the presence of 1 mM GTP. Only small differences were observed between the analyses, but the parameter estimation was more precise when the *in vitro* pKi of sufentanil in the presence of 100 mM NaCl was constrained. The estimates of *in vivo* affinity (pK_A) and efficacy (log τ) are shown in table 3. The pK_A ranged from 5.64 (morphine) to 9.15 (sufentanil) and of the log τ from 0.421 (alfentanil) to -0.342 (nalbuphine).

Table 3: Estimates of pK_A, log τ and $EC_{50,u}$ as derived from simultaneous analysis with the operational model of agonism. Results are presented as mean ± SE

Compound	pK_A	Log τ
Alfentanil	6.42 ± 0.23	0.421 ± 0.215
Sufentanil	9.15 *	0.393 ± 0.060
Fentanyl	7.81 ± 0.14	0.296 ± 0.177
Morphine	5.64 ± 0.06	-0.064 ± 0.058
Nalbuphine	6.73 ± 0.09	-0.342 ± 0.073
Butorphanol	7.25 ± 0.22	-0.326 ± 0.165

** pK_A of sufentanil has been fixed to the pK_i value in the presence of 100 mM NaCl as obtained in in vitro receptor bindings assay*

In vitro receptor binding assays

The results of the binding assays are shown in table 4. In buffer, the receptor affinity for the μ-opioid receptor ranged from 0.09 nM for sufentanil to 5.84 nM for alfentanil. In the presence of either 100 mM NaCl or 1 mM GTP, the receptor affinity of the opioids decreased substantially. As a measure of intrinsic efficacy, both the Na-shift and the GTP-shift were calculated. In the presence of Na, alfentanil showed the highest efficacy, whereas in the presence of GTP, fentanyl had the highest agonist character. The sodium-shift ranged from 22 (alfentanil) to 3.8 (morphine) and the GTP-shift ranged from 11. (fentanyl) to 2.4 (butorphanol).

Table 4: *In vitro* receptor binding characteristics as obtained in the displacement studies. Results are presented as mean ± SEM

Compound	Ki (nM)	Ki +Na (nM)	Ki +GTP (nM)	Na-shift	GTP-shift
Alfentanil	5.84 ± 1.69	129.27 ± 32.59	59.88 ± 12.30	22	10
Sufentanil	0.09 ± 0.01	0.70 ± 0.22	0.43 ± 0.22	7.7	4.8
Fentanyl	1.28 ± 0.46	15.13 ± 5.57	14.36 ± 4.54	12	11
Morphine	5.55 ± 1.38	21.22 ± 6.89	25.14 ± 10.33	3.8	4.5
Nalbuphine	0.67 ± 0.20	5.33 ± 0.74	7.44 ± 1.04	7.9	11
Butorphanol	0.45 ± 0.12	2.12 ± 0.78	1.07 ± 0.44	4.7	2.4

In vitro – in vivo correlations

When the estimated *in vivo* pK_A values were correlated with the *in vitro* pK_i values, evidence for two distinct subpopulations was obtained. Figure 3 shows the correlation between the apparent *in vivo* pK_A estimates with the pK_i values found *in vitro* in the presence of either 1 mM GTP (left panel) or 100 mM NaCl (right panel). When taking all data together, no statistically significant correlation between the *in vivo* pK_A and the *in vitro* pK_i values was obtained. On contrast, for the subset containing alfentanil, fentanyl and sufentanil highly significant correlations were obtained. These correlations could be best described by $pK_A = 1.3096*pK_i - 2.7991$ ($R^2 = 0.9584$, P = 0.131) and by $pK_A = 1.1911*pK_i - 1.681$ ($R^2 = 0.9873$, P = 0.072) for 1 mM GTP and 100 mM NaCl, respectively. In addition, for the second set containing morphine, butorphanol and nalbuphine the correlation for 1 mM GTP could be best described by $pK_A = 1.1231*pK_i - 2.7064$ ($R^2 = 0.8932$, P = 0.211), whereas for 100 mM NaCl the correlation was best described by $pK_A = 1.6264*pK_i - 6.8076$ ($R^2 = 0.9925$, P = 0.055). For alfentanil, fentanyl and sufentanil the correlation between the *in vivo* pK_A and the *in vitro* pK_i in the presence of 100 mM NaCl was closest to the line of unity. In general, for morphine, butorphanol and nalbuphine a rightward shift was observed compared to the line of unity.

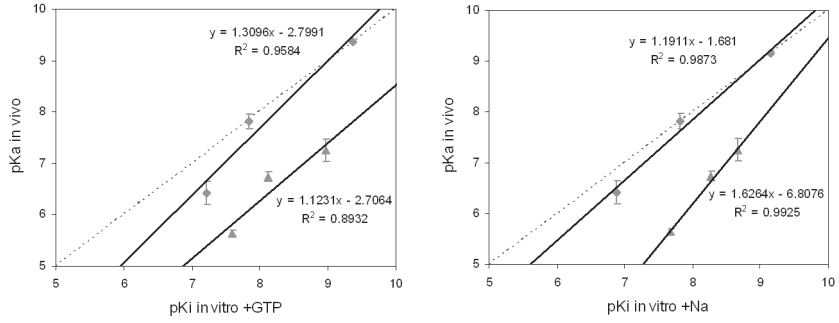

Figure 3: Relationship between the apparent *in vivo* pK_a estimates for the EEG effect of opioids and the *in vitro* pK_i values for the opioids in the presence of 1mM GTP (left panel) or 100 mM NaCl (right panel). The dashed line represents the line of identity. The solid lines were obtained by linear regression. The compounds are depicted with the first letter of the opioid name

Figure 4 depicts the relationship between *in vivo* measure for efficacy log τ and the *in vitro* efficacy parameter GTP-shift (left panel) and Na-shift (right panel). No statistically significant relationship between the *in vivo* efficacy parameter log τ and the *in vitro* efficacy measures was observed (P > 0.1). When describing the correlations between the two parameters with the equation $pK_A = a*pK_i + b$, the correlation between log τ and Na-shift was $R^2 = 0.4096$ (P = 0.171), while the correlation was $R^2 = 0.1332$ between log τ and GTP-shift (P = 0.478).

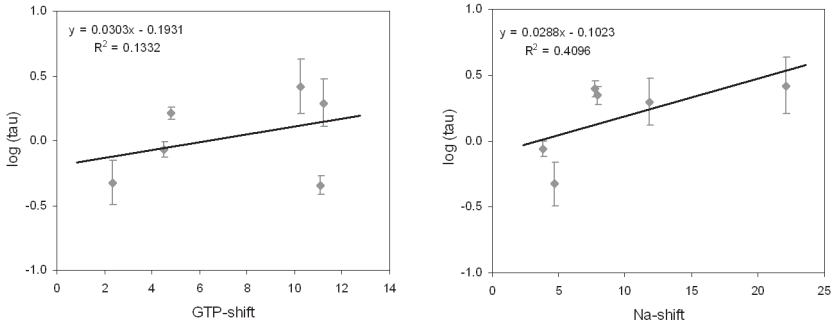

Figure 4: Relationship between the in *vivo* logt estimates for the EEG effect of opioids and the *in vitro* GTP-shift (left panel) and Na-shift (right panel). The solid line was obtained by linear regression. The compounds are depicted with the first letter of the opioid name.

DISCUSSION

The objective of the current study was to develop a mechanism-based pharmacodynamic model for the characterisation of the biophase concentration-EEG effect relationships of opioids. To this end, the unbound biophase concentration-effect relationships of a series of opioids which consisted of alfentanil, fentanyl, sufentanil, morphine, butorphanol and nalbuphine were simultaneously analysed with both the empirical sigmoid E_{max} model and the mechanistic operational model of agonism. The values of the parameters obtained with the operational model of agonism, characterizing the *in vivo* affinity (pK_A) and intrinsic efficacy (log τ) were compared with the estimates of the receptor affinity and intrinsic efficacy as determined in *in vitro* binding assays.

An important feature of this investigation was that the *in vivo* biophase concentration-EEG effect relationships have been determined using previously developed biophase distribution models (chapter 7). For morphine it has been demonstrated that the biophase distribution kinetics is best described with an extended-catenary biophase distribution model consisting of a transfer and an effect compartment model. In contrast, the biophase distribution kinetics of fentanyl, sufentanil, butorphanol and nalbuphine were best described with the effect-compartment model, whereas for alfentanil a direct relationship was observed between blood concentrations and EEG-effect.

In the current investigations, EEG monitoring was used as a pharmacodynamic endpoint.

Quantitative analysis of drug effects on the electroencephalogram (EEG) yields an attractive biomarker, which is continuous, sensitive and reproducible (Dingemanse *et al*. 1988). It has been shown that the synthetic opioid alfentanil, which is frequently used in anesthesia produces a progressive slowing of the EEG with a pre-dominant increase in the delta frequency band (0.5-4.5 Hz) of the EEG power spectrum in both animals (Cox *et al*. 1997; Mandema & Wada 1995; Wauquier *et al*. 1988; Young & Khazan 1984) and humans (Scott *et al*. 1985; Wauquier *et al*. 1984; Young & Khazan 1984). Meanwhile the increase in the delta frequency band of the EEG has been widely used as a biomarker in numerous studies on the PK-PD correlations of synthetic opioids. In preclinical studies evidence has been obtained that the increase in the delta frequency band of the EEG reflect μ-opioid receptor activation (Cox *et al*. 1997; 1998; 1999). However, it remains to be elucidated whether changes in the delta frequency band are solely caused by μ-opioid receptor activation.

Simultaneous PK-PD analysis with the Hill equation showed that alfentanil had the highest intrinsic activity (123 ± 13 μV). This analysis was performed in order to enable a ranking in intrinsic activity for the set of opioids. This fraction (α) ranged from 0.81 to 0.10 for sufentanil and butorphanol, respectively which corresponds to an Emax value of 100 μV for sufentanil and 12 μV for butorphanol. Previously, the biophase concentration-effect relationships have been investigated with the Hill equation for each opioid separately (chapter 7). The parameters derived from the simultaneous analysis are not distinctly different compared to the separate analysis except for the E_{max} of nalbuphine. In the separate analysis an E_{max} of 56 μV was found, whereas in the simultaneous analysis an E_{max} fraction of 0.16 was obtained, which corresponds to an E_{max} of 20 μV. A possible explanation for this difference is that with the simultaneous analysis one residual error is estimated whereas with the separate analysis a residual error is estimated for each compound.
A limitation of the Hill equation is that, although very useful for descriptive purposes, it is only of limited value to understand factors which determine the shape and location of the concentration-effect relationship. Specifically, the pharmacodynamic parameters of the Hill equation are mixed parameters which depend on both the properties of the drug and the biological system (van der Graaf *et al*. 1997; 1997a). To fully understand the *in vivo* concentration-effect relationship, more mechanistic modeling approaches are needed to describe target binding and activation processes, including a clear distinction between drug-specific and biological system specific properties (Danhof *et al*. 2005; 2007). Recently, the operational model of agonism has been successfully applied for explaining and predicting the effects of differential expression of agonism *in vivo* (Black & Leff 1983; van der Graaf *et al*. 1997; Zuideveld *et al*. 2004).

Previously, simulation on the basis of the operational model of agonism indicated that the μ-opioid receptor functions with high efficiency. As a result, the synthetic opioids

alfentanil, fentanyl and sufentanil were all found to behave as full agonists, which complicated identification of the operational model of agonism (van der Graaf *et al.* 1997; 1997b). The simultaneous analysis of the six opioids with the Hill equation has shown that these compounds display a wide range in intrinsic efficacy and were therefore particularly useful for identification of the operational model of agonism.
For the analysis of the operational model of agonism, the comparative method (Black & Leff 1983; Leff *et al.* 1990; van der Graaf *et al.* 1997) was applied where E_{max} (123 μV) and n (1.44) were constraint to alfentanil which displays the highest intrinsic activity *in vivo* as proposed by Leff and co-workers. In addition, the pK_A of sufentanil was fixed to the *in vitro* pK_i (9.15), since this opioid displays the highest affinity. The constraint of the *in vivo* pK_A to the *in vitro* pK_i has been applied previously (Black & Leff 1983; Jonker *et al.* 2005; van der Graaf *et al.* 1997; Zuideveld *et al.* 2004). When analyzing the concentration-effect relationships of the opioids two subsets were seen in the efficacy parameter log τ which ranged from 0.3 to 0.4 for alfentanil, fentanyl and sufentanil and from -0.3 to -0.06 for morphine, nalbuphine and butorphanol.
The *in vitro* K_i values of alfentanil, fentanyl and sufentanil were slightly lower compared to the results reported previously, whereas the values for the sodium shift were largely similar (Cox *et al.* 1998). The observed difference in binding affinity may be explained by differences in the method of membrane preparation and the source of the membranes. When using both the Na-shift and the GTP-shift as measures of the *in vitro* intrinsic efficacy, the opioids alfentanil, fentanyl, and nalbuphine displayed the highest efficacy. The GTP-shift ranged from 11 for fentanyl to 2.4 for butorphanol and the Na-shift ranged from 22 for alfentanil to 3.8 for morphine. Interestingly, nalbuphine showed a relatively high efficacy in both assays, whereas the effect *in vivo* is relatively small (E_{max} fraction 0.16 compared to alfentanil).

When taking all compounds together, the correlations between the *in vivo* pK_A and the *in vitro* pK_i determined in the presence of 1 mM GTP or 100 mM NaCl were not statistically significant (P>0.05). However, there were clear indications for two (sub-) populations of opioids. The estimated *in vivo* pK_A for alfentanil, fentanyl and sufentanil were similar to the values obtained *in vitro*, whereas for morphine, butorphanol and nalbuphine, the pK_A was higher. A possible explanation for this observation is the influence of complex biophase distribution processes with emphasis on interaction with transporters. Although analysis with the biophase distribution models has resulted in accurate biophase concentration- effect relationships, it could still be possible that interaction with active transporters influences the biophase concentration-time profiles and thereby the estimation of the pharmacodynamic parameters. The influence of active transport mechanisms as a confounder of the analysis of the *in vitro-in vivo* corrlations of pK_A values has also been identified for 5-HT_{1A} receptor agonists in particular with regard to flesinoxan (Zuideveld *et al.* 2004). No significant correlations between *in vitro* pK_i and *in vivo* pK_A were observed for a set of 5-HT_{1A} receptor agonists

including flesinoxan. However, when flesinoxan was excluded from the analysis the correlation became statistically significant. Zuideveld and co-workers concluded that the *in vivo* pK_A determined on the basis of blood concentrations was not representative for the flesinoxan concentrations at the site of the 5-HT_{1A} receptor due to interaction with transporters at the BBB which had previously been shown by Van der Sandt and co-workers (2001).
Another possible explanation for the existence of two sub-populations is the interaction with different μ-opioid receptor subtypes. After pre-treatment with β-FNA, the Hill factor of alfentanil is increased to 2.75 (Garrido *et al.* 2000). It has been speculated that antagonist-induced curve-steepening could be indicative for receptor heterogeneity (van der Graaf *et al.* 1996) and that the EEG effect of alfentanil is mediated via multiple receptor types which differ in their sensitivity to β-FNA (Garrido *et al.* 2000). Recently, alternative spliced μ-opioid receptor isoforms have been identified, which might be involved with different aspects of the pharmacology of alfentanil (Pasternak, 2005; Zernig *et al.* 1994). In addition, for the opioids morphine, butorphanol and nalbuphine it is known that they have affinity for both the μ- and κ-opioid receptor, whereas fentanyl is a specific μ-opioid receptor agonist (Chen *et al.* 1993). In literature, little is known about the receptor affinity of alfentanil and sufentanil, but they have been specifically designed to bind exclusively to the μ-opioid receptor (Chen *et al.* 1988). Furthermore, it is known that heterodimerisation of opioid receptors can potentiate the effects of opioids (Gomes *et al.* 2000).

Finally, the correlation between the *in vitro* measures for efficacy, the GTP-shift and the Na-shift, and the *in vivo* log τ were poor. This indicates that the EEG effects of opioids are not determined by interaction with a single receptor system. For example, nalbuphine shows a relatively high efficacy *in vitro* (Na-shift = 7.94) whereas the *in vivo* efficacy is the lowest of the six opioids tested (log τ = -0.342). As mentioned above, nalbuphine has affinity for both μ- and κ-opioid receptors suggesting that interaction with both receptors determines the *in vivo* EEG effect.

In conclusion, analysis with the operational model of agonism has provided insight into the complex process of receptor interaction in the EEG effect of opioids. Since many opioids have affinity for both the μ- and the κ-opioid receptor, the predictive value of the *in vitro* K_i at the μ-opioid receptor is of limited value.

ACKNOWLEDGMENTS

The authors gratefully acknowledge the technical assistance M.C.M. Blom-Roosemalen, S.M. Bos-van Maastricht and P. Looijmans. The financial support by GlaxoSmithKline, Clinical Pharmacokinetics Neurology, Harlow, United Kingdom is gratefully acknowledged.

REFERENCES

Beal SL, Sheiner LB (1999) *NONMEM users guide* San Francisco, CA

Black JW, Leff P (1983) Operational models of pharmacological agonism *Proc.R.Soc.Lond B Biol.Sci.* **220:** 141-162

Chen JC, Smith ER, Cahill M, Cohen R, Fishman JB (1993) The opioid receptor binding of dezocine, morphine, fentanyl, butorphanol and nalbuphine. *Life Sci.* **52:** 389-396

Cox EH, Kerbusch T, van der Graaf PH, Danhof M (1998) Pharmacokinetic-pharmacodynamic modeling of the electroencephalogram effect of synthetic opioids in the rat: correlation with the interaction at the mu-opioid receptor. *J Pharmacol.Exp.Ther.* **284:** 1095-1103

Cox EH, Langemeijer MW, Gubbens-Stibbe JM, Muir KT, Danhof M (1999) The comparative pharmacodynamics of remifentanil and its metabolite, GR90291, in a rat electroencephalographic model. *Anesthesiology* **90:** 535-544

Cox EH, Van Hemert JG, Tukker EJ, Danhof M (1997) Pharmacokinetic-pharmacodynamic modelling of the EEG effect of alfentanil in rats. *J Pharmacol.Toxicol.Methods* **38:** 99-108

Danhof M, Alvan G, Dahl SG, Kuhlmann J, Paintaud G (2005) Mechanism-based pharmacokinetic-pharmacodynamic modeling-a new classification of biomarkers. *Pharm.Res.* **22:** 1432-1437

Danhof M, de Jongh J, de Lange EC, Della Pasqua O, Ploeger BA, Voskuyl RA (2007) Mechanism-Based Pharmacokinetic-Pharmacodynamic Modeling: Biophase Distribution, Receptor Theory, and Dynamical Systems Analysis. *Annu.Rev.Pharmacol Toxicol.* **47:** 357-400

Dingemanse J, Sollie FA, Breimer DD, Danhof M (1988) Pharmacokinetic modeling of the anticonvulsant response of oxazepam in rats using the pentylenetetrazol threshold concentration as pharmacodynamic measure. *J.Pharmacokinet.Biopharm.* **16:** 203-228

Garrido M, Gubbens-Stibbe J, Tukker E, Cox E, von Frijtag-Drabbe Künzel J, IJzerman A, Danhof M, van der Graaf PH (2000) Pharmacokinetic-pharmacodynamic analysis of the EEG effect of alfentanil in rats following beta-funaltrexamine-induced mu-opioid receptor “knockdown” in vivo. *Pharm.Res.* **17:** 653-659

Gomes I, Jordan BA, Gupta A, Trapaidze N, Nagy V, Devi LA (2000) Heterodimerization of mu and delta opioid receptors: A role in opiate synergy. *J.Neurosci.* **20:** RC110

Groenendaal D, Blom-Roosemalen MC, Danhof M, de Lange EC (2005) High-performance liquid chromatography of nalbuphine, butorphanol and morphine in blood and brain microdialysate samples: application to pharmacokinetic-pharmacodynamic studies in rats. *J.Chromatogr.B Analyt.Technol.Biomed.Life Sci.* **822:** 230-237

Jonker DM, Kenna LA, Leishman D, Wallis R, Milligan PA, Jonsson EN (2005) A pharmacokinetic-pharmacodynamic model for the quantitative prediction of dofetilide clinical QT prolongation from human ether-a-go-go-related gene current inhibition data. *Clin Pharmacol Ther* **77:** 572-582

Kenakin T (1996) The classification of seven transmembrane receptors in recombinant expression systems. *Pharmacol Rev.* **48:** 413-463

Leff P, Prentice DJ, Giles H, Martin GR, Wood J (1990) Estimation of agonist affinity and efficacy by direct, operational model-fitting. *J.Pharmacol.Methods* **23:** 225-237

Lohse MJ, Lenschow V, Schwabe U (1984) Interaction of barbiturates with adenosine receptors in rat brain. *Naunyn Schmiedebergs Arch.Pharmacol* **326:** 69-74

Mandema JW, Wada DR (1995) Pharmacodynamic model for acute tolerance development to the electroencephalographic effects of alfentanil in the rat. *J.Pharmacol.Exp.Ther.* **275:** 1185-1194

Meuldermans WE, Hurkmans RM, Heykants JJ (1982) Plasma protein binding and distribution of fentanyl, sufentanil, alfentanil and lofentanil in blood. *Arch.Int.Pharmacodyn.Ther.* **257:** 4-19

Pasternak GW (2005) Molecular biology of opioid analgesia *J.Pain Symptom.Manage.* **29:** S2-S9

Pert CB, Snyder SH (1974) Opiate Receptor Binding of Agonists and Antagonists Affected Differentially by Sodium. *Molecular Pharmacology* **10:** 868-879

Scott JC, Ponganis KV, Stanski DR (1985) EEG quantitation of narcotic effect: the comparative pharmacodynamics of fentanyl and alfentanil. *Anesthesiology* **62:** 234-241

Tuk B, van Gool T, Danhof M (2003) Mechanism-based pharmacodynamic modeling of the interaction of midazolam, bretazenil, and zolpidem with ethanol. *J Pharmacokinet Pharmacodyn* **29:** 235-250

Tuk B, van Oostenbruggen MF, Herben VM, Mandema JW, Danhof M (1999) Characterization of the pharmacodynamic interaction between parent drug and active metabolite in vivo: midazolam and alpha-OH-midazolam. *J.Pharmacol Exp.Ther* **289:** 1067-1074

van der Graaf PH, Danhof M (1997a) Analysis of drug-receptor interactions in vivo: a new approach in pharmacokinetic-pharmacodynamic modelling. *Int.J Clin.Pharmacol.Ther.* **35:** 442-446

van der Graaf PH, Danhof M (1997b) On the reliability of affinity and efficacy estimates obtained by direct operational model fitting of agonist concentration-effect curves following irreversible receptor inactivation. *J.Pharmacol.Toxicol.Methods* **38:** 81-85

van der Graaf PH, Shankley NP, Black JW (1996) Analysis of the activity of alpha 1-adrenoceptor antagonists in rat aorta. *Br.J.Pharmacol* **118:** 299-310

van der Graaf PH, Van Schaick EA, Mathot RA, IJzerman AP, Danhof M (1997) Mechanism-based pharmacokinetic-pharmacodynamic modeling of the effects of N6-cyclopentyladenosine analogs on heart rate in rat: estimation of in vivo operational affinity and efficacy at adenosine A1 receptors. *J.Pharmacol.Exp.Ther.* **283:** 809-816

van der Graaf PH, Van Schaick EA, Visser SA, De Greef HJ, IJzerman AP, Danhof M (1999) Mechanism-based pharmacokinetic-pharmacodynamic modeling of antilipolytic effects of adenosine A(1) receptor agonists in rats: prediction of tissue-dependent efficacy in vivo. *J.Pharmacol Exp.Ther* **290:** 702-709

van der Sandt I, Smolders R, Nabulsi L, Zuideveld KP, de Boer AG, Breimer DD (2001) Active efflux of the 5-HT(1A) receptor agonist flesinoxan via P-glycoprotein at the blood-brain barrier. *Eur.J.Pharm.Sci.* **14:** 81-86

Visser SA, Gladdines WW, van der Graaf PH, Peletier LA, Danhof M (2002) Neuroactive steroids differ in potency but not in intrinsic efficacy at the GABA(A) receptor in vivo. *J.Pharmacol Exp.Ther* **303:** 616-626

Visser SA, Wolters FL, Gubbens-Stibbe JM, Tukker E, van der Graaf PH, Peletier LA, Danhof M (2001) Mechanism-based pharmacokinetic/pharmacodynamic modeling of the electroencephalogram effects of GABAA receptor modulators: in vitro-in vivo correlations. *J Pharmacol Exp Ther* **304:** 88-101

Wauquier A, Bovill JG, Sebel PS (1984) Electroencephalographic effects of fentanyl-, sufentanil- and alfentanil anaesthesia in man. *Neuropsychobiology* **11:** 203-206

Wauquier A, De Ryck M, Van den Broeck W, Van Loon J, Melis W, Janssen P (1988) Relationships between quantitative EEG measures and pharmacodynamics of alfentanil in dogs. *Electroencephalogr.Clin Neurophysiol.* **69:** 550-560

Yeadon M, Kitchen I (1988) Comparative binding of mu and delta selective ligands in whole brain and pons/medulla homogenates from rat: affinity profiles of fentanyl derivatives. *Neuropharmacology* **27:** 345-348

Young GA, Khazan N (1984) Differential neuropharmacological effects of mu, kappa and sigma opioid agonists on cortical EEG power spectra in the rat. Stereospecificity and naloxone antagonism. *Neuropharmacology* **23:** 1161-1165

Zernig G, Butelman ER, Lewis JW, Walker EA, Woods JH (1994) In vivo determination of mu opioid receptor turnover in rhesus monkeys after irreversible blockade with clocinnamox. *J.Pharmacol.Exp.Ther.* **269:** 57-65

Zuideveld KP, van der Graaf PH, Newgreen D, Thurlow R, Petty N, Jordan P, Peletier LA, Danhof M (2004) Mechanism-based pharmacokinetic-pharmacodynamic modeling of 5-HT1A receptor agonists: estimation of in vivo affinity and intrinsic efficacy on body temperature in rats. *J.Pharmacol Exp.Ther* **308:** 1012-1020

Section 4

CONCLUSIONS AND GENERAL DISCUSSION

Chapter 9

MECHANISM-BASED PHARMACOKINETIC-PHARMACODYNAMIC MODELLING OF OF OPIOIDS: SUMMARY, CONCLUSIONS AND PERSPECTIVES

CONTENTS

1. SCOPE OF THESIS AND GENERAL BACKGROUND

The objective of the research described in this thesis was to develop a mechanism-based pharmacokinetic-pharmacodynamic (PK-PD) model for the electro-encephalogram (EEG) effects of opioids. The central effects of opioids are determined by four main processes: (1) blood/plasma pharmacokinetics, (2) biophase distribution, which is largely determined by blood-brain barrier (BBB) transport, (3) kinetics of target binding and activation and (4) transduction (figure 1).

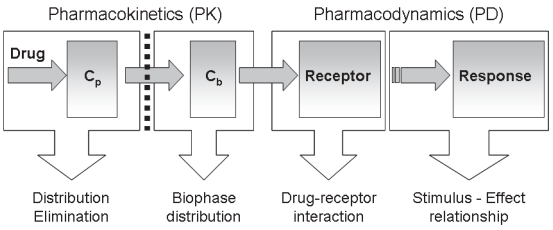

Figure 1: Determinants of in vivo drug effects

Under the assumption that within a single species the transduction mechanisms are similar for all opioids, the focus of this thesis was on the role of biophase distribution kinetics and the kinetics of target binding and activation on the pharmacokinetic-pharmacodynamic (PK-PD) relationships of opioids in the rat.
The opioids selected were alfentanil, fentanyl, sufentanil, morphine, butorphanol and nalbuphine because they differ widely in their brain distribution kinetics and efficacy.

Biophase distribution is considered to be a major determinant of the effects of opioids because they have to cross the blood-brain barrier (BBB) to enter the brain and to exert their central effect. Transport across the BBB can be a critical factor in the PK-PD relationships of opioids, since it determines the rate and extent of biophase distribution. For BBB transport, apart from restricted paracellular diffusion by the presence of tight junctions between the endothelial cells of the BBB, active transport mechanisms may play an important role, especially the efflux transport mediated by P-glycoprotein (Pgp).
In order to develop a mechanism-based PK-PD model, the influence of receptor binding and activation should also be considered. A distinction between affinity and intrinsic efficacy at the μ-opioid receptor can be made using concepts of receptor theory (i.e. the operational model of agonism).

In this chapter, the results of the investigations described in this thesis are reviewed and discussed. Furthermore, considerations and perspectives are presented.

2. MECHANISMS OF BIOPHASE DISTRIBUTION *IN VITRO*

The membrane transport characteristics of opioids were investigated *in vitro* with the focus on the relative contribution of passive permeability and P-glycoprotein (Pgp)-mediated efflux. Such information was also present in literature for some of the opioids (Schinkel *et al.* 1995; 1996; Wandel *et al.* 2002). However, in the context of the development of mechanistic PK-PD models for opioids, it is important to have comparative data for Pgp interaction on the selected opioids, obtained in a single test system an using an identical experimental design. To this end, for all selected opioids, studies were conducted in an *in vitro* cell system using monolayers of either the MDCK: MDR1 cells, which were transfected with the MDR1 gene encoding for human Pgp, or LLC-PK1:MDR1a cells, which were transfected with the MDR1a gene encoding for rodent Pgp. Moreover, unlike in previous studies, here the Pgp mediated transport relative to the passive membrane transport component was explicitely addressed. In these investigations, the passive permeability, as reflected by the Papp, of the different opioids was determined in the presence of a relatively high concentration of the potent and specific Pgp-blocker GF120918 (Hyafil *et al.* 1993).

2.1 Interaction with P-glycoprotein

The interaction of the opioids with Pgp was determined indirectly by investigating the inhibition of Pgp-mediated efflux of ^{3}H-digoxin and directly by a substrate assessment study. In the latter study, the transport of opioids was determined in the presence and absence GF120918.

The 3H-digoxin inhibition studies showed that alfentanil, fentanyl, sufentanil, morphine and loperamide were able to reduce the efflux transport of 3H-digoxin. The fact that loperamide is a strong Pgp substrate and therefore does not cross the BBB is a quantifiable extent (Schinkel *et al.* 1996; Wandel *et al.* 2002) explains why this anti-diarrhoeal agent with an opioid-like structure and receptor pharmacology does not exert any opioid-like effect *in vivo* (DeHaven-Hudkins *et al.* 1999; Niemegeers *et al.* 1979).

In the substrate assessment studies only morphine and loperamide were identified as Pgp substrates. For alfentanil, fentanyl and sufentanil no Pgp mediated transport could be detected, which is in accordance with literature (Wandel *et al.* 2002). For nalbuphine, literature values were included (Mahar Doan *et al.* 2002) to calculate a Pgp substrate efflux ratio, since in the present study no quantifiable transport could be obtained at the concentration tested. A transport ratio of 2 was found, which indicates that nalbuphine is a substrate for Pgp, while no inhibition of Pgp mediated transport of 3H-digoxin by nalbuphine was found. This apparent contradiction might be explained by the existence of several Pgp binding sites (Martin *et al.* 2000).

2.2 Apparent permeability and QSAR

From the Pgp substrate assessment data after pre-incubation with GF120918, the apparent passive permeability (P_{app}) could be calculated. It was shown that the P_{app} of alfentanil, fentanyl, sufentanil and butorphanol was high (>500 nm/sec) whereas for loperamide and nalbuphine the Papp was below 200 nm/sec. For morphine the lowest value of Papp (16 nm/sec) was observed. A schematic overview of the results of the *in vitro* transport studies is shown in table 1. It shows that the relative contributions of

Table 1: Results of the biophase distribution studies *in vitro*

Compound	Inhibitory activity	Substrate Assessment	Apparent permeability
Alfentanil	+	-	Very high
Fentanyl	++	-	Very high
Sufentanil	++	-	Very high
Morphine	+/-	+	Low
Butorphanol	-	-	Very high
Nalbuphine	-	+	Moderate
M3G	-	n.d.	n.d.
M6G	-	n.d.	n.d.
Loperamide	++	++	moderate

Inhibition/Substrate: ++ strong, + moderate, +/- weak, - none

Permeability: very high > 400 nm/sec, high 250-400 nm/sec, moderate 50-250 nm/sec, low <50 nm/sec

Pgp transport and passive permeability to the overall membrane transport were widely different between the opioids. Specifically, as a result of the high passive permeability, the relative contribution of Pgp-mediated transport to the overall transport of alfentanil, fentanyl and sufentanil are minimal. In contrast, for morphine, with a very low passive permeability, Pgp has a significant influence on the membrane transport of morphine, because the passive permeability is very low. This implicated the need for further *in vivo* BBB transport measurements in order to characterise the biophase distribution kinetics in the PK-PD relationships of morphine.

An interesting question is to what extent the passive permeability of opioids could be predicted on the basis of their physicochemical properties. To this end, regression analysis was performed to investigate the relationships between the physico-chemical properties and the P_{app} values. No statistically significant correlations were found in this analysis. This is in contrast with the results of an earlier study on the transport characteristics of adenosine A_1 receptor agonists. Here it has been found that the dynamic polar surface area (non-linear) and logBB as calculated by the Abraham equation (linear) were significantly related to the *in vitro* BBB clearance values of a set of 11 structurally highly related adenosine A1 receptor agonists (Schaddelee *et al*. 2003). An important

factor with the opioids tested here is that three clusters exist: four compounds with a very high passive permeability (alfentanil, fentanyl, sufentanil and butorphanol), two compounds with an intermediate permeability (nalbuphine and loperamide) and one with a low permeability (morphine). It is therefore expected that the *in silico-in vitro* correlations may improve upon inclusion of more opioids representing a more equal distribution of passive permeabilities.

3. MODELLING OF THE BIOPHASE DISTRIBUTION KINETICS OF MORPHINE *IN VIVO*

For morphine, the role of biophase distribution kinetics in the PK-PD correlation was investigated using a novel combined EEG/microdialysis technique that allows simultaneous characterisation of both the brain extracellular fluid (ECF) distribution and the EEG effect. In these investigations a wide dose range was investigated (4 to 40 mg/kg). The influence of Pgp was investigated by co-infusion of the Pgp blocker GF120918. In these investigations, the pharmacokinetics of morphine was investigated by non-linear mixed effect modelling (NONMEM).
The pharmacokinetics of morphine in blood was best described by a three-compartment model, whereas in previous studies plasma pharmacokinetics was described with a two-compartment model (Bouw *et al.*, 2000; Tunblad *et al.*, 2004). A possible explanation of this difference is that in the current investigations samples were collected for a much longer period of time (up to 350 minutes after the end of the infusion), whereas in previous studies samples were only collected up to 180 minutes. The blood pharmacokinetics of morphine was further shown to be independent of the dose administered. Moreover, co-administration of GF120918 did not influence the blood pharmacokinetic parameters.

3.1 Non-linear brain distribution model

To study BBB transport characteristics, intracerebral microdialysis is a valuable tool, since its allows the determination of detailed profiles of the free drug concentrations in the ECF as a function of time, which can be related to the (free) concentration-time profile in blood. However, the dialysate concentrations do not directly equal the real extracellular fluid (ECF) concentrations, because of the existence of a constant flow of the perfusion fluid. This results in a recovery value below 100%. The recovery can be determined *in vitro*, but to account for periprobe tissue processes, the recovery of the microdialysis should also be determined *in vivo* (Bungay *et al.*, 1990). For example, co-infusion of GF120918 can alter the elimination of morphine from the ECF and in addition, the *in vivo* recovery can also be changed by GF120918. It is therefore crucial the determine the *in vivo* recovery in the presence and absence of this Pgp efflux blocker.
For morphine, the *in vivo* recovery is typically determined using the retrodialysis-by-drug method (Bouw *et al.* 2000; Hyafil *et al.* 1993; Tunblad *et al.* 2004). In the current investigation, the *in vivo* recovery was determined with the retro-DNNF method (Bouw

& Hammarlund-Udenaes, 1998; Olson & Justice, Jr., 1993) in order to obtain concentration- as well as time-dependent recovery values of morphine. The retro-DNNF method consists of a retrodialysis period before intravenous administration of morphine to determine whether the loss of morphine from the probe was concentration dependent or influenced by GF120918. These perfusion concentrations were maintained until the end of the experiment, according to the DNNF principle (Olson & Justice, Jr., 1993). *In vivo* recovery was calculated from the retrodialysis period, in order to determine time-dependent values for *in vivo* recovery after iv administration of morphine. However, in contradiction to previous results for morphine in mice (Xie *et al.* 1999), in this case no conclusions could be drawn from the microdialysis data obtained for the DNNF rats after iv administration of morphine. Therefore these data were omitted from further analysis.

Upon administration of morphine, a rapid increase in morphine concentrations in the brain ECF was observed. A non-linearity was observed between the two dose groups as reflected in a reduction of the dose normalized AUC with increasing dose (chapter 5). Moreover, for the 4 mg/kg dose group a characteristic relatively stable plateau of the morphine concentration was reached in the brain ECF which was not observed for the 40 mg/kg dose group for which a clear decline was observed in time. To describe this non-linearity, a transport model was proposed which consisted of a passive diffusion, an active saturable influx and an active efflux component (figure 2). The active efflux was influenced by GF120918. This model is based on earlier indications for active uptake of morphine into the brain (Xie *et al*., 1999), simulations of the influence of different transport processes on the ECF concentration-time profiles (Hammarlund-Udenaes *et al*. 1997) and the models proposed by Upton and Geldof for the brain distribution of fluvoxamine (Upton *et al*. 2000; Xie *et al.* 1999; Geldof *et al*., 2007). The value of the passive diffusion rate constant was 0.0014 min^{-1} and the values of the active efflux rate constant were 0.0113 min^{-1} and 0.0195 min^{-1} in the presence and absence of GF120918, respectively. The active influx has a low capacity as indicated by the maximum transport rate of 0.66 $ng.min^{-1}.ml^{-1}$ and was readily saturated at low concentrations of morphine (C_{50} = 9.9 ng/ml). The active influx was not influenced by GF120918. Interestingly, the active efflux component could not be blocked completely with GF120918 indicating that BBB efflux of morphine is also mediated by transporters other than Pgp. Tunblad and co-workers showed that morphine is also substrate for the probenecid-sensitive transporters at the BBB. Specifically, co-administration of probenecid was found to result in a decrease in efflux clearance of morphine from the brain (Tunblad *et al.* 2004). Taken together, it can be concluded that the distribution of morphine is dependent by multiple transport mechanisms.

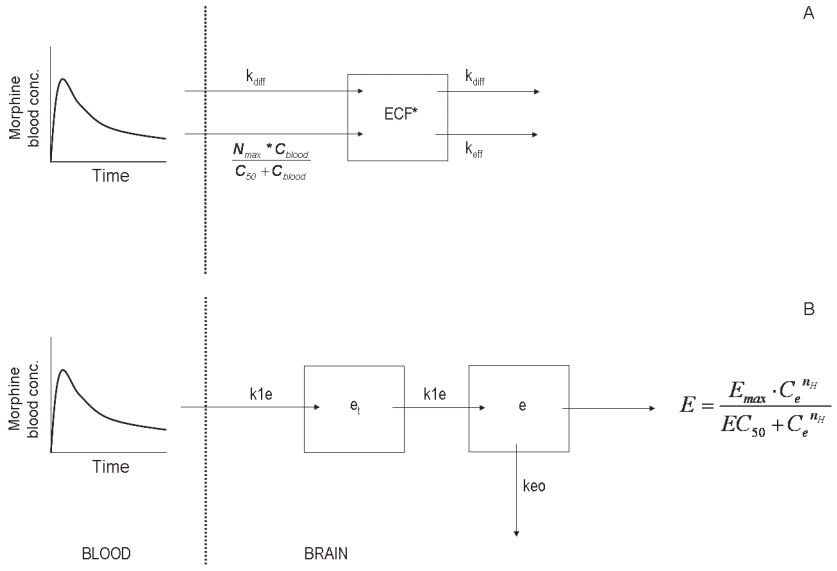

Figure 2: Schematic diagram of the non-linear brain distribution model as determined by microdialysis (panel A) and the extended-catenary biophase distribution model (panel B)

3.2 Biophase distribution model

In the current investigations, EEG monitoring was used as a pharmacodynamic endpoint. Quantitative analysis of drug effects on the electroencephalogram (EEG) yields an attractive biomarker, which is continuous, sensitive and reproducible (Dingemanse *et al.* 1988). It has been shown that the synthetic opioid alfentanil, which is frequently used in anesthesia produces a progressive slowing of the EEG with a pre-dominant increase in the delta frequency band (0.5-4.5 Hz) of the EEG power spectrum in both animals (Cox *et al.* 1997; Mandema & Wada 1995; Wauquier *et al.* 1988; Young & Khazan 1984) and humans (Scott *et al.* 1985; Wauquier *et al.* 1984; Young & Khazan 1984). Meanwhile the increase in the delta frequency band of the EEG has been widely used as a biomarker in numerous studies on the PK-PD correlations of synthetic opioids. In preclinical studies evidence has been obtained that the increase in the delta frequency band of the EEG reflect μ-opioid receptor activation (Cox *et al.* 1997; 1998; 1999). However, it remains to be elucidated whether changes in the delta frequency band are solely caused by μ-opioid receptor activation or whether more complex interactions at multiple receptor subtypes are involved.

After the start of the morphine infusion, a gradual increase in the EEG effect, expressed as the absolute amplitude in the 0.5-4.5 Hz frequency range, was observed. After the start of the morphine infusion, a gradual increase in the EEG effect was observed. The maximal effect was 60 μV and was observed around 20 minutes after the end of the morphine infusion. The duration of the effect (from the start of the infusion until the

return to baseline values) was dependent on dose and co-infusion of GF120918 and around 180 minutes following the infusion of 4 and 10 mg/kg morphine whereas after a dose of 4 mg/kg combined with GF120918 or 40 mg/kg morphine the duration of the effect was around 360 minutes. It was found that the derived blood concentration-EEG effect relationships showed profound hysteresis for all experimental groups. To describe this hysteresis, a biophase distribution model was developed. Initially, the biophase equilibration kinetics was fitted according to the one-compartment biophase distribution model. The utility of both a symmetrical (with identical values of the rate constants k_{1e} and k_{eo}) and an asymmetrical (with different values for k_{1e} and k_{eo}) effect compartment distribution model to describe the data was tested. However, neither the symmetrical nor the asymmetrical effect compartment model was able to estimate the biophase concentrations accurately. Therefore, the extended-catenary biophase distribution model was proposed, consisting of two sequential effect compartments; a transfer and an effect compartment (figure 2). The structure of this model is similar to the two-compartment "tank in series" model described by Upton and co-workers and provides a simple method to account for dispersion of drug in transit through the brain (Upton *et al.* 2000). The value of the rate constant for transport through the transfer compartment (k_{1e}) was 0.038 min^{-1} and was unaffected by the co-administration of GF120918. The values for transport rate constants for the loss from the effect compartment (k_{eo}) in the presence and absence of GF120918 were 0.0015 min^{-1} and 0.043 min^{-1}, respectively. Interestingly, the observation of the involvement of Pgp-mediated efflux in the brain distribution of morphine as observed on the basis of the EEG effect is consistent with observations on the basis of the brain ECF concentrations as obtained with intracerebral microdialysis.

3.3 Evaluation of the brain and biophase distribution models

In the investigations on the brain distribution kinetics and the PK-PD correlations, two structurally different models are proposed for characterization of the biophase distribution. The brain distribution model consisted of one brain ECF compartment with distinction between passive diffusion, active saturable influx and active efflux whereas the biophase distribution model consisted of two sequential biophase compartments with two rate constants for transport through the transfer compartment and efflux from the effect compartment . A schematic diagram of both models is shown in figure 2. When comparing the concentration-time profiles in brain ECF and biophase, it could be noted that they were distinctly different (figure 3). The concentration in brain ECF peaked early, whereas the maximum biophase concentration showed a profound delay. In addition, at the low dose of morphine a "plateau" was observed in brain ECF whereas in the biophase concentrations a clear decline over time was observed. These observations indicate that the brain ECF cannot be used to explain the hysteresis. This is in contrast with the observation by Bouw and co-workers where 85% of the observed hysteresis for the anti-nociceptive effect could be explained by distribution into the

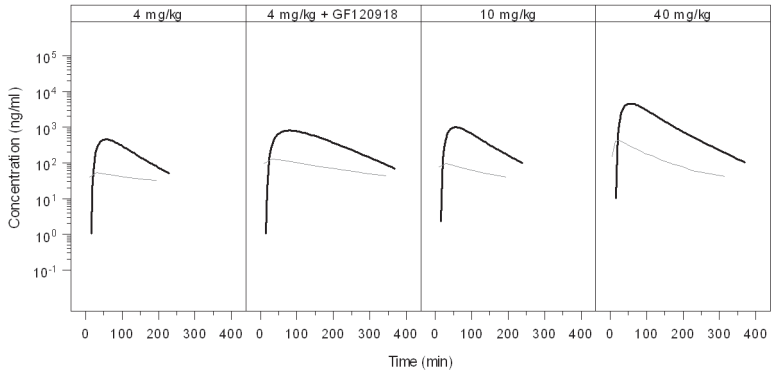

Figure 3: Comparison of the population predicted biophase concentration-time profiles (black lines) and the population predicted brain ECF fluid concentration-time profiles (grey lines) as obtained previously. It is shown that the time-course of the biophase concentrations differs substantially from the time-course of the brain ECF concentrations indicating that biophase distribution is slower than transport to the brain ECF.

brain ECF (2000). In addition, Bouw and co-workers did not identify the active uptake of morphine in the brain ECF. This indicates that the site of action for the anti-nociceptive effects is different from that for the EEG effect.

A discrepancy between the predicted biophase concentration and the measured CNS concentration-time course has also been observed for the EEG effects of amobarbital and baclofen, where the biophase concentrations did not reflect the measured cerebrospinal fluid concentrations (Mandema *et al.* 1991; 1992). In addition, Chenel and co-workers showed that the extensive time delay between EEG effect and plasma concentrations of norfloxacin, best described with an effect-compartment model, could not be explained by slow distribution to the biophase (Chenel *et al.* 2004). For norfloxacin the brain ECF concentrations peaked very early, whereas the EEG effect was delayed, which was also seen for morphine. For norfloxacin the brain ECF profiles were parallel to the plasma profiles whereas for morphine a non-linearity was observed at the low dose (4 mg/kg). Chenel and co-workers showed that the keo did not decrease when the ECF data were included in the PK-PD analysis, whereas for morphine the brain ECF and EEG effects could not be analysed simultaneously.

A number of possibilities can explain these observations. First, from a pharmacokinetic perspective it may be that the biophase distribution of morphine is not mainly determined by BBB transport but also to a significant extent by distribution and elimination processes in relation to the regional distribution of the target (de Lange & Danhof 2002). The location of the microdialysis probe in the specific area of the brain, and the concentrations measured in that region, may differ from the biophase as determined by receptor density (Mansour *et al.* 1988). In addition, while the free concentrations in the brain ECF are quantified by intracerebral microdialysis, also intracellular concentrations of morphine may contribute to the EEG effects.

Alternatively, from a pharmacodynamic perspective, it could be that morphine does not exclusively exerts its EEG effects by binding to the μ-opioid receptor. It is known that morphine has affinity for both the μ and κ receptor (Chen *et al*. 1993; Kilpatrick & Smith 2005; Ulens *et al*. 2001) and therefore it is possible that although the EEG is considered to be a biomarker for μ-opioid receptor activation, the other receptor subtypes can influence the EEG effect of morphine.

In addition, the observed discrepancy could also be explained by the influence of receptor association-dissociation kinetics. Recently it has been shown that the onset and offset of the anti-nociceptive and respiratory depressant effects of buprenorphine are determined by both biophase distribution and receptor association-dissociation kinetics, although the major determinant was the biophase distribution kinetics (Yassen *et al.* 2005; 2006). Buprenorphine is an opioid which is structurally related to morphine and kinetics of binding to and dissociation from the μ-opioid receptor is slow (Boas & Villiger 1985; Cowan *et al*. 1977). In contrast, for fentanyl it was shown that the hysteresis could be completely explained by biophase distribution kinetics. Since buprenorphine is structurally related to morphine, it may be possible that receptor association-dissociation kinetics also influence the onset and offset of the EEG effect. Finally, transduction processes can also influence the time-course of the EEG effect. In the current investigations, the biophase concentration-effect relationships were described with the sigmoidal E_{max} model. However, in theory, the transduction function may take any shape. Depending on the behaviour of the drug in the biological system, a hyperbolic or linear transduction is chosen (Black & Leff 1983). The receptor theory by Clark states that for partial agonists, the pharmacological response is directly related to the number of receptors occupied (Clark 1937). So, when information is available in the *in vivo* receptor binding, a linear transduction function is able to describe the receptor occupancy-effect relationship.

4. PK-PD MODELLING OF THE EEG EFFECTS OF OPIOIDS

In addition to morphine, the EEG effects of the opioids alfentanil, fentanyl, sufentanil, nalbuphine and butorphanol have been investigated. The data for alfentanil, fentanyl and sufentanil have been collected and published previously (Cox *et al*. 1998). The blood pharmacokinetics of all opioids could be successfully described using population PK analysis. For fentanyl, sufentanil and butorphanol, a two-compartment model best described the data whereas for alfentanil, morphine and nalbuphine a three-compartment model was most suitable.

4.1 Role of complex biophase distribution kinetics

From the previous studies it can be concluded that the modelling of complex biophase distribution kinetics of opioids is important, given the potential interaction with active transporters and the wide range in lipophilicity. It was shown the biophase distribution

kinetics of morphine could be best described with the extended-catenary biophase distribution model which consists of two sequential compartments (chapter 6). To describe the time-course of the EEG effect of fentanyl, sufentanil, butorphanol and nalbuphine two structurally different biophase distribution models were investigated: 1) the one-compartment biophase distribution model (the effect-compartment model) and 2) the extended-catenary biophase distribution model. For alfentanil, a direct relationship between the blood concentrations and the EEG effect was observed. For fentanyl, sufentanil and butorphanol, the one-compartment distribution model, with identical values of the distribution rate constants k_{1e} and k_{eo} yielded the most accurate description of the pharmacodynamics. This was expected since the delay in pharmacodynamic effect was relatively short, as is confirmed by the k_{1e} values of 0.47 min^{-1}, 0.17 min^{-1} and 0.21 min^{-1} for fentanyl, sufentanil and butorphanol, respectively. The biophase distribution kinetics of nalbuphine could be equally well described with both distribution models. However, since the accuracy of the parameter estimates did not change when the model was simplified from the extended-catenary to the one-compartment distribution model, the latter model was accepted as the most appropriate model to describe the biophase distribution kinetics of nalbuphine. In addition, asymmetrical distribution could not be identified for nalbuphine and the estimated k_{1e} (and k_{eo}) value was 0.20 min^{-1}.

Interestingly, a statistically significant correlation was observed between the values of the *in vivo* k_{1e} and the *in vitro* P_{app} as determined in the *in vitro* assays (chapter 4). However, it should be taken into consideration that for biophase distribution processes, apart from BBB transport, also distribution within the brain can influence the hysteresis (Liu *et al.* 2005). An important question is whether the estimates of the biophase concentrations that have been obtained with this PK-PD modelling approach indeed reflect the true biophase concentrations. In this respect, it is important that the role of active transporters at the BBB other than Pgp has not been taken into considerations. The findings on the effect of the Pgp blocker GF120918 on the biophase distribution and the EEG effect of morphine indicate that such an effect might be significant. Whether this also applies to the other opioids will be discussed in a subsequent paragraph.

4.2 Identification of the kinetics of target binding and activation

As the first step in the pharmacodynamic analysis, the unbound biophase concentration effect relationships were analysed with the Hill equation. This analysis showed that alfentanil is the opioid with the highest intrinsic activity (123 ± 13 μV). This analysis was performed in order to enable a ranking in intrinsic activity for the set of opioids. The relative intrinsic activity of the various opioids (α) ranged from 0.81 to 0.10 for sufentanil and butorphanol, respectively which corresponds to an E_{max} value of 100 μV for sufentanil and 12 μV for butorphanol. In addition, the $EC_{50,u}$ ranged from 0.21 nM for sufentanil to 1223 nM for morphine. Thus, a wide range of both E_{max} and EC50,u values was observed (figure 4).

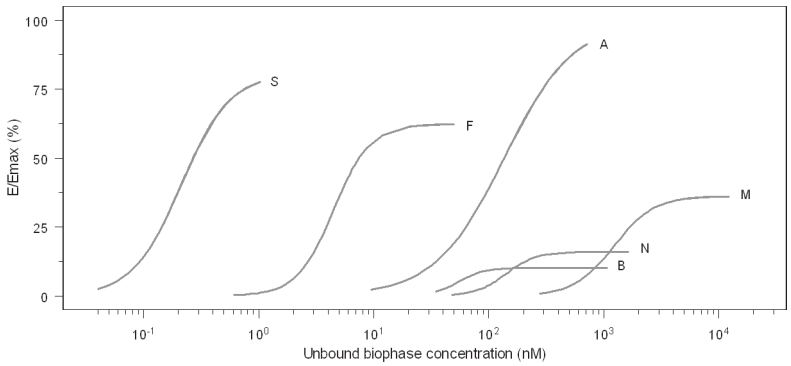

Figure 4: Unbound biophase concentration-EEG effect relationships of opioids as obtained by simultaneous analysis with the Hill equation. From left to right the opioids are: sufentanil, fentanyl, alfentanil, butorphanol, nalbuphine and morphine. The EEG effect is presented as the net EEG amplitude as a percentage of the maximum achievable effect in the system (123 μV).

A limitation of the Hill equation is that, although very useful for descriptive purposes, it is only of limited value to understand factors which determine the shape and location of the concentration-effect relationship. Specifically, the pharmacodynamic parameters of the Hill equation are mixed parameters which depend on both the properties of the drug and the biological system (van der Graaf *et al*. 1997; van der Graaf & Danhof 1997). As a result, observed values of the E_{max} may depend on the drug or the biological system. Moreover, values of the EC_{50} depend on both the target affinity and the intrinsic efficacy. Recently, the concepts of receptor theory have been used to make a strict distinction between drug-specific and biological-system specific factors as determinants of *in vivo* concentration-effect relationships. Especially, the operational model of agonism (Black & Leff 1983;) has been successfully applied for explaining and predicting the effects of differential expression of agonism *in vivo* (Black & Leff 1983; van der Graaf *et al*. 1997; Zuideveld *et al*. 2004).

The comparative method (Black & Leff 1983; Leff *et al*. 1990; van der Graaf *et al*. 1997) was applied for analysis of the concentration-effect relationships by the operational model of agonism with the values of E_{max} (123 μV) and n (1.44) constrained to the values of alfentanil which displays the highest intrinsic activity *in vivo*. In addition, the pK_A of sufentanil, as the opioid with the highest receptor affinity, was fixed to the *in vitro* pK_i (9.15). The constraint of the *in vivo* pK_A to the *in vitro* pK_i has also been applied in previous analyses of concentration-effect relationships (Black & Leff 1983; Jonker *et al*. 2005; van der Graaf *et al*. 1997; Zuideveld *et al*. 2004). When analyzing the concentration-effect relationships of the opioids, the efficacy parameter τ ranged from 0.452 for nalbuphine to 2.618 for alfentanil. In addition, the K_A ranged from $4.3*10^{-10}$ to $2.3*10^{-6}$ M for sufentanil and morphine, indicating that large differences existed in the set of opioids.

When taking all compounds together, the correlations between the *in vivo* pK_A and the *in vitro* pK_i determined in the presence of 1 mM GTP or 100 mM NaCl were not statistically significant (P>0.05). However, there were clear indications for two (sub-)populations of opioids. The estimated *in vivo* pK_A for alfentanil, fentanyl and sufentanil were similar to the values obtained *in vitro*, whereas for morphine, butorphanol and nalbuphine, the pKa was higher. For these opioids, this may be explained by biophase distribution processes, including BBB transport, as has been specifically addressed for morphine. Another explanation may be that these opioids interact not only with a specific μ-opioid receptor subtype, but also with other μ, κ and δ-opioid receptor subtypes.

a) Biophase distribution processes

As discussed in section 3, for morphine it has been shown that biophase distribution is influenced by the functionality of Pgp at the BBB. Specifically, co-infusion of GF120918 reduced the rate constant for efflux of morphine from the effect compartment with 60%. As a result, in the absence of Pgp blockers the free drug concentrations in the brain ECF are substantially lower than the corresponding free blood concentrations. This could well explain the observed discrepancy between the *in vitro* and *in vivo* K_A values. However, it is important to note that morphine is not only transported by Pgp, but also by other transporters like the probenecid-sensitive transporter which is also present at the BBB (Tunblad *et al.* 2004). The influence of active transport mechanisms as a confounder of the analysis of the *in vitro-in vivo* corrlations of pK_A values has also been identified for 5-HT_{1A} receptor agonists in particular with regard to flesinoxan (Zuideveld *et al.* 2004). In addition, regional differences in brain kinetics can also explains the differences between the local pharmacokinetic in the brain ECF and the overall kinetics responsible for the EEG effect.

b) Interaction with μ opioid receptor subtypes and κ and δ opioid receptors

Another possible explanation of the existence of two (sub-)populations is the interaction with different μ-opioid receptor subtypes or the interaction with κ and δ opioid receptors. Upon reducing the number of available μ-opioid receptors by irreversible binding by β-funaltrexamine (β-FNA), it has been found that the Hill factor of alfentanil is increased to 2.75 (Garrido *et al.* 2000). It has been speculated that antagonist-induced curve-steepening could be indicative for receptor heterogeneity (van der Graaf *et al.* 1996) and that the EEG effect of alfentanil is mediated via multiple receptor types which differ in their sensitivity to β-FNA (Garrido *et al.*,2000). Recently, several spliced μ-opioid receptor isoforms have been identified, which might be involved with different aspects of the pharmacology of opioids (Pasternak 2005; Zernig *et al.* 1994). Specifically, for the opioids morphine, butorphanol and nalbuphine it is known that they have affinity for both the μ- and κ-opioid receptor, whereas fentanyl is a specific μ-opioid receptor agonist (Chen *et al.* 1993). In literature, little is known about the receptor affinity of alfentanil and sufentanil, but they have been specifically designed to bind exclusively

to the μ-opioid receptor (Chen *et al.* 1993; Yeadon & Kitchen 1988). Furthermore, it is known that heterodimerisation of opioid receptors can potentiate the effects of opioids (Gomes *et al.* 2000).

5. CONCLUSIONS AND PERSPECTIVES

The objective of the research described in this thesis was to develop a PK-PD model for the EEG effects of opioids, to get insight into the mechanisms that determine the pharmacological effects of opioids. The results described in this thesis indicate that the major determinants of the EEG effects of opioids are biophase distribution processes and kinetics of target binding. This illustrates that the biophase distribution kinetics should be explicitly addressed in great detail as an integral part of the investigations into the pharmacodynamics of opioids.

Biophase distribution kinetics

In the current investigations, the biophase distribution kinetics has been studied with emphasis on BBB transport and the influence of Pgp. However, multiple (efflux) transporters are present at the BBB which could influence biophase distribution. These transporters include the multidrug resistance proteins (MRP) (Zhang *et al.* 2000) and other probenicid-sensitive transporters, which have shown to be involved in the transport of morphine and morphine-3-glucuronide (Tunblad *et al.* 2004; Xie *et al.* 2000). In addition, modelling of the BBB transport of morphine has revealed the influence of a yet unknown influx transporter (chapter 5). Active influx was also found for oxycodone (Bostrom *et al.* 2006). In addition, other yet unknown transporters could also play a role in the BBB transport of opioids. In order to be able to exclude the influence of such transporters a cocktail of different selective blockers could be administered in each experiment or single or multiple transporter knock-out animals (e.g. mdr1a/1b(-/-), mrp1(-/-) mice (Johnson *et al.* 2001)). As an alternative, detailed information on the brain concentrations should be obtained, for example including intracerebral microdialysis combined with EEG monitoring (chapter 5 and 6), though the location of the biophase does not need to be represented by that of the ECF surrounding the microdialysis probe as shown for morphine in relation to the EEG effect.

Other *in vivo* techniques could be considered as well. For example, Positron Emission Tomography (PET) would be very useful to study the distribution of a (radio labelled) opioid across the brain thereby enabling detailed information on total brain concentration distribution of the radiolabel and its specific binding within the brain as a function of time and location. Recently, Liefaard and co-workers have established a population pharmacokinetic model to describe and predict these processes for 11C-flumazenil (2005). Important disadvantages of PET are that it requires radioisotopes which are often instable resulting in a very short half-life and that it cannot distinguish between parent compound and metabolites.

Simultaneous analysis of biophase distribution and kinetics of target binding

Biophase distribution models were proposed for all opioids and biophase concentration-effect relationships were derived. Subsequently, the estimated biophase concentration-effect relationships were analysed according to the operational model of agonism to get insight into the kinetics of target binding and activation. As an alternative to this sequential approach, simultaneous analysis of the biophase distribution and kinetics of target binding could be performed. Recently, Yassen and co-workers have presented a mechanism-based PK-PD model that is based on receptor theory and aims at the separate characterisation of biophase distribution and receptor association/dissociation kinetics as determinants of hysteresis between plasma concentrations and effect (Yassen *et al*. 2005; 2006). It was shown that for the anti-nociceptive and respiratory depressant effects of opioids, reliable parameter estimates could be obtained for both biophase distribution and receptor association/dissociation. However, for fentanyl, no reasonable values could be obtained for the receptor association/dissociation kinetics, indicating that receptor binding for fentanyl is instantaneous and therefore does not contribute to the hysteresis. A prerequisite for this approach is that receptor binding is not instantaneous. On that basis it is expected that this approach cannot be applied for fentanyl-like opioids. Since buprenorphine is structurally related to morphine, it may be possible that receptor association-dissociation kinetics also influence the onset and offset of the EEG effect of morphine, butorphanol and nalbuphine.

Specificity of EEG as biomarker of μ-opioid receptor activation

In this thesis, EEG is used as a biomarker for μ-opioid receptor activation. EEG is an attractive biomarker because it can be monitored continuously. However, it remains to be elucidated whether changes in the δ-frequency band are solely caused by μ-opioid receptor activation. In order to investigate this, EEG experiments should be performed with specific agonists for the different receptor subtypes. A list of specific agonists and antagonists as derived from available literature is shown in table 2. See (Alexander *et al*. 2000; Baker & Meert 2002; Chen *et al*. 1993) for additional references.

Table 2: Selective agonists and antagonists for the different opioid receptor subtypes

Receptor subtype	Agonists	Antagonists
μ	Endomorphine-1 and -2	Naloxone
	DAMGO	β-funaltrexamine (irreversible)
		naloxonazine (μ_1)
κ	U50,488H	Nor-binaltorphine
	U69,593	DIPPA (irreversible)
δ	DPDPE	Naltrindole
	DSBULET	BNTX (δ_1)
	[dAla2]deltorphine I or II	Naltriben (δ_2)
	SNC80	

Influence of other μ-opioid receptor subtypes

It is known from literature that opioids bind to different opioid-receptor subtypes. First, the receptor binding characteristics at these receptor subtypes should be investigated *in vitro* using radioligand binding studies as described in section 3 of this discussion and by Chen and co-workers (1993).

Next, the influence of the different receptor subtypes should be investigated by co-administration of selective blockers for each receptor subtype (table 3). Recently, a study has been described which investigates the roles of peripheral and central μ, δ and κ receptors and their subtypes in opioid-induced hypothermia in mice (Baker & Meert 2002). The effects of morphine and selective agonists for the opioid receptor subtypes, (fentanyl, SNC80, U50,488H and loperamide), on the body temperature were assessed directly. All selected opioids produced hypothermia, which was (partly) counteracted by a selection of receptor specific antagonist (naloxone, β-funaltrexamine, naloxonazine, naltrindole, BNTX, naltriben, nor-binaltorphine and DIPPA). For morphine and fentanyl, the hypothermia was shown to involve a composite action on μ, κ and possible δ receptors after initial activation. Such findings indicate that for the development of a mechanistic PK-PD model also the influence of the interaction between different receptor subtypes has to be considered.

Other pharmacodynamic end-points

In the current investigations, EEG was used as a pharmacodynamic endpoint. It has the advantages of being continuous and subjective. However, for opioids to produce changes in the EEG effect, relatively high concentrations are required, often resulting in the occurrence of respiratory depression. In addition, for example for buprenorphine, no clear effect on the EEG could be observed (Yassen, personal communication), while also for butorphanol and nalbuphine, the EEG effect was difficult to quantify. The high dose group of nalbuphine had to be excluded because of severe systemic side effects during and after the opioid infusion. Another disadvantage of EEG in rats is that it is a rather invasive technique involving the implantation of cortical electrodes. For research of opioids, antinociception is often used as a pharmacodynamic endpoint. Antinociception can be investigated using the tailflick latency test (Letrent *et al.* 1998; 1999; Yassen *et al.* 2005) or the electrical stimulation-vocalisation test (Bouw *et al.* 2000; 2001; Ekblom *et al.* 1993). Disadvantages of these tests are censoring of the data (values above cut-off value), possible interference between measurement and the limited number of observations that can be obtained in one animal.

All opioids produce respiratory depression to some extent. Respiratory depression is often measured using arterial carbon dioxide tension (P_ACO_2) as a surrogate biomarker of minute ventilation (V_i) (Megarbane *et al.* 2006; Ohtani *et al.* 1997). Recently, Yassen and co-workers have developed a more sensitive method in which minute ventilation is measured by whole body plethysmography at a fixed inspired CO_2 concentration of 6.5% (Yassen *et al.* 2006).

Conclusions

The effects of opioids are mainly determined by biophase distribution kinetics and kinetics of target binding. For the development of a mechanism-based PK-PD model which also has predictive value, these processes should be investigated in great detail. In addition, supportive data for each of the processes are essential for model validation and prediction.

6. REFERENCES

Alexander S, Peters J (2000) Opioid and opioid-like receptors. *Trends in pharmaceutical sciences* receptor and ionchannel nomenclature supplement 70-71

Baker AK, Meert TF (2002) Functional effects of systemically administered agonists and antagonists of mu, delta, and kappa opioid receptor subtypes on body temperature in mice. *J.Pharmacol.Exp.Ther.* **302:** 1253-1264

Black JW, Leff P (1983) Operational models of pharmacological agonism. *Proc.R.Soc.Lond B Biol.Sci.* **220:** 141-162

Boas RA, Villiger JW (1985) Clinical actions of fentanyl and buprenorphine. The significance of receptor binding. *Br.J.Anaesth.* **57:** 192-196

Bostrom E, Simonsson US, Hammarlund-Udenaes M (2006) In vivo blood-brain barrier transport of oxycodone in the rat: indications for active influx and implications for pharmacokinetics/pharmacodynamics. *Drug Metab Dispos.* **34:** 1624-1631

Bouw MR, Gardmark M, Hammarlund-Udenaes M (2000) Pharmacokinetic-pharmacodynamic modelling of morphine transport across the blood-brain barrier as a cause of the antinociceptive effect delay in rats--a microdialysis study. *Pharm.Res.* **17:** 1220-1227

Bouw MR, Xie R, Tunblad K, Hammarlund-Udenaes M (2001) Blood-brain barrier transport and brain distribution of morphine-6-glucuronide in relation to the antinociceptive effect in rats--pharmacokinetic/pharmacodynamic modelling. *Br.J.Pharmacol* **134:** 1796-1804

Chen JC, Smith ER, Cahill M, Cohen R, Fishman JB (1993) The opioid receptor binding of dezocine, morphine, fentanyl, butorphanol and nalbuphine. *Life Sci.* **52:** 389-396

Chenel M, Marchand S, Dupuis A, Lamarche I, Paquereau J, Pariat C, Couet W (2004) Simultaneous central nervous system distribution and pharmacokinetic-pharmacodynamic modelling of the electroencephalogram effect of norfloxacin administered at a convulsant dose in rats. *Br.J.Pharmacol* **142:** 323-330

Clark AJ (1937) General Pharmacology. in *Heffner's Handbuch der experimentellen Pharmacologie Erganzungsband* Springer 38-51

Cowan A, Doxey JC, Harry EJ (1977) The animal pharmacology of buprenorphine, an oripavine analgesic agent. *Br.J.Pharmacol* **60:** 547-554

Cox EH, Kerbusch T, van der Graaf PH, Danhof M (1998) Pharmacokinetic-pharmacodynamic modeling of the electroencephalogram effect of synthetic opioids in the rat: correlation with the interaction at the mu-opioid receptor. *J Pharmacol.Exp.Ther.* **284:** 1095-1103

Cox EH, Langemeijer MW, Gubbens-Stibbe JM, Muir KT, Danhof M (1999) The comparative pharmacodynamics of remifentanil and its metabolite, GR90291, in a rat electroencephalographic model. *Anesthesiology* **90:** 535-544

Cox EH, Van Hemert JG, Tukker EJ, Danhof M (1997) Pharmacokinetic-pharmacodynamic modelling of the EEG effect of alfentanil in rats. *J Pharmacol.Toxicol.Methods* **38:** 99-108

de Lange EC, Danhof M (2002) Considerations in the use of cerebrospinal fluid pharmacokinetics to predict brain target concentrations in the clinical setting: implications of the barriers between blood and brain. *Clin. Pharmacokinet.* **41:** 691-703

DeHaven-Hudkins DL, Burgos LC, Cassel JA, Daubert JD, DeHaven RN, Mansson E, Nagasaka H, Yu G, Yaksh T (1999) Loperamide (ADL 2-1294), an opioid antihyperalgesic agent with peripheral selectivity. *J.Pharmacol. Exp.Ther.* **289:** 494-502

Dingemanse J, Sollie FA, Breimer DD, Danhof M (1988) Pharmacokinetic modeling of the anticonvulsant response of oxazepam in rats using the pentylenetetrazol threshold concentration as pharmacodynamic measure. *J.Pharmacokinet.Biopharm.* **16:** 203-228

Ekblom M, Gardmark M, Hammarlund-Udenaes M (1993) Pharmacokinetics and pharmacodynamics of morphine-3-glucuronide in rats and its influence on the antinociceptive effect of morphine. *Biopharm.Drug Dispos.* **14:** 1-11

Garrido M, Gubbens-Stibbe J, Tukker E, Cox E, von Frijtag-Drabbe Künzel J, IJzerman A, Danhof M, van der Graaf PH (2000) Pharmacokinetic-pharmacodynamic analysis of the EEG effect of alfentanil in rats following beta-funaltrexamine-induced mu-opioid receptor “knockdown” in vivo. *Pharm.Res.* **17:** 653-659

Geldof M, Freijer J, van Beijsterveldt L, Danhof M, (2007) Physiological pharmacokinetic modeling of non-linear brain distribution of fluvoxamine in the rat. *in press*

Gomes I, Jordan BA, Gupta A, Trapaidze N, Nagy V, Devi LA (2000) Heterodimerization of mu and delta opioid receptors: A role in opiate synergy. *J.Neurosci.* **20:** RC110

Hammarlund-Udenaes M, Paalzow LK, de Lange EC (1997) Drug equilibration across the blood-brain barrier--pharmacokinetic considerations based on the microdialysis method. *Pharm.Res.* **14:** 128-134

Hyafil F, Vergely C, Du VP, Grand-Perret T (1993) In vitro and in vivo reversal of multidrug resistance by GF120918, an acridonecarboxamide derivative. *Cancer Res.* **53:** 4595-4602

Johnson DR, Finch RA, Lin ZP, Zeiss CJ, Sartorelli AC (2001) The pharmacological phenotype of combined multidrug-resistance mdr1a/1b- and mrp1-deficient mice. *Cancer Res.* **61:** 1469-1476

Jonker DM, Kenna LA, Leishman D, Wallis R, Milligan PA, Jonsson EN (2005) A pharmacokinetic-pharmacodynamic model for the quantitative prediction of dofetilide clinical QT prolongation from human ether-a-go-go-related gene current inhibition data. *Clin Pharmacol Ther* **77:** 572-582
Kilpatrick GJ, Smith TW (2005) Morphine-6-glucuronide: actions and mechanisms. *Med.Res.Rev.* **25:** 521-544

Leff P, Prentice DJ, Giles H, Martin GR, Wood J (1990) Estimation of agonist affinity and efficacy by direct, operational model-fitting. *J.Pharmacol.Methods* **23:** 225-237

Letrent SP, Pollack GM, Brouwer KR, Brouwer KL (1998) Effect of GF120918, a potent P-glycoprotein inhibitor, on morphine pharmacokinetics and pharmacodynamics in the rat. *Pharm.Res.* **15:** 599-605

Letrent SP, Pollack GM, Brouwer KR, Brouwer KL (1999) Effects of a potent and specific P-glycoprotein inhibitor on the blood- brain barrier distribution and antinociceptive effect of morphine in the rat. *Drug Metab Dispos.* **27:** 827-834

Liefaard LC, Ploeger BA, Molthoff CF, Boellaard R, Lammertsma AA, Danhof M, Voskuyl RA (2005) Population pharmacokinetic analysis for simultaneous determination of B (max) and K (D) in vivo by positron emission tomography. *Mol Imaging Biol.* **7:** 411-421

Liu X, Smith BJ, Chen C, Callegari E, Becker SL, Chen X, Cianfrogna J, Doran AC, Doran SD, Gibbs JP, Hosea N, Liu J, Nelson FR, Szewc MA, Van Deusen J (2005) Use of a physiologically based pharmacokinetic model to study the time to reach brain equilibrium: an experimental analysis of the role of blood-brain barrier permeability, plasma protein binding, and brain tissue binding. *J.Pharmacol.Exp.Ther.* **313:** 1254-1262

Mandema JW, Heijligers-Feijen CD, Tukker E, de Boer AG, Danhof M (1992) Modeling of the effect site equilibration kinetics and pharmacodynamics of racemic baclofen and its enantiomers using quantitative EEG effect measures. *J.Pharmacol Exp.Ther* **261:** 88-95

Mandema JW, Veng-Pedersen P, Danhof M (1991) Estimation of amobarbital plasma-effect site equilibration kinetics. Relevance of polyexponential conductance functions. *J.Pharmacokinet.Biopharm.* **19:** 617-634

Mandema JW, Wada DR (1995) Pharmacodynamic model for acute tolerance development to the electroencephalographic effects of alfentanil in the rat. *J.Pharmacol.Exp.Ther.* **275:** 1185-1194

Mansour A, Khachaturian H, Lewis ME, Akil H, Watson SJ (1988) Anatomy of CNS opioid receptors. *Trends Neurosci.* **11:** 308-314

Martin C, Berridge G, Higgins CF, Mistry P, Charlton P, Callaghan R (2000) Communication between multiple drug binding sites on P-glycoprotein. *Mol.Pharmacol.* **58:** 624-632

Megarbane B, Marie N, Pirnay S, Borron SW, Gueye PN, Risede P, Monier C, Noble F, Baud FJ (2006) Buprenorphine is protective against the depressive effects of norbuprenorphine on ventilation. *Toxicol.Appl. Pharmacol* **212:** 256-267

Niemegeers CJ, McGuire JL, Heykants JJ, Janssen PA (1979) Dissociation between opiate-like and antidiarrheal activities of antidiarrheal drugs. *J.Pharmacol.Exp.Ther.* **210:** 327-333

Ohtani M, Kotaki H, Nishitateno K, Sawada Y, Iga T (1997) Kinetics of respiratory depression in rats induced by buprenorphine and its metabolite, norbuprenorphine. *J.Pharmacol.Exp.Ther.* **281:** 428-433

Pasternak GW (2005) Molecular biology of opioid analgesia. *J.Pain Symptom.Manage.* **29:** S2-S9

Schaddelee MP, Voorwinden HL, Groenendaal D, Hersey A, IJzerman AP, Danhof M, de Boer AG (2003) Blood-brain barrier transport of synthetic adenosine A1 receptor agonists in vitro: structure transport relationships. *Eur. J Pharm.Sci* **20:** 347-356

Schinkel AH, Wagenaar E, Mol CA, van Deemter L (1996) P-glycoprotein in the blood-brain barrier of mice influences the brain penetration and pharmacological activity of many drugs. *J.Clin.Invest* **97:** 2517-2524

Schinkel AH, Wagenaar E, van Deemter L, Mol CA, Borst P (1995) Absence of the mdr1a P-Glycoprotein in mice affects tissue distribution and pharmacokinetics of dexamethasone, digoxin, and cyclosporin A. *J.Clin. Invest* **96:** 1698-1705

Scott JC, Ponganis KV, Stanski DR (1985) EEG quantitation of narcotic effect: the comparative pharmacodynamics of fentanyl and alfentanil. *Anesthesiology* **62:** 234-241

Tunblad K, Jonsson EN, Hammarlund-Udenaes M (2004) Morphine blood-brain barrier transport is influenced by probenecid co-administration. *Pharm Res* **20:** 618-623

Ulens C, Baker L, Ratka A, Waumans D, Tytgat J (2001) Morphine-6beta-glucuronide and morphine-3-glucuronide, opioid receptor agonists with different potencies. *Biochem.Pharmacol.* **62:** 1273-1282

Upton RN, Ludbrook GL, Grant C, Doolette DJ (2000) The effect of altered cerebral blood flow on the cerebral kinetics of thiopental and propofol in sheep. *Anesthesiology* **93:** 1085-1094

van der Graaf PH, Danhof M (1997) Analysis of drug-receptor interactions in vivo: a new approach in pharmacokinetic-pharmacodynamic modelling. *Int.J Clin.Pharmacol.Ther.* **35:** 442-446

van der Graaf PH, Shankley NP, Black JW (1996) Analysis of the activity of alpha 1-adrenoceptor antagonists in rat aorta. *Br.J.Pharmacol* **118:** 299-310

van der Graaf PH, Van Schaick EA, Mathot RA, IJzerman AP, Danhof M (1997) Mechanism-based pharmacokinetic-pharmacodynamic modeling of the effects of N6-cyclopentyladenosine analogs on heart rate in rat: estimation of in vivo operational affinity and efficacy at adenosine A1 receptors. *J.Pharmacol.Exp.Ther.* **283:** 809-816

Wandel C, Kim R, Wood M, Wood A (2002) Interaction of morphine, fentanyl, sufentanil, alfentanil, and loperamide with the efflux drug transporter P-glycoprotein. *Anesthesiology* **96:** 913-920

Wauquier A, Bovill JG, Sebel PS (1984) Electroencephalographic effects of fentanyl-, sufentanil- and alfentanil anaesthesia in man. *Neuropsychobiology* **11:** 203-206

Wauquier A, De Ryck M, Van den Broeck W, Van Loon J, Melis W, Janssen P (1988) Relationships between quantitative EEG measures and pharmacodynamics of alfentanil in dogs. *Electroencephalogr.Clin Neurophysiol.* **69:** 550-560

Xie R, Bouw MR, Hammarlund-Udenaes M (2000) Modelling of the blood-brain barrier transport of morphine-3-glucuronide studied using microdialysis in the rat: involvement of probenecid-sensitive transport. *Br.J.Pharmacol* **131:** 1784-1792

Xie R, Hammarlund-Udenaes M, de Boer AG, de Lange EC (1999) The role of P-glycoprotein in blood-brain barrier transport of morphine: transcortical microdialysis studies in mdr1a (-/-) and mdr1a (+/+) mice. *Br.J.Pharmacol.* **128:** 563-568

Yassen A, Kan J, Olofsen E, Suidgeest E, Dahan A, Danhof M (2006) Mechanism-based pharmacokinetic-pharmacodynamic modeling of the respiratory-depressant effect of buprenorphine and fentanyl in rats. *J.Pharmacol Exp.Ther* **319:** 682-692

Yassen A, Olofsen E, Dahan A, Danhof M (2005) Pharmacokinetic-pharmacodynamic modeling of the antinociceptive effect of buprenorphine and fentanyl in rats: role of receptor equilibration kinetics. *J.Pharmacol.Exp.Ther.* **313:** 1136-1149

Yeadon M, Kitchen I (1988) Comparative binding of mu and delta selective ligands in whole brain and pons/medulla homogenates from rat: affinity profiles of fentanyl derivatives. *Neuropharmacology* **27:** 345-348

Young GA, Khazan N (1984) Differential neuropharmacological effects of mu, kappa and sigma opioid agonists on cortical EEG power spectra in the rat. Stereospecificity and naloxone antagonism. *Neuropharmacology* **23:** 1161-1165

Zernig G, Butelman ER, Lewis JW, Walker EA, Woods JH (1994) In vivo determination of mu opioid receptor turnover in rhesus monkeys after irreversible blockade with clocinnamox. *J.Pharmacol.Exp.Ther.* **269:** 57-65

Zhang Y, Han H, Elmquist WF, Miller DW (2000) Expression of various multidrug resistance-associated protein (MRP) homologues in brain microvessel endothelial cells. *Brain Res.* **876:** 148-153

Zuideveld KP, van der Graaf PH, Newgreen D, Thurlow R, Petty N, Jordan P, Peletier LA, Danhof M (2004) Mechanism-based pharmacokinetic-pharmacodynamic modeling of 5-HT1A receptor agonists: estimation of in vivo affinity and intrinsic efficacy on body temperature in rats. *J.Pharmacol Exp.Ther* **308:** 1012-1020

Samenvatting

SAMENVATTING IN HET NEDERLANDS

SYNOPSIS IN DUTCH

1. ALGEMENE INLEIDING EN DOEL VAN HET ONDERZOEK

Het onderzoek in dit proefschrift heeft betrekking op de relaties tussen farmacokinetiek (PK) en farmacodynamiek (PD) van opiaten, met speciale aandacht voor de distributie vanuit het bloed naar de plaats van werking (de biofase) in het centrale zenuwstelsel en de interactie met de μ-opiaat receptor. In hoofdstuk 1 wordt een inleiding gegeven over de achtergronden van de PK-PD modellering in het algemeen en van opiaten in het bijzonder.

1.1 Farmacokinetisch-farmacodynamische modellering

Het doel van farmacokinetisch-farmacodynamische (PK-PD) modellering is de beschrijving en voorspelling van het tijdsverloop van geneesmiddel effecten *in vivo* in gezonde en zieke toestand. Klassieke PK-PD modellen bestaan uit drie componenten: 1) een farmacokinetisch model, 2) een farmacodynamisch model en 3) een link model. Het farmacokinetische model beschrijft het verloop van de concentratie van het geneesmiddel in bloed/plasma in de tijd. In deze modellen wordt de farmacokinetiek vaak beschreven met hypothetische compartimentele modellen die de processen van absorptie, distributie en eliminatie nabootsen. Het farmacodynamische model beschrijft de relatie tussen de geschatte biofase concentratie en het farmacologische effect. Het meest bekende farmacodynamische model is het sigmoidale E_{max} model dat de relatie tussen concentratie en effect beschrijft met een s-vormige curve, de zogenaamde Hill vergelijking. Een beperking van dit model is dat het geen mechanistisch model is. Dat wil zeggen dat er geen onderscheid gemaakt wordt tussen stof-specifieke en systeem-specifieke eigenschappen die de vorm en de ligging van de concentratie-werkingsrelatie bepalen. Het link model tenslotte wordt gebruikt voor het beschrijven van de vertraging tussen het verloop van de concentratie in bloed/plasma en het effect (hysterese). Hysterese wordt vaak beschreven op basis van distributie naar een hypothetisch effect-compartiment, waarbij de intensiteit van het effect wordt gerelateerd aan de concentratie in het hypothetische effect compartiment (de biofase).

1.2 Mechanistische PK-PD modellering: onderscheid tussen de verschillende processen die het verloop van het farmacologische effect bepalen

Er is een duidelijke trend in de richting van de ontwikkeling van mechanistische PK-PD modellen waarbij onderscheid wordt gemaakt tussen de verschillende (deel-) processen die bepalend zijn voor het verloop van het farmacologische effect. Deze modellen bevatten beschrijvingen van 1) het verloop van de concentratie in bloed/plasma, 2) de biofase distributie, 3) de binding en activatie van het doeleiwit op de plaats van werking, 4) de transductie en 5) de homeostatische terugkoppelings mechanismen. Het onderzoek dat in dit proefschrift wordt beschreven richt zich met name op 1) de rol van biofase distributie, dat de concentratie op de plaats van werking bepaalt, en 2) de beschrijving van de binding aan en de activatie van de receptoren op de plaats van werking.

Biofase distributie

Biofase distributie is afhankelijk van de bloedperfusiesnelheid van het weefsel waarin zich het doeleiwit bevindt en weefseldistributie processen waarbij de laatste kunnen worden onderverdeeld in passieve diffusie en transporter-gemedieerd transport. Voor stoffen met een werking binnen het centrale zenuwstelsel, wordt de biofase distributie in belangrijke mate bepaald door het transport over de bloed-hersen barriere (BBB). De BBB bevindt zich in de wanden van de bloedvaten in de hersenen en onderscheidt zich van andere vaatwanden in het lichaam onder meer doordat de vaatwanden in de hersenen sterk vernauwde ruimtes hebben tussen aangrenzende vaatwandcellen. Dit maakt dat het transport van stoffen die niet over celmembranen kunnen diffunderen in hoge mate beperkt wordt. Daarnaast bezit de BBB een diversiteit aan actieve transporter-eiwitten waaronder P-glycoproteine (Pgp), een efflux-transporter die stoffen vanuit de hersenen terug naar het bloed pompt. Experimenten *in vitro*, in cellijnen die getransfecteerd waren met het MDR1 gen, dat codeert voor het humane Pgp, hebben inzicht gegeven in de functionele rol van Pgp op het transport van veel stoffen. Daarnaast hebben *in vivo* studies waarin specifieke blokkers zijn toegediend, inzicht gegeven in de functionele rol van specifieke transporters bij de distributie naar de hersenen. Een gevoelige techniek om het transport naar de hersenen *in vivo* te kwantificeren is intracerebrale microdialyse. Hierbij wordt een microdialyse probe in een specifiek gedeelte van de hersenen geïmplanteerd. De probe wordt geperfuseerd met een artificiële extracellulaire vloeistof (ECF). Moleculen die klein genoeg zijn om het semi-permeabele membraan aan de punt van de probe te passeren, zullen de probe in diffunderen en worden meegenomen met de perfusiestroom. Vervolgens kunnen *ex vivo* fracties te worden opgevangen om geanalyseerd te worden. Op deze manier wordt een afspiegeling van de concentratie van de te meten stof in de hersen ECF verkregen.

Hersen en biofase distributie modellen

Wanneer het verloop van de concentratie in bloed/plasma en in de hersen ECF bepaald is, kan een farmacokinetisch model worden opgesteld waarmee het transport naar de hersenen beschreven kan worden en waarmee de invloed van transporters kan worden gekarakteriseerd. Op die manier kan inzicht worden verkregen in de mechanismen die bepalend zijn voor de distributie naar de plaats van werking.

Recent is deze benadering toegepast in PK-PD experimenten waarbij gelijktijdig de distributie naar de hersenen, met behulp van microdialyse, en de concentratie-EEG effect relatie van het geneesmiddel norfloxacin zijn bepaald. Er werd hysterese waargenomen, die het beste beschreven kon worden met het effect-compartiment model. De waarde van de snelheidsconstante voor distributie naar het effect compartiment was verschillend van die voor de distributie over de BBB. Dit geeft aan dat de ECF concentratie niet representatief is voor de norfloxacin concentratie op de plaats van werking voor het EEG. Echter, voor morfine kon de hysterese die is waargenomen in het anti-nociceptieve effect voor 80% verklaard worden door het transport over de BBB.

1.3 PK-PD modellering van opiaten

Biofase distributie kinetiek van opiaten

Voor de PK-PD modellering van opiaten is het van belang de biofase distributie in detail te karakteriseren vanwege de sterk verschillende fysisch-chemische eigenschappen van de opiaten, alsook vanwege de mogelijke interactie met transporters op de BBB. In de literatuur zijn verschillende studies beschreven waarin de biofase distributie kinetiek van opiaten is bestudeerd in *in vitro* en *in vivo* modellen. Daarbij werd voor morfine en loperamide aangetoond dat Pgp een functionele rol speelt bij het transport over de BBB. Voor alfentanil en sufentanil werd geen interactie gevonden, terwijl voor fentanyl de resultaten niet eenduidig waren. De biofase distributie kinetiek van morfine en metabolieten is uitvoerig bestudeerd met behulp van intracerebrale microdialyse. PK-PD studies hebben aangetoond dat onder invloed van de Pgp blokker GF120918 het anti-nociceptieve effect van morfine langer duurt door een langere halfwaardetijd in de hersenen.

EEG als biomarker voor receptor activatie

Om in PK-PD studies de biofase distributie kinetiek in detail te kunnen bestuderen is de keuze van het farmacodynamische eindpunt erg belangrijk. Electroencephalogram (EEG) metingen vormen bij uitstek een geschikt farmacodynamisch eindpunt omdat het een continu eindpunt is, het effect met hoge resolutie in de tijd kan worden gemeten en het effect zowel bij proefdieren als bij de mens kan worden gekwantificeerd. Opiaten laten een specifiek effect zien in de delta-band van het EEG; onder invloed van opiaten verandert het EEG van een signaal met hoge frequentie en lage amplitude naar een signaal met lage frequentie en hoge amplitude.

PK-PD modellering van de EEG effecten van opiaten

In eerdere studies zijn de EEG effecten van de synthetische opiaten alfentanil, fentanyl en sufentanil bestudeerd in ratten. Daarbij werd hysterese waargenomen voor fentanyl en sufentanil. Deze kon goed beschreven worden met het effect-compartiment model. Voor alfentanil werd een directe relatie tussen bloed concentratie en EEG effect waargenomen. De biofase concentratie-effect relatie van de drie opiaten kon gekarakteriseerd worden met het sigmoidale E_{max} model. Aanvullend is er ook mechanistisch onderzoek verricht naar de factoren die de vorm en de ligging van deze concentratie-effect relaties bepalen. Dit had vooral betrekking op de rol van receptor binding en activatie. De receptor bindingskarakteristieken werden bepaald met behulp van een *in vitro* model en de PK-PD relaties werden geanalyseerd op basis van het zogenaamde "operational model of agonism". Dit leverde aanwijzingen op voor een aanzienlijke receptor reserve, wat inhoudt dat niet alle receptoren bezet hoeven te zijn om het maximale effect te bereiken. Dit werd bevestigd in studies naar de invloed van voorbehandeling met de irreversibele antagonist β-FNA, wat resulteert in een

afname van het aantal functionele receptoren (experimentele receptor "knock-down"). Voorbehandeling met β-FNA resulteerde in een verschuiving van de concentratie-effect relatie naar hogere alfentanil concentraties met een gelijkblijvend maximaal effect. De verschuiving in de concentratie-effect relatie kwam overeen met een 40-60% afname in het aantal beschikbare receptoren.

1.4 Doel van het in dit proefschrift beschreven onderzoek

Het onderzoek in dit proefschrift heeft betrekking op de ontwikkeling van mechanistische PK-PD modellen voor de effecten van opiaten, met speciale aandacht voor 1) de distributie naar de plaats van werking in de hersenen en 2) de binding en activatie van de μ-opiaat receptor. Hiertoe werden de PK-PD relaties van een serie van opiaten met sterk verschillende fysisch-chemische en farmacologische eigenschappen onderzocht. De opiaten werden voornamelijk gekozen op basis van (partiële) agonistische eigenschappen op de μ-opiaat receptor. De veranderingen in de delta-frequentieband van het EEG werden gebruikt als farmacodynamisch eindpunt. De volgende opiaten zijn bestudeerd: alfentanil, fentanyl, sufentanil, morfine, nalbuphine en butorphanol.

2. KARAKTERISERING VAN DE ROL VAN BIOFASE DISTRIBUTIE

2.1 Bepaling van morfine, nalbuphine en butorphanol concentraties in bloed en hersenmicrodialysaat monsters met behulp van HPLC

Om de PK-PD relaties van morfine, nalbuphine en butorphanol te kunnen karakteriseren werd een gevoelige HPLC methode ontwikkeld voor de bepaling van de concentratie in bloed en hersen microdialysaat monsters (hoofdstuk 3). Deze methode bestond uit een vloeistof-vloeistof extractie van de bloedmonsters met ethylacetaat. Voor de hersen-microdialysaat monsters was geen monstervoorbewerking nodig. De (voorbewerkte) monsters werden geïnjecteerd op een HPLC systeem dat gekoppeld was aan een electrochemische detector. De detectielimiet lag tussen 25 en 50 ng/ml voor de bloedmonsters en was 0.5 ng/ml voor morfine in microdialysaat. Voor de analyses kon worden volstaan met kleine monster volumina van rond de 50 μl wat de methode zeer geschikt maakt voor PK-PD studies in ratten.

2.2 Membraan transport van opiaten *in vitro*: invloed van P-glycoproteine en passieve permeabiliteit.

In hoofdstuk 4 wordt het onderzoek beschreven naar de relatieve bijdrage van het door het P-glycoproteine gemedieerde efflux transport en de passieve diffusie aan het totale membraan transport van opiaten. De experimenten werden uitgevoerd in MDCKII: MDR1 en LLC-PK1:MDR1a cellen. Deze cellen zijn getransfecteerd met respectievelijk het humane MDR1 gen of het muizen MDR1a gen. De interactie van de opiaten met P-glycoproteine werd zowel indirect, op basis van de inhibitie van de Pgp-gemedieerde efflux van ^{3}H-digoxine, als direct, op basis van het transport van het betreffende opiaat

in aan- en afwezigheid van de Pgp-blokker GF120918 bepaald. De passieve permeabiliteit van de opiaten werd bepaald in aanwezigheid van GF120918, waarmee de actieve efflux door Pgp werd geblokkeerd. De resultaten zoals verkregen met de digoxine assay lieten zien dat alfentanil, fentanyl, sufentanil, morfine en loperamide mogelijk substraten zijn voor Pgp omdat zij de actieve efflux van digoxine kunnen remmen. Echter, in de transport studies kon niet worden aangetoon dat alfentanil, fentanyl en sufentanil substraat zijn voor Pgp. Een mogelijke verklaring hiervoor is dat de bijdrage van Pgp-gemedieerd transport aan het totale transport van deze opiaten niet significant is door de hoge passieve permeabiliteit (>500 nm/sec). Omgekeerd geldt dat Pgp transport een belangrijke invloed heeft op het totale BBB transport van morfine en loperamide omdat de passieve permeabiliteit van deze opiaten relatief laag is.
De relaties tussen de passieve permeabiliteit en de fysisch chemische eigenschappen (LogP, LogBBB, PSA) werden bestudeerd met regressie analyse. Er konden echter geen significante verbanden worden geïdentificeerd. Dit betekent dat de fysisch-chemische eigenschappen geen voorspellende waarde hebben met betrekking tot de passieve permeabiliteit. In dit verband is het van belang dat slechts een beperkt aantal opiaten is bestudeerd en bovendien dat de bestudeerde opiaten, qua structuur, tot twee afzonderlijke groepen behoren.

2.3 Populatie pharmacokinetische modellering van de hersen distributie van morfine: invloed van actieve verzadigbare influx and Pgp-gemedieerde efflux

Voor morfine werd de rol van biofase distributie kinetiek bestudeerd *in vivo* in chronisch geïnstrumenteerde ratten. In deze ratten kan simultaan het verloop van de concentratie in de ECF en het EEG effect worden bestudeerd. Daartoe werden bij ratten vier corticale EEG electroden en een microdialyse probe geïmplanteerd. Voor de toediening van morfine, de Pgp blokker GF120918 (of het oplosmiddel) en midazolam en om bloed monsters af te kunnen nemen, werden vier permanente arteriële en veneuze cannules ingebracht. In elk experiment werd midazolam toegediend via een continu infuus om mogelijke opiaat-geïnduceerde convulsies te onderdrukken. In de verschillende studies varieerde de morfine dosering van 4 mg/kg tot 40 mg/kg. Om de invloed van Pgp te onderzoeken werd bij één serie van ratten ook GF120918 toegediend via een continu infuus. In hoofdstuk 5 lag de nadruk op het karakteriseren van het transport over de BBB en de invloed van Pgp hierop. De farmacokinetiek van morfine in bloed kon het beste beschreven worden met een drie-compartimenten model. De farmacokinetiek van de distributie naar de hersenen was niet-lineair over de verschillende doseringsgroepen. Bovendien werd een duidelijk effect van Pgp waargenomen. Om de distributie van morfine naar de hersenen te beschrijven werd een farmacokinetisch model opgesteld met verschillende wiskundige vergelijkingen voor het transport door passieve diffusie van en naar de hersenen, een verzadigbare actieve influx en een actieve efflux door Pgp. De actieve influx was al bij lage morfine concentraties verzadigd (C_{50} = 9.9 ng/ml). Er is op dit moment nog geen aanwijzing welke transporter betrokken is bij deze actieve

influx, maar in andere studies in mdr1a knock-out muizen is hetzelfde waargenomen. De actieve efflux door Pgp werd voor 42% geremd door GF120918. Deze resultaten laten zien dat de actieve efflux (voor een deel) via Pgp verloopt. Uit deze analyse kon geconcludeerd worden dat de kinetiek van distributie naar de hersenen van morfine complex is, wat belangrijke gevolgen kan hebben voor het karakteriseren van de PK-PD relaties.

2.4 PK-PD modellering van de EEG effecten van morfine: invloed van biofase distributie en de interactie met Pgp.

In hoofdstuk 6 werd de invloed van biofase distributie en Pgp op de EEG effecten van morfine bestudeerd. Er werd een significante hysterese waargenomen tussen het verloop van de bloed concentraties en het verloop van het EEG effect in de tijd. Bovendien leidde toediening van GF120918 tot een sterke verlenging van de duur van het EEG effect. De hysterese kon niet beschreven worden met een eenvoudig effect compartiment model. Uiteindelijk werd een "extended catenary biophase distribution model" voor het EEG effect van morfine ontwikkeld. In dit model wordt de distributie van morfine van het bloed naar de plaats van werking in de hersenen beschreven op basis van twee in serie geschakelde compartimenten; een transfer compartiment en een effect compartiment. Daarbij worden twee snelheidsconstantes bepaald , k_{1e} die de snelheid van het transport door het transfer compartiment beschrijft en de k_{eo} die de snelheid van het transport uit het effect compartiment beschrijft. Vervolgens werd de relatie tussen de geschatte concentraties in het effect compartiment en het EEG effect beschreven met het sigmoidale E_{max} model.

Gelijktijdige toediening van GF120918 had alleen invloed op de k_{eo}. Deze waarneming is geheel in overeenstemming met de bevindingen in het hersendistributie model waar GF120918 ook alleen invloed had op de actieve efflux. In tegenstelling tot het hersendistributie model kon voor het extended catenary biophase distributie model geen actieve influx worden geïdentificeerd. Een opmerkelijke bevinding was verder dat de voorspelde biofase concentratie-tijd profielen duidelijk verschilden van de ECF concentratie-tijd profielen zoals bepaald met intracerebrale microdialyse. De maximale concentratie in ECF werd snel bereikt, terwijl een duidelijke vertraging werd waargenomen in de maximale biofase concentratie. Ook werd na toediening van een lage dosering van morfine in het ECF concentratie-tijd profiel een plateau waargenomen, terwijl dat voor de voorspelde biofase concentratie niet het geval was. Dit betekent dat bestudering van de hersendistributiekinetiek met behulp van intracerebrale microdialyse weliswaar belangrijke informatie kan opleveren over de mechanismen die de verdeling van morfine naar de plaats van werking in de hersenen bepalen, maar dat uiteindelijk geïntegreerde PK-PD studies nodig zijn om het concentratieverloop op de plaats van werking vast te stellen.

3. PK-PD MODELLERING VAN DE EEG EFFECTEN VAN OPIATEN DIE VERSCHILLEN IN FYSISCH-CHEMISCHE EN FARMACOLOGISCHE EIGENSCHAPPEN

3.1 De rol van complexe biofase distributie kinetiek

Het doel van het onderzoek dat wordt beschreven in dit deel van het proefschrift is gericht op de ontwikkeling van een mechanistisch PK-PD model voor opiaten. Daartoe werden de PK-PD relaties van de gehele set van opiaten, die onderling sterk verschillen in fysisch-chemische (lipofilie) en farmacologische (receptor affiniteit en intrinsieke effectiviteit) eigenschappen bestudeerd. De EEG effecten van de opiaten werden onderzocht in ratten waarbij corticale electrodes waren geïmplanteerd voor het monitoren van het EEG en permanente cannules voor de infusie van de opiaten, midazolam en vecuronium bromide en voor het afnemen van bloed monsters. Evenals in de studies met morfine, werd in alle ratten midazolam toegediend via een continue infusie om mogelijke opiaat geïnduceerde convulsies te onderdrukken. Na toediening van opiaten kan ademhalingsdepressie optreden. Bij toediening van alfentanil, fentanyl, sufentanil en de hoge dosering van morfine (40 mg/kg) moesten de ratten beademd worden, waarvoor toediening van de spierverslapper vecuronium bromide noodzakelijk was. Eerst werd de invloed van biofase distributie kinetiek in kaart gebracht (hoofdstuk 7). Met uitzondering van alfentanil werd voor alle opiaten een significante hysterese waargenomen tussen het verloop van de concentratie in bloed en het verloop van het EEG effect. Voor deze opiaten werden twee verschillende biofase distributie modellen getest om de hysterese te beschrijven, 1) het effect compartiment model en 2) het extended-catenary biophase distributie model zoals beschreven voor morfine. Alleen voor morfine was het extended-catenary biophase distributie model het beste model wat erop duidt dat alleen morfine een complexe biofase kinetiek laat zien.

Regressie analyse liet zien dat er een relatie bestaat tussen de passieve permeabiliteit en de waarde van k1e, dat het transport naar het effect compartiment beschrijft.

3.2 Identificatie van het operational model of agonism voor de EEG effecten van opiaten: schatting van de *in vivo* affiniteit en intrinsieke activiteit op de μ-opioid receptor

In hoofdstuk 8 werd de relatie tussen de *in vivo* concentratie-effect relatie en de interactie met de μ-opioid receptor onderzocht. De voorspelde biofase concentratie-effect relaties werden eerst simultaan geanalyseerd met het sigmoidaal E_{max} model.

De analyse was uitgevoerd om de opiaten te rangschikken op de waarde voor intrinsieke activiteit (maximale effect). Alfentanil had de hoogste intrinsieke activiteit (123 ± 13 μV). Voor de andere opiaten werd de intrinsieke activiteit uitgedruk als een fractie van alfentanil en deze fracties lagen tussen 0.81 en 0.10. Echter, om de *in vivo* concentratie-effect relaties volledig te begrijpen zijn meer mechanistische modellen noodzakelijk.

Hierbij dienen zowel de binding aan de receptor als de daaropvolgende signaal transductie processen te worden meegenomen en zal een duidelijk onderscheid gemaakt moeten worden tussen specifieke eigenschappen van zowel de stof als het biologische systeem. Daarom werden de pharmacodynamische data verder geanalyseerd op basis van het "operational model of agonism". Het daarin te gebruiken systeem maximum (oftewel het maximaal bereikbare effect in het biologische systeem) werd gelijk gesteld aan de intrinsieke activiteit van alfentanil, terwijl ook de helling van de concentratie-effect relatie van alfentanil werd gebruikt. Op basis van het operational model of agonism werden grote verschillen gevonden tussen de opiaten in zowel *in vivo* affiniteit als intrinsieke effectiviteit.
Het verband tussen de *in vivo* affiniteit (pK_A) en de *in vitro* affiniteit (pK_i) was een aanwijzing voor het bestaan van twee subgroepen binnen deze set van opiaten. Ook werd het verband tussen de *in vivo* effectiviteit (log τ) en de *in vitro* effectiviteit (Na/GTP-shift) onderzocht, maar er werd voor deze set van opiaten geen duidelijk verband gevonden. Mogelijke verklaringen hiervoor zijn het bestaan van meerdere μ-opiaat receptor subtypes en de mogelijke interactie van de opiaten met andere types opiaat receptoren.

4. CONCLUSIES

Het doel van het onderzoek beschreven in dit proefschrift was om een PK-PD model te ontwikkelen voor de EEG effecten van opiaten, waarbij inzicht zou worden verkregen in de mechanismen die de farmacologische effecten van opiaten bepalen. Dit proefschrift laat zien dat zowel biofase distributie als receptor interactie van invloed zijn op deze PK-PD relaties. Om een mechanistisch model te ontwikkelen dat ook nog voorspellende waarde heeft, moeten deze processen in detail bestudeerd worden. Daarnaast zijn ondersteunende data (bijv *in vitro* bindings data) essentieel voor de validatie en voorspelbaarheid van het model.

LIST OF ABBREVIATIONS

List

α	Maximum response (intrinsic activity) or Fraction of E_{max}
α^H_2	Hydrogen bond acidity
A	Area of the monolayer
a→b	Apical to basolateral
AUC	Area under the curve
β-FNA	β-Funaltrexamine
β^H_2	Hydrogen bond basicity
B	Number of receptors occupied
b→a	Basolateral to apical
BBB	Blood-brain barrier
BCEC	Brain capillary endothelial cells
B_{max}	Total number of specific binding sites
BW	Bodyweight
C_{50}	Morphine concentration in the blood compartment at which 50% of the maximal active infux is reached
C_b	Blood concentration
C_d	Concentration of the displacer added
$C_D(t)$, $C_R(t)$	Drug concentration in the donor/receiver chamber
C_e	Effect-site concentration
C_{ecf}	ECF concentration
C_{et}	Concentration in the transfer compartment
C_f	Free ligand (^{3}H-naloxone) concentration
Cl	Clearance of the drug from the body
(c)LogP	(calculated) octanol/water patitioning coefficient
C_{max}	Maximum concentration
CNS	Central nervous system
CSF	Cerebrospinal fluid
‹C(t)›	Average concentration of the compound on both sides of the monolayer
ε	Residual error
E_0	No-drug response (baseline)
EC_{50}	Concentration at which 50% of the maximum effect is reached (potency)
$EC_{50,u}$	Unbound EC_{50}
ECD	Electrochemical detection
ECF	Extracellular fluid
EEG	Electroencephalogram
E_m	Maximum effect achievable in the system
f_u	Free fraction in plasma
η	Interindividual variation
HPLC	High-performance liquid chromatography
IC_{50}	Opiod concentration that displaces 50% of the radioligand (^{3}H-naloxone)
ICS	Intracellular space
IIV	Interindividual variability
k_{1e}	Rate constant for transport to the effect-site
K_A	Agonist dissociation equilibrium constant

K_d*	Equilibrium dissiciation constant of ^{3}H-naloxone
K_{diff}	Diffusion rate constant
K_E	Concentration of the drug-receptor complex required to produce half-maximal effect
K_{eff}	Active efflux rate constant
k_{eo}	Rate constant for drug loss from the effect compartment
K_i	Equilibrium inibition constant
L*	Concentration of ^{3}H-naloxone
LogBB	Logarithm of the blood-brain concentration ratio
M3G	Morphine-3-glucuronide
M6G	Morphine-6-glucuronide
MD	Microdialysis
MDR1	Multidrug resistance gene (human)
MDR1a	Multidrug resistance gene (rodent)
MRP	Multidrug resistance protein
n	Slope index for the occupancy effect relationship
n_H	Hill factor (expressing the slope of the sigmoid relationship)
N_{max}	Maximal active influx
π^H_2	Dipolarity/polarizability
P	Population parameter
P_{app}	Apparent permeability
PBPK	Physiologically-based pharmacokinetics
Pgp	P-glycoprotein
P_i	Individual value of the model parameter P
PK-PD	Pharmacokinetic-pharmacodynamic
PSA	Polar surface area
Q	Intercompartmental clearance
Q_{diff}	Diffusion clearance
$Q_{eff}.C_{ecf}$	Active efflux by Pgp
R_0	Total number of available receptors
R_2	Excess molar refraction
τ	Efficacy parameter
$t_{1/2}$	Elimination half-life
TEER	Trans epithelial electrical resistance
θ	Fixed effect
V1	Volume of distribution of the central compartment
V2, V3	Volume of distribution of the peripheral compartments
V_D, V_R	Donor and receiver chamber volumes

Nawoord
NAWOORD

Na

Aan het einde van lang promotietraject is mijn proefschrift dan eindelijk afgerond. Echter, dit was niet mogelijk geweest zonder de bijdragen van een groot aantal mensen die ik hier graag even wil noemen.
In de eerste plaats natuurlijk Jan Freijer. Eindeloze discussies hebben we gevoerd over de verschillende modellen, maar het resultaat mag er wezen. Ik heb er heel veel van geleerd en ben het modelleren echt leuk gaan vinden. En nu gaan we als collega's gewoon verder met onze discussies.
Om de data te verkrijgen waren er een heleboel experimenten nodig, die ik op verschillende afdelingen heb uitgevoerd. Allereerst de EEG en microdialyse experimenten die zonder de expertise van Erika Tukker, Susanne Bos-van Maastricht en Pieter Looijmans niet mogelijk waren geweest. Ook mijn stagestudenten Andrea Rosier en Dennis de Mik hebben veel uurtjes doorgebracht bij de experimenten. Ik heb het erg leuk gevonden om samen met jullie aan het project te werken en hoop dat ik jullie wat heb kunnen leren.
During my research project, I have performed a series of *in vitro* experiments at GlaxoSmithKline, Drug Metabolism and Pharmacokinetics in Ware, United Kingdom, together with Dennis de Mik. I think we have made quite an impression there and it was a really good experience. I would especially like to mention Glynis Nicholls and Andy Ayrton who made it possible for me to do the research and guide me through the processes. But also the help of Nipa Shah and Caroline Brough with the cell-cultures and Rebecca Scott and Phil Deniff from the World-wide bioanalysis department with the analysis of all the samples is highly appreciated.
In mijn laatste jaar heb ik ook een serie *in vitro* experimenten uitgevoerd bij de afdeling farmacochemie van het LACDR onder begeleiding van professor IJzerman en Jacobien von Frijtag-Drabbe Kunzel. Jacobien, helaas kun je dit niet meer meemaken, maar zonder jou waren de experimenten nooit zo succesvol verlopen. Ik zal je nooit vergeten. Daarnaast ben ik professor IJzerman zeer erkentelijk dat mij de mogelijkheid geboden is om de experimenten uit te voeren. Al de verschillende technieken hebben mijn promotie juist zo aantrekkelijk gemaakt.
Maar natuurlijk mag ik mijn collega-aio's ook niet vergeten, het was een echte vrouwenclub met Corine, Lia, Tamara, Dymphy, Paulien en Marian, af en toe echt een kippenhok, maar zo gezellig. Wat zullen jullie mannen, Hugo, Ashraf, Gijs, weleens gedacht hebben.
En dan mijn paranimfen, Margret en Paulien. Margret, zonder jouw steun en hulp had ik die HPLC allang het raam uitgegooid. Hoeveel monsters we samen we niet gemeten hebben?! Het heeft ook onze persoonlijke band sterk gemaakt en ben heel blij dat jij als paranimf aan mijn zijde wilt staan. Paulien, we zijn al vriendinnen vanaf het introductieweekend in Leiden en ook al was het soms lastig om collega's te zijn, ik had het niet willen missen en ben blij dat ik ook nu weer op je steun kan rekenen.
Mijn vrienden en familie hebben mijn promotie van dichtbij meegemaakt. Ik ben niet altijd even sociaal geweest, maar jullie hadden altijd er altijd begrip voor en waren

altijd geïnteresseerd in hoe het ging. In het bijzonder wil ik graag mijn ouders, Bas en mijn schoonouders noemen die me altijd hebben gesteund en op wie ik altijd kon rekenen voor een luisterend oor. Roel, zonder jouw hulp had mijn proefschrift er nu niet zo mooi uitgezien.
En tot slot, lieve Michiel, zonder jouw onvoorwaardelijke liefde, steun en hulp had ik het nooit gered. Hoe vaak ging je niet met me mee naar het lab om te pipetteren of moest je mijn frustraties aanhoren? Ik hoop dat ik voor jou nu hetzelfde kan doen. Een leven zonder jou kan ik me gewoon niet meer voorstellen.

Dorien

CURRICULUM VITAE

Dorien Groenendaal werd geboren op 11 april 1978 te Velsen. Na het behalen van het diploma Gymnasium in 1996 aan het Augustinus College te Beverwijk, begon zij de studie Bio-Farmaceutische Wetenschappen aan de Universiteit Leiden, waar zij in 1998 het propedeutisch diploma verkreeg. Tijdens de doctoraal fase heeft zij haar hoofdvakstage gedaan op de afdeling Farmacologie van het Leiden/Amsterdam Center for Drug Research, onder begeleiding van Dr. M.P. Schaddelee, Dr. A.G. de Boer en Prof. Dr. M. Danhof. Het verslag van het stage project was getiteld: The Blood-brain barrier transport of the adenosine A_1 receptor agonists CPA, MCPA and 2'dCPA. Aansluitend volgde zij een tweede onderzoeksstage bij Pfizer Global Research and Development, Discovery Biology, Sexual Health Group te Sandwich, United Kingdom. Dit project werd begeleid door Dr. P.H. van der Graaf, Dr. C. Wayman and Prof. Dr. M. Danhof en het stageverslag was getiteld: *In vitro* studies to investigate novel targets for the treatment of Male Erectile Dysfunction. In december 2000 behaalde zij haar doctoraal diploma Bio-Farmaceutische Wetenschappen.

Van december 2000 tot en met juli 2005 was zij als assistent in opleiding verbonden aan de afdeling Farmacologie van het Leiden/Amsterdam Center for Drug Research onder begeleiding van Dr. E.C.M. de Lange en Prof. Dr. M. Danhof, alwaar het in dit proefschrift beschreven onderzoek werd uitgevoerd. In het kader van dit onderzoek werd samengewerkt met de afdeling Farmacochemie van het Leiden/Amsterdam Center for Drug Research en de afdelingen Drug Metabolism and Pharmacokinetics en Clinical Pharmacokinetics Neurology van GlaxoSmithKline in het Verenigd Koninkrijk.

Sinds augustus 2005 is zij werkzaam als Clinical Pharmacokineticist bij Astellas Pharma Europe B.V. te Leiderdorp, Nederland.

LIST OF PUBLICATIONS

Groenendaal D, Freijer F, von Frijtag Drabbe Kunzel J, van der Graaf PH, IJzerman AP, Danhof M, de Lange ECM (2007). Identfication of the operational model of agonism for the EEG effects of opioids: estimation of the role of in vivo affinity and intrinsic efficacy at the mu-opioid receptor. *In preparation*

Groenendaal D, Freijer J, Rosier A, de Mik D, Nicholls G, Hersey A, Ayrton AD, Danhof M, de Lange ECM (2007). Pharmacokinetic-pharmacodynamic modelling of the EEG effects of opioids: the role of complex biophase distribution kinetics. *Eur. J. Pharm. Sci., Submitted*

Groenendaal D, Freijer J, de Mik D, Bouw MR, Danhof M, de Lange ECM (2007). Population pharmacokinetic modelling of non-linear brain distribution of morphine: influence of active saturable influx and P-glycoprotein mediated efflux. *Br J Pharmacol.* **515:** 701-712

Groenendaal D, Freijer J, de Mik D, Bouw MR, Danhof M, de Lange ECM (2007). Influence of biophase distribution and P-glycoprotein interaction on pharmacokinetic-pharmacodynamic modelling of the effects of morphine on the EEG. *Br J Pharmacol.* **515:** 713-720

de Lange ECM, Ravenstijn PGM, Groenendaal D, van Steeg TJ (2005). Toward the prediction of CNS drug-effect profiles in physiological and pathological conditions using microdialysis and mechanism-based pharmacokinetic-pharmacodynamic modeling. *AAPS Journal* **7:** E532-E543

Groenendaal D, Blom-Roosemalen MC, Danhof M, de Lange ECM (2005). High-performance liquid chromatography of nalbuphine, butorphanol and morphine in blood and brain microdialysate samples: application to pharmacokinetic/pharmacodynamic studies in rats. *J Chromatogr B Analyt Technol Biomed Life Sci.* **822:** 230-237

Schaddelee MP, Groenendaal D, DeJongh J, Cleypool CG, IJzerman AP, De Boer AG,
Danhof M (2004). Population pharmacokinetic modeling of blood-brain barrier transport of synthetic adenosine A1 receptor agonists. *J Pharmacol Exp Ther.* **311:** 1138-1146

Schaddelee MP, Voorwinden HL, Groenendaal D, Hersey A, Ijzerman AP, Danhof M,
De Boer AG (2003). Blood-brain barrier transport of synthetic adenosine A1 receptor agonists in vitro: structure transport relationships. *Eur J Pharm Sci.* **20:** 347-356